FINAL REPORT

CONTRACT NO. NAS 9-2792

1 May 1964 through 31 January 1966

THERMALLY REGENERABLE CARBON DIOXIDE ABSORBENT SYSTEM

BY

Harry P. Gregor, Project Supervisor
Irving F. Miller, Research Associate
Oscar W. Weber, Research Fellow

FOR

NATIONAL AERONAUTICS AND SPACE ADMINISTRATION
NASA MANNED SPACECRAFT CENTER
CREW SYSTEMS DIVISION
HOUSTON, TEXAS 77058
APRIL 1966

HARRY P. GREGOR, Ph. D.
150 LAKEVIEW AVENUE
LEONIA, NEW JERSEY

FINAL REPORT

CONTRACT NO. NAS 9-2792

1 May 1964 through 31 January 1966

THERMALLY REGENERABLE CARBON DIOXIDE ABSORBENT SYSTEM

by

Harry P. Gregor, Project Supervisor
Irving F. Miller, Research Associate
Oscar W. Weber, Research Fellow

FOR

NATIONAL AERONAUTICS AND SPACE ADMINISTRATION
NASA MANNED SPACECRAFT CENTER
CREW SYSTEMS DIVISION
HOUSTON, TEXAS 77058
APRIL 1966

HARRY P. GREGOR, Ph. D.
150 LAKEVIEW AVENUE
LEONIA, NEW JERSEY

ACKNOWLEDGMENT

The work reported herein was supported by a Contract (NAS 9-2792) issued by the National Aeronautics and Space Administration, NASA Manned Spacecraft Center, Houston, Texas, to Harry P. Gregor, Ph. D. of Leonia, New Jersey. The experimental studies were performed by O. W. Weber, a Research Fellow in the Department of Chemical Engineering at the Polytechnic Institute of Brooklyn, New York, under a sub-contract from Harry P. Gregor, Ph. D.

ABSTRACT

This investigation was conducted in order to ascertain the feasibility of the application of ion exchange resins in gaseous systems. While some previous work has been done in the field of gas absorption with chemical reaction by solutions of polyelectrolytes, this represents the first time that the ion exchange materials have been utilized in the solid state. The major effort was directed toward the removal of carbon dioxide from an air stream by weak-base resins. Commercial products, Dowex WGR, Dowex-3, Dowex-4, Amberlite IRA-93, and a resin synthesized by cross-linking polyethylenimine with epichlorohydrin, were tested.

Unique packed beds were constructed to eliminate channeling, and CO_2 removal from a gas stream was studied at various levels of carbon dioxide partial pressure, temperature, and relative humidity. A correlation of equilibrium capacity with these variables was obtained. The capacities found appear to be consistent with those found for similar materials in dilute solutions.

A four step reaction mechanism is postulated, consisting of:

1. Absorption of CO_2 from the bulk gas stream across a gaseous boundary layer to a thin liquid film surrounding the resin particle, governed by the equation: rate = $k_G(P_{GAS} - \frac{C_{LIQ}}{s})$ where s is the solubility of CO_2 in the liquid;

2. Transfer of CO_2 across the liquid film via a linear concentration gradient to the surface of the solid, where a distribution coefficient, R, between the solid and liquid concentrations operates, to give: rate = $k_L(C_{LIQ} - \frac{C_{SOLID}}{R})$;

3. Slow diffusion of CO_2 away from the surface towards the interior of the spherical particle by Fick's Law:

$$\frac{\partial c_{SOLID}}{\partial \theta} = D\nabla^2 c_{SOLID}$$

4. Rapid reaction of CO_2 with resin inside the particle by

$$R_3NH^+OH^- + CO_2 + H_2O = H_2CO_3 + R_3NH^+OH^- = R_3NH^+HCO_3^- + H_2O$$

For this mechanism, the solutions of the diffusion equations have been found and employed to give good correlation of the data.

Finally, a feasible system using such resins as air purifiers in enclosed areas, such as space capsule cabins, was designed for the best material, the polyethylenimine-epichlorohydrin resin. The equipment required to maintain an atmosphere of 0.65% CO_2 and 50% relative humidity at 20°C for two men consisted of four packed beds (two large, for CO_2 absorption, and two small, for water absorption) containing a total of 37 pounds of resin, a shell-and-tube air humidifier to saturate the column feed stream, and a heat exchanger to condense the water vaporized during regeneration. The important numerical values associated with the design are:

Total Volume: Less than ten cubic feet

Power (Heating): 1134 watts

Condenser cooling: 2970 Btu/hr.

Capacity: 96.1 grams of CO_2 and 82 grams of water per hour

The system is regenerated by heating the beds to 80°C and applying a vacuum. Use of the space vacuum available eliminates the need for a vacuum pump and permits the CO_2 to be immediately dumped.

TABLE OF CONTENTS

LIST OF TABLES

LIST OF TABLES (CONTINUED)

LIST OF TABLES (CONTINUED)

LIST OF FIGURES

LIST OF FIGURES (CONTINUED)

LIST OF FIGURES (CONTINUED)

LIST OF FIGURES (CONTINUED)

I. INTRODUCTION

A. Background

With the advent of vehicles such as submarines and spacecraft which remove man from his natural environment, where he has an inexhaustible supply of breathable air, it has become mandatory that a method be developed to sustain him in a small, finite atmosphere. All the water and carbon dioxide which he continuously introduces into this atmosphere by perspiration and exhalation must therefore be continuously removed if he is to survive. Neither of these substances would present much difficulty if the duration of the man's encapsulation were short and physical requirements not critical.

Air conditioning systems easily remove moisture by cooling and condensation, but the equipment involved is heavy, large in volume, and very consuming of power. The current atmosphere control method employed in submarines utilizes the chemical reaction between CO_2 and the weak base monoethanolamine (MEA) (1), but this is a toxic, volatile, combustible liquid which requires large storage volumes and high regeneration temperatures (with the accompanying high power load), and which degenerates after a time in the presence of atmospheric oxygen to give off noxious ammonia gas (2). The current space program utilizes the chemical reaction between CO_2 and the strong base lithium hydroxide (LiOH) (1), but this requires a large inventory of fresh material, for the reaction is irreversible. It would appear that the criteria for finding a more suitable system are:

1. Ability to remove CO_2 and dispose of it;
2. Ability to remove water and save it for further use;
3. High capacities for both these substances;

4. Compactness;

5. Low power requirement;

6. Reversible reaction, with ease of regeneration, for continuous, long-term operation.

The qualifications could be met by a substance with the following properties:

1. A base, so that it could react with the weak acid H_2CO_3;

2. A porous, hygroscopic material, to absorb water;

3. Large usable capacity, namely, large pore volume and accessible basic constituents;

4. A solid, so that large solution volumes and leakage problems could be done away with;

5. Small temperature changes (low heat of reaction and favorable equilibrium constants) to minimize the power load;

6. Fast and complete reverse reaction.

An anionic ion-exchange resin which is a basic polyamine solidified by a small amount of crosslinking fits these requirements.

The groundwork for this investigation of gaseous ion exchange was laid by Robins (3), who through experiments with dilute solutions found that polymers, particularly poly-N-methylethylenimine, were available which were capable of the CO_2 absorption needed, by Saber (4), who was able to synthesize a solid resin from polyethylenimine which had enough available -NH- sites to give a capacity for strong acid of over 9 milli-equivalents per gram of resin when in its basic state (by comparison, the theoretical strong acid capacity for potassium hydroxide is only 17.9 meq per gram), and by Tetenbaum and Gregor (5), who investigated the existence of a coupled film-particle diffusion mechanism for liquid-solid

ion exchange (for a lightly cross-linked resin of polystyrenesulfonic acid). High capacity commercial resins were also readily available, and merited consideration because the synthesis of Saber's resin is perhaps too time-consuming to put on a large scale.

This method could be easily extended (with the appropriate resins) to the efficient removal of small amounts of other ionic components, such as NH_3, HCl, SO_2, and SO_3, from gas streams.

B. Statement of the Problem

Polyamine, weak-base ion exchange resins were to be tested for their ability to absorb carbon dioxide from an air stream under various operating conditions of temperature, CO_2 concentration, and relative humidity. Having found a compound with both high CO_2 capacity and reasonable absorption rates, an atmospheric conditioning system employing this material and suitable for the maintenance of a closed volume, containing two breathing human beings, at a CO_2 level of 0.65 volume per cent and a relative humidity of 50% (at 20°C), was to be designed.

II. RESINS

A. Polyethylenimine-Epichlorohydrin

The structure of polyethylenimine has as its repeating (monomer) unit the group $-CH_2-CH_2-NH-$ which arises from the opening of the three-membered ethylenimine ring. This polymerization is normally initiated by a protonation reaction with HCl acting on one ring. (6) The highly reactive $\backslash NH_2^+ Cl^-$ configuration (still in the cyclic state) then opens its ring with a second molecule to form:

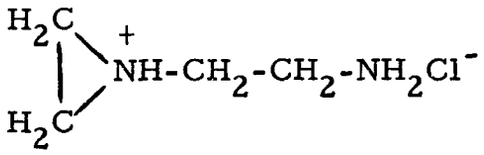

The trailing NH_2Cl^- continues the process.

With such a structure, it would appear that, if each of the repeating nitrogens in the final polymer could be made reactive, the polymer would have an equivalent weight of 43. If one were then to protonate the polymer with a strongly basic solution, a strong acid capacity of 1000/43 or 23.2 meq per gram would be found. However, the smallness of the monomer unit prevents this from happening; the -NH- groups are too close together. The charge density associated with the $-NH^+OH^-$- structure is too high to permit the existence of another such group separated from it by only a $-CH_2-CH_2-$ group (7). Thus it has been found that the strong acid capacity should be very nearly one-half of the above, or 11.6 meq per gram. The polymer, as supplied by the Chemirad Corp., is a 50% by weight water solution. The polymer cannot be completely dried by freeze drying or evaporation, so that its measured capacity (per moist gram) is again slightly less. The residual water is usually about 5 to 10 per cent, since temperatures higher than about 90°C cannot be employed in the

drying operation. Cross-linking, in order to form a mechanically strong solid, reduces the capacity per gram of the resultant resin even further.

Epichlorohydrin was used as a cross-linking agent. Its structure, containing two reactive groups in a short chain, is ideal for use with a straight chain polymer containing a multitude of NH sites. When the recommended (8) ratio (based on a PEI equivalent weight of 43) of 4.2 moles of PEI per mole of ECH was employed and the resultant product crushed and refluxed with methanol, a whitish solid was obtained for the finely ground material. The particles in the 28 to 48 mesh range had, however, a yellowish tinge due to trapped linear polymer which the methanol was unable to extract. The solid took on more of a bluish-green hue when treated with strong base (1M KOH). This resin could be expected to have a strong acid capacity in the neighborhood of 9 meq/gram.

This material was prepared according to the method of Saber (4), who also suggested (8) that the 4.2 molar ratio of dehydrated PEI to ECH afforded the best combination of capacity and mechanical strength. The PEI was dehydrated for at least 24 hours in a rotary vacuum evaporator at 90°C. Subsequent analysis (9) showed that this treatment could result in a PEI product containing as little as 2% water by weight-a distinct improvement upon Saber's original freeze-drying technique.

First 200 g. of 50% PEI (unit monomer molecular weight of 43) solution equivalent to 2.33 moles of PEI were placed in a flask and subjected to the rotary vacuum evaporation treatment. Then 5.1 grams of ECH (equivalent to the required 4.2 molar ratio) were slowly added to the dehydrated PEI (which had been dissolved in about 250 grams of methanol) with continuous rapid agitation to insure more uniform mixing.

After an hour's agitation period, the material, now quite viscous, was poured into four large pyrex baking dishes to give a large surface to volume ratio for drying. The dishes were heated in a vented oven at 65° for two hours. After remaining in the oven overnight at close to room temperature, they were reheated at 65°C for an additional hour (8).

The resulting sheets, which had cracked into small flexible pieces roughly 1/4" x 1/4", were ground in a ball mill (using ceramic cylinders to do the grinding) for one day, and then further pulverized in a blender using dodecane as a non-solvent, liquid medium. The fine particles were then treated for several days in a Soxhlet extraction apparatus with methanol to dissolve the uncrosslinked PEI. The extracted material was dried overnight in the oven under low heat to remove the remaining methanol. The dried particles were sieved, with the 28 to 48 mesh cut retained for fixed bed use, the greater-than-48 mesh cut retained for fluidized bed use, and the less-than-28 mesh cut returned to the blender for further grinding.

B. Commercial Resins

Dowex WGR is made by reacting the polymer

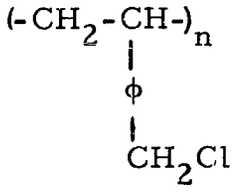

(where the symbol ϕ denotes the phenyl group) with tetraethylene pentamine (TEP) :

$$H_2N\text{-}(CH_2\text{-}CH_2\text{-}NH)_3\,CH_2\text{-}CH_2\text{-}NH_2$$

The nitrogen atoms provide five active sites per molecule. The reaction should progress favorably in basic media by virture of the formation of HCl as the inorganic product. The TEP provides cross-linkages for the original polymer because more than one of the nitrogens in each molecule can react.

The equivalent weight of this material should be the unit weight, 305, divided by the average number of amine sites which are protonated. Where the PEI-ECH resin was concerned, it was noted that only alternating sites could take on the $R_2NH_2^+OH^-$ configuration needed due to high charge density. In the present case also, the nitrogen atoms are separated by only a $-CH_2-CH_2-$ group. One should then be able to protonate only the 2 and 4 positions or the 1, 3 and 5 positions, so that the equivalent weight on this basis alone should be 305/2.5, or 122, for a theoretical strong electrolyte capacity of 1000/122 or 8.2 meq/gm.

An additional decrease in capacity should be observed because of the effect of TEP as a cross-linking agent. Each linkage involves <u>one</u> TEP chain and <u>two</u> monomer units of the original polymer. If each TEP molecule cross-linked, the resultant equivalent weight would be 421/2.5 or 168.3, so that a strong acid capacity of 5.94 (=1000/168.3)

meq/gm would be exhibited.

Each cross-linkage makes the particular amine site involved a stronger base. Basicity increases with the degree of substitution of R groups for hydrogen atoms on the nitrogen, making these atoms more likely sites for protonation. It is also possible for one TEP molecule to react with more than two polymer chains. The degree to which these multiple linkages occur depends strongly on steric hindrance exhibited by the long chains and by the phenyl groups. Multiple linkages also introduce more three-dimensional charge density effects which inhibit protonation. These additional complications make an accurate capacity prediction unfeasible; only an acid-base titration can provide the information.

Rohm & Haas Amberlite IRA-93 is a styrene-divinyl benzene copolymer containing only tertiary amine groups (which cannot form carbamates (22)). Its protonated reactive sites thus have the

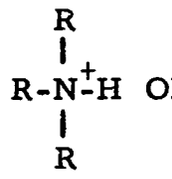

configuration. Titrations performed by the manufacturer show this material to have a strong acid capacity of 4.4 meq/gm. The outstanding feature of this resin is its so-called "macroreticularity", that is, its possession of many large-diameter pores, which increase the diffusion rate, in each spherical particle.

C. Treatment Prior to Use

Dowex-3 and Dowex WGR are available in the strongly acidic chloride form, while Dowex-4 and Rohm & Haas Amberlite IRA-93 are shipped in the free base form. Since an acid-base neutralization reaction is required for resin operation ($R_3NH^+OH^- + H_2CO_3 \rightleftharpoons R_3NH^+HCO_3^- + H_2O$) the higher the initial pH of the material, the higher its capacity. Therefore all resins were soaked for a minimum of twelve hours in an agitated 1M KOH solution to convert them to the hydroxide form. This KOH solution was decanted, and the particles agitated with deionized water down to a pH of 11 to wash away excess KOH which is itself, of course, a high capacity CO_2 absorbent. In addition, it has been found that the chloride ion catalyzes the hydration of carbon dioxide (10). The data of Robins (3) indicate a substantial increase in total exchange capacity for CO_2 when these resins are suspended (in base form) in KCl solutions instead of just in pure deionized water. The final step in preparation was to soak the resins in a 1M KCl solution. The pH of this solution was raised to 11 by the addition of a small amount of solid KOH (which rapidly dissolved) to prevent lowering the pH of the particles to less than 11 during the several hours duration of the agitation. The resin was thereafter considered ready for packing in the column.

The resin particles tend to agglomerate when moist. The material could not be dried before packing since carbamates are formed at higher temperatures when the dry resin exhibits a pH greater than 8.0 (3). A liquid was thus required to aid distribution of the particles among the meshes of the "Vexar" screens. In order to maintain the resin in its correct final condition the wash liquid used was again a one molar KCl solution having a pH of 11. Excess solution was drained with the help of vibration.

D. Titrations to Determine Strong Electrolyte Capacity

Five different ion exchange resins were available for study: Dowex-3, Dowex-4, Dowex WGR, Rohm & Haas IRA-93, and the aforementioned PEI-ECH. Accompanying literature gave the strong electrolyte capacity of IRA-93 as 4.4 milliequivalents per dry gram. It was necessary to titrate the remaining resins with NaOH and HCl to determine their capacities. The procedure follows.

Between one and three grams of moist resin were placed in a flask and agitated overnight in the presence of a 1M NaOH solution. The liquid was decanted and the resin washed with deionized water until the pH of the wash water, as determined by pH indicator paper, was slightly less than 11. A measured amount of standard .2N HCl solution (obtained from Fisher Scientific, standardized and sealed) was added—either 100 or 125 ml., depending on the amount of resin being used. The flasks were again stoppered and agitated overnight. These resin suspensions were then titrated with .2N NaOH solution (also obtained standardized and sealed from Fisher Scientific) to the phenolphthalein end-point. Capacity was calculated by: (.2 meq/ml) (ml HCl - ml NaOH)/wt. of resin. The weight of the moist resin was known; to obtain the dry weight, the resin was filtered and the particles placed in a weighing tin of known weight. The tin was placed in an oven at 80°C and weighed every few hours until a constant weight was noticed for two consecutive measurements.

The results of these titrations are shown in Table 1. Comparison of the capacities shows the PEI-ECH to be highest, with Dowex WGR next. These two were therefore chosen for extensive packed bed treatment with dilute mixtures of CO_2 in air to determine their ability to neutralize the weak acid H_2CO_3. Dilute-solution data (11) indicated that dilute solutions

TABLE I

TITRATIONS TO DETERMINE STRONG ACID CAPACITIES AT 20°C

MATERIAL	MOIST WT.	ml. HCl	ml. NaOH	DRY WT.	CAPACITY
Dowex-3	1.5286gm	100.3	78.9	1.3671	3.14 meq/dry gm
Dowex-4	1.7835gm	100.3	77.5	1.3003	3.51 meq/dry gm
DowexWGR	1.3461gm	125.0	103.0	.7568	5.81 meq/dry gm
PEI-ECH	1.0056gm	125.1	98.0	.5970	9.08 meq/dry gm

of methyl polyethylenimine, $+HCCH_3\text{-}CH_2\text{-}NH+_n$ would absorb between 0.16 and 0.24 grams of CO_2 per gram of resin when exposed to an atmosphere of 3.0% CO_2, the actual value increasing with the salt concentration in the solution. The IRA-93 was also tested further, since it was hoped that its large pore volume would make diffusion within the particles less of a rate-determining step.

III. EQUIPMENT AND PROCEDURES

A. Instrumentation

The quantities whose magnitudes are required for the material balance and reaction rate calculations are carbon dioxide concentration (exit only), inlet and exit humidity, volumetric gas flow, reaction temperature, and time.

The inlet carbon dioxide concentration is determined by the Matheson Company which analyses the composition of the cylinders of compressed gas used as feed. The exit CO_2 concentration is measured by means of a Liston-Becker infrared analyzer, supplied and serviced by the Beckman Co. This device yields a signal which varies (non-linearly) with volumetric CO_2 percentage, from zero to ten volts. A standard calibration curve (Figure 1) was obtained from four reproducible experimental points: 0.00%, 0.30%, 0.65%, and 1.00% carbon dioxide. It was found that prepurified grade nitrogen and compressed ambient air which had been passed through a bed of Fisher Scientific "Indicarb" reagent gave the same "zero" point. The aforementioned Matheson-analyzed gases were used as standards. The zero and top-scale (1% CO_2) points were checked before and after each run, since the device is prone to some time-variation in its calibration. Occasionally, the intermediate (0.30% and 0.65% CO_2) points were checked, but their positions relative to the two end-points were found to be invariant. (That this should be so is intuitively obvious since the initial steps of calibration always result in setting 0.00% CO_2 at zero volts and 1.00% CO_2 at 10.0 volts.)

Two additional precautions were necessitated by the analyzer's sensitivity to humidity and pressure. To accommodate the first difficulty,

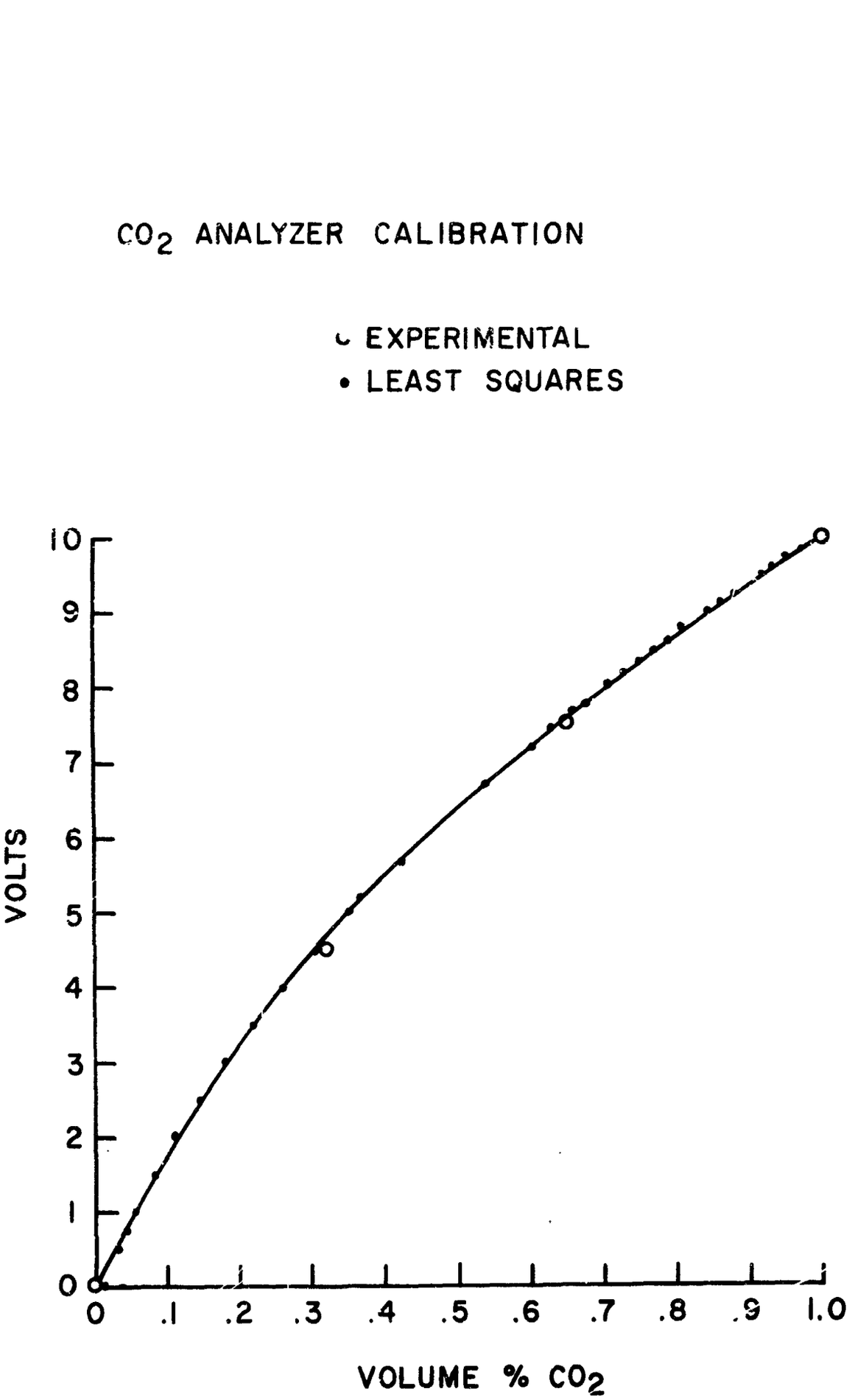

FIGURE 1
PAGE 15

the detecting probe for the outlet humidity was placed between the reactor and the analyzer, and the gas was then dehumidified by passage through a bed of Drierite (anhydrous $CaSO_4$). The second problem was compensated for by making all calibration readings at a gas flow rate approximately the same as that used during the actual run, and sufficient to keep the analyzer from lagging behind the actual concentration by more than about thirty seconds. (The manufacturer states that the analyzer is pressure-sensitive, but not flow-sensitive; however, since we are dealing with a compressible fluid flowing through a myriad of small tubes and fittings, pressure and flow rate are definitely inter-related through the Navier-Stokes equations.)

Combination wide-range relative humidity and temperature probes and accompanying amplifiers and indicators were supplied by the Hygrodynamics Division of the American Instrument Company. Each of these elements was calibrated by the manufacturer. The calibrations were guaranteed invariant as long as no liquid water contacted the sensors (lest the Li Cl coating, upon which measurements depend, be washed off). As a check, the probes were occasionally calibrated against each other when it was suspected that condensation of moisture might have occurred on one of them. In two cases this was found to have occurred, and these elements were replaced.

Both the CO_2 analyzer and the humidity sensor amplifiers were provided with cables for connections with potentiometric recorders, and Bausch and Lomb VOM-5 recorders (with one second full scale response time) were used. Their time-accuracy was excellent. Time for the individual runs was kept with a stopwatch.

Volumetric gas flow was measured by a dry test meter supplied and calibrated by the Brooklyn Union Gas Company; this device could be read to about .003 cubic feet.

The resin bed itself was kept at a constant temperature by submersion in an insulated, stirred tank of water (or water/ice mixture) containing two immersion heaters powered by varible voltage supplies. The feed gas was first passed through a twenty-foot coil of copper tubing submerged in the same bath so that its temperature coincided with that of the bed. Temperatures were read from a Fisher thermometer accurate to about $0.2^{\circ}C$.

B. The Packed Bed

1. Packing Scheme

The properties of the resins which were responsible for the low, inaccurate capacities obtained early in this work were low density and swelling. The former made gas channeling, especially along the container wall, easy. The result was that the gas failed to contact most of the particles. Since diffusion through the untouched particles (and the resultant stagnant void spaces among them) is slow, it follows that the inlet and exit CO_2 concentrations would quickly become essentially equal, and one would erroneously conclude that saturation had been reached. If, after allowing the bed to sit for awhile, gas flow was again initiated, more CO_2 take-up would be observed, that which had previously been absorbed having distributed itself by diffusion more uniformly throughout the remainder of the bed. Swelling of the wet particles prevented use of tight packing at the top and bottom of the bed as a corrective measure.

It was necessary to create a more tortuous path for the gas to traverse, with special attention given to making the cylinder wall an undesirable fluid highway. The gas was forced to constantly change its direction of flow by stacking the column with 6 mesh DuPont "Vexar" screening which had been stamped out in circles conforming to the inside diameter of the tube. The interstices of the screens were completely filled with the resin particles, accompanied by vibration to obtain the densest possible packing. The gas was further prevented from traveling along the walls for any considerable distance by packing the column in inch-long sections, each section being marked by a brass plate with the following features: (Figure 2) a few holes drilled in the center (less than 25% of the surface perforated) completely encircled by an airtight O-ring

AM 1-3-66

COLUMN SECTIONING AND PLATES

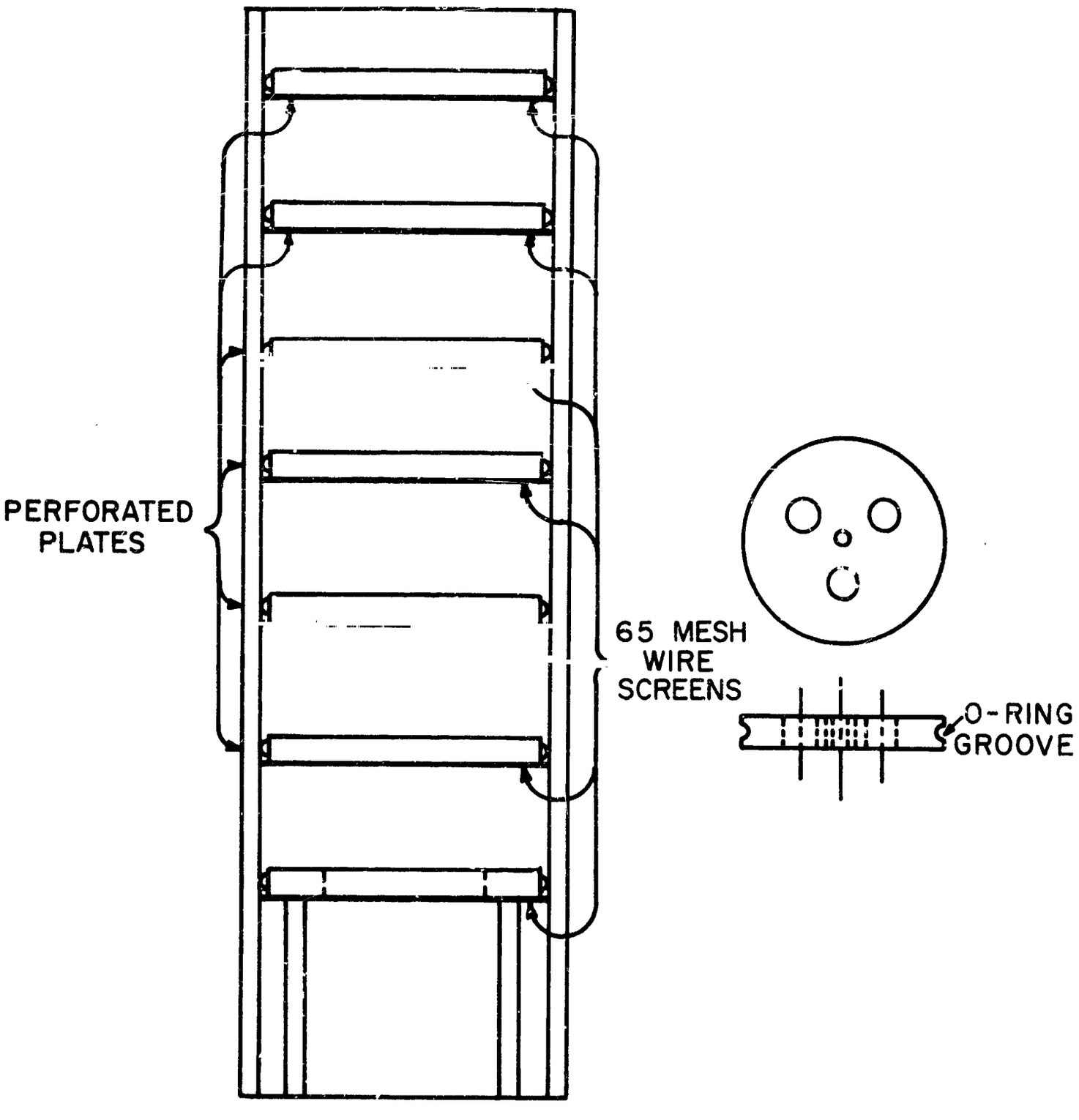

FIGURE 2
PAGE 19

6-3-66

gasket; a 65 mesh screen epoxied to one face; all exposed faces lacquered with epoxy resin. The center holes and the O-ring forced the gas to leave each section only through the center; yet no two consecutive plates had their holes completely aligned lest the gas adopt the center as a preferred path. The screening prevented any particles from leaving their own section, either by gravity or fluidization, and the epoxy coating kept the extremely basic and ammoniacal resins from reacting with the copper portion of the brass alloy (12).

The column used was a one foot length of borosilicate glass of 44 mm inside diameter with a 2 mm thick wall. Glass was chosen so that the arrangement of the particles, screens, and plates could be seen.

The column was assembled as follows: The bottom plate (and its accompanying stand) was put into place, and the first "Vexar" screen laid flat on top of it. The meshes were filled with the wet resin and a small amount of KCl solution. When no more settling was observed after a period of mechanical vibration, more resin was added until the thickness of the particle layer was slightly greater than the "Vexar" thickness. Further vibration then equalized these thicknesses. These steps were repeated until eight screens had been filled, each screen rotated between 30° and 45° with respect to its predecessor. A perforated brass plate was then slowly worked down the column until it rested in contact with the completed section; the next section was begun by stacking right on top of this plate.

AM 1-3-66

2. The Column

A transparent column was used so that: 1) any non-uniformities in the packing could be observed and immediately corrected during the stacking process, and: 2) any unfavorable action during an experimental run, such as channeling, excess surface moisture, excessive surface drying, and fluidization were also visible. Channeling prevents complete gas-solid contacting. Excessive surface moisture is injurious to the relative humidity probes if entrainment occurs, besides yielding slightly false capacity since its basic condition permits it to absorb some CO_2. Excessive surface drying lowers the resin's capacity by failing to provide sufficient water for carbon dioxide hydration and bicarbonate ion formation. Fluidization is a further consequence of excessive drying, wherein the density of the particles is sufficiently reduced to permit the gas to fluidize some of them, leading to channeling through the now-vacant portion of the bed.

Borosilicate glass tubing was chosen not only for its great mechanical strength, necessary to withstand the pressures of the mass of wet resin, the tight 0-ring gaskets, and the feed gas, but also for its low thermal expansion coefficient, lest it deform under the application of the 70°C to 80°C temperatures of the regeneration process. This low coefficient of expansion was, however, responsible for the overall design shown in Figure 3. Since the stainless steel rods holding the brass plates expanded, in the hot bath, more than the glass tube, it was necessary to introduce springs between the plates and the securing nuts. These springs maintained sufficient tension to prevent the gaskets of the plates from separating from the ends of the glass tubing, thus providing leakproof seals.

OVERALL COLUMN DESIGN

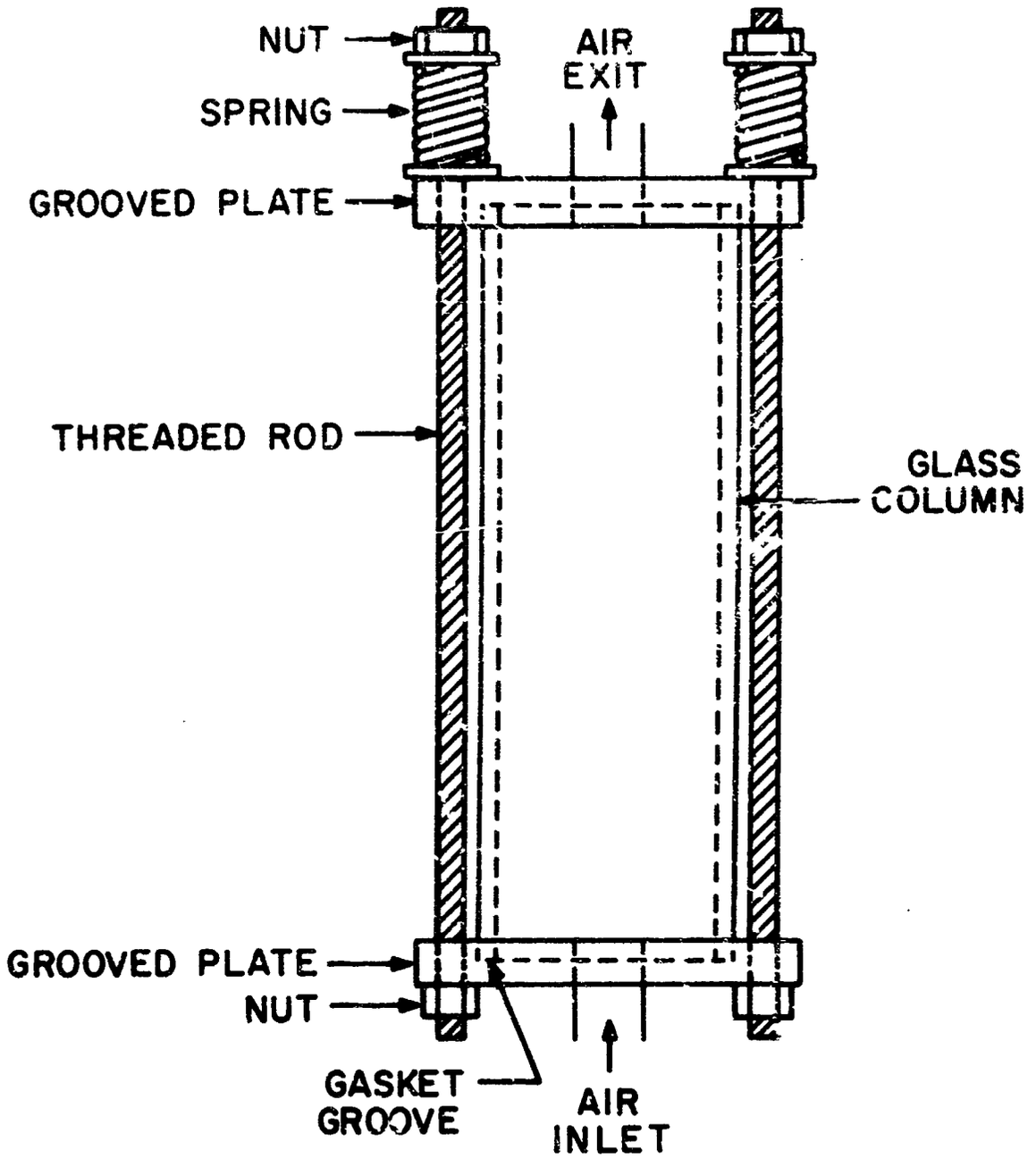

FIGURE 3
PAGE 22

C. Operating Procedures

1. Absorption

Figure 4 is a schematic flow diagram of the entire experimental system. After the resin bed was inserted into the bath, and the connecting joints tightened, it was pretreated by blowing 100% relative humidity, CO_2-free air, at the desired reaction temperature through it until no evolution of CO_2 or liquid was detected. Then it was isolated from the remainder of the equipment by the exit-and entrance-line needle valves. The CO_2 analyzer was recalibrated, with the final calibration point utilizing the same gas composition as the actual run. At the same time, this gas was bubbled through the humidifier column for approximately one-half hour to insure that the deionized water in the column was in equilibrium with this feed gas. The water temperature and bypass ratio also were adjusted to provide the desired feed relative humidity. When all of the above was accomplished and the bath temperature had reached its required value, the reactor bypass was closed and the reactor inlet and exit valves opened. The gas meter reading was taken and the stop-watch and recorders were started. Intermittent readings of bath temperature, cumulative gas flow, and inlet gas relative humidity and temperature were taken. Since every run which was made to complete CO_2 saturation demonstrated a linear concentration versus time dependency over the concluding portion, suitable shorter times were utilized together with linear extrapolation to determine some of the total CO_2 absorption capacities. A run was considered concluded when the exit and inlet carbon dioxide concentrations coincided. [Since the inlet and exit gas flow rates were equal, a CO_2 mass balance shows this criterion for lack of further CO_2 takeup by the resin.] The total time and cumulative

FLOW DIAGRAM OF EXPERIMENTAL SYSTEM

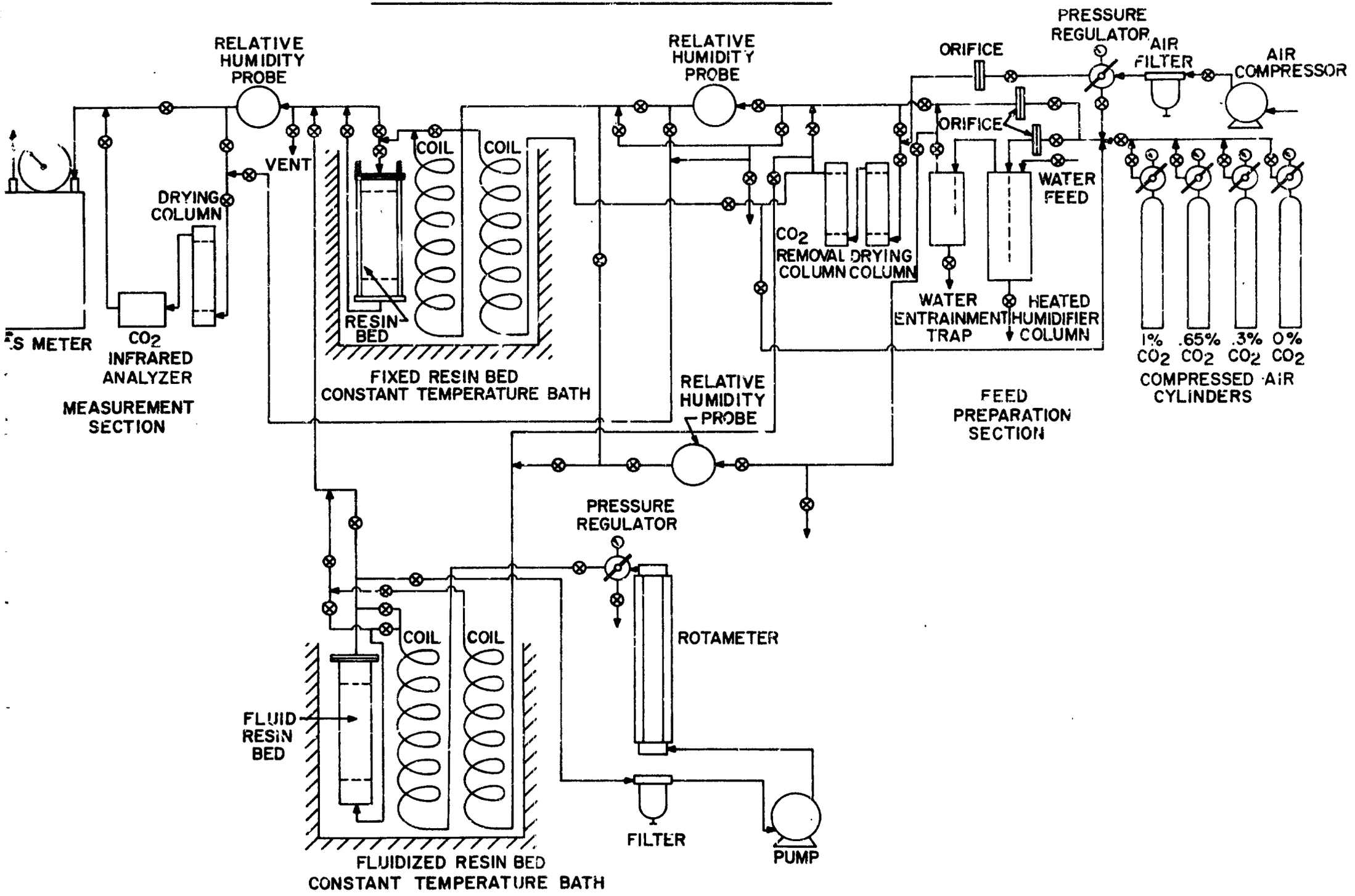

FIGURE 4

volumetric gas flow were noted. The infrared calibration was then checked. Any necessary corrections (always minor, because the drift of this apparatus was small) of concentration readings were made.

2. Regeneration

Since the requirements for absorption included low temperature (increasing the value of the equilibrium constant) and positive concentration gradients from fluid to interface and interface to particle interior, regeneration was effected by setting up conditions favorable to the reverse reaction: no CO_2 in the gas feed, to change the direction of the concentration gradient, and elevated temperature (70°C to 80°C), to decrease the equilibrium constant while increasing the reaction rate. The carbon dioxide was removed from the air supplied by the compressor by Fisher "Indicarb" reagent, a strongly basic solid which indicated through color change when replacement was needed. Regeneration was usually carried out in two steps. The temperature during the first portion was maintained at the same value as that which was used during the absorption run. Thus the rate of the reverse reaction at this temperature was obtained. The amount of carbon dioxide removed was always less than the amount absorbed during absorption. The bath was then heated at least to 70°C, high humidity, CO_2-free gas fed, and most of the remainder of the CO_2 thus removed. Since the resin became somewhat dried out during this high temperature step, the bed was wet down with a KCl solution of pH 11 (cf. RESINS: Treatment Prior to Use) before the next run.

D. Calculation Procedures

The major data obtained directly were potentiometric recorder graphs of output voltage from the CO_2 analyzer of the reactor exit gas stream versus time. These data were converted to output-carbon-dioxide mol percentage-versus-time plots through the analyzer calibration curve. This curve was drawn from the parabolic equation extracted from a curvilinear regression analysis (13) done on the four replicated calibration points (Figure 1). For a constant gas flow rate, the milliequivalents of carbon dioxide transferred per unit mass of resin was equal to

$$(V)\left(\frac{492}{460+T}\right)(1263)\left(\frac{1}{100}\right)(A)/W$$

where:

V = measured volumetric gas flow rate, ft^3/min;

$\frac{492}{460+T}$ = correction to standard conditions, T in ^oF

(Since the gas meter outlet is open to the atmosphere no pressure correction is necessary.);

1263 = number of milliequivalents of CO_2 per standard cubic foot of pure CO_2 (assuming H_2CO_3 is only singly ionized);

$$= \frac{1 \text{ lb. mole}}{359 \text{ s c f}} \times \frac{453.6 \text{ g moles}}{\text{lb. mole}} \times \frac{1 \text{ eq}}{\text{g mole}} \times 1000 \frac{\text{meq}}{\text{eq}}$$

$\frac{1}{100}$ = conversion of mole % to mole fraction

A = area between curve and horizontal feed gas concentration line (concentrations given as mole %)

W = dry weight of resin

This equation can be derived from a differential material balance:

accumulation = material in - material out

$$Wd\left(\frac{\text{accumulation}}{W}\right) = V\left(\frac{492}{460+T}\right)\left(\frac{1263}{100}\right)c_{in}dt - V\left(\frac{492}{460+T}\right)\left(\frac{1263}{100}\right)c_{out}dt$$

$$W \int_0^t \left(\frac{\text{accumulation}}{W} \right) dt = \frac{5737\ V}{460+T} \int_0^t (c_{in} - c_{out})\, dt$$

$$\therefore \frac{\text{accumulation}}{W} = \text{accumulation per unit mass} = \frac{5737\ V}{460+T} (A/W).$$

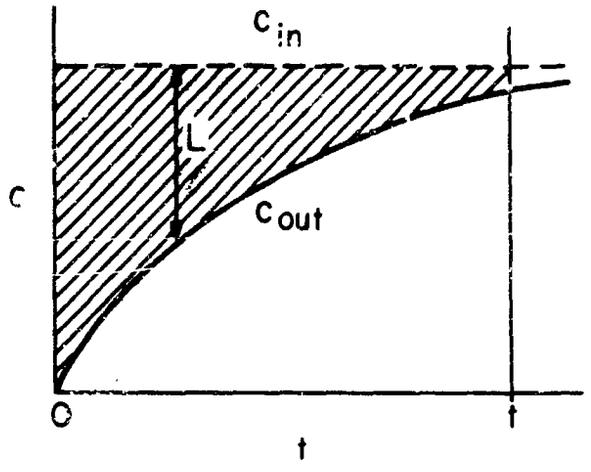

The cross-hatched area is A.

$L = (c_{in} - c_{out})$

The rate of reaction at any time can be determined through the same balance:

rate = moles absorbed per unit time

$$\text{rate} = \frac{W \int_{t_1}^{t_2} d\left(\frac{\text{accumulation}}{W}\right)}{t_2 - t_1} = \frac{\frac{5737\ V}{460+T} \int_{t_1}^{t_2} (c_{in} - c_{out})\, dt}{t_2 - t_1}$$

Since $(t_2 - t_1)$ can be represented as $\int_{t_1}^{t_2} dt$ and $\int_{t_1}^{t_2} (c_{in} - c_{out})\, dt$

by the mean value theorem as $(c_{in} - c_{out})_{avg} \int_{t_1}^{t_2} dt$, we can write:

$$\text{rate} = \frac{\frac{5737\ V}{460+T} (c_{in} - c_{out})_{avg} \int_{t_1}^{t_2} dt}{\int_{t_1}^{t_2} dt}$$

The limit of this expression as $t_2 \rightarrow t_1$ i.e. the instantaneous rate, is

$\left(\frac{5737\ V}{460+T}\right)\left(c_{in} - c_{out}\right)_{instant}$. The magnitude of the rate is then proportional to the distance L in the accompanying figure, i.e

$$\text{rate} = \frac{5737\ VL}{460 + T}\ .$$

Apparently then, the rate is a function of the gas flow rate V. However it was determined experimentally that the rate was independent of V, the reason being the value of c_{out} so adjusts itself that the product $V(c_{in} - c_{out})$ varies only with t. Therefore, in order to make comparison of the results more convenient, all graphs have been drawn on a common-basis volumetric gas flow rate of 0.2 standard cubic feet per minute.

The water capacity of the resin was obtained by vacuum-filtering a water-suspension of the resin, which had been left to soak for several hours with agitation, quickly weighing four small samples of the wet filtrate, and oven-drying them to constant weight. The water capacity is then simply:

$$\frac{\text{Wt. of wet sample} - \text{Wt. of dry sample}}{\text{Wt. of dry sample}} \text{ grams } H_2O/\text{gram dry resin.}$$

IV POSTULATED REACTION MECHANISM

Consider a porous, spherical resin particle, as shown in Figure 5, of radius a, whose interior is completely saturated with liquid and whose exterior is completely surrounded by a very thin film, of thickness δ, of the same liquid. Assume that a gas, one of whose components is soluble in this liquid, surrounds the film. Let P_{GAS} denote the partial pressure of the soluble gaseous component in atmospheres, s the solubility of this component in the liquid in moles per unit volume per atmosphere, R the distribution coefficient defined as the ratio of the concentration in the solid phase to the concentration in the liquid phase, k_G the mass transfer coefficient between the gaseous phase and the film phase in moles per unit surface area per unit time and k_L the mass transfer coefficient between the film phase and the resin phase in moles per unit surface area per unit time. If the gas is not stagnant, but instead flows past the sphere, albeit at a low enough velocity that the film remains undisturbed, then constantly supplying fresh gas should keep P_{GAS} constant. For isothermal conditions k_G, k_L, R, and s, which should be functions of temperature only, will be invariant. The gas phase mass transfer coefficient k_G has associated with it the partial pressure during force $P_{GAS} - P_{INTERFACE}$, the gas at the interface being considered to be in equilibrium with the liquid at the interface. Suppose that the liquid film concentration also varies linearly, and that diffusion from the surface to the inside of the resin particle is very slow. Unsteady state material balances are now made at the two phase boundaries. Calling the molar concentration in the liquid at the gas-liquid interface c_L and the molar concentration in the solid c_R (so that $(c_R)_{r=a}$ is the concentration in the solid at

MULTI-PHASE MODEL AND CONCENTRATION PROFILES

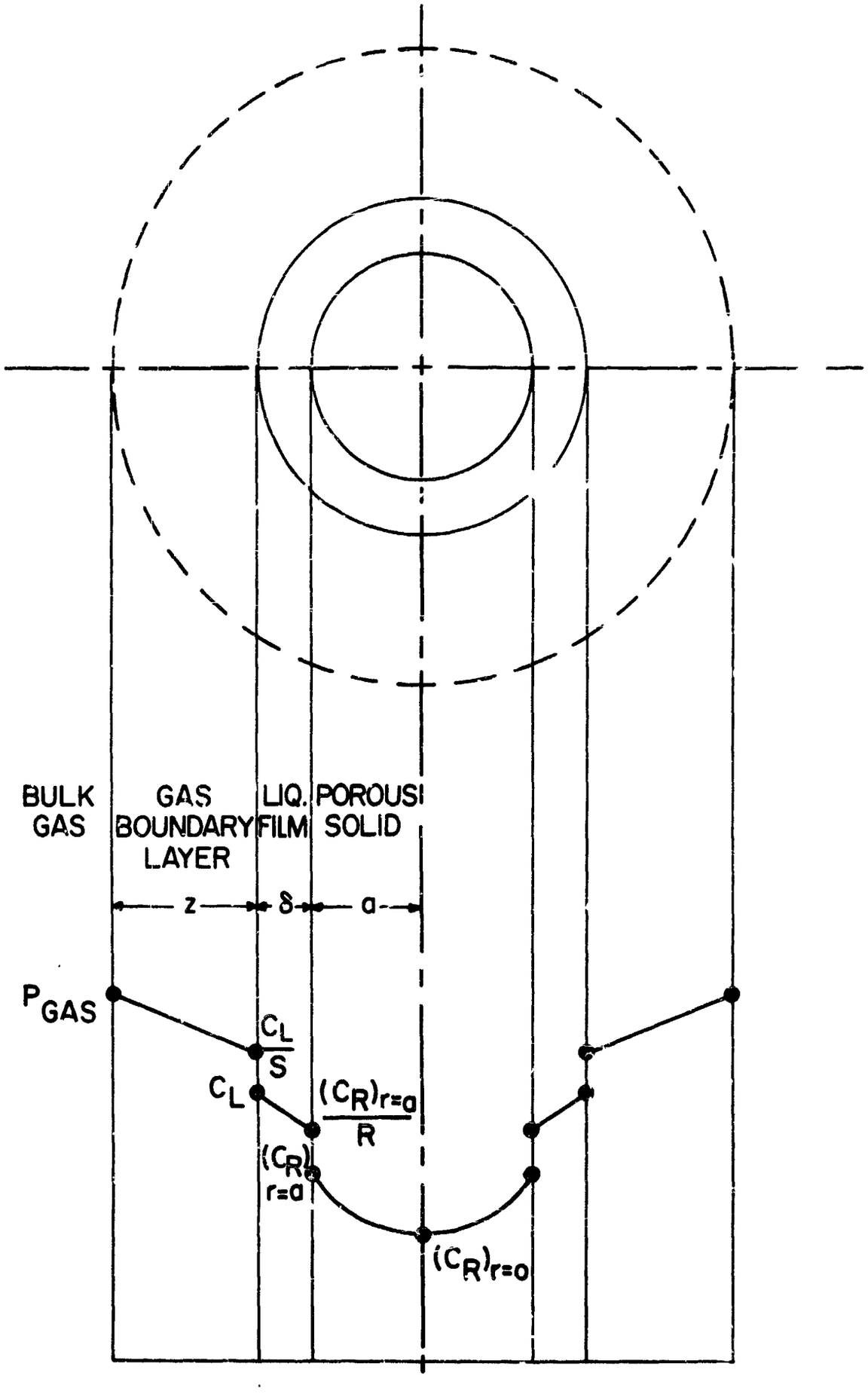

FIGURE 5
PAGE 31

the film-particle interface, assumed to be in equilibrium with the liquid at the interface) we have (see Figure 5):

$$\frac{4}{3}\pi\left[(a+\delta)^3 - a^3\right]\frac{dc_L}{dt} = k_G\left[4\pi(a+\delta)^2\right](P_{GAS}-P_{INTERFACE}) - k_L(4\pi a^2)\left(c_L - \frac{(c_R)_{r=a}}{R}\right) \text{ and,} \quad (1)$$

$$\left(\frac{4}{3}\pi a^3\right)\left(\frac{dc_R}{dt}\right)_{r=a} = k_L(4\pi a^2)\left(c_L - \frac{(c_R)_{r=a}}{R}\right) - D_R\left(\frac{\partial c_R}{\partial r}\right)_{r=a}(4\pi a^2) \quad (2)$$

With $\delta << a$, and $P_{INTERFACE} = \frac{c_L}{s}$, these reduce to:

$$\frac{dc_L}{dt} = \frac{k_G}{\delta}\left(P_{GAS} - \frac{c_L}{s}\right) - \frac{k_L}{\delta}\left(c_L - \frac{(c_R)_{r=a}}{R}\right)$$

$$\frac{d(c_R)_{r=a}}{dt} = \frac{3k_L}{a}\left(c_L - \frac{(c_R)_{r=a}}{R}\right)$$

Differentiating equation 1 with respect to time and substituting first equation 2 for $\frac{d(c_R)_{r=a}}{dt}$ and then again equation 1 for $(c_R)_{r=a}$ yields:

$$\frac{d^2c_L}{dt} + \left(\frac{k_G}{s\delta} + \frac{k_L}{\delta} + \frac{3k_L}{aR}\right)\frac{dc_L}{dt} + \left(\frac{3k_G k_L}{a\delta Rs}\right)c_L = \left(\frac{3k_G k_L}{a\delta R}\right)P_{GAS}$$

The boundary conditions are: $(c_R)_{r=a} = c_I$ and $c_L = \frac{c_I}{R}$ at $t=0$ (i.e. some of the diffusing substance is already present, but there is phase equilibrium). The particular integral is $c_L = s\,P_{GAS}$.

Setting $\left(\frac{k_G}{s\delta} + \frac{k_L}{\delta} + \frac{3k_L}{aR}\right) = 2\xi$ and $\left(\frac{3k_G k_L}{a\delta Rs}\right) = \eta$

The complementary solution is found (14) from the indicial equation: $m^2 + 2\xi m + \eta = 0$, whose two roots are: $m_1 = -\xi + \sqrt{\xi^2 - \eta}$ and

$$-\xi - \sqrt{\xi^2 - \eta} \quad .$$

Then $c_L = A e^{m_1 t} + B e^{m_2 t} + s P_{GAS}$ (4)

which yields $\frac{c_1}{R} = A + B + s P_{GAS}$ from the first boundary condition.

Putting equation 4 into equation 2 and solving by the integrating factor method gives:

$$(c_R)_{r=a} = \frac{3k_L AR}{3k_L + aRm_1} e^{m_1 t} + \frac{3k_L BR}{3k_L + aRm_2} e^{m_2 t} + Rs P_{GAS} \qquad (5)$$

Inserting the second boundary condition and solving for A and B with the previous boundary equation yields:

$$(c_R)_{r=a} - c_1 = \left(\frac{m_2}{m_1 - m_2} e^{m_1 t} - \frac{m_1}{m_1 - m_2} e^{m_2 t} + 1 \right) (Rs P_{GAS} - c_1) \qquad (6)$$

Substituting into equation 6 the values of m_1 and m_2:

$$(c_R)_{r=a} - c_1 = \left[\frac{-\xi - \sqrt{\xi^2 - \eta}}{2\sqrt{\xi^2 - \eta}} e^{-(\xi - \sqrt{\xi^2 - \eta})t} - \frac{-\xi + \sqrt{\xi^2 - \eta}}{2\sqrt{\xi^2 - \eta}} e^{-(\xi + \sqrt{\xi^2 - \eta})t} + 1 \right] (Rs P_{GAS} - c_1). \qquad (7)$$

If $\eta << \xi^2$, which is reasonable for small $\frac{\delta}{a}$ and large R, then

$\frac{-\xi + \sqrt{\xi^2 - \eta}}{2\sqrt{\xi^2 - \eta}} \to 0$ and $e^{-(\xi + \sqrt{\xi^2 - \eta})t}$ damps out very quickly. At the same time $\frac{-\xi - \sqrt{\xi^2 - \eta}}{2\sqrt{\xi^2 - \eta}} \to -1$, and, by application of the binomial expansion to $\xi\sqrt{1 - \frac{\eta}{\xi^2}}$, retaining only the first two terms, finally yields:

$$(c_R)_{r=a} - c_1 = (Rs P_{GAS} - c_1)\left[1 - e^{-\frac{\eta t}{2\xi}}\right] \qquad (8)$$

The final (equilibrium) value of $(c_R)_{r=a} = c_{EQ} = Rs\, P_{GAS}$ which is certainly correct.

Now apply Fick's Law (15) to a sphere whose surface concentration is described by $(c_R)_{r=a} - c_1 = (c_{EQ} - c_1)(1-e^{-\beta t})$ and within which a chemical reaction is taking place which immobilizes the diffusing substance according to the relation $c_{IMMOBIL.} = a\, c_R$:

$$\frac{\partial c_R}{\partial t} = \frac{D}{a+1} \nabla^2 c_R = D' \nabla^2 c_R \qquad (9)$$

where D is the actual diffusivity in the resin phase and $D' = \frac{D}{a+1}$

Rewriting equation 9 in terms of a new variable $u = c_R r$ (assuming no angular concentration dependence):

$$\frac{\partial u}{\partial t} = \frac{D}{a+1} \frac{\partial^2 u}{\partial r^2} \qquad (10)$$

The initial condition is $u = r c_1$ at $t=0$ for all r.

The boundary conditions are: $u - c_1 = a(c_{EQ} - c_1)(1-e^{-\beta t})$ for $t=0$ at $r=a$ and $u = 0$ at $r = 0$ for all t.

Applying Laplace Transform methods to equation 10 yields (16):

$$\frac{c_R - c_1}{c_{EQ} - c_1} = 1 - \frac{a}{r} e^{-\beta t} \frac{\sin\left\{(\beta a^2/D')^{1/2} (r/a)\right\}}{\sin\left\{(\beta a^2/D')^{1/2}\right\}} - \frac{2\beta a^3}{\pi D' r} \sum_{n=1}^{\infty} \frac{(-1)^n \sin \frac{n\pi a}{r} e^{\frac{-D' n^2 \pi^2 t}{a^2}}}{n(n^2\pi^2 - \beta a^2/D')} \qquad (11)$$

Taking $\int_0^t \left(\frac{\partial c_R}{\partial r}\right)_{r=a} dt$ gives:

$$\frac{M_t}{M_\infty} = 1 - \frac{3D'}{\beta a^2} e^{-\beta t}\left[1 - \sqrt{\frac{\beta a^2}{D'}} \cot\sqrt{\frac{\beta a^2}{D'}}\right] + \frac{6\beta a^2}{\pi^2 D'} \sum_{n=1}^{\infty} \frac{\exp(-D' n^2 \pi^2 t/a^2)}{n^2(n^2\pi^2 - \beta a^2/D')} \quad (12)$$

where M_t is the cumulative amount of material which has diffused into the sphere and M_∞ is the final total amount which has diffused in, given by $\frac{4}{3}\pi a^3 (c_{EQ} - c_1)$. M_∞ is equal to the resin capacity only if the initial concentration, c_1, is equal to zero. Figures 70 through 78 of Appendix C show the curves of M_t/M_∞ versus $\sqrt{\frac{D't}{a^2}}$ with $\beta a^2/D'$ as the third parameter. Table 2 lists the Fortran IV computer program which can be used to obtain the results. (The variables have been redefined as follows:

$A = \beta a^2/D'$, $B = (D't/a^2)^{1/2}$, FRAC = M_t/M_∞,

and SIGMA = $\sum_{n=1}^{\infty} \frac{e^{-n^2\pi^2 B^2}}{n^2(n^2\pi^2 - A)}$.)

The rate at which absortion into the particle from the surface is taking place is: $\frac{dM_t}{dt} = M_\infty \frac{d(M_t/M_\infty)}{dt}$

Differentiating equation 12 with respect to time

$$\text{Rate} = M_\infty\left[\frac{3D'}{a^2}\left(1 - \sqrt{\frac{\beta a^2}{D'}} \cot\sqrt{\frac{\beta a^2}{D'}}\right) e^{-\beta t} - 6\beta \sum_{n=1}^{\infty} \frac{\exp(-D' n^2 \pi^2 t/a^2)}{(n^2\pi^2 - \beta a^2/D')}\right] \quad (13)$$

TABLE 2

FORTRAN IV COMPUTER PROGRAM TO OBTAIN M_t/M_∞ AS A FUNCTION OF $\frac{D't}{a^2}$ AT V .RIOUS PRESCRIBED VALUES OF $\beta a^2/D'$

```
      READ (5, 2) K, L
2     FØRMAT (2I4)
      DIMENSIØN A (150, 8), B(150, 8), EN (100), SIGMA (150, 8),
     1FRAC (150, 8)
      CØT(x) = CØS (X)/SIN(X)
      DØ 10 I = 1, K
      DØ 10 J = 1, 8
      SIGMA (I, J) = 0.0
      A (1, J) = 0.0
10    B (I, 1) = 0.0
      DØ 20 I = 2, K
      DØ 20 J = 2, 8
      A (I, J) = A(I-1, J) + 1.0
20    B (I, J) = B (I, J-1) + 0.1
      DØ 30 I = 1, L
30    EN (I) = FLØAT (I) **2
      DØ 50 I = 2, K
      DØ 50 J = 2, 8
      DØ 40 N = 1, L
      AN = -EN (N) *9.869588*B (I, J)**2
      IF (ABS(AN). LE. 88.) EAN = EXP (AN)
      IF (ABS(AN). GT. 88.) EAN = 0.0
40    SIGMA (I, J) = SIGMA (I, J) + EAN/(EN(N)*
     1 (EN(N)*9.869588 - A(I, J)))
      AX = SQRT (A(I, J))
      BB = -A(I, J)* B(I, J)**2
      IF(ABS(BB). LE. 88.) AB = EXP(BB)
      IF(ABS(BB). GT. 88.) AB = 0
50    FRAC (I, J) = 1.0-(3.0*AB/A(I, J) *(1.0 - AX*
     1CØT (AX))+ 6.0 * A(I, J) * SIGMA (I, J)/9.869588
      WRITE (6, 60) ((FRAC (I, J), A(I, J), B(I, J), I = 1, K) J = 1, 8)
60    FØRMAT (3F8.4)
      CALL EXIT
      END
```

Substituting equation 12 into equation 13:

$$\text{Rate} = \beta M_\infty \left[\left(\frac{M_\infty - M_t}{M_\infty} \right) - \frac{6}{\pi^2} \sum_{n=1}^{\infty} \frac{\exp(-D'^2 n^2 \pi^2 t/a^2)}{n^2} \right]$$

However Crank (16) gives as the solution to Fick's Law for a sphere with a constant surface concentration c_{EQ} and an initial uniform concentration c_1 (i.e. for $\beta = \infty$) that:

$$\frac{M_\infty - M_t}{M_\infty} = \frac{6}{\pi^2} \sum_{n=1}^{\infty} \frac{\exp(-D'^2 n^2 \pi^2 t/a^2}{n^2} .$$

It is therefore possible to represent the rate by:

$$\text{Rate} = \beta M_\infty \left[\frac{M_\infty - M_t}{M_\infty} - \left(\frac{M_\infty - M_t}{M_\infty} \right)_{\beta=\infty} \right] \quad \text{or,} \tag{14}$$

by rearranging and equation with the rate equation developed in the "Calculation Procedures" section

$$\text{Rate} = \beta M_\infty \left[\left(\frac{M_t}{M_\infty} \right)_{\beta=\infty} - \frac{M_t}{M_\infty} \right] = \frac{5737V}{460+T} (c_{in} - c_{out})_{\text{instant}} \tag{15}$$

Realizing that both of the M_t/M_∞ terms are complicated functions involving finite series, it would appear that the use of the usual kinetic expressions for reaction rate, involving only temperature-dependent constants and products of concentrations, is not feasible for this type of reaction mechanism.

Now let us examine the experimental results to determine the extent to which this model agrees with them.

V. DISCUSSION OF RESULTS

A. General

1. Equilibrium

The values obtained for the equilibrium carbon dioxide absorption at 100% relative humidity were plotted, at the four different temperature levels, against CO_2 partial pressure (cf. Figures 6, 7, 8 and 9). Since the literature data for dilute polymer solutions (3) indicated that this relationship might well follow a power law through its obedience of the Katchalsky and Spitnik (17) modification of the Henderson-Hasselbach equation (18), the curves were drawn on both linear and logarithmic coordinates. The slopes of the linear correlations and the (log 1) intercepts of the logarithmic correlations were employed to define an equilibrium constant, i.e. $K = (\text{CAPACITY})/P_{CO_2}^{n}$ (Tables 3 and 4). The derived K values were then plotted against 1/T on semi-logarithmic paper and the least-squares lines drawn. (Figures 10 and 11)

Difficulties arise when an attempt is made to attribute the usual thermodynamic significance to this equilibrium constant. It has been established (19) that ion exchange equilibrium constants are really functions of concentration if defined in the same manner as thermodynamic equilibrium constants (meaning selectivity coefficients) i.e. ratio of the activities of the reaction products to the activities of the reactants, each raised to the appropriate stoichiometric power (20). Thermodynamic equilibrium constants show no such concentration dependence. A thermodynamically rigorous ion exchange equilibrium constant must involve additional terms in free solvent concentrations in both the resin and solvent phases which can only be calculated for dilute solutions from

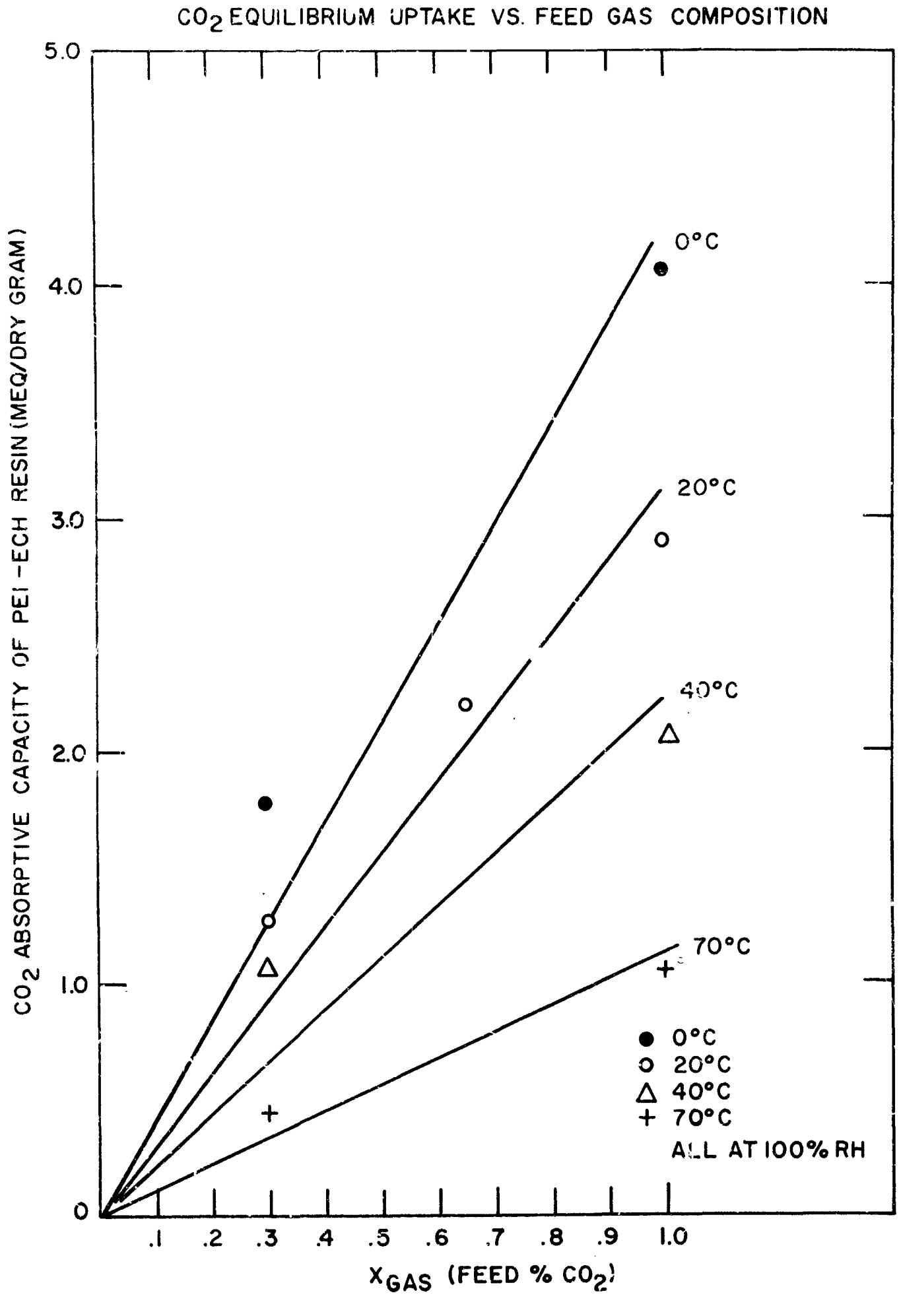

FIGURE 6
PAGE 39

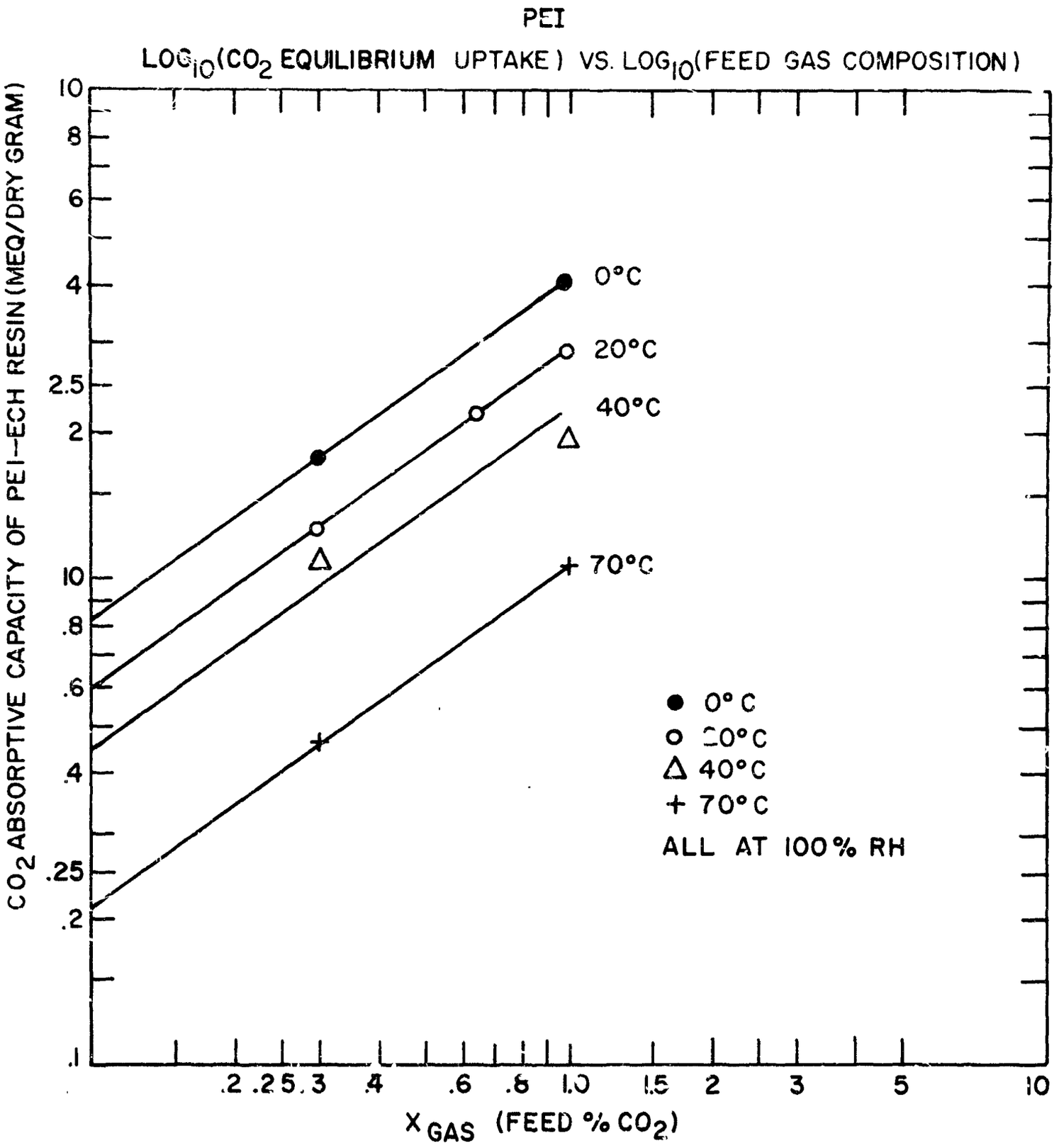

FIGURE 7
PAGE 40

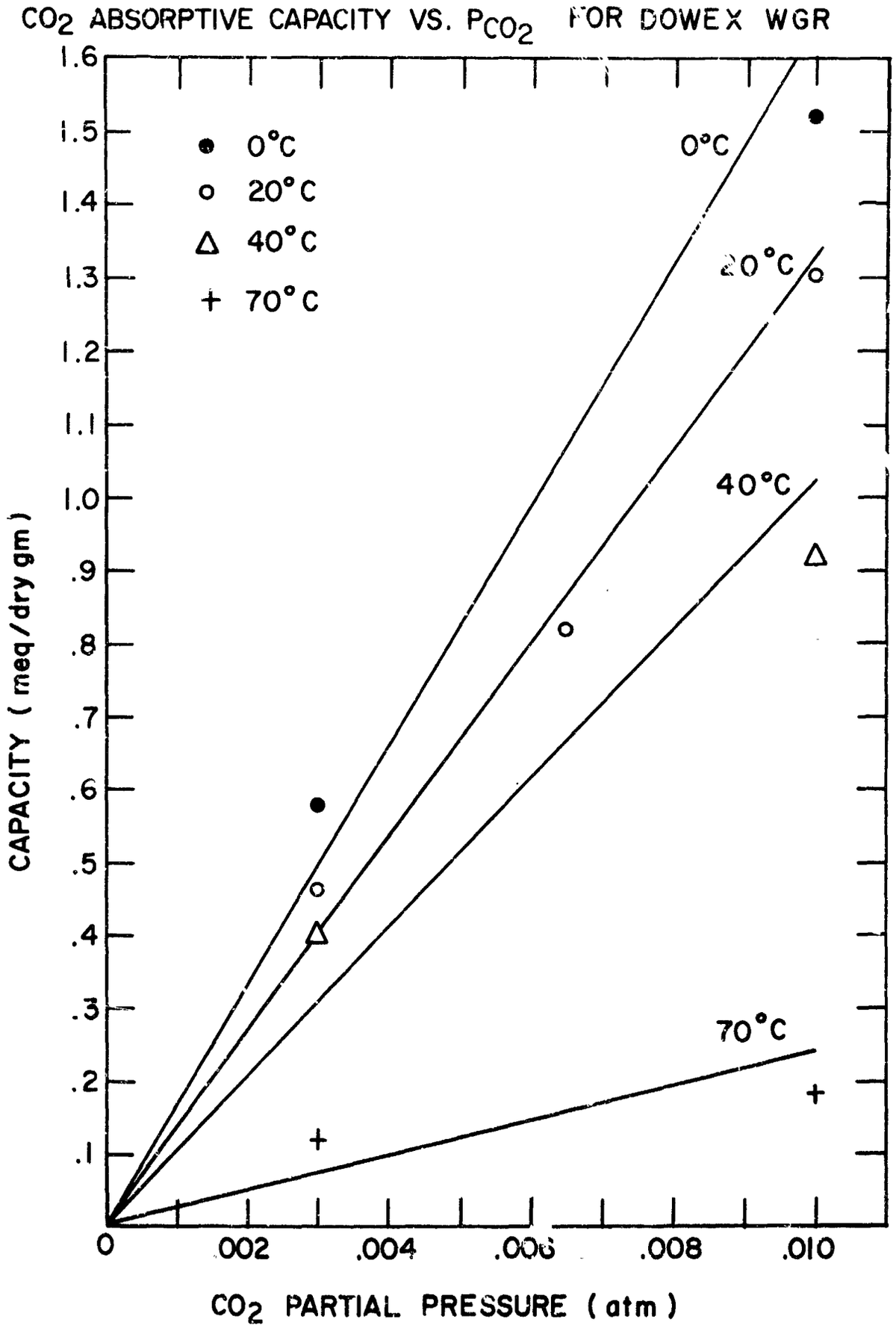

FIGURE 8
PAGE 41

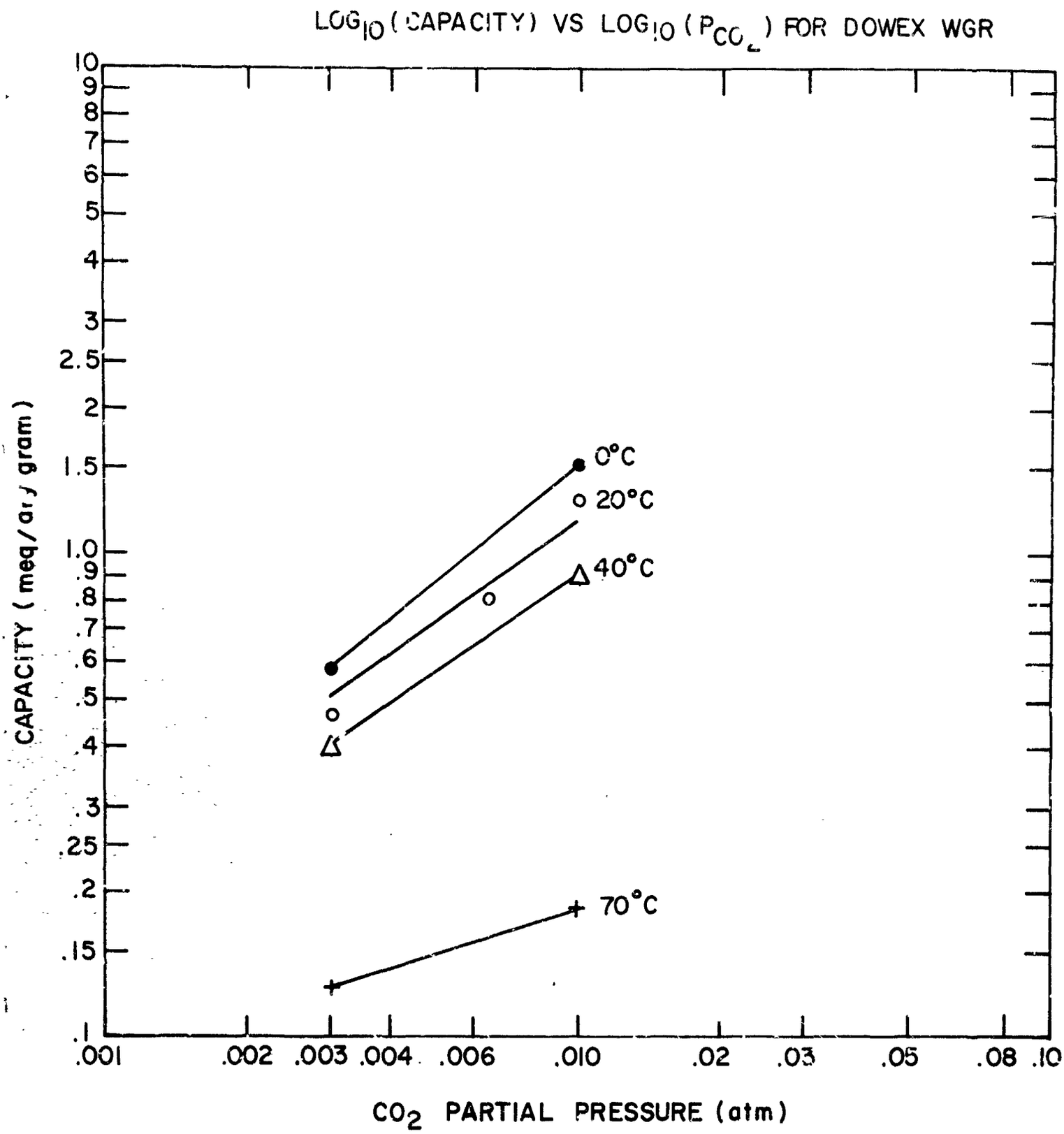

FIGURE 9
PAGE 42

TABLE 3

SUMMARY OF CO_2 EQUILIBRIUM DATA AND CALCULATIONS FOR PEI-ECH RESIN

$$K = \frac{CAP.}{(P_{CO_2})^n}$$

REACTION CONDITIONS			CAPACITY	"EQUIL. CONSTANT",			
			(meq per	n = 1		n = 0.684	
TEMP (°C)	P_{CO_2}(atm)	%RH	dry gr.)	K_{calc}	$K_{l.sq.}$	K_{calc}	$K_{l.sq.}$
0	0.01	100	4.06	406	422	95 0	94.8
0	0.003	100	1.78	594		94.7	
20	0.01	100					
20	0.01	100	2.90	290		67.8	
20	0 01	100					
20	0.0065	100	2.20	348	312	69.0	68.0
20	0.003	100	1.27	424		67.6	
20	0.01	55	1.03	187*		43.7*	
20	0.01	70	1.82	260*		60.8*	
40	0.01	100	2.06	206	219	48.2	49.5
40	0.003	100	1.07	357		56.9	
70	0.01	100	1.06	106	110	24.8	24.6
70	0.003	100	0.45	150		24.0	

*These K values are corrected for the lowered relative humidity. The equilibrium constant should be inversely proportional to the product of the reactant concentrations raised to the stoichiometric powers, and $[H_2O]$ varies directly with %RH. Therefore, the equation employed was:

$$K_{reaction} = (CAPACITY / P_{CO_2}{}^n)\ (100/\%RH).$$

NOTE: Least-square values of K were calculated for the best straight line plot of CAPACITY versus $P_{CO_2}{}^n$ passing through the origin

($K = \sum(CAPACITY)\ (P_{CO_2}{}^n) / \sum(P_{CO_2}{}^{2n})$) (13), since no CO_2 will be absorbed if none is present in the gas stream.

TABLE 4

SUMMARY OF CO_2 EQUILIBRIUM DATA AND CALCULATIONS FOR DOWEX WGR RESIN

REACTION CONDITIONS			CAPACITY (meq per dry gr.)	"EQUIL. CONSTANT", $K = \frac{CAP.}{(P_{CO_2})^n}$			
				n = 1		n = .620	
TEMP (°C)	P_{CO_2} (atm)	%RH		K_{calc}	$K_{l.sq.}$	K_{calc}	$K_{l.sq.}$
0	0.01	100	1.520	152	155	26.5	25.3
0	0.003	100	0.578	193		21.2	
20	0.01	100	1.305	130		22.7	
20	0.01	100					
20	0.0065	100	0.821	126	131	18.7	20.5
20	0.003	100	0.466	155		17.1	
20	0.003	100*	0.394	131		14.3*	
40	0.01	100	0.912	91	95	15.9	15.5
40	0.003	100	0.401	134		14.7	
70	0.01	100	0.185	18	20	3.22	3.46
70	0.003	100	0.126	42		4.61	

* This run was made with 100%RH in the gas feed stream, but the particles were unsaturated initially. This run immediately followed the 70°C regeneration of the 20°C, 0.30% CO_2, 100%RH run. Taking its equilibrium constant as the true value yields an equilibrium relative humidity of 84%.

cf. NOTE accompanying Table 2 for method of calculating least-squares K values.

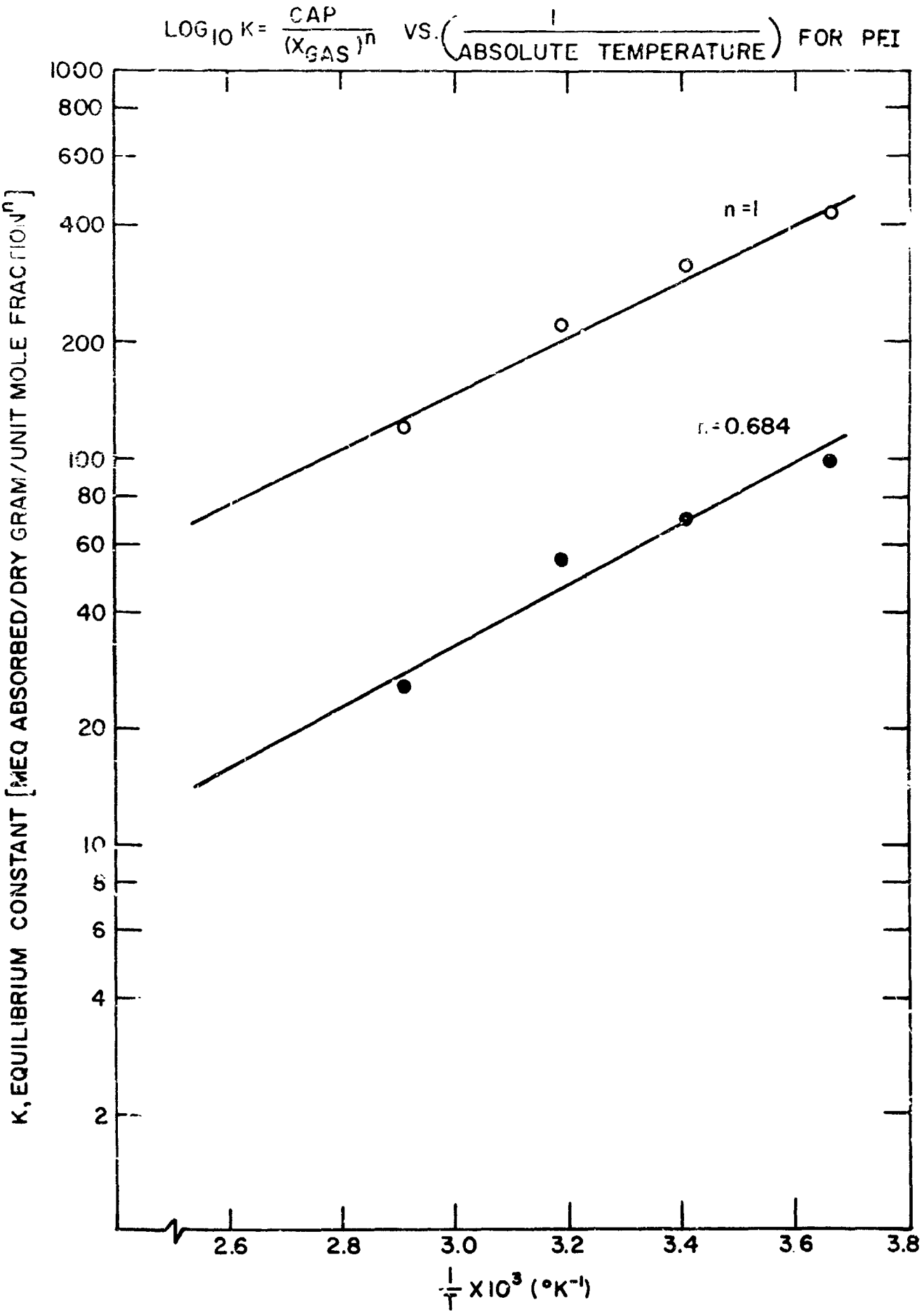

FIGURE 10
PAGE 45

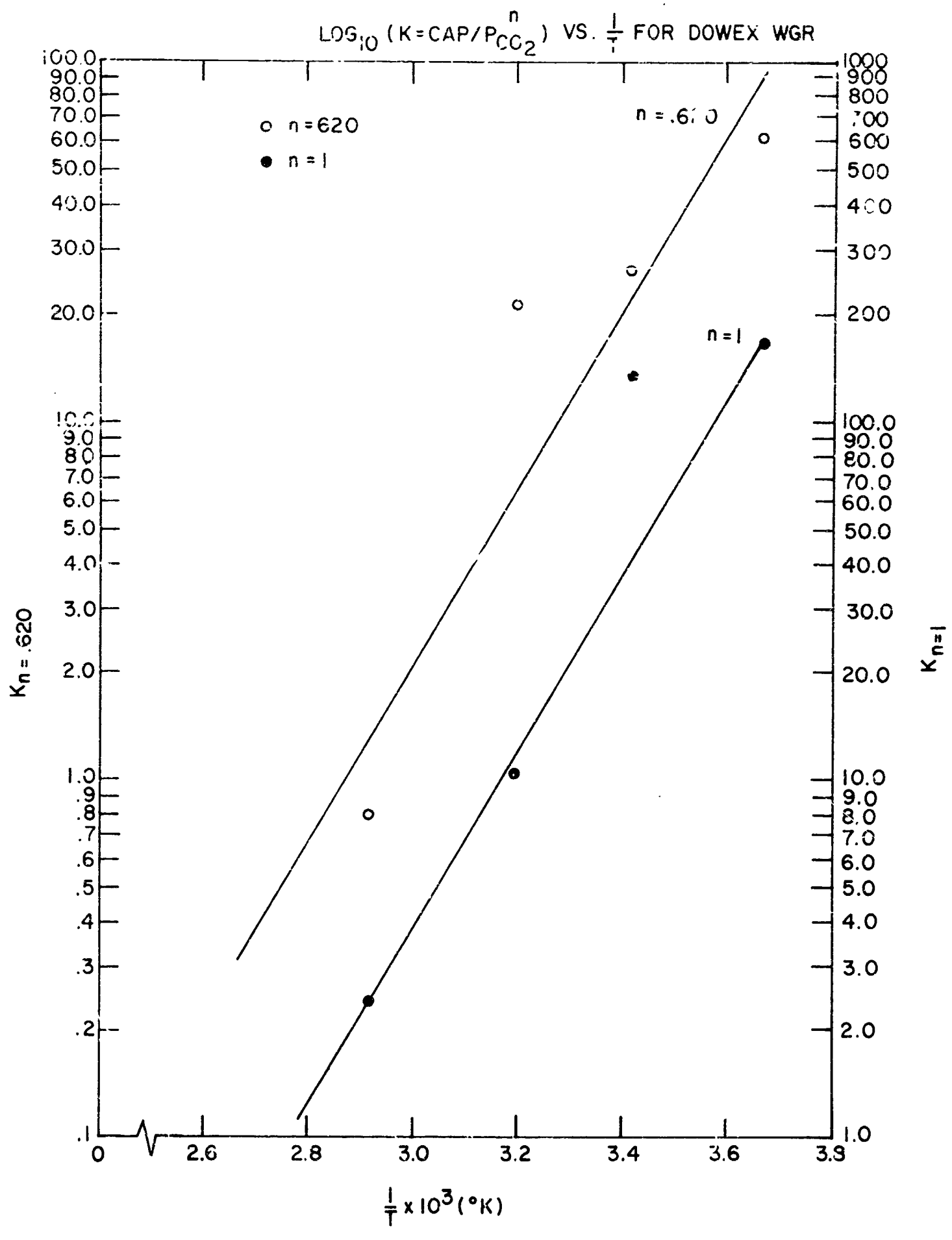

FIGURE 11
PAGE 46

observations of swelling volumes and swelling pressures (21). Therefore, even if a straight line correlation is found for the log K versus 1/T plot, it is not possible to assign the title "Heat of Reaction" to the resultant slope as was done in a previous investigation (3). It would appear necessary to apply calorimetric techniques to determine the actual changes in the thermodynamic state functions which occur during the course of the reaction.

The significance of the constant K as defined in this work rests not only on the excellence with which it describes the data but also on its relationship to the distribution coefficients employed by the mathematical model. Rewriting the capacity and partial pressure terms as concentrations gives:

$$K = f\left(\left[H CO_3^-\right]\right)/\left(\left[CO_2\right]/s\right)^n \qquad (16)$$

(where f is a conversion factor to maintain consistent units and the brackets represent molar concentrations) for it is known that the capacity of the resin (over and above the absorption by the attendant liquid) is entirely in the form of bicarbonate ion (11). Dividing both sides of equation 16 by the quantity $f(P_{CO_2})^{1-n}$ and substituting for P_{CO_2} again yields:

$$\frac{K}{f(P_{CO_2})^{1-n}} = (s)\frac{\left[HCO_3^-\right]}{\left[CO_2\right]} = sR \qquad (17)$$

First it can be seen that K is not the rigorous thermodynamic function since it contains no resin concentration terms. Secondly, a system which involves a series of simultaneous equilibria should be governed by an overall equilibrium constant which is the product of all the individual ones. Two equilibria are involved in the postulated

model:

1. Between the gas and the liquid film, for which the constant is the equilibrium solubility, s
2. Between the liquid film and the resin sphere, for which the constant is the distribution coefficient R.

Then, $K_{reaction} = fsR = K/P_{CO_2}^{1-n} = (CAPACITY/P_{CO_2}^{n})/P_{CO_2}^{1-n}$

so that, since $n \neq 1$, $K_{reaction} = CAPACITY/P_{CO_2}$ which is a function of the carbon dioxide concentration (only the "constant" defined by $CAPACITY/P_{CO_2}^{n}$ is concentration independent).

Values of s are shown in Table 5, as is the Harned and Davis (22) equation from which they were calculated. The R values found from the results with dilute solutions of the linear polymer as discussed in reference 3 are presented in Figure 12. Since the same numbers arise whether the modified Henderson-Hasselbach equation is graphically solved for the ratio of bicarbonate ion to carbon dioxide or the ratio of (Total absorption - water absorption) to water absorption is used, the latter method was applied to our case, as shown in Tables 5 and 6. (That both methods give the same results proves that the resin absorbs only HCO_3^-, and not CO_2.)

TABLE 5

COMPUTATIONS FOR R, THE RATIO OF CARBON DIOXIDE ABSORBED BY PEI-ECH RESIN TO THAT ABSORBED BY THE ASSOCIATED SALT SOLUTION UNDER VARIOUS REACTION CONDITIONS (ALL, HOWEVER, AT 100%RH)

TEMP (°C)	P_{CO_2}(atm)	CAPACITY (total meq)	CAPACITY (total gms)	SOLUBILITY s	SORBED BY H_2O (gms)	R
0	0.01	334.4	14.73	6.187×10^{-2}	4.49×10^{-3}	3283
0	0.003	146.8	6.460	"	1.35×10^{-3}	4790
20	0.01	238.2	10.49	3.266×10^{-2}	2.37×10^{-3}	4432
20	0.0065	181.4	7.985	"	1.54×10^{-3}	5180
20	0.003	104.7	4.605	"	7.09×10^{-4}	6485
40	0.01	170.0	7.437	2.028×10^{-2}	1.47×10^{-3}	5050
40	0.003	88.1	3.875	"	4.41×10^{-4}	8797
70	0.01	86.9	3.824	1.265×10^{-2}	9.06×10^{-4}	4385
70	0.003	37.7	1.659	"	2.75×10^{-4}	6335

NOTES

CAPACITY (total meq) is the total number of milliequivalents of carbon dioxide absorbed by the bed (dry weight of resin = 82.35 gms) at equilibrium.

CAPACITY (total gms) is the above CAPACITY converted by the factor of 44 gms of CO_2 per equivalent of CO_2 (i.e. per 1000 milliequivalents), which assumes that carbonic acid is only singly ionized (26).

SOLUBILITY s (units of moles of CO_2 per 1000 grams of H_2O per atmosphere of CO_2 partial pressure) is obtained from the Harned and Davis (22) equation: $\log s = (2195.84/T) - 12.9875 + 0.013605\ T$ corrected by the multiplier 1.05 for the ratio of solubility in KCl solutions to that in NaCl solutions (22, 3).

SORBED BY WATER (gms) = (2 gms water/gm resin) x (82.35 gms resin) $(s \times 44 P_{CO_2})/1000$.

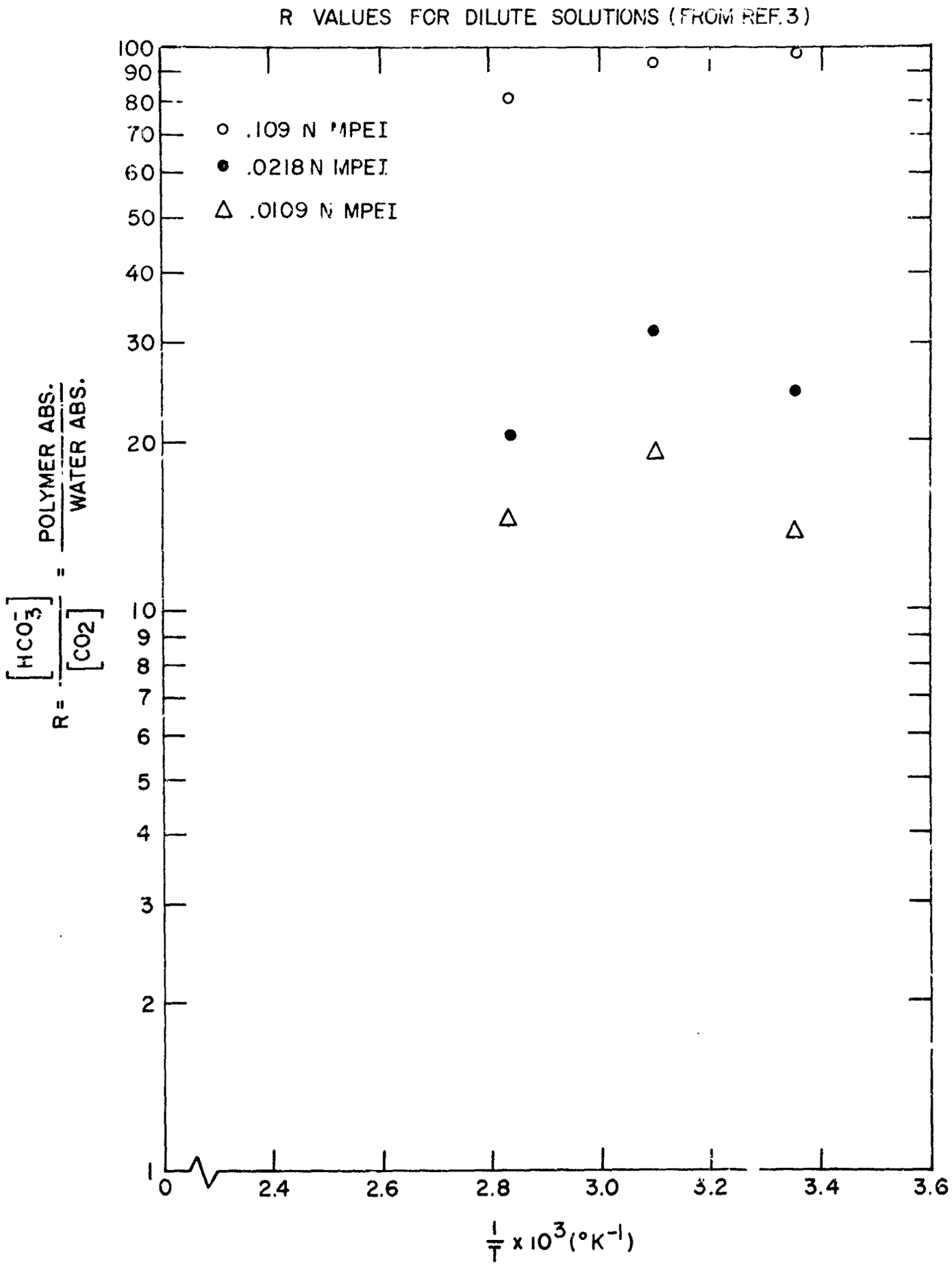

FIGURE 12
PAGE 50

TABLE 6

COMPUTATIONS FOR R, THE RATIO OF CARBON DIOXIDE ABSORBED BY DOWEX WGR RESIN TO THAT ABSORBED BY THE ASSOCIATED WATER UNDER VARIOUS REACTIONS CONDITIONS (ALL, HOWEVER, AT 100%RH)

TEMP (°C)	P_{CO_2}(atm)	CAPACITY (total meq)	CAPACITY (total gms	SOLUBILITY s	SORBED BY H_2O (gms)	R
0	0.01	106.7	4.690	7.705×10^{-2}	2.89×10^{-3}	1623
0	0.003	57.8	2.542	"	8.67×10^{-4}	2931
20	0.01	91.6	4.030	3.840×10^{-2}	1.44×10^{-3}	2798
20	0.0065	57.6	2.535	"	9.37×10^{-4}	2704
20	0.003	32.7	1.439	"	4.32×10^{-4}	3328
40	0.01	64.0	2.816	2.405×10^{-2}	9.03×10^{-4}	3118
40	0.003	28.2	1.241	"	2.71×10^{-4}	4580
70	0.01	12.94	.569	1.359×10^{-2}	5.10×10^{-4}	1117
70	0.003	8.85	.389	"	1.53×10^{-4}	2543

NOTES (viz. TABLE 5)

Dry weight of resin = 70.2 grams.

SOLUBILITY for CO_2 in pure water from Harned and Davis (22) and Perry (31)

SORBED BY WATER (gms) = (1.245) (70.2) (s x 44 P_{CO_2})/1000 = 3.75 x s x P_{CO_2}

2. Reaction Mechanism

Evidence in support of the diffusion model was compiled by first taking successive increments of the concentration versus time curves, integrating to obtain the cumulative mass M_t scrubbed from the gas as a function of time and plotting the ratio of M_t to the equilibrium capacity prevalent at the given reaction conditions against time. A choice of $\beta a^2/D'$ was made and, for at least five widely distant times, $(D't/a^2)^{1/2}$ found at the applicable M_t/M_∞ values using Figures 70 to 78, and $(D'/a^2)^{1/2}$ calculated (cf. Tables 18 through 30 and 34 through 44 of Appendix B). This sequence of steps was iterated until the best agreement among the several $(D'/a^2)^{1/2}$ values was achieved. Of course β was then simply $(\beta a^2/D')(D'/a^2)$.

Semilogarithmic plots of D'/a^2 and $D'(R+1)/a^2 = D/a^2$ against $1/T$ were made (23), the least squares lines drawn, and the diffusion activation energy calculated from the slope $(=E_D/R_oT)$. The β values had to be correlated with the various parameters involved in the surface concentration portion of the model: $\beta = \eta/2\xi$. Returning to the definitions of η and ξ it follows that:

$$\beta = (3k_G k_L/a\delta Rs)/(k_G/s\delta + k_L/\delta + 3k_L/aR) \qquad (18)$$

Combining the second group of terms under one common denominator with the additional stipulation that $3\delta << aR$ because $\delta << \underline{a}$ and $R >> 3$ leads to:

$$\beta = (3k_G k_L)/(k_G aR + k_L aRs) \qquad (19)$$

Upon inverting and rearranging this expression we have:

$$\frac{3}{\beta aR} = \frac{1}{k_L} + \frac{s}{k_G} \qquad (20)$$

so that, upon recognition of the form of the equation, the overall mass transfer coefficient K_L is actually equal to $\beta aR/3$:

$$K_L = \left(\frac{1}{k_L} + \frac{s}{k_G}\right)^{-1} = \beta aR/3; \therefore \beta = (K_L)\left(\frac{1}{R}\right)\left(\frac{3}{a}\right) \qquad (21)$$

The significance of β can now be easily seen —— K_L is the overall mass transfer coefficient between the bulk gas and the liquid-solid interface, R the ratio of the concentration on the solid side of this interface to the concentration on the liquid state of it, and $3/a$ the surface to volume ratio of the particle. In addition, if either the gaseous or the liquid film is "controlling" mass transfer to the solid, then $K_L = k_L$ or $K_L = \frac{k_G}{s}$. Only in the former case, over the small 273 to 343° K temperature range, should K_L obey an exponential 1/T relationship ($k_L = \frac{D_L}{\delta} = \frac{D_L/a}{(\delta/a)}$, (24); $\ln D_L \sim \frac{1}{T}$, (23); $k_G = \frac{D_G P}{R_o T z}$, (24) In the gas-film-controlled case, pressure P is constant at 1 atm and the boundary layer thickness z (25) is virtually temperature independent but the temperature T appears explicitly as well as in D_G. For liquid film control, one can plot $\ln \beta$ versus $1/T$ and expect a straight-line correlation, provided that R also obeys this same form of equation.

3. Effect of Relative Humidity

Most of the experiments took place with water-saturated (actually 1M KCl solution) resin fed with a gas stream of 100% RH at the reaction temperature. Actually the K values given do have an implicit dependence on the amount of water due to the effect of the R ratio:

$$R = \frac{[HCO_3^-]}{[CO_2]} \cdot \frac{\text{moles of } HCO_3^-}{\text{moles of } CO_2} = \frac{\text{moles of } HCO_3^-}{(\text{moles of } H_2O)(s)(P_{CO_2})} \qquad (22)$$

$$K_{reaction} = fsR = f(\text{moles of } HCO_3^-)/(\text{moles of } H_2O \times P_{CO_2})$$

$$\therefore (K_{react.})(\text{moles of } H_2O) = f(\text{moles of } HCO_3^-)/P_{CO_2}$$

This means that the capacity should be proportional to the amount of water present, and therefore to the fraction of water saturation attained, i.e. the equilibrium relative humidity.

A second effect which is encountered, though, makes the observed capacity even lower. The moist particles are obviously heavier, but they also have a tendency to agglomerate. With the given column design, channeling in the water-saturated state is negligible. Drying the particles out makes them lighter and more individual, and it is then not very difficult for the gas to select a preferred path through the bed. Likewise, this channeling should become more severe, and the observed capacity consequently lower, the lower the relative humidity.

The dryness of the material also seriously effects the rate of reaction and the adherence to the proposed absorption diffusion model. The liquid film surrourding the particle sphere is obviously the first water which is removed by drier air. Then the derived mechanism ought no longer to hold.

4. Decay of Resin Capacity

It was expected that the CO_2 absorptive capacity exhibited by the freshly packed column in run number one would decline with the succeeding runs for two reasons. First, the resin was usually not completely regenerated. Because the particle diffusion was controlling, the absorption-regeneration cycle was usually quite time-consuming. When regeneration with hot CO_2-free air was nearly complete, linear extrapolation was relied upon to give the final value for the meq per gram removed so that the time

required to remove the final 5% or so remaining could be saved. Secondly, the drying out of the resin during the regeneration process due to lack of ability to maintain 100% RH air at 80°C combined with the high pH of the resin made for conditions favorable to carbamate formation (25), which happens by a highly irreversible reaction. It was not feasible to further regenerate the material with strong base. The one molar KOH solution would have had to be completely washed away as in the steps preceding the column packing (cf. Treatment Prior to Use), which could not be done with the column still tightly packed. It is assumed that the pH 11 1M KCl solution added after each run to resaturate with liquid easily had its hydroxide content (for the size column used and an estimated voidage for spheres of .39, only a total of .123 meq of OH^- ion was introduced each time) quickly and completely exhausted by the CO_2 still present within the particles. This CO_2 was probably what was observed to be driven off during the preliminary purging with CO_2-free air that preceded each run.

Since it was also not feasible to regenerate further the next day with hot CO_2-free air because the bed would again have had to be wet down with KCl solution for several hours prior to the beginning of the next run, an attempt was made to correlate the loss of capacity with the number of regenerations which the resin had undergone. It was thus necessary to repeat the standard (20°C, 1.00% CO_2, 100% RH) absorption at one or two other places during the set of experiments. The results of these runs were then compared to number one, which had employed the fresh material, and the appropriate resultant correlated (with run number) correction factor applied to each individual run. The capacities obtained in this fashion are those presented as the true values. It must also be pointed out

that the curves for fractional mass uptake (M_t / M_∞) are not affected by the initial presence of CO_2 within the sphere. As shown during the derivation of the equations for the mathematical model, M_t and M_∞ are defined as the amounts of diffusing substance which have entered the particle during the run, which are the actual quantities measured and employed.

An additional difficulty was introduced into our system by the presence of brass plates as section dividers and end pieces for the column. These metal discs were initially all coated with epoxy to prevent exposure of their surfaces. However the temperature cycles involved in each run because of the regeneration process broke the bonds between the epoxy and the metal surfaces by virtue of the difference in thermal expansion coefficients of the two materials. The resin was always allowed to soak overnight while remaining in the column because packing it was such a tedious and time-consuming task. The basicity of the regenerating solution was then responsible for the solution of some of the copper from the brass alloy. Since these resins are both ammoniacal and basic to begin with, it seems only logical that they should form copper complexes (12). These complexes are obviously not formed with the CH_2 groups but with the NH^+OH^- groups which represent the only sites which could be reactive toward HCO_3^- ions. The absorptive capacity is thus reduced.

B. Polyethylenimine-Epichlorohydrin Resin

1. Equilibrium

Figures 24 through 31 of Appendix C show how the reactor outlet gas composition varies with time under different reaction conditions of temperature, CO_2 partial pressure, and percentage relative humidity. These curves all have the same general shape, with a rapid rise at the beginning and an asymptotic approach to equilibrium. The equilibrium constants derived from these data, after correction for loss of capacity with time (cf. Decay of Resin Capacity), are given in Table 3 and Figures 6 and 7 as CAPACITY/ $P_{CO_2}^n$. Calculations were made on the usual basis of n=1, for which the equation $K_{reaction} = fsR$ is applicable, and on the basis that n equals its best value (the one which makes K independent of concentration) which, for this material, is seen from the slopes of the logarithmic plots to be 0.684.

For comparison, the data of Robins (3) for dilute solutions of the polymer methyl polyethylenimine (MPEI) in water containing various concentrations of KCl are given in Table 7 for two partial pressures of carbon dioxide. These data show that the capacity decreases with increasing resin concentration to a marked extent, so that the approximately 5N "solution" which our water-saturated solid might be considered to be should exhibit capacities such as we found. (The resin was seen to have a water capacity of 2.0 grams per gram, cf. Appendix B, Table 45.) Note that there is only a minor weight correction term involved, since MPEI exhibits an equivalent weight of 2 x 57 or 114 while a solid of 4.2 PEI monomer units to one ECH molecule exhibits an equivalent weight of $2 \times (43 \times 4.2) + 92.5)/5.2$ or 105.1. These data also show capacity proportional to about the two-tenths power of the carbon dioxide partial pressure whereas ours have an almost seven-tenths power relationship.

TABLE 7

CO_2 ABSORPTIVE CAPACITY OF MPEI BASE (FROM REFERENCE 3)

[MPEI BASE]	[KCl]	MEQ OF CO_2/DRY GRAM OF RESIN					
		P_{CO_2} = .03 atm			P_{CO_2} = .003 atm		
		25°C	50°C	80°C	25°C	50°C	80°C
.109N	0	3.58	2.58	1.33	1.91	1.14	0.54
.0218N	0	4.43	3.36	1.82	2.18	1.63	0.57
.0109N	0	4.90	3.74	2.12	3.06	2.12	1.20
.109N	0.1N	4.30	3.06	1.51	2.04	1.26	0.48
.109N	1.0N	5.44	3.90	2.13	3.04	1.84	0.65
.0218N	1.0N	6.64	5.60	3.62	4.63	2.96	1.61

But again, the value of this exponent is seen to increase with the polymer's concentration quite markedly (n=.155 for .0218N solution and n=.252 for .109N solution, both one molar in KCl). Since n increases by 66% for a fivefold concentration rise, it is quite possible that our "solution", being still fifty times stronger, could exhibit a value of n as large as .7. Again the differences in the systems must be emphasized.

The calculated equilibrium constants for both values of n were plotted on semilogarithmic coordinates against 1/T and two reasonably straight lines produced (Figure 10). That the 70°C points in both instances seemed to drop is probably another reflection of the peculiar behavior demonstrated by the R factor (cf. next two paragraphs) at elevated temperatures. The slopes of the two plots were almost identical, namely $3480/2.303R_o$ and $3616/2.303R_o$. One might be tempted to say that the heat of reaction is then about 3550 calories per gram mole of CO_2 absorbed. Robins' application of this procedure gave a value which varied with resin and salt concentrations from 8000 to 15000 calories per gram mole. Since Helffe·ich (19) states that the heat of reaction associated with ion exchange is normally about 2000 calories per gram mole, but that it does occasionally reach 10000, it might be said that either source's value could be correct, but they surely could not both be correct. In all likelihood, as stated in the general discussion, neither is correct because in ion exchange, the "equilibrium constants" that do not vary with concentration do not conform to thermodynamic definitions.

Remembering that our concentration dependent K was equivalent to a series of simultaneous equilibria represented by the product $f_s R$, and realizing the closeness of the two slopes obtained, it is quite likely

that the 3550 value is the sum of the heat of solution of CO_2 in water, which is 1130 calories per gram mole at $27^{\circ}C$ (26) and the heat of reaction, which would then be 2420. But this would not be ion exchange, and subtracting the 1010 calories per mole associated with the first ionization of carbonic acid gets the heat of reaction down to 1410, which is not unreasonable. The semilogarithmic plots of s and R versus 1/T unfortunately do not bear this out, the slope of the s line being $4210/2.303R_o$ and of the R line (an average for the two concentration-dependent lines) being $-910/2.303R_o$. As a whole, the best equilibrium correlation is: $\text{CAPACITY} = .0715\,(P_{CO_2})^{.684}\,(\frac{\%KH}{100})\,e^{\frac{-3616}{R_oT}}$

An important assumption must now be introduced. Originally R was defined as the distribution coefficient between the solid and liquid phases. In the derivation of the equation for spherical diffusion with chemical reaction there was introduced the stipulation that the concentration of the solute which had been immobilized through the reaction was directly proportional to the concentration of the diffusing solute. The proportionally constant we called α. Since we know from Robins (3) that the absorption by the resin is entirely in the form of the bicarbonate ion, and that, by virtue of its preponderance over all other species, CO_2 is the diffusing form, α is seen to be $[HCO_3^-]/[CO_2]$. But the diffusion that is taking place is not into something which is just solid, but rather into the liquid trapped in the pores of the solid. The data of Robins (3) show that, since the absorbed forms are completely different from each other, α can also be calculated as the ratio of polymer absorption to water absorption, which can be rewritten as (total absorption minus water absorption)/(water absorption). But this last expression is the definition of R, so that R must be equal to α.

The data presented in Table 8 show that the value of R should increase with increasing polymer concentration and increasing salt content, so that the order of magnitude for our system ought to be something like $1x10^3$ to $1x10^4$. Our calculated values of R appear in Table 5, and they range from about $3x10^3$ to $9x10^3$. R should show no relationship with CO_2 partial pressure. For Robins this is emphatically not so; he shows R proportional to $P_{CO_2}^{-0.7}$. For our system the dependence is to the minus 0.316 power throughout. This is unfortunate from the standpoint that constancy of R is required for the derivation of both major equations of the mathematical model. However, as discussed in the "Validity of Assumptions" section, the dependence is minor and is greatly aided by the relative constancy of the entire reactor gas profile after a very short fraction of the total equilibrium time has elapsed. R seems also to have some of the peculiar temperature dependency evinced by Robins' data, i.e. there seems to be the usual simple exponential of 1/T variation at the lower temperatures, but above 60^oC seems to take a noticeable drop. For correlation purposes, we have ignored this final dip and applied a least squares line to the exponential form of the equation over the entire temperature range employed (Figure 13).

TABLE 8

R, THE RATIO OF CO_2 ABSORBED BY MPEI TO THAT ABSORBED BY THE WATER IN THE SOLUTION (FROM REFERENCE 3)

[MPEI BASE]	[KCl]	TEMP ($^{\circ}C$)	P_{CO_2} (atm)	R
.109N	0	25	.01	97.0
.109N	0	50	.01	94.5
.109N	0	80	.01	81.9
.0218N	0	25	.01	24.6
.0218N	0	50	.01	31.4
.0218N	0	80	.01	20.4
.0109N	0	25	.01	13.8
.0109N	0	50	.01	19.1
.0109N	0	80	.01	15.0
.109N	0	25	.03	42.5
.109N	0	25	.003	227.2
.0109N	0	25	.003	32.3
.109N	1N	25	.01	174.2
.0218N	1N	25	.01	49.6

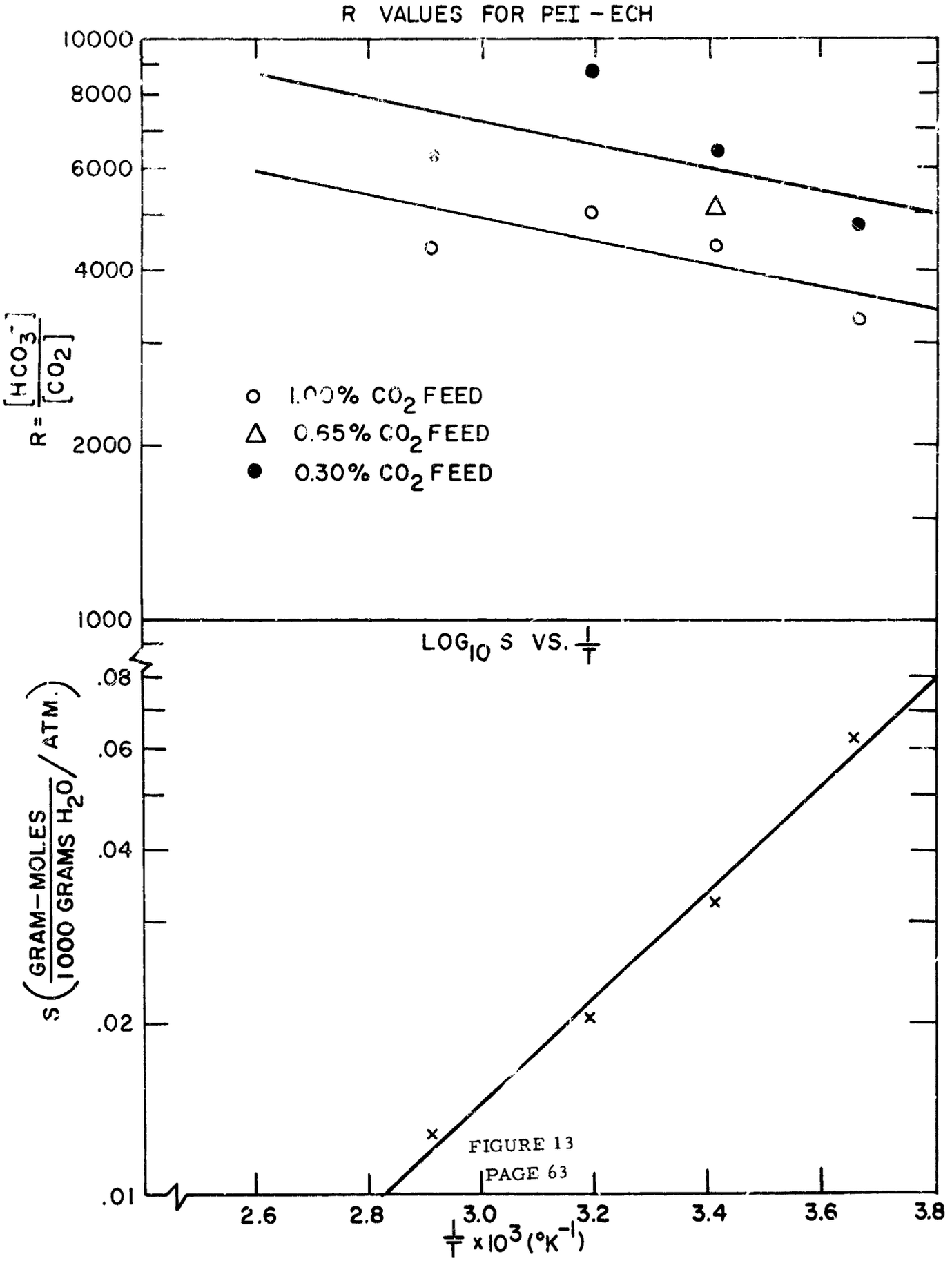
R VALUES FOR PEI – ECH
10000
8000
6000
4000
2000
1000
R = [HCO3-] / [CO2]
1.00% CO2 FEED
0.65% CO2 FEED
0.30% CO2 FEED
LOG10 S VS. 1/T
.08
.06
.04
.02
.01
S (GRAM-MOLES / 1000 GRAMS H2O / ATM.)
2.6
2.8
3.0
3.2
3.4
3.6
3.8
1/T x 10^3 (°K^-1)

FIGURE 13

2. Reaction Mechanism

Figures 32 through 36 of Appendix C show the fractional uptake curves and Tables 18 through 30 in Appendix B show the calculations involved in determining the best values of β and D'/a^2 for the diffusion model. It is immediately noticeable that the parameter $(D'/a^2)^{1/2}$ is relatively insensitive to shifts in $\beta a^2/D'$. This occurs by virtue of the fact that the term $D't/a^2$ occurs in only one place in the mass uptake equation, as part of a rapidly deteriorating exponential, whereas the $\beta a^2/D'$ parameter appears five times. The excess of scatter of the β data over the diffusivity data is attributible to this difference in sensitivity. The excellent agreement among the $(D'/a^2)^{1/2}$ values across the entire time coordinate is however indicative of the applicability of this model. Table 9 and Figures 14 and 15 show the relative lack of dependence of the effective (D') and real (D=D' (R+1)) diffusivities on concentration and the good semilogarithmic $1/T$ relationships From the slope of the "real" line an activation energy for diffusion of 8610 calories per mole was calculated. This is well within the customary limits described in the literature (23) of 2400 to 10000 calories per gram mole. Both obey the same sort of correlation because R+1, which for all practical purposes equals R, pretty well exhibits the same sort of exponential temperature variation.

As was discussed during the derivation of the equations for the mathematical model, β could be easily correlated only if the liquid film controlled the flux of carbon dioxide to the particle surface. If the liquid film controls, one would plot $\ln(\beta R)$ versus $1/T$, since $3/\beta aR$ would equal $1/k_L = \delta/D_L$.

If the gaseous film controls, we would have $3/\beta aR = s/k_G = szTR_o/D_G$.

TABLE 9

VARIABLES WHOSE TEMPERATURE DEPENDENCE CAN BE DESCRIBED BY AN EXPONENTIAL EQUATION OF THE FORM:

$y = (\text{constant}) \times (\exp(\pm E/R_o T))$ FOR PEI-ECH RESIN

T(°C)	P_{CO_2} (atm)	R	D'/a^2 (min)$^{-1}$	β (min)$^{-1}$	D/a^2 (min)$^{-1}$	βR	sx10^{-}
273	0.01	3283	0.846×10^{-4}	0.846×10^{-2}	0.278	27.79	6.187
273	0.003 (FIRST)	4790	1.237×10^{-4}	1.546×10^{-2}	0.593	74.05	6.187
293	0.01 (SECOND)	4432	3.011×10^{-4}	1.807×10^{-2}	1.336	80.30	3.266
293	0.01 (THIRD)	4432	4.220×10^{-4}	2.531×10^{-2}	1.872	50.70	3.266
293	0.01	4432	2.903×10^{-4}	2.033×10^{-2}	1.288	90.30	3.266
293	0.0065	5180	2.340×10^{-4}	2.573×10^{-2}	1.212	133.2	3.266
293	0.003	6485	3.313×10^{-4}	1.657×10^{-2}	2.14	107.4	3.266
313	0.01	5050	$8.[illegible] \times 10^{-4}$	4.083×10^{-2}	4.0[illegible]	206.2	2.028
313	0.003	8797	6.440×10^{-4}	2.515×10^{-2}	[illegible]55	221.3	2.028
343	0.01	4385	2.046×10^{-3}	9.840×10^{-2}	5.983	431.2	1.265
343	0.003	6335	1.816×10^{-3}	5.810×10^{-2}	11.50	368.0	1.265

NOTE: $D/a^2 = (D'/a^2) \cdot (R+1)$

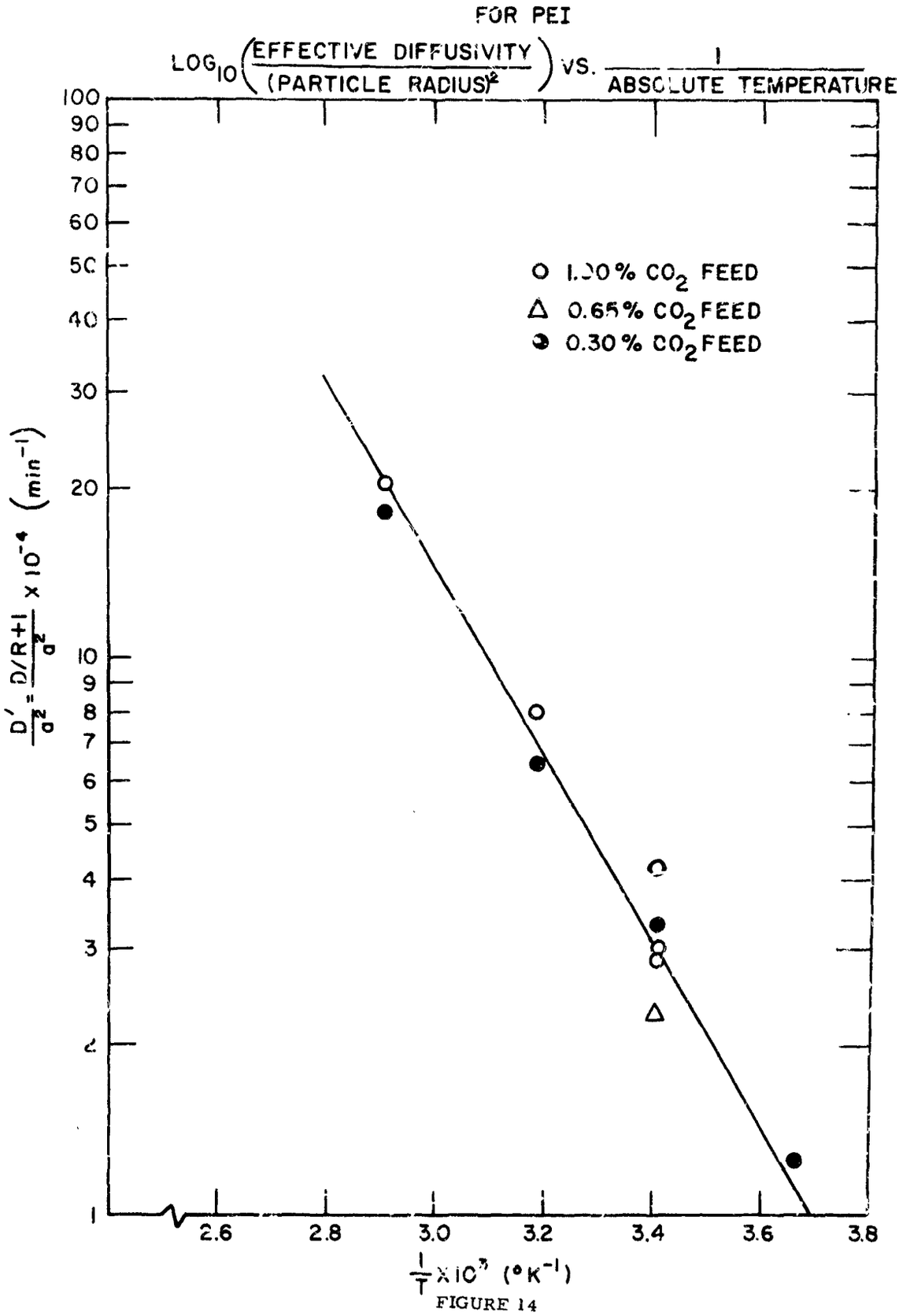
FOR PEI
LOG10 (EFFECTIVE DIFFUSIVITY / (PARTICLE RADIUS)²) VS. 1 / ABSOLUTE TEMPERATURE
O 1.00% CO2 FEED
Δ 0.65% CO2 FEED
● 0.30% CO2 FEED
D'/a² = D/R+1/a² x 10⁻⁴ (min⁻¹)
1/T X 10³ (°K⁻¹)
100
90
80
70
60
50
40
30
20
10
9
8
7
6
5
4
3
2
1
2.6
2.8
3.0
3.2
3.4
3.6
3.8

FIGURE 14

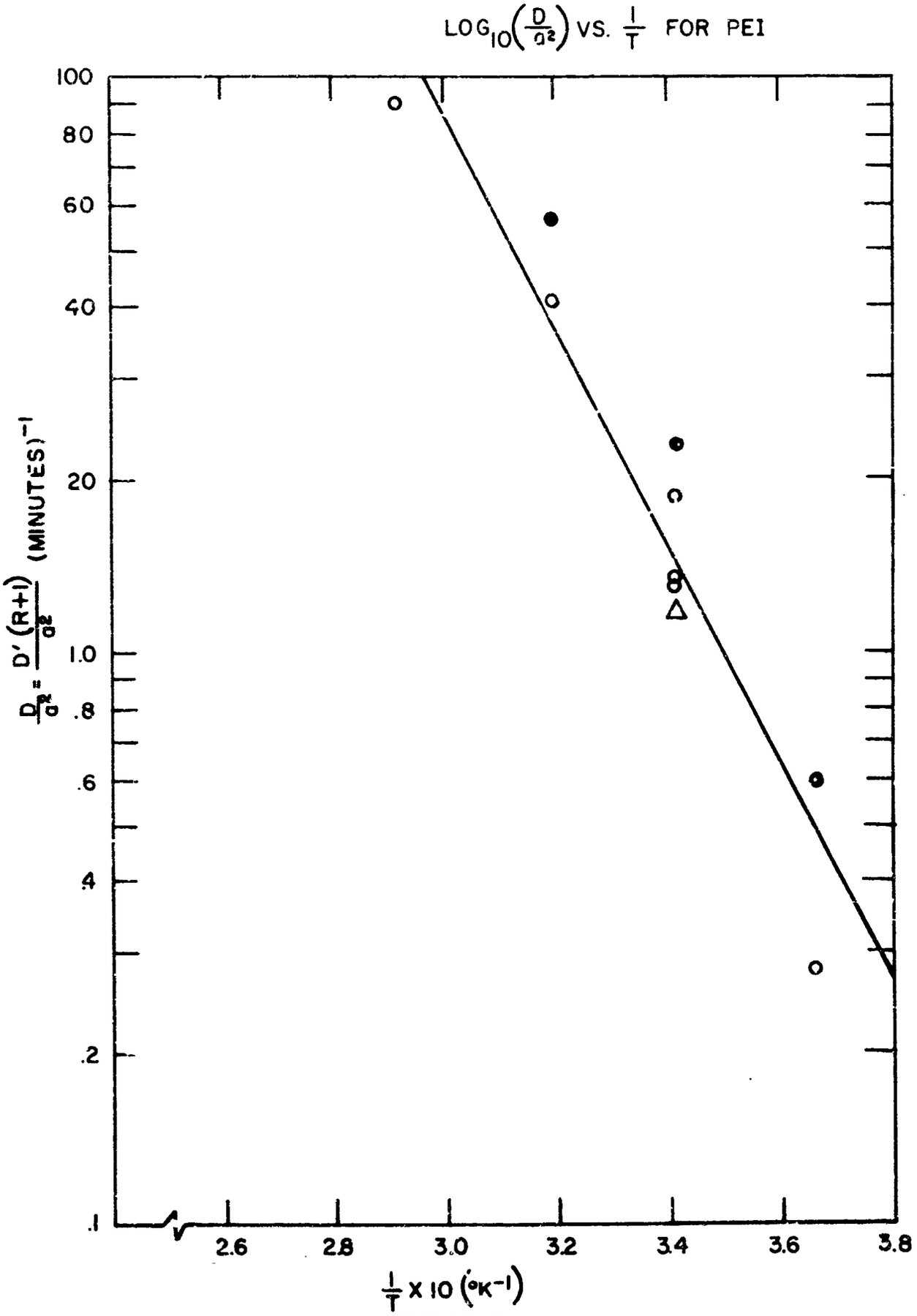
LOG10(D/a²) VS. 1/T FOR PEI
100
80
60
40
20
1.0
.8
.6
.4
.2
.1
D/a² = D'(R+1)/a² (MINUTES)⁻¹
2.6
2.8
3.0
3.2
3.4
3.6
3.8
1/T X 10 (°K⁻¹)

FIGURE 15

The boundary layer thickness z can be approximated by the Blasius solutions to the Navier-Stokes equations (15) given by Schlichting (25). It is found that $z = \phi a$, where ϕ is a function of the angle between the desired location and the forward stagnation point, and z is a minor function of temperature due to its dependence on the square root of the Reynolds number. For air flow past uniform spheres in a bed of 39% voids at a flow rate of .2 standard cubic feet per minute, at 20° C the Reynolds number is 30.6. The value of ϕ then ranges from .307 at the forward stagnation point to .562 at the points of separation (which almost surely do not exist here because the next layer of particles would bend the gas stream back) at angles of 109.6° to the direction of the flow. The gas constant R_o and the radius a are independent of temperature, and s presumably follows an exponential $1/T$ relationship. However, the T/D_G term follows only a complex semi-empirical temperature dependence (15). The only plotting method available would be to graph $(\beta R s z)$ versus D_G/T. An approximate calculation was made for 20°C to determine whether a simplified plot could be made. Taking the value of D_L for pure water (instead of 1M KCl) from Sherwood and Pigford (23) as 1.77×10^{-5} cm^2/sec and D_G for CO_2 in pure air (dry) as .1382 cm^2/sec from the same source and the average value (of the five) of $60/\beta R$ (converting to units of seconds) as .719, we have:

$$.719 = 9.20\,(\delta/a) + 9.25 \times 10^{-4}(\phi) \qquad (23)$$

We have seen that ϕ is at most about 0.5, so that the first term clearly predominates. As a matter of fact, we can now estimate the value of δ/a from equation 23 by ignoring the last term entirely. Thus $\delta/a = 0.078$. The actual value is somewhat smaller by virtue of the diffusivity of CO_2 in a 1M KCl solution being less than in pure water.

It is now possible to plot βR versus $1/T$ on semilogarithmic coordinates and expect a straight line correlation. Table 9 and Figure 16 show this to be the case. In addition, Table 9 summarizes the calculated values of all the temperature dependent variables, and the equations of all the resultant least-squares correlations appear in Table 10.

The final test of any correlation, though, must be the accuracy of with which it predicts the experimental results. Therefore, starting only with the correlated values of all the variables, the curves of M_t/M_∞ and exit CO_2 concentration Table 11 were drawn for the standard 20°C, 1% CO_2, 100%R.H runs from equations 12 and 15 on the same pages (Figures 25 to 27 and 32 to 34 of Appendix C) as the originals representing the actual data. The results are gratifying.

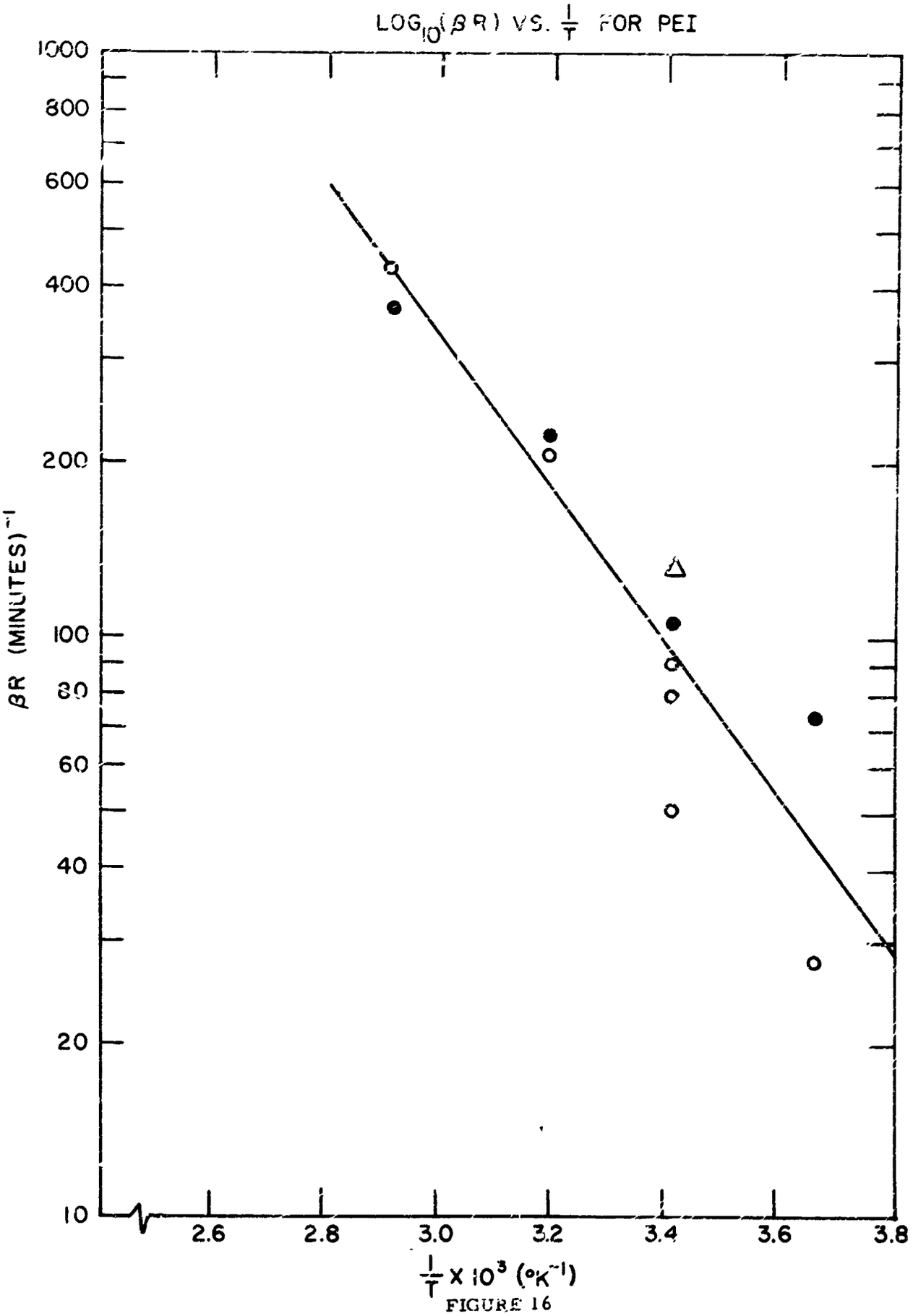
LOG10(βR) VS. 1/T FOR PEI
1000
800
600
400
200
100
80
60
40
20
10
βR (MINUTES)⁻¹
2.6
2.8
3.0
3.2
3.4
3.6
3.8
1/T X 10³ (°K⁻¹)

FIGURE 16

TABLE 10

EQUATIONS FOR THE LEAST-SQUARES CORRELATIONS OF THE TEMPERATURE DEPENDENT VARIABLES PRESENTED IN TABLE 9 FOR PEI-ECH RESIN

(24) $R = (4947)\,(P_{CO_2})^{-0.316} \exp(-910/R_o T)$

(25) $D'/a^2 = (172.9)\exp(-7740/R_o T)$

(26) $\beta R = (2.858 \times 10^6)\exp(-6012/R_o T)$

(27) $D/a^2 = (3.783 \times 10^6)\exp(-8610/R_o T)$

(28) $s = (2.466 \times 10^{-5})\exp(+4215/R_o T)$

NOTES

The units which apply to the above variables are: R, dimensionless; D'/a^2, βR, and D/a^2, minutes^{-1}; s, gram moles per 1000 grams of water (or better, gram moles per liter of water); R_o, 1.987 calories/gram mole; T, ^oK. Since the resin particles employed passed through a 28 mesh sieve but not a 48 mesh sieve, the radius a can be considered to be one half the size of the average sieve opening, namely $(\frac{1}{2})(\frac{1}{2})(.589+.294)$ mm or 2.21×10^{-2} cm.

TABLE II

CALCULATIONS FOR COMPARISON OF FRACTIONAL MASS UPTAKE AND EXIT VOLUME PER CENT CO_2 VERSUS TIME CURVES WITH EXPERIMENTAL RESULTS FOR 20°C, 1.00% CO_2, 100% RH FOR PEI-ECH RESIN

t(min)	$(t)^{\frac{1}{2}}$	$(D't/a^2)^{\frac{1}{2}}$	(M_t/M_∞)	$(M_t/M_\infty)_{\beta=\infty}$	C_{exit}
30	5.48	.0942	.100	.281	.730
60	7.75	.1333	.218	.394	.738
90	9.49	.1632	.322	.470	.779
120	10.96	.1884	.410	.533	.817
150	12.24	.2107	.476	.578	848
180	13.42	.2308	.533	.620	.870
210	14.49	.2495	.581	.656	.888
240	15.49	.2664	.623	.688	.903
270	16.43	.2827	.660	.716	.916
300	17.32	.2980	.693	.743	.925
330	18.17	.3127	.723	.767	.934
360	18.98	.3264	.750	.785	.948
390	19.74	.3398	.774	.804	.955
420	20.48	.3525	.793	.819	.961
450	21.22	.3647	.810	.835	.963
480	21.92	.3771	.825	.849	.964
510	22.57	.3885	.839	.863	.965
540	23.23	.3997	.853	.876	.966
570	23.86	.4108	.865	.887	.967
600	24.49	.4213	.877	.896	.972
630	25.09	.4315	.888	.905	.975
660	25.68	.4415	.898	.913	.978

NOTES

$D'/a^2 = 2.96 \times 10^{-4} min^{-1}$; $\beta = 2.110 \times 10^{-2} min^{-1}$

$\beta a^2/D' = 71.3$; $(D/a^2)^{\frac{1}{2}} = 1.721 \times 10^{-2}$; $M_\infty = 2.95$ meq/dry gram

3. Effect of Relative Humidity

As stated in the general discussion, the unsaturated (with water) runs were not expected to fit the equilibrium or kinetic models. It was expected that the deviations would become more severe as the material became drier, and this was indeed encountered. It was found that the 55% RH run had an equilibrium capacity only 36% of the saturated value, while the 70% RH run had a capacity of 63% of the saturated value. Tables 29 and 30 of Appendix B show that the diffusion equation is even less well-served. The most consistent values of the diffusivity for the 70% case were two to three times the size of those obtained for the saturated case, and the β value somewhat smaller. One expects the diffusivity to rise when the pores are no longer completely filled with water, since the diffusivity in the gas phase is 10000 times as large as in the liquid and it is now possible for gas to penetrate the particle. A smaller β means that the gas film is exerting more influence, quite likely since the liquid film has diminished in size. The 55% data never gave a constant diffusivity with time; for all β, D'/a^2 increased with time. This increase probably indicates that all the water is now entirely within the particle, and in fact does not fill the particle pores. This means that the first fractions of gas quickly diffuse into the center where the liquid is residing, and the remainder, since it sees progressively more gas-filled pores, diffuses in even faster.

4. Decay of Resin Capacity

For the PEI-ECH resin the replicated runs were numbers 1, 4, and 9 (out of a total of 15 involving temperature cycles). The CO_2 absorptive capacity obtained after 300 minutes was used as the standard, since only number four was run to complete equilibrium. The cumulative mass uptake M_t was normalized to the value exhibited by run number 1 (fresh resin). Figure 17 shows the actual value of $M_t/(M_t)_1$ obtained and the parabola drawn through them; Table 12 contains the values of the normalizing factors taken from this parabola and applied to the remaining runs. A second order equation was chosen rather than a linear one because, with the sources of copper ions fixed within the column, these ions had greater distances to migrate to uncomplexed resin each time. The amount of complexing per regeneration ought to then decrease with time.

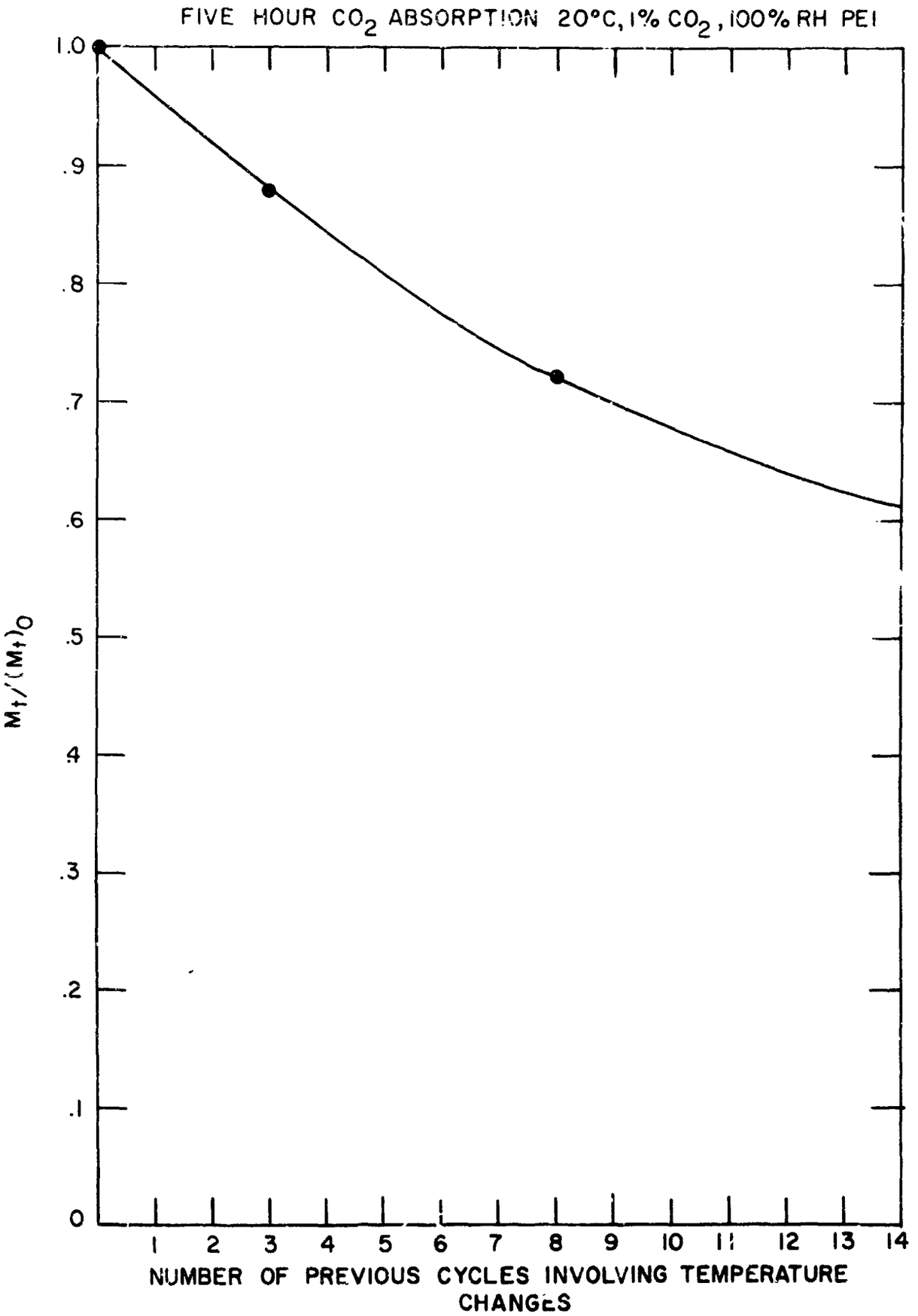
FIVE HOUR CO_2 ABSORPTION 20°C, 1% CO_2, 100% RH PEI
1.0
.9
.8
.7
.6
.5
.4
.3
.2
.1
0
$M_t/(M_t)_0$
1 2 3 4 5 6 7 8 9 10 11 12 13 14
NUMBER OF PREVIOUS CYCLES INVOLVING TEMPERATURE CHANGES

FIGURE 17

TABLE 12

CORRECTION FACTOR FOR LOSS OF CO_2 CAPACITY BY PEI-ECH RESIN, DUE TO REACTIONS BOTH WITH CO_2 AND COPPER IONS

NUMBER OF PREVIOUS REGENERATIONS	REACTION CONDITIONS			CO_2 UPTAKE CORRECTION FACTOR
	TEMP (°C)	P_{CO_2}(atm)	%RH	
0	20	0.01	100	1.000
1	40	0.01	100	1.045
1	70	0.01	-	1.045
2	0	0.01	100	1.092
2	70	0.01	-	1.092
3	20	0.01	100	1.139
3	70	0.003	-	1.139
4	20	0.003	100	1.188
5	40	0.003	100	1.237
6	0	0.003	100	1.287
7	70	0.003	100*	1.337
8	20	0.01	100	1.384
9	20	0.01	55	1.433
10	20	0.0065	100	1.481
11	40	0.01	100	1.522
12	70	0.01	100*	1.562
13	40	0.003	100	1.600
14	20	0.01	70	1.632

* These runs were begun with freshly regenerated (wet) material. While it was not possible with this equipment to maintain a feed-gas relative humidity of 100% at 70°C, these high temperature experiments were sufficiently rapid that one could reasonably assume the presence of a continuous liquid water film surrounding each particle for the duration of the run, even in the presence of the unsaturated (50-60%RH) atmosphere. Numbers 9 and 14 were run under reduced-humidity equilibrium ($\%RH_{inlet} = \%RH_{exit}$) conditions.

C. Commercial Resins

1. Rohm & Haas Amberlite IRA-93

Only, the standard 20°C, 1.00% CO_2, 100% RH absorption run was made with this material, for the capacity which it exhibited was far too low for our applications. With 78 grams of resin (dry weight) saturated with pure deionized water (no KCl), only a total of 11.97 milliequivalents of CO_2 were absorbed, for a capacity of 0.153 meq/gm. Figure 37 of Appendix C shows the curves of exit CO_2 concentration and fractional mass uptake versus time obtained.

Table 33 of Appendix B shows the calculations involved in applying the postulated diffusion model to this material. The extremely high porosity of this resin manifested itself in two ways: the time required to reach carbon dioxide equilibrium was only 71 minutes, roughly one-tenth of that required at the same conditions by the other two resins: and the diffusivity D' was more than an order of magnitude greater than for the other two resins. The true diffusivity D in the resin phase was also greater, having a value of 1.93×10^{-5} cm^2/sec. This value must be slightly large, since the resin could not be expected to have a diffusivity greater than that for water (which represents unlimited porosity) at the same temperature, which is 1.77×10^{-5}.

The high value of β, .248, is consistent, for it implies that 27.8 minutes are required for the particle surface to reach 99.9% of its equilibrium value. Most of the calculations for the other materials do show that this time should be slightly less than half the time required for the particle to come to equilibrium. Using the water absorptive capacity presented in the Company's literature as

1.17 grams of water per gram of dry resin and the Henry's Law constant for CO_2 in water at 20°C (22), the value of $\underline{R}$ was found to be 331. This factor should be about one-tenth the value found for the other resins because IRA-93 has only about one-tenth their capacity.

Substituting the β and $\underline{R}$ values into equation 23 shows δ/a to be 0.077, which is in the same range as previously.

2. Dowex WGR

a. Equilibrium

The same analysis as was presented in the discussion of the PEI-ECH results was applied here. The best value of n in the expression K = CAPACITY/$(P_{CO_2})^n$ was found to be .620, which agrees well with the PEI value of .684. The computed K values given in Table 4 show good agreement with the experimental results when this n (obtained from the slopes of the lines shown in Figure 9) is used.

Figure 11 shows the semilogarithmic plots of K versus 1/T for both values of n (.620 and 1.0). The slopes of the least-squares lines are the same and, if the correlation is in the form $K = (\text{constant}) \times (P_{CO_2})^{n-1} \exp(E_K/R_oT)$, then the constant should be 1.892×10^{-3} and E_K should be 5337 calories per gram-mole. (This E_K compares well with the 3550 for PEI-ECH.)

Table 6 shows the computations involved in obtaining the values of R. When these results are plotted (Figure 18) the dependence of R on $(P_{CO_2})^{n-1}$ is again evident. In this case, the temperature effect is so severely non-linear above 40°C that a linear least-squares relationship with 1/T is out of the question. (The dashed line is the linear extrapolation of the correlation involving the three low temperatures.) Both dilute MPEI solutions (Figure 12) and the PEI-ECH resin (Figure 13) exhibit the same sort of temperature dependence of R, but not in so pronounced a fashion.

The capacities obtained were slightly less than half those demonstrated by PEI-ECH (Table 3). Since Dowex WGR is supposedly the highest-capacity resin commercially available, PEI-ECH was assumed to have an unsurpassed CO_2 absorptive capacity. Therefore

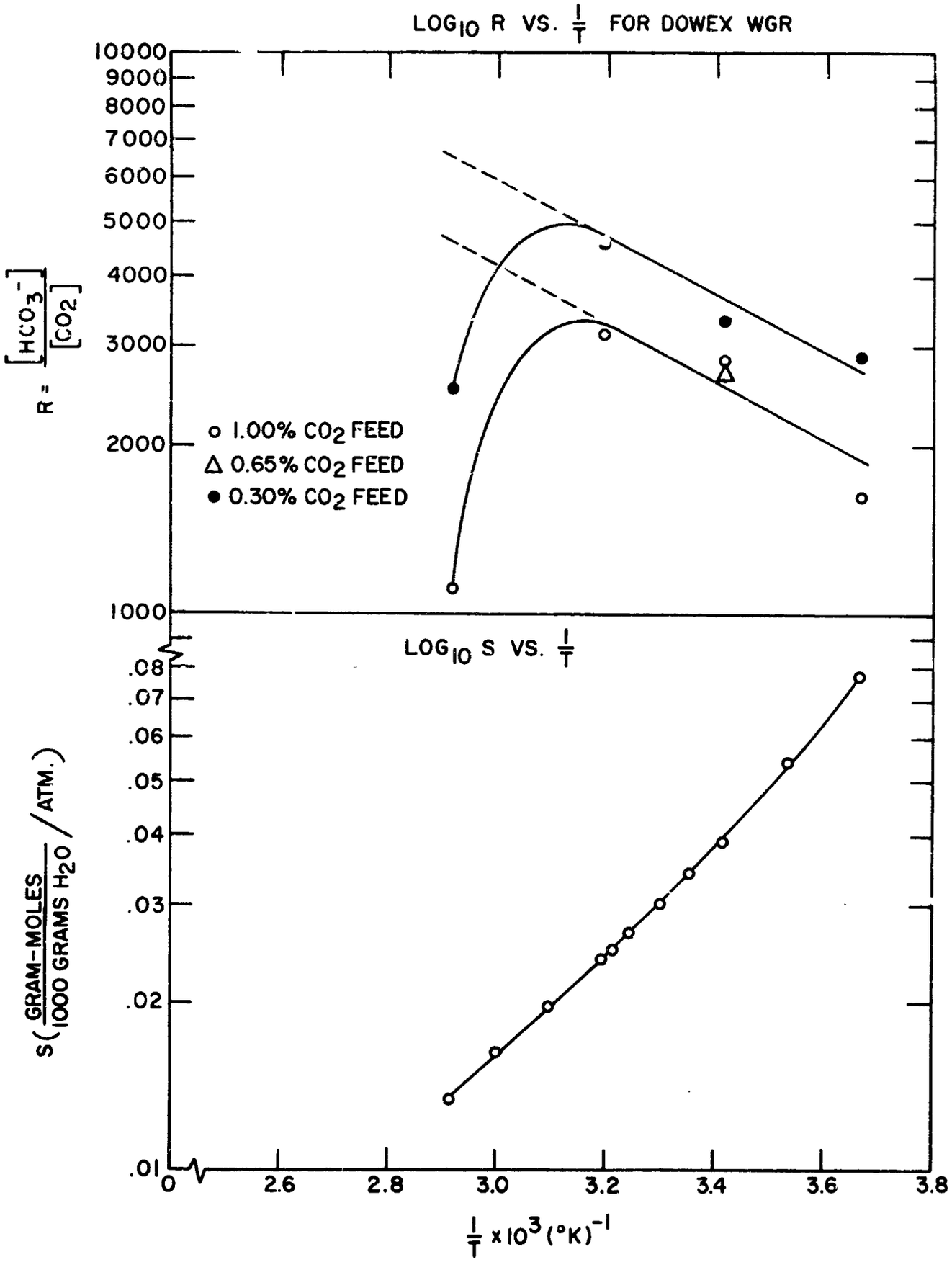

FIGURE 18

PAGE 80

PEI-ECH was chosen as the basic material for the design of an operational air purification system(cf. SECTION VI).

b. Reaction Mechanism

Tables 34 through 44 of Appendix C show the trial and error calculations involved in determining the best values of D'/a^2 and $\beta a^2/D'$ for Dowex WGR. As can be seen, the postulated reaction mechanism is applicable to this material also. Figure 19 shows the relationship of D'/a^2 to temperature. Unlike the PEI-ECH case, the semilogarithmic plot does not yield a linear correlation. This can be attributed to the behavior of R, for, when $D/a^2 = (D'/a^2)(R + 1)$ is plotted in Figure 20 on the same coordinates, a straight line results, the slope of which is the diffusion activation energy. PEI-ECH exhibited a value of 8610 calories per gram-mole for this quantity; Dowex WGR exhibits a value of 6270. Both lie within the accepted range of 2400 to 10000.

The value of the diffusivity at 20°C is not as acceptable, however. The diffusivity of CO_2 in water at this temperature was seen to be 1.77×10^{-5} cm^2/sec while D at 20°C in the resin phase was calculated to be 3.60×10^{-5} cm^2/sec. It seems highly unlikely that the coefficient for diffusion of CO_2 through the water contained in a material of limited porosity could exceed that for pure water, which can be thought of as representing maximum porosity.

Table 13 presents the derived values of D/a^2 and βR for this set of experiments. The plot of LOG(βR) versus 1/T is given in Figure 21. The least-squares correlation was obtained without making use of the 0°C, 0.30%CO_2 point, which was far away from the calculated line. Table 14 shows the equations of the correlations of the temperature variables given in Table 13 and Figures 19, 20, and 21.

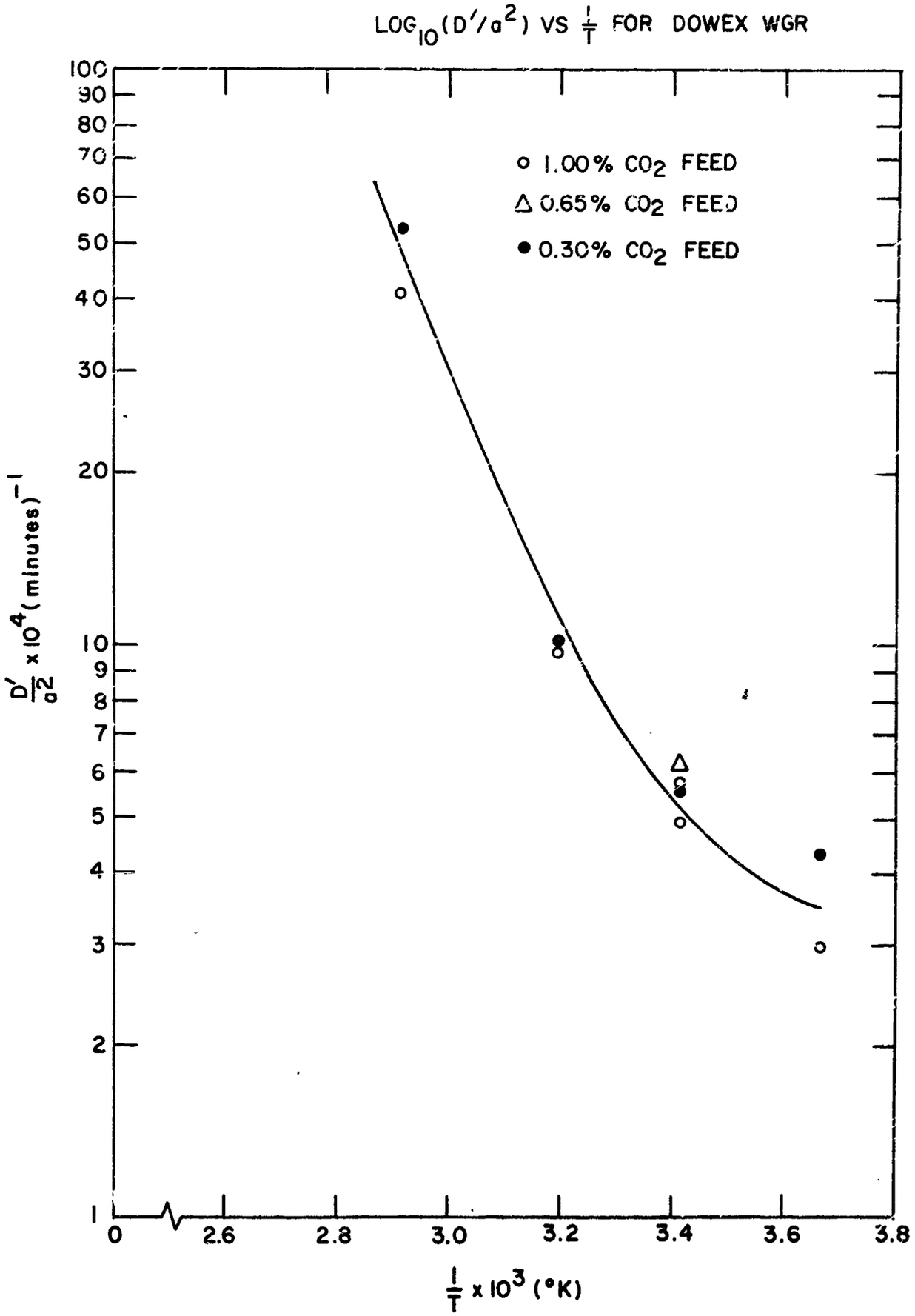

FIGURE 19

PAGE 82

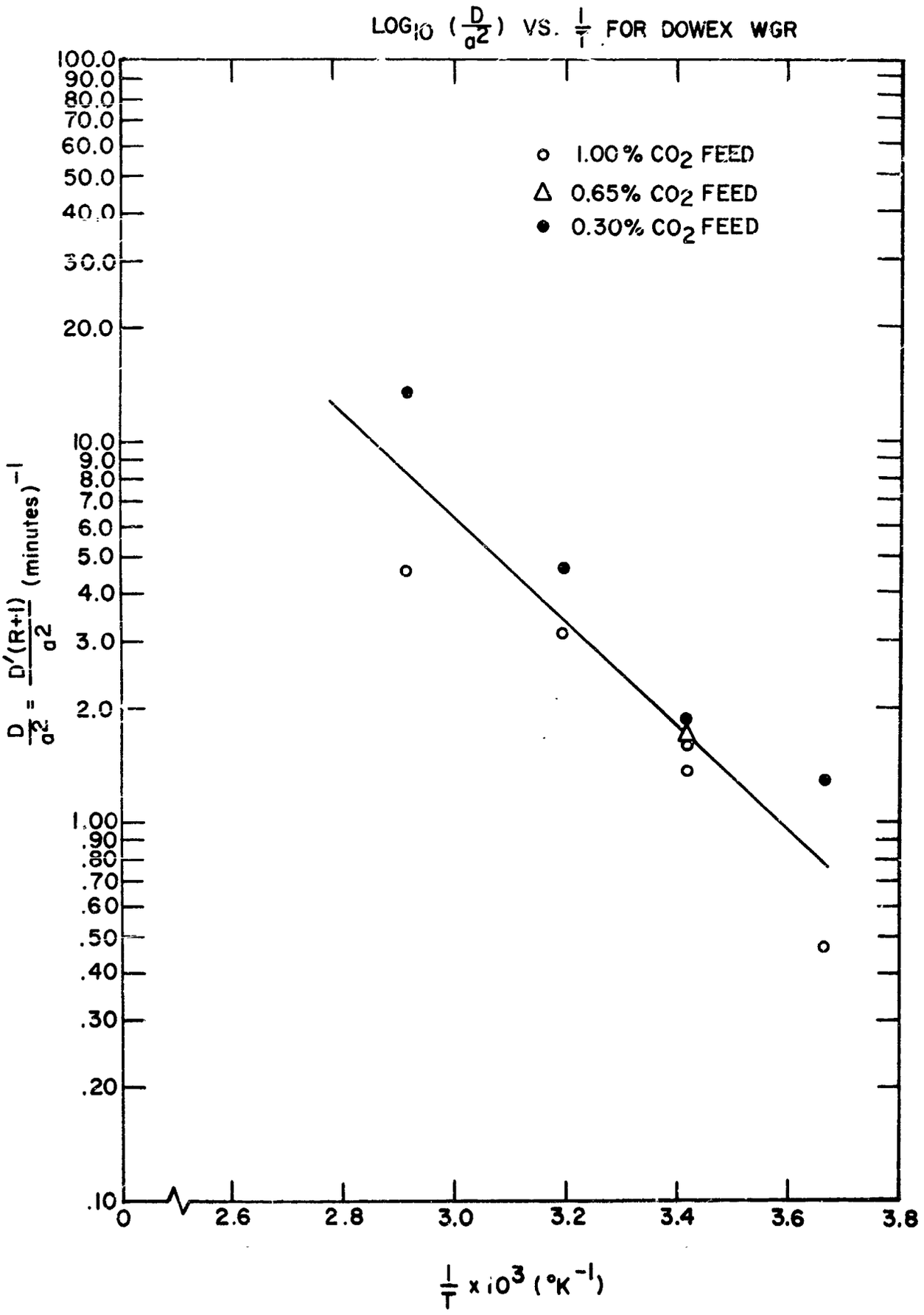
LOG10 (D/a2) VS. 1/T FOR DOWEX WGR
1.00% CO2 FEED
0.65% CO2 FEED
0.30% CO2 FEED
D/a2 = D'(R+1)/a2 (minutes)-1
1/T x 10^3 (°K-1)
100.0
90.0
80.0
70.0
60.0
50.0
40.0
30.0
20.0
10.0
9.0
8.0
7.0
6.0
5.0
4.0
3.0
2.0
1.00
.90
.80
.70
.60
.50
.40
.30
.20
.10
0
2.6
2.8
3.0
3.2
3.4
3.6
3.8

FIGURE 20

TABLE 13

VARIABLES (D/a^2, βR, s) WHOSE TEMPERATURE DEPENDENCE CAN BE DESCRIBED BY AN EXPONENTIAL EQUATION OF THE FORM: $y = (\text{constant}) \times (\exp(\pm E/R_o T))$, FOR DOWEX WGR RESIN

T (^oK)	P_{CO_2} (atm)	R	D'/a^2 (min)$^{-1}$	β (min)$^{-1}$	D/a^2 (min)$^{-1}$	βR	$s \times 10^2$
273	0.01	1623	2.97×10^{-4}	0.861×10^{-2}	0.483	13.98	7.705
273	0.003	2931	4.37×10^{-4}	1.882×10^{-2}	1.282	56.15	7.705
293	0.01 (first)	2798	4.90×10^{-4}	1.717×10^{-2}	1.372	48.03	3.840
293	0.01 (second)	2798	5.73×10^{-4}	1.433×10^{-2}	1.603	40.13	3.840
293	0.0065	2704	6.18×10^{-4}	1.236×10^{-2}	1.671	33.42	3.840
293	0.003	3328	5.58×10^{-4}	1.228×10^{-2}	1.857	40.88	3.840
313	0.01	3118	9.71×10^{-4}	2.757×10^{-2}	3.126	86.0	2.405
313	0.003	4580	10.12×10^{-4}	2.837×10^{-2}	4.633	129.9	2.405
343	0.01	1117	40.96×10^{-4}	26.63×10^{-2}	4.570	297.4	1.359
343	0.003	2513	52.87×10^{-4}	18.52×10^{-2}	13.30	465.0	1.359

NOTE: $D/a^2 = (D'/a^2) \times (R + 1)$

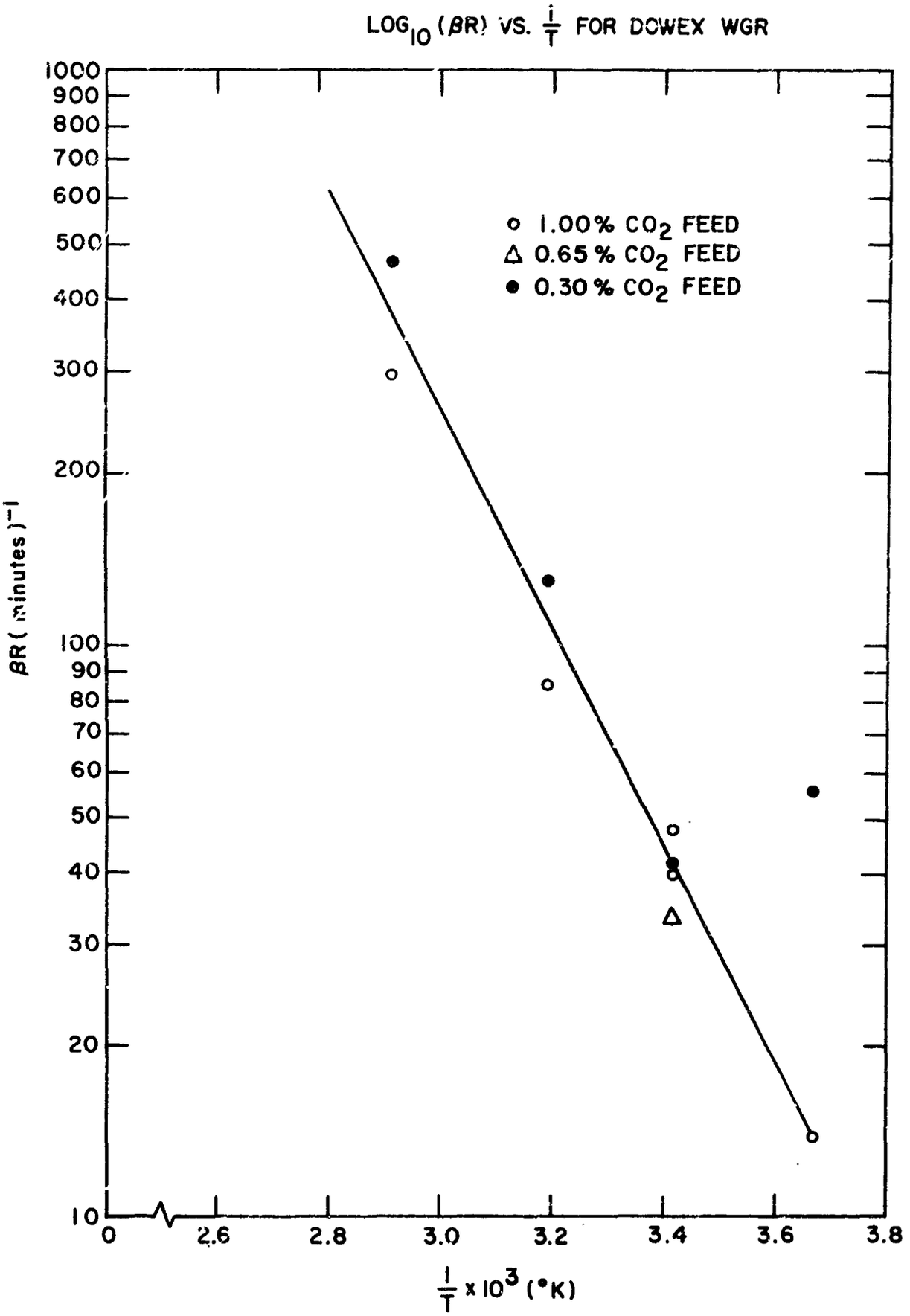

FIGURE 21

PAGE 85

TABLE 14

EQUATIONS FOR THE LEAST-SQUARES CORRELATIONS OF THE TEMPERATURE - DEPENDENT VARIABLES PRESENTED IN TABLE 13

(29) $D/a^2 = (7.99 \times 10^4) \exp(-6270/R_o T)$

(30) $\beta R = (1.430 \times 10^8) \exp(-8780/R_o T)$

(31) $S = (1.615 \times 10^{-5}) \exp(4568/R_o T)$

NOTES

See Table 10 for the units associated with these quantities

The radius a for these 20 to 28 mesh particles can be considered to be one half the size of the average sieve opening, namely $(\frac{1}{2})(\frac{1}{2})(.833 + .589)$ mm $= 3.555 \times 10^{-2}$ cm

Taking the average value of βR at 20°C, liquid film diffusion is again found to control the transfer of CO_2 from the bulk gas to the solid surface. Calculating the film thickness of water yields $\delta/a = 0.062$, which compares favorably with the 0.078 for PEI-ECH and 0.077 for IRA-93.

The results of applying this correlation in an attempt to duplicate the experimental data are shown in Table 15 and Figure 43 of Appendix C.

TABLE 15

FRACTIONAL MASS UPTAKE AND EXIT CONCENTRATION DATA, DERIVED FROM THE GENERAL CORRELATIONS, FOR 20°C, 1.00%CO_2, 100%RH FEED WITH DOWEX WGR.

TIME t(min)	$t^{\frac{1}{2}}$	$(D't/a^2)^{\frac{1}{2}}$	M_t/M_∞	$(M_t/M_\infty)_{\beta=\infty}$	c_{out}
40	6.56	.163	.178	.473	.841
80	8.94	.222	.324	.608	.848
120	10.96	.272	.468	.697	.877
160	12.65	.314	.592	.768	.906
200	14.14	.350	.680	.818	.926
240	15.49	.384	.757	.858	.946
280	16.74	.415	.810	.892	.956
320	17.89	.443	.851	.917	.965
360	18.98	.470	.883	.933	.973
400	20.00	.496	.908	.949	.978
440	20.97	.520	.927	.959	.983
480	21.93	.544	.943	.969	.986

NOTES

From Equation 29, $D/a^2 = (7.99 \times 10^4) \exp(-6270/1.987 \times 293)$

$= (7.99 \times 10^4)(2.14 \times 10^{-5}) = 1.719$

From Table 6, $R = 2798$; $\therefore D'/a^2 = 6.14 \times 10^{-4} (min)^{-1}$

From Equation 30, $\beta R = (1.430 \times 10^8) \exp(-8780/1.987 \times 293)$

$= (1.430 \times 10^8)(28.96 \times 10^{-8}) = 41.40$

$\therefore \beta = (\beta R)/R = 41.40/2798 = 1.480 \times 10^{-2}$; $\frac{\beta a^2}{D'} = 24.1$

From Table 4, $M_\infty = 1.305$ meq/dry gr.

c. Decay of Resin Capacity

The regeneration runs for Dowex WGR are presented in Figures 59 through 69 of Appendix C. Of course, most of the CO_2 evolution took place in the first few minutes at elevated temperatures, and normally at least 80% of the absorbed material was removed.

The same problems existed with this material as with the PEI-ECH namely, partial drying of the bed, small concentration differences at low temperatures, off-scale voltages at high temperatures, and unknown initial profiles within the particles. Likewise, copper complexes formed during the overnight soaking periods, as before. Since only two standard 20°C, 1.00% CO_2, 100% RH runs were made, a linear relationship for loss of capacity with time had to be assumed. Table 16 presents the resulting correction factors. These were used in obtaining the equilibrium capacities given in Table 4.

TABLE 16

CORRECTION FACTOR FOR LOSS OF CO_2 CAPACITY BY DOWEX WGR

Number of Previous Temp. Cycles	Reaction Conditions	Correction factor
0	20°C 1.00% CO_2 100% RH	1.000
	(Capacity = 91.6 meg/dry gm.)	
1	40°C, 1.00% CO_2, 100% RH	1.045
2	70°C, 1.00% CO_2, 100% RH	1.094
3	0°C, 1.00% CO_2, 100% RH	1.147
4	20°C, 0 30% CO_2, 100% RH	1.207
5	20°C, 0.30% CO_2, 100% RH	1.272
	[Without Re-Wetting Surface]	
6	40°C, 0.30% CO_2, 100% RH	1.347
6	70°C, 0.30% CO_2, 100% RH	1.347
7	0°C, 0.30% CO_2, 100% RH	1.428
8	20°C, 0.65% CO_2, 100% RH	1.521
9	20°C, 1.00% CO_2, 100% RH	1.627
	(Capacity = 56.7 meg/dry gm.)	

D. Validity of Assumptions

A number of assumptions were involved in the derivation of the equation for the concentration of solute at the solid surface which must be examined in the light of the experimental results:

1.) The particle interior is completely saturated with liquid and its surface is completely covered by a thin liquid film. This situation is a matter of experimental procedure, and involves only complete soaking in liquid prior to each run and maintaining a relative humidity of 100% at the bed temperature in the gaseous phase.

2.) The gas composition is constant with time. While the inlet gas composition is time invariant, the same cannot be said for the exit composition. To reduce experimental measurement error a shallow packed bed is inadvisable, since composition differences across the bed provide the only mass uptake data. Truly, therefore, only the section of the bed closest to the gas inlet experiences a constant CO_2 partial pressure. However, after the first few minutes of gas flow (less than 10% of the total reaction time; see Figure 24, for example) the exit gas CO_2 concentration has reached 80% of its final (equilibrium) value, which is the same as the inlet. Thus for at least the remaining 90% of the run, the top section of the column sees a gas whose CO_2 partial pressure changes by only 20%, while the remainder of the column sees even progressively less variation.

3.) Isothermal conditions prevail.

The presence of the large constant temperature bath and its attendant coil for the feed gas combined with a heat of reaction (19) of the order of 10 kcal/mole (or a maximum total heat evolution of the order of 3000 calories ($0^{\circ}C$, 1% CO_2) spread over many hours of

reaction time insures against even local hot spots.

4.) The values of k_G, k_L, $\underline{R}$, and $\underline{s}$ are functions only of temperature and not of concentration. These assumptions usually require dilute solutions, and it must be remembered that the feed gas containers at most 1% CO_2 by volume, and the minimum ratio of moles of water per mole of CO_2 absorbed (under reaction conditions of 0°C, 1% CO_2, 199% RH) was found to be (164.7/18) / (14.73/44) = 9.15/.334 = 27.4. Sherwood and Pigford (24) present the general defining equations for gaseous and liquid mass transfer and apply them to more concentrated solutions than these with reasonable results; k_G and k_L should then not be suspect. Harned and Davis (22) provided the correlation for $\underline{s}$ used in this work, for solutions of these strengths, which gives $\underline{s}$ only in terms of $\underline{T}$.

The distribution coefficient $\underline{R}$, however, demonstrates a correlation with gaseous CO_2 partial pressure raised to about the -.3 power. Since it has been stated in the discussion of assumption number two that P_{GAS} is really not a constant, variations in $\underline{R}$ will exist. The fact that the most changing value of P_{GAS}, — namely the exit value at the top of the column — quickly reaches 80% of the inlet value shows that, from then on, $\underline{R}$ will change by less than 7% [i.e. $100\,(1-(.8)^{.3})$] at worst, and by less elsewhere in the column. This situation should not be intolerable.

5.) $\delta << a$

The data of Tetenbaum and Gregor (5) prove this for liquid feed, but in their case the film thickness is the boundary layer thickness in a continuous liquid medium. For our case $\underline{\delta}$ represents the affinity of the particles for liquid so that a direct comparison is not possible.

The computation of $\frac{\delta}{a}$ at 20°C given in the discussion section shows that $\frac{\delta}{a}$ for PEI-ECH is less than .078, .077 for IRA-93, and .062 for WGR

6.) $n << \xi^2$

This is the crucial assumption in that it permits reduction of the surface concentration equation to the form $(c_{EQ} - c_l)e^{-\frac{\eta}{2\xi}t}$.

Going back to the definitions of these quantities, we have:

$\xi = \frac{1}{2}\left(\frac{k_G}{s\epsilon} + \frac{k_L}{\delta} + \frac{3k_L}{aR}\right)$ and $\eta = \frac{3k_G k_L}{aRs}$

$$\therefore \frac{\eta}{\xi^2} = \frac{12k_G k_L \delta s}{aR\,(k_G^2 + 2s k_G k_L + s^2 k_L^2)} < \frac{12k_G k_L \delta s}{aR\,(2sk_G k_L)}$$

since all the terms are positive in sign.

(29) $\frac{\eta}{\xi^2} < \frac{12\,k_G k_L \delta s}{aR(2sk_G k_L)} = \frac{6\delta}{aR}$ which is far, far less than 1 since $\delta << a$ and R is of the order of 10^{+3}.

The assumptions involved in the derivation of the diffusion equations, and the corresponding arguments supporting these assumptions, are:

1.) The surface concentration of diffusing substance is described by $\left(c_R\right)_{r=a} - c_l = \left(c_{EQ} - c_l\right)\left(1 - e^{-\beta t}\right)$.

The verification of all the assumptions in the previous section which lead to this form of equation justify its use.

2.) The immobilization of the diffusing substance follows the relationship $c_{IMMOBIL.} = \alpha\ c_R$.

Here two tacit points are involved: the reaction is sufficiently fast compared to the diffusion rate so that diffusion is not impeded, and α is not a function of C_R. Since it has been concluded that CO_2 is the only diffusing substance, it is necessary to examine the steps involved in the chemical reaction. First the CO_2 must hydrate to form H_2CO_3. Normally the ratio of carbon dioxide to carbonic acid is

about 300 (from the value of the hydration equilibrium constant (26)). The reaction is sufficiently rapid—at 25°C, k ≈ .03 sec^{-1} (27)—that its half time of 23 seconds is inconsequential in comparison to the length of time required for the system to reach equilibrium (about 600 minutes at this temperature).

The second step is the ionization of carbonic acid to HCO_3^- by hydroxide ion which, according to Edsall and Wyman (25) is much more rapid than the first step. The resin, since it is in the $R_3NH^+OH^-$ form, provides the OH^- ions. We have seen that $\underline{a}$ and the distribution coefficient $\underline{R}$ are identical. But $\underline{R}$ varies as $P_{CO_2}^{-.3}$ while c_R varies as $P_{CO_2}^{1.0}$. Again it must be pointed out that the value of $\underline{R}$ varies at most by 7% over the last 90% of the reaction time so that for by far the major portion of an experiment it may be considered constant.

3.) The diffusivity $\underline{D}$ is not a function of concentration.

Actually $D' = D/(a + 1) + D/(R + 1)$ must be independent of concentration, and the trial-and-error solutions for D'/a^2 and $\beta a^2/D'$ were obtained for the best agreement among the $\underline{D'}$ values calculated across the time span of the run. The diffusivity $\underline{D}$ can be expected to be constant for dilute solutions such as these (23). The temporary dependence of $\underline{R}$ on concentration has already been discussed.

4.) M_∞ is the equilibrium total mass transfer.

Since almost all total uptakes were determined by linear extrapolation because of the slowness of the diffusion, values of M_∞ might be suspect. However, in all cases equilibrium was closely enough approached that even a radical error in the slope of the extrapolation line would mean an error of only a few per cent in M_∞.

5.) The rate of absorption is given by equation 15.

If this is so, then concentration curves can be drawn using the rate equation developed in the PROCEDURES section and matching its results with those from equation 15:

$$\frac{5737\ V}{460+T}\left(c_{in} - c_{out}\right)_{instant} \stackrel{?}{=} \beta M_{\infty}\left[\left(\frac{M_t}{M_{\infty}}\right)_{\beta=\infty} - \frac{M_t}{M_{\infty}}\right]$$

At $t = 0$, $\left(c_{in} - c_{out}\right)_{instant}$ has its maximum value, while $\left[\left(\frac{M_t}{M_{\infty}}\right)_{\beta=\infty} - \frac{M_t}{M_{\infty}}\right]$ equals zero. This relation is clearly inapplicable at the beginning, the reason being that the absorption that is observed at this time involves transfer to the water film rather than to the particle. But again, after a short time, the diffusion equation does agree with the experimental results. An operational system can now be designed.

E. Miscellaneous

1. Rate of Absorption Independent of Gas

In several instances flow disturbances occurring during an experiment caused variations in the gas velocity. Manipulating the delivery pressure gauges in order to restore normal operating conditions led to more velocity perturbations. It was noticed that, when the disturbances occurred during the more linear portions of the concentration versus time curves, the same amount of CO_2 was absorbed during the transient period as would have occurred if the prevailing smooth curve were interpolated into this region, i.e. if the velocity had not changed.

It is well-known that a particle diffusion mechanism would show no gas stream effect because the slow motion of the reacting substance away from the particle surface and toward the interior compared to the rate at which the stream delivered the substance to the outside surface controlled the rate. However, when it was found that this simple diffusion mechanism did not adequately describe the process — that indeed the delivery of CO_2 to the solid surface was not instantaneous — the validity of this conclusion was opened to question. That it has been certified as correct came about with the discovery that the liquid film, and not the gas film, was the rate-controlling step in the transfer of CO_2 from the bulk gas stream to the liquid-solid interface. Since this is so, the fact that the thickness of the gas boundary layer is a function of the Reynolds number (and hence of the gas velocity) is no longer any problem. The gas velocity would have to decrease by a factor of one hundred in order to have even a slight effect (provided it didn't disturb the liquid film) since z varies as $N_{Re}^{-\frac{1}{2}}$ (25).

2. Regeneration

The concentration versus time curves for the regeneration process are presented in Appendix C in Figures 46 through 69. Suffice it to say that the usual situation was that 85 to 95 per cent of the material absorbed during a run was removed by this passage of hot, CO_2-free gas through the bed, and that the unregenerated part was in the main responsible for the loss of capacity noticed with each succeeding run (cf. Decay of Resin Capacity). It was not possible to correlate the regeneration data in the manner of the absorption data for the following reasons:

1. At low temperatures the diffusion process is slow and the equilibrium extremely unfavorable. This means that the concentration of CO_2 in the exit gas stream is very close to zero. Combining this with the tendency of the analyzer to drift makes the results obtained very prone to large errors.

2. At high temperatures the resin begins to dry out, so that we have an unsteady-state moisture condition. We have shown how lower humidity equilibria give spurious results due to stripping away the water film and the pore liquid. Adding to this a time-dependency negates our diffusion analysis completely.

3. At high temperatures with somewhat dry resin we also have the possibilities of channeling and carbamate formation (26).

4. For the sake of rapidity, a number of the regenerations were conducted under non-isothermal conditions.

5. One of the basic requirements for the use of the diffusion equations is that the initial concentration distribution within the particle be either constant of fully-known. Since only an occasional absorption was run to completion because of the long equilibration time, it follows that a concentration gradient exists within the particle at the time the run

was terminated. But it was not possible to immediately begin regeneration since gas lines had to be purged of CO_2, as well as the humidifier column water supply, and the infrared analyzer had to be recalibrated. The time required for these operations was always in the neighborhood of twenty minutes. During this hiatus, the concentration profile within the particle must have been adjusting itself to become horizontal, but how far the adjustment had proceeded when regeneration was initiated was not possible to tell. If a long wait occurred because it was desired to heat up to 80°C before beginning, then the equilibrium and kinetics became so favorable that the exit gas concentration at the very beginning was quite a bit greater than the upper calibration point of the analyzer. Most of the regeneration took place right at the beginning, since that was when the most CO_2 was present in the solid, and the accuracy of the calculations was here in severest doubt because the recorder pen was off scale for the first few minutes.

If all these difficulties were overcome, it is assumed that the regeneration would have to follow the same model as the absorption, since Crank (16) derives the diffusion equation for mass transfer in either direction.

3. Fluidization

Prior to the discovery of the method of packing the column with screens and in sections as outlined in the "Packing Scheme" section an attempt was made to circumvent the problem of gas channeling through the bed by fluidizing the resin. It was reasoned that maximum contact between the gaseous and resinous phases could be achieved this way, since a sufficient flow of gas had to contact each individual particle in order to keep that particle aloft. The minimum fluidization velocity calculated for spheres in the 28 to 48 mesh diameter range (28) was found to exceed the maximum that could be provided by the compressed gas cylinders or the outside air compressor, even when the delivery pressure was set as high as fifty pounds per square inch gage. In addition, such hign flow rates would have presented very small concentration differences to the infrared analyzer; combined with the flow sensitivity of this measuring device, the results would have been highly inaccurate.

A bypass line was introduced into the column's inlet and exit. A large recycle of the gas leaving the bed was shunted into this line, where an auxiliary gas compressor delivered it to the bottom (entrance) of the column at the prevailing inlet pressure. A recycle ratio of 9 to 1 brought the external gas flow back to the .2 scfm rate normally employed. A material balance envelope which does not cut the recycle stream shows that the feed gas supplied by the cylinders is the same as this, so that the amount of absorption is independent of the recycle ratio.

One of the assumptions involved was that the fluidization would be particulate, not aggregative. Zenz and Othmer (28) have stated that a good many fine powers aggregate, even in an atmosphere whose relative

humidity was as low as one per cent. When the expected improvement in absorptive capacity was not found, and the pressure drop at incipient fluidization was seen to rise as soon as something other than bone-dry air (which had been used to obtain the value of this pressure drop for this bed) was introduced, an alternative column of clear plastic was constructed. When this bed was seen to slug in its entirety, fluidization was abandoned.

VI. DESIGN OF OPERATIONAL SYSTEM

A. Description

The carbon dioxide atmosphere control system is shown diagrammatically in Fig. 22 Inlet air can be fed to the system by compressing it or by creating a partial vacuum and pulling the air back to the cabin by a return system. Air leaving the cabin is first passed into a humidification unit to raise the relative humidity of the influent air from approximately 50% to 90% relative humidity of higher. The purpose of this is, as shown earlier, to increase the capacity of the carbon dioxide absorbing system. In a space cabin, the water humidification system will operate by a wick assembly wherein liquid water is in contact with strips of a felt-like material which absorbs water and passes it along the fabric at good rates of speed. There are many designs which can be employed here, but a wick system appears to be most suitable and most simple.

The humidified air is then passed into the carbon dioxide absorbing system, which has previously been regenerated. After regeneration, this system is near saturation with respect to water vapor, so that the amount of water which is supplied by the humidifier is small. Also, since the inlet air to the carbon dioxide absorber in presaturated and the carbon dioxide absorption takes place at the bottom of the column, a good capacity is achieved even though the top of the column is not as near saturation. The effluent air from the carbon dioxide absorber enters a water absorbing column which is comprised of the same resin but which has been previously regenerated to remove most of its water content.

SCHEMATIC DIAGRAM FOR OPERATIONAL AIR PURIFICATION SYSTEM

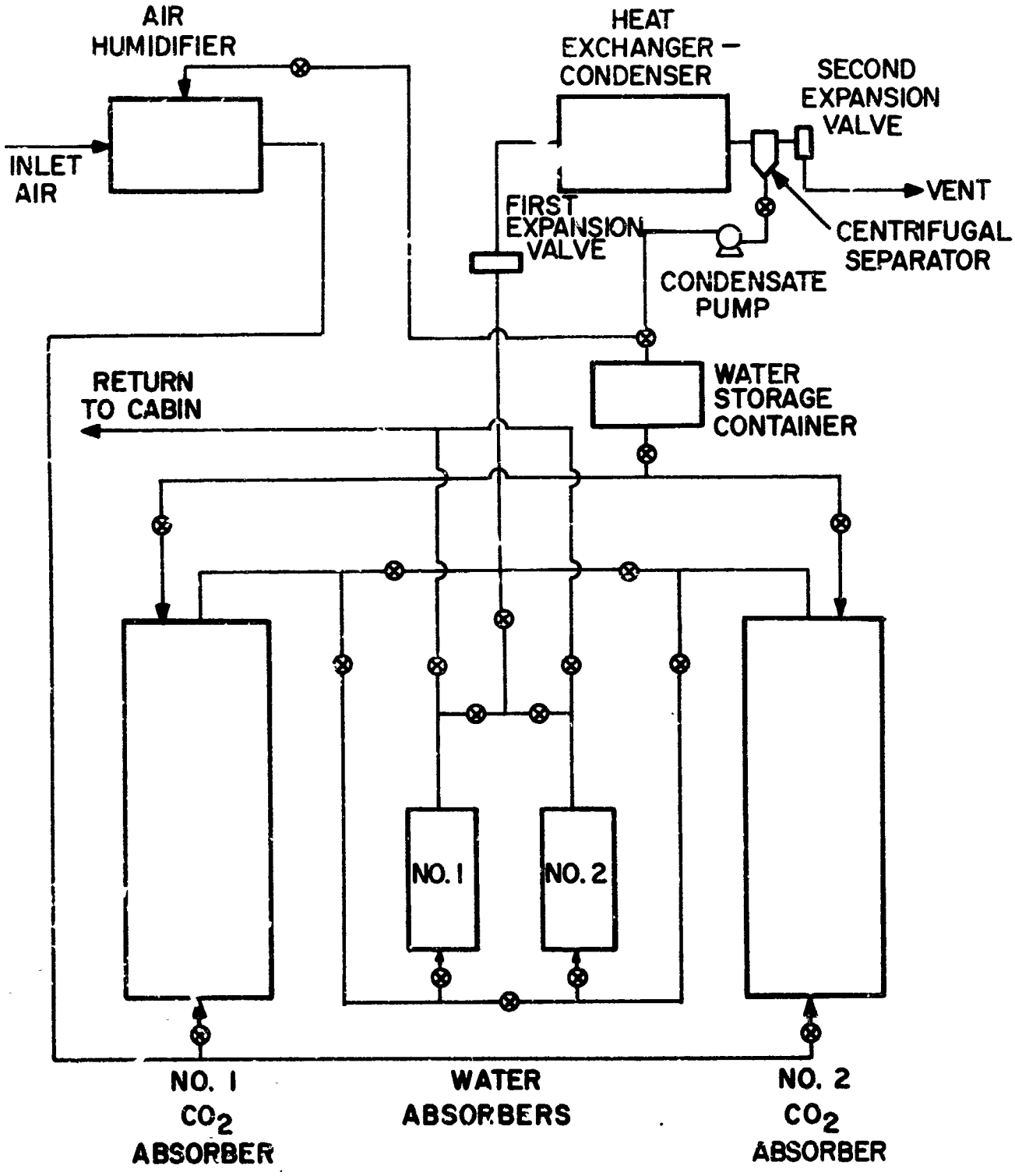

FIGURE 22

The air leaving the water absorber is near the ambient relative humidity in the cabin, namely, 50%. This entire system has duplicate carbon dioxide and water absorber beds, which are operated on alternate cycles for continous control of atmospheric CO_2 levels.

During the regeneration cycle, the valve at the bottom of the carbon dioxide absorber is closed and the carbon dioxide absorbing system is heated to 80°C. This can be done by electric heating elements or by the passage of a high frequency alternating current across the bed which is itself a good electrical conductor. The electric heaters are probably most efficient, but there are many ways of heating these columns efficiently. The carbon dioxide absorber column contains a negligible amount of air, since the volume is taken up almost entirely by the solid resin particles themselves. As the temperature in the carbon dioxide absorber is raised, the partial pressure of carbon dioxide is increased sharply. An automatically controlled expansion valve opens when the pressure on the upstream side exceeds a given preset level, which would presumably be at approximately 1/2 atmosphere. The vapor pressure of water at 80°C is 355 mm. The pressure setting of the expansion valve can be modified to obtain the most efficient regeneration in terms of maximum carbon dioxide and minimum water removal. Prior to the vent is a heat exchanger-condenser where the water vapor is condensed on a cold surface. In order to pass the condensate into the water storage container, one could employ a centrifugal device.

After the proper interval of time, the CO_2 absorber bed has been regenerated. Most of the carbon dioxide has been removed with a relatively small loss of water, as will be shown later.

At the same time, the water absorber unit is also heated to 80°C but its regeneration is continued until most of the water has been removed, condensed and centrifuged into the hold-up tank. The period of time required for this is relatively short because of the small size of the unit.

The second expansion valve opens only when the upstream pressure is less than the preset pressure. This valve follows the heat exchanger and vents the gas therein only after sufficient water has condensed so that the gas finally vented is much more concentrated in carbon dioxide than in water.

A small liquid pump distributes the condensate among the beds and humidifier column, while a holding tank provides storage for the condensate, which cannot be returned to the beds until their regeneration is complete.

A summary of the numerical values associated with this design appears in Table 17.

TABLE 17

NUMERICAL VALUES ASSOCIATED WITH DESIGN

CONDITIONS TO BE MAINTAINED IN CABIN:

1. 0.65% CO_2 by volume
2. 50% relative humidity at 20°C
3. CO_2 introduced into air only by exhalation, and water by both exhalation and perspiration, of two human beings.

LENGTH OF ABSORPTION CYCLE:

314 minutes

GAS FLOW:

5.114 standard cubic feet per minute

CO_2 ABSORBERS:

1. NUMBER: 2
2. FRACTION OF CAPACITY USED: 70%
3. WEIGHT OF PEI-ECH RESIN (DRY): 7538 grams per bed
4. ASSOCIATED WATER: 15076 grams per bed
5. CO_2 ABSORBED PER CYCLE: 503.7 grams per bed

WATER ABSORBERS:

1. NUMBER: 2
2. FRACTION OF CAPACITY USED: 50%
3. WEIGHT OF PEI-ECH (DRY): 899 grams per bed
4. WATER ABSORBED PER CYCLE: 899 grams per bed

HUMIDIFIER:

1. WATER DEPLETED PER CYCLE: 471.3 grams
2. SUGGESTED WATER INVENTORY: 6(471.3) = 2833 grams

PUMP CAPACITY:

5500 grams in 314 minutes

TABLE 17 (CONTINUED)

VOLUMES:

1. BEDS: Approximately 1.5 cubic feet total
2. AIR HUMIDIFIER: Less than 2.2 cubic feet
3. WATER STORAGE TANK: Less than two-tenths cubic feet
4. HEAT EXCHANGER-CONDENSER: Less than two cubic feet
5. TOTAL VOLUME (INCLUDING PIPING): Less than 10 cubic feet

HEAT LOADS:

1. CO_2 ABSORBER: 17880 Btu per cycle
2. WATER ABSORBER: 2400 Btu per cycle
3. TOTAL: 20280 Btu per cycle
4. POWER (AVERAGE): 1134 watts
5. CONDENSER (REFRIGERATION) (MAXIMUM): 2970 Btu per hr.
6. ABSORBER COOLING (REFRIGERATION): 4717 Btu per cycle.

B. Principles of Operation

ABSORPTION:

1.) About 5 scfm of air at 20°C and 50% RH containing 0.65% CO_2 by volume is blown through the air humidifier to raise it to 90% RH at 20°C.

2.) This gas then passes to the number one CO_2 absorber column where its CO_2 content is reduced to close to zero.

3.) From there, the excess water is absorbed in the number one water absorber column; the exit gas stream is returned to the cabin.

4.) At the end of the 314 minute period flow is transferred to the number two CO_2 and water absorbers by the control valves, and regeneration of the number one columns is begun.

REGENERATION:

1.) The small amount of air trapped in the void spaces of the packed beds is exhausted.

2.) The CO_2 absorber bed is heated to 80°C. The first automatically controlled expansion valve will open when the CO_2 and H_2O in the vapor phase exert the set point pressure.

3.) This gas then passes to the heat exchanger where most of the water is condensed. When the total pressure becomes less than the set point for the second automatic expansion valve, that valve will open to vent the remaining gas, which is mostly CO_2, to the space vacuum.

4.) Condensate is pumped into the water storage container.

5.) When CO_2 removal from this bed is finished, the heaters are turned off and the water from step 4 is pumped back into the column to resaturate the resin.

6.) The water absorber column is heated to 80°C now, and the identical procedure followed (there must of necessity be some CO_2 in this column too)

7.) Water is pumped back to the air humidifier only in the amount needed to replace what had been vaporized during the absorption cycle.

C. Additional Information

1.) The first expansion valve should be an automatic controller which has its inlet side set for a pressure of about 200 mm of mercury. In this way the regenerating absorber will be exhausted of air rapidly; with CO_2 escaping more rapidly from the resin than water at 80°C it may be possible to lower the water evaporation by not using the vapor pressure of water out of the resin as a set point but a lesser value instead. This will be true if the CO_2 partial pressure reaches equilibrium before H_2O partial pressure does. The greater the water equilibrium time compared to CO_2, the less the value of this pressure set point can be. The second valve should be set to open only when the pressure is less than about 20 mm of mercury, to exhaust CO_2 after the water is condensed.

2.) It is assumed that the heat exchanger-condenser (which saves the water vaporized during regeneration) can be maintained at 20°C or less by a combination of radiation to space and convection to the cooling medium of the cabin air conditioning system. It must provide a maximum of only about 3000 Btu/hr. The same applies to the cooling requirement of the beds after regeneration (a total of 4700 Btu per cycle).

3.) A blower or air compressor capable of providing at least 5.1 standard cubic feed per minute of gas at a maximum pressure of about 15 or 20 psig and a pump capable of a flow of .194 ft^3/314 min or 6.18×10^{-4} ft^3/min of water are needed.

VII. CONCLUSIONS

The polyethylenimine-epichlorohydrin resin is a good absorbing material for carbon dioxide. In fact, it is better than any other known resin, for Dowex WGR is the best commercial product available.

Carbon dioxide absorption capacity increases with increasing gaseous carbon dioxide partial pressure and increasing water content, and decreasing temperature.

A unique packing method and complete water saturation were required to prevent any effects of gas channeling, since these resins are such lightweight solids.

The reaction apparently takes place in four steps, with diffusion within the particles the major rate-controlling step. Diffusion through the surrounding liquid film is also an important contributing factor.

The PEI-ECH system should have immediate applicability to closed-volume air purification systems in both spacecraft and submarines. The general method of employing solid ion exchange resins to gas streams containing small amounts of contaminant should be useful for any contaminant which is reasonably soluble and forms an ionic compound in water, provided the proper resin is chosen (for example, ammonia could be absorbed by a high capacity acidic resin such as an acrylic).

It is recommended that future work also take place with the resins in a form such that the diffusion influence is reduced, thereby speeding up the reaction rate. Such a form is the ion-exchange membrane.

VIII. BIBLIOGRAPHY

1. R.R. Miller and V.R. Piatt, ed., NRL Report No. 5465 for U.S. Naval Research Laboratory, Washington, D.C. (1960).

2. V.R. Piatt and E.A. Ramskill, ed., NRL Report No. 5630 for U.S. Naval Research Laboratory, Washington, D.C. (1961).

3. J. Robins, Doctoral Dissertation in Chemistry, Polytechnic Institute of Brooklyn, 1959.

4. T.M.H. Saber, Doctoral Dissertation in Chemistry, Polytechnic Institute of Brooklyn, 1965.

5. M. Tetenbaum and H.P. Gregor, J. Am. Chem. Soc., 58, 1156 (1954).

6. G.D. Jones, et al. J. Org. Chem., 9, 125, 484 (1944).

7. H.P. Gregor, Chemistry Dept., Polytechnic Institute of Brooklyn, Brooklyn, N.Y., Private Communication (1965).

8. T.M.H. Saber, Polytechnic Institute of Brooklyn, Brooklyn, N.Y., Private Communication (1965).

9. R.G. Wolfe, Polytechnic Institute of Brooklyn, Brooklyn, N.Y., Private Communication (1966).

10. J.P. Allen, Technical Report AFFDL-TR-65-48 for Air Force Flight Dynamics Laboratory, Wright-Patterson Air Force Base, Ohio.

11. H.P. Gregor, Final Report, Contract No. nr-839(20) for U.S. Naval Research Laboratory, Washington, D.C. (1959).

12. S. Nonogaki, S. Makishima and Y.K. Yoneda, J. Phys. Chem., 62, 601 (1958).

13. W. Volk, "Applied Statistics for Engineers", McGraw-Hill Book Co., Inc., New York, 1958.

14. W. Kaplan, "Ordinary Differential Equations", Addison-Wesley Publishing Co., Inc., Reading, Mass., 1958.

15. R.B. Byrd, W.E. Stewart and E.N. Lightfoot, "Transport Phenomena", John Wiley and Sons, Inc., New York, 1960.

16. J. Crank, "The Mathematics of Diffusion", Oxford University Press, London, 1957.

17. A. Katchalsky and P. Spitnik, J. Polymer Sci., 2, 432 (1947).

18. D.H. Gold, Doctoral Dissertation in Chemistry, Polytechnic Institute of Brooklyn, 1956.

19. F. Helfferich, "Ion Exchange", McGraw-Hill Book Co., Inc., New York, 1962.

Bibliography (continued)

20. B.F. Dodge, "Chemical Engineering Thermodynamics", McGraw-Hill Book Co., Inc., New York, 1944.

21. H.P. Gregor, J. Am. Chem. Soc., 70, 1293 (1948).

22. H.S. Harned and R. Davis, J. Am. Chem. Soc., 65, 2030 (1943).

23. J. Frenkel, "Kinetic Theory of Liquids", Dover Publications, Inc., New York, 1955.

24. T.K. Sherwood and R.L. Pigford, "Absorption and Extraction", McGraw-Hill Book Co., Inc., New York, 1952.

25. H. Schlichting, "Boundary Layer Theory", 4th edition, McGraw-Hill Book Co., Inc., New York, 1960.

26. J.T. Edsall and J. Wyman, "Biophysical Chemistry", Vol. 1, Academic Press Inc., New York, 1958.

27. H.P. Gregor and K. Liu, J. Am. Chem. Soc., 87, 1678 (1965).

28. F.A. Zenz and D.F. Othmer, "Fluidization and Fluid Operations", Reinhold Publishing Corp., New York, 1960.

29. A.C. Guyton, "Textbook of Medical Physiology", W.B. Saunders Co., Philadelphia, 1961.

30. Special Report, Chemical and Engineering News, April 27, 1964, p. 79.

31. J.H. Perry, ed., Chemical Engineers Handbook, 3rd edition, McGraw-Hill Book Co., Inc., New York, 1950.

32. C.J. Major, Final Report, Contract No. NASr-73, for National Aeronautics and Space Administration, Houston, Texas (1965).

APPENDIX A

After work on the above contract had been completed, studies were continued without support of NASA to attempt to find improved methods for carbon dioxide control without the use of a granular material. Solid films have been prepared by the combination of polyethylenimine and epichlorohydrin together with a film-forming polymer such as a copolymer of vinyl chloride and acrilonitrile. The film-forming polymer is dissolved in a solution along with the basic polymer and the cross-linking agent and a film is cast which is dried and cured. Films having thicknesses varying from 1 mil to several mils have been prepared. These have strong acid and carbon dioxide capacities which are approximately the same as the granular resin because, under these circumstances, much less cross-linking agent is required. The water absorbing capacity is also lower, which is a pronounced weight advantage. The principal advantage of sheets of this material is the considerably simplified mechanical design which can be employed. Fig. 23 shows a few designs which have been tested in a preliminary cell. Here, a high rate of absorption is achieved because the thickness of the diffusion layer can be controlled at will and there is no problem of channeling of the beds. The changes in volume of the resin which occur during operation are handled by either a spring-loaded sandwich-type design or negative pressure design. The operating characteristics of such a device should compare quite favorably with those of the packed beds described in this report.

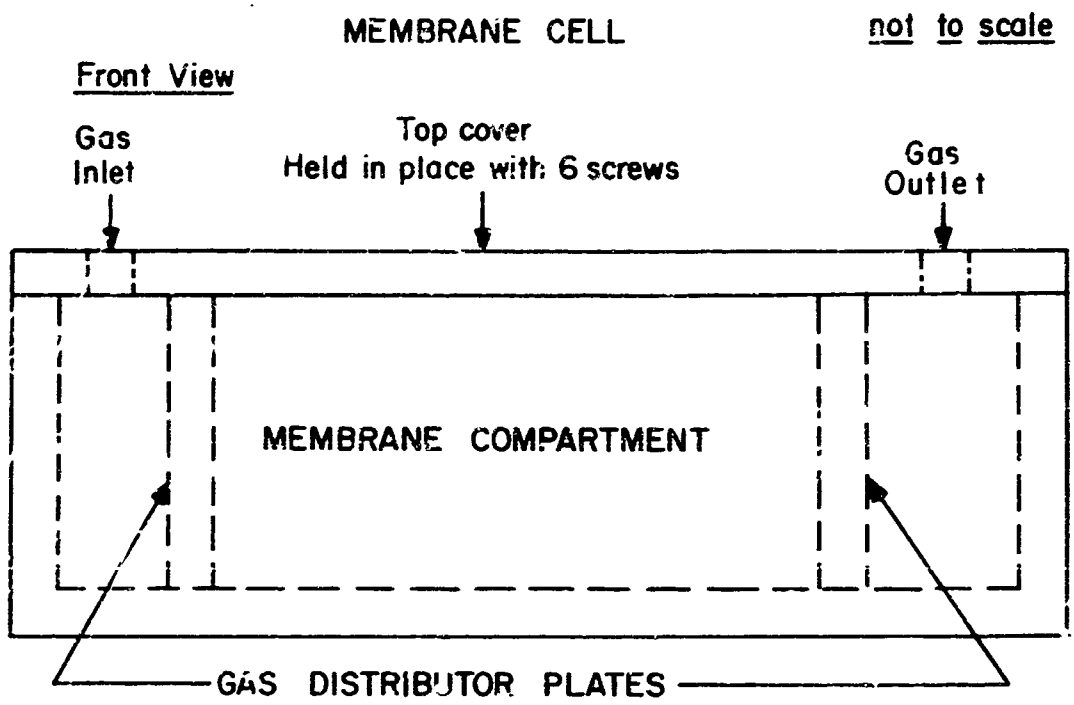
MEMBRANE CELL
not to scale
Front View
Gas Inlet
Top cover
Held in place with 6 screws
Gas Outlet
MEMBRANE COMPARTMENT
GAS DISTRIBUTOR PLATES

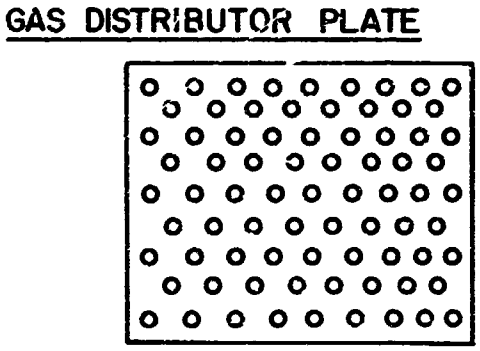
GAS DISTRIBUTOR PLATE

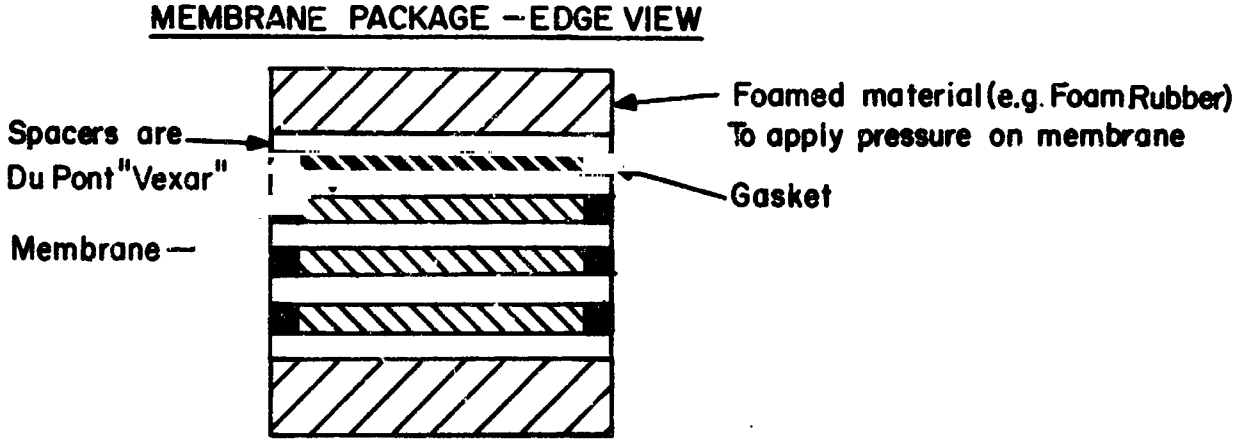
MEMBRANE PACKAGE – EDGE VIEW
Spacers are Du Pont "Vexar"
Membrane
Foamed material (e.g. Foam Rubber) To apply pressure on membrane
Gasket

FIGURE 23

APPENDIX B: TABLES AND CALCULATIONS

TABLE 18

TRIAL AND ERROR CALCULATIONS FOR BEST VALUES OF (D'/a^2) AND $(\beta a^2/D')$ FOR PEI - ECH RESIN

CONDITIONS: 0°C, 1.00% CO_2, 100% RH

$\frac{\beta a^2}{D'}$	t(min)	100	200	300	400	500	600	700	800
	$t^{\frac{1}{2}}$	10.00	14.14	17.32	20.00	22.37	24.49	26.44	28.28
	M_t/M_∞	.149	.229	.309	.389	.469	.552	.627	.692
80	$(D't/a^2)^{\frac{1}{2}}$	.109	.133	.155	.178	.2035	.233	.263	.293
	$(D'/a^2)^{\frac{1}{2}}$	.01090	.00994	.00894	.00890	.00909	.00951	.00994	.01037
125	$(D't/a^2)^{\frac{1}{2}}$	.096	.1165	.138	.161	.188	.2165	.251	.2815
	$(D'/a^2)^{\frac{1}{2}}$	.00960	.00823	.00796	.00809	.00892	.00892	.00949	.00994
100	$(D't/a^2)^{\frac{1}{2}}$	.1017	.124	.1465	.170	.194	.225	.2568	.2872
	$(D'/a^2)^{\frac{1}{2}}$	.01017	.00876	.00846	.00850	.00868	.00919	.00971	.01016

$(D'/a^2)_{avg} = 8.46 \times 10^{-5}$; $\beta = 100 \times 8.46 \times 10^{-5}$; $\therefore \beta = 8.46 \times 10^{-3}$ (minutes)$^{-1}$

TABLE 19

TRIAL AND ERROR CALCULATIONS FOR BEST VALUES OF (D'/a^2) AND $(\beta a^2/D')$ FOR PEI - ECH RESIN

CONDITIONS: 0°C, 0.30% CO_2, 100% RH

	t(min)	60	120	180	240	300	360	420
	$t^{\frac{1}{2}}$	7.75	10.95	13.42	15.49	17.32	18.97	20.49
$\frac{\beta a^2}{D'}$	M_t/M_∞	.158	.257	.340	.413	.476	.540	.586
80	$(D't/a^2)^{\frac{1}{2}}$	.1065	.141	.169	.185	.206	.228	.246
	$(D'/a^2)^{\frac{1}{2}}$	.01374	.01288	.01288	.01194	.01194	.01202	.01201
125	$(D't/a^2)^{\frac{1}{2}}$	.0985	.1235	.147	.169	.190	.2135	.2322
	$(D'/a^2)^{\frac{1}{2}}$	.01272	.01128	.01096	.01092	.01097	.01126	.01133

Ignoring the first column, the results are:

$(D'/a^2)_{avg} = 1.237 \times 10^{-4}$; $\beta = 125 \times 1.237 \times 10^{-4} = 1.546 \times 10^{-2}$

TABLE 20

TRIAL AND ERROR CALCULATIONS FOR BEST VALUES OF (D'/a^2) AND $(\beta a^2/D')$ FOR PEI - ECH RESIN

CONDITIONS: (FIRST RUN) 20°C, 1.00% CO_2, 100% RH

	t(min)	60	120	180	240	300
	$t^{\frac{1}{2}}$	7.75	10.95	13.42	15.49	17.32
$\frac{\beta a^2}{D'}$	M_t/M_∞	.244	.391	.520	.619	.689
13	$(D't/a^2)^{\frac{1}{2}}$	.236	.296	.341	.383	.416
	$(D'/a^2)^{\frac{1}{2}}$	.0304	.0268	.0254	.0247	.0240
20	$(D't/a^2)^{\frac{1}{2}}$	.205	.261	.302	.339	.368
	$(D/a^2)^{\frac{1}{2}}$	.0265	.0238	.0227	.0219	.0212
31	$(D't/a^2)^{\frac{1}{2}}$	.176	.229	.272	.304	.334
	$(D'/a^2)^{\frac{1}{2}}$	.0227	.0209	.0203	.0196	.0193
50	$(D't/a^2)^{\frac{1}{2}}$	.155	.200	.242	.280	.309
	$(D'/a^2)^{\frac{1}{2}}$	.0200	.0183	.0180	.0181	.0178
100	$(D't/a^2)^{\frac{1}{2}}$	.128	.1705	.2125	.253	.286
	$(D'/a^2)^{\frac{1}{2}}$	.01652	.01557	.01584	.01632	.01651
60	$(D'ta^2)^{\frac{1}{2}}$	.1465	.1905	.232	.269	.3005
	$(D'/a^2)^{\frac{1}{2}}$	.01891	.01739	.01730	.01736	.01736

Ignoring the first column, the results are:

$(D'/a^2)_{avg} = 3.011 \times 10^{-4}$; $\beta = 60 \times 3.011 \times 10^{-4} = 1.807 \times 10^{-2}$

TABLE 21

TRIAL AND ERROR CALCULATIONS FOR BEST VALUES OF (D'/a^2) AND $(\beta a^2/D')$ FOR PEI - ECH RESIN

CONDITIONS: (SECOND RUN) 20°C. 1.00% CO_2, 100% RH

	t(min)	80	160	240	320	400
	$t^{\frac{1}{2}}$	8.94	12.65	15.49	17.89	20.00
$\frac{\beta a^2}{D'}$	M_t/M_∞	.252	.434	.598	.722	.835
60	$(D't/a^2)^{\frac{1}{2}}$	.149	.204	.261	.317	.387
	$(D'/a^2)^{\frac{1}{2}}$	.01667	.01613	.01685	.01772	.01935
40	$(D't/a^2)^{\frac{1}{2}}$	.166	.222	.2795	.333	.402
	$(D'/a^2)^{\frac{1}{2}}$	.01857	.01755	.01803	.01861	.02010
20	$(D't/a^2)^{\frac{1}{2}}$	.2085	.275	.331	.383	.446
	$(D'/a^2)^{\frac{1}{2}}$	.02331	.02174	.02137	.02141	.02230
27	$(D't/a^2)^{\frac{1}{2}}$	.189	.254	.307	.358	.423
	$(D'/a^2)^{\frac{1}{2}}$	.02115	.02007	.01982	.02001	.02115

$(D'/a^2)_{avg} = 4.220 \times 10^{-4}$; $\beta = 27 \times 4.220 \times 10^{-4} = 1.141 \times 10^{-2}$

TABLE 22

TRIAL AND ERROR CALCULATIONS FOR BEST VALUES OF (D'/a^2) AND $(\beta a^2/D')$ FOR PEI - ECH RESIN

CONDITIONS: (THIRD RUN) 20°C, 1.00% CO_2, 100% RH

	t(min	60	120	180	240	300
	$t^{\frac{1}{2}}$	7.75	10.96	13.42	15.49	17.32
$\frac{\beta a^2}{D'}$	M_t/M_∞	.260	.403	.524	.614	.689
60	$(D't/a^2)^{\frac{1}{2}}$	.151	.194	.2337	.2665	.3005
	$(D'/a^2)^{\frac{1}{2}}$	.01948	.01771	.01741	.01721	.01736
75	$(D't/a^2)^{\frac{1}{2}}$	.144	.184	.225	.259	.2935
	$(D'/a^2)^{\frac{1}{2}}$	.01858	.01679	.01685	.01672	.01696
80	$(D't/a^2)^{\frac{1}{2}}$	.142	.182	.2215	.2565	.2918
	$(D'/a^2)^{\frac{1}{2}}$	.01832	.01662	.01651	.01657	.01684
70	$(D't/a^2)^{\frac{1}{2}}$	.1453	.1867	.228	.2635	.296
	$(D'/a^2)^{\frac{1}{2}}$	.01876	.01702	.01701	.01700	.01709

Ignoring the first column, the results are:

$(D'/a^2)_{avg} = 2.903 \times 10^{-4}$; $\beta = 70 \times 2.903 \times 10^{-4} = 2.033 \times 10^{-2}$

TABLE 23

TRIAL AND ERROR CALCULATIONS FOR BEST VALUES OF (D'/a^2) AND $(\beta a^2/D')$ FOR PEI - ECH RESIN

CONDITIONS: 20°C, 0.65% CO_2, 100% RH

	t(min)	60	120	180	240	300
	$t^{\frac{1}{2}}$	7.75	10.96	13.42	15.49	17.32
$\frac{\beta a^2}{D'}$	M_t/M_∞	.245	.363	.471	.579	.686
60	$(D't/a^2)^{\frac{1}{2}}$	.1465	.182	.2155	.2533	.299
	$(D'/a^2)^{\frac{1}{2}}$	.01890	.01662	.01605	.01634	.01727
51	$(D't/a^2)^{\frac{1}{2}}$	.1553	.192	.226	.264	.3082
	$(D'/a^2)^{\frac{1}{2}}$	.02040	.01753	.01686	.01705	.01778
75	$(D't/a^2)^{\frac{1}{2}}$	.1359	.172	.206	.246	.2915
	$(D'/a^2)^{\frac{1}{2}}$	.01753	.01572	.01572	.01588	.01682
100	$(D't/a^2)^{\frac{1}{2}}$	.1283	.162	.195	.236	.2837
	$(D'/a^2)^{\frac{1}{2}}$	.01657	.01479	.01453	.01523	.01638
115	$(D't/a^2)^{\frac{1}{2}}$	.124	.158	.191	.232	.278
	$(D'/a^2)^{\frac{1}{2}}$	.01601	.01443	.01424	.01498	.01605
110	$(D't/a^2)^{\frac{1}{2}}$	.126	.1595	.1925	.233	.282
	$(D'/a^2)^{\frac{1}{2}}$	.01628	.01457	.01435	.01504	.01628

$(D'/a^2)_{avg} = 2.340 \times 10^{-4}$; $\beta = 110 \times 2.340 \times 10^{-4} = 2.573 \times 10^{-2}$

TABLE 24

TRIAL AND ERROR CALCULATIONS FOR BEST VALUES OF (D'/a^2) AND $(\beta a^2/D')$ FOR PEI - ECH RESIN

CONDITIONS: 20°C, 0.30% CO_2, 100% RH

	t(min)	60	120	180	240	300
	$t^{\frac{1}{2}}$	7.75	10.96	13.42	15.49	17.32
$\frac{\beta a^2}{D'}$	M_t/M_∞	.215	.362	.501	.620	.725
60	$(D't/a^2)$	.137	.182	.226	.269	.319
	(D'/a^2)	.01768	.01662	.01683	.01737	.01832
49	$(D't/a^2)$	.153	.203	.246	.284	[illegible]
	(D'/a^2)	.0 973	[illegible]	[illegible]	[illegible]	[illegible]
55	$(D't/a^2)$	.143	.186	.2305	.2735	.322
	(D'/a^2)	.01845	.01699	.01719	.01765	.01858
48	$(D't/a^2)$	.147	.194	.238	.280	.328
	(D'/a^2)	.01896	.01772	.01773	.01807	.01893
50	$(D't/a^2)$	.1455	.193	.2365	.280	.3265
	(D'/a^2)	.01878	.01764	.01763	.01807	.01884

$(D'/a^2)_{avg} = 3.314 \times 10^{-4}$; $\beta = 50 \times 3.313 \times 10^{-4} = 1.657 \times 10^{-2}$

TABLE 25

TRIAL AND ERROR CALCULATIONS FOR BEST VALUES OF (D'/a^2) AND $(\beta a^2, D')$ FOR PEI - ECH RESIN

CONDITIONS: 40°C, 1.00% CO_2, 100% RH

	t(min)	30	60	90	120	150	180	210	240
	$t^{\frac{1}{2}}$	5.48	7.75	9.49	10.96	12.24	13.42	14.49	15.49
$\frac{\beta a^2}{D'}$	M_t/M_∞	.262	.437	.579	.682	.755	.8125	.861	.897
60	$(D't/a^2)^{\frac{1}{2}}$	.1518	.2042	.2532	.297	.335	.3715	.4095	.448
	$(D'/a^2)^{\frac{1}{2}}$	.02773	.02636	.02667	.02710	.02737	.02827	.02827	.02828
33	$(D't/a^2)^{\frac{1}{2}}$	.181	.236	.286	.328	.364	.397	.434	.469
	$(D'/a^2)^{\frac{1}{2}}$	.03303	.03045	.03015	.02995	02973	.02958	.02998	.03029
48	$(D't/a^2)^{\frac{1}{2}}$	.161	.215	.263	.307	.345	.380	.414	.450
	$(D'/a^2)^{\frac{1}{2}}$	.02939	.02777	.02773	.02802	.02818	.02832	.02832	.02903
51	$(D't/a^2)^{\frac{1}{2}}$	.159	.2143	.264	.305	.342	.378	.415	.4505
	$(D'/a^2)^{\frac{1}{2}}$	.02903	.02770	.02782	.02783	.02792	.02818	.02864	.02906

$(D'/a^2)_{avg} = 8.010 \times 10^{-4}$; $\beta = 51 \times 8.010 \times 10^{-4} = 4.085 \times 10^{-2}$

TABLE 26

TRIAL AND ERROR CALCULATIONS FOR BEST VALUES OF (D'/a^2) AND $(\beta a^2/D')$ FOR PEI-ECH RESIN

CONDITIONS: 40°C, 0.30% CO_2, 100% RH

	t(min)	40	80	120	160	200
	$t^{\frac{1}{2}}$	6.32	8.94	10.96	12.65	14.14
$\frac{\beta a^2}{D'}$	M_t/M_∞	.248	.427	.565	.682	.786
40	$(D't/a^2)^{\frac{1}{2}}$	.164	.220	.267	.314	.3685
	$(D'/a^2)^{\frac{1}{2}}$	.02593	.02461	.02438	.02482	.02604
36	$(D't/a^2)^{\frac{1}{2}}$	.170	.2275	.2753	.322	.374
	$(D'/a^2)^{\frac{1}{2}}$	.02687	.02546	.02513	.02546	.02644
38	$(D't/a^2)^{\frac{1}{2}}$	.167	.2238	.2713	.3195	.372
	$(D'/a^2)^{\frac{1}{2}}$	.02640	.02503	.02477	.02524	.02629
39	$(D't/a^2)^{\frac{1}{2}}$	.1655	.222	.2698	.317	.3805
	$(D'/a^2)^{\frac{1}{2}}$	.02617	.02482	.02462	.02505	.02619

$(D'/a^2)_{avg} = 6.44 \times 10^{-4}$; $\beta = 39 \times 6.44 \times 10^{-4} = 2.515 \times 10^{-2}$

TABLE 27

TRIAL AND ERROR CALCULATIONS FOR BEST VALUES OF (D'/a^2) AND $(\beta a^2/D')$ FOR PEI - ECH RESIN

CONDITIONS: 70°C, 1.00% CO_2, 100% RH

	t(min	20	40	60	80	100
	$t^{\frac{1}{2}}$	4.46	6.32	7.75	8.94	10.00
$\frac{\beta a^2}{D'}$	M_t/M_∞	.407	.623	.750	.844	.911
36	$(D't/a^2)^{\frac{1}{2}}$	.221	.298	.355	.4125	.476
	$(D'/a^2)^{\frac{1}{2}}$	.0496	.0471	.0458	.0461	0476
40	$(D't/a^2)^{\frac{1}{2}}$	.214	.289	.348	.409	.473
	$(D'/a^2)^{\frac{1}{2}}$	.0480	.0457	.0449	.0458	.0473
48	$(D't/a^2)^{\frac{1}{2}}$	.2063	.2803	.342	.401	.463
	$(D'/a^2)^{\frac{1}{2}}$	.0462	.0444	.0441	.0449	.0463

$(D'/a^2)_{avg} = 20.46 \times 10^{-4}$; $\beta = 48 \times 20.46 \times 10^{-4} = 9.84 \times 10^{-2}$

TABLE 28

TRIAL AND ERROR CALCULATIONS FOR BEST VALUES OF (D'/a^2) AND $(\beta a^2/D')$ FOR PEI - ECH RESIN

CONDITIONS: 70°C, 0.30% CO_2, 100% RH

	t(min)	20	40	60	80	100
	$t^{\frac{1}{2}}$	4.46	6.32	7.75	8.94	10.00
$\frac{\beta a^2}{D'}$	M_t/M_∞	.305	.515	.666	.778	.864
50	$(D't/a^2)^{\frac{1}{2}}$	.174	.241	.299	.356	.419
	$(D'/a^2)^{\frac{1}{2}}$	.0390	.0381	.0386	.0398	.419
40	$(D't/a^2)^{\frac{1}{2}}$	.183	.249	.307	.363	.425
	$(D'/a^2)^{\frac{1}{2}}$	.0411	.0394	.0396	.0496	.0425
31	$(D't/a^2)^{\frac{1}{2}}$	.198	.270	.324	.379	.437
	$(D'/a^2)^{\frac{1}{2}}$	.0444	.0427	0418	.0423	.0437
36	$(D't/a^2)^{\frac{1}{2}}$	.189	.257	.316	.369	.430
	$(D'/a^2)^{\frac{1}{2}}$	.0424	.0406	.0408	.0413	.0430
33	$(D't/a^2)^{\frac{1}{2}}$	.195	.262	.321	.377	.436
	$(D'/a^2)^{\frac{1}{2}}$	.0428	.0414	.0414	.0421	.0436

By linear interpolation, the results are:

$(D'/a^2)_{avg} = 18.16 \times 10^{-4}$; $\beta = 32 \times 18.16 \times 10^{-4} = 5.81 \times 10^{-2}$

TABLE 29

TRIAL AND ERROR CALCULATIONS FOR BEST RESULTS OF $(D't/a^2)$ AND $(\beta a^2/D')$ FOR PEI - ECH RESIN

CONDITIONS: 20°C, 1.00% CO_2, 70% RH

	t(min)	60	120	180	240	300
	$t^{\frac{1}{2}}$	7.75	10.96	13.42	15.49	17.32
$\frac{\beta a^2}{D'}$	M_t/M_∞	.248	.521	.588	.753	.876
20	$(D't/a^2)^{\frac{1}{2}}$	.2065	.271	.3265	.3985	.478
	$(D'/a^2)^{\frac{1}{2}}$	.02666	.02473	.02434	.02573	.02761
10	$(D't/a^2)^{\frac{1}{2}}$	.256	.332	.400	.4815	.565
	$(D'/a^2)^{\frac{1}{2}}$	.03303	.03013	.02982	.03110	.03265
12	$(D't/a^2)^{\frac{1}{2}}$	.2413	.315	.3815	.457	.537
	$(D'/a^2)^{\frac{1}{2}}$	.03112	.02877	.02842	.02952	.03104

$(D'/a^2)_{avg} = 8.86 \times 10^{-4}$; $\beta = 12 \times 8.86 \times 10^{-4} = 1.064 \times 10^{-2}$

TABLE 30

TRIAL AND ERROR CALCULATIONS FOR BEST VALUES OF (D'/a^2) AND $(\beta a^2/D')$ FOR PEI - ECH RESIN

CONDITIONS: 20°C, 1.00% CO_2, 55% RH

	t(min)	60	120	180	240	300
	$t^{\frac{1}{2}}$	7.75	10.96	13.42	15.49	17.32
$\frac{\beta a^2}{D'}$	M_t/M_∞	.176	.355	.573	.756	.888
51	$(D' t/a^2)^{\frac{1}{2}}$	.133	.190	.262	.342	.442
	$(D'/a^2)^{\frac{1}{2}}$	.01716	.01734	.01953	.02207	.02553
13	$(D't/a^2)^{\frac{1}{2}}$	.204	.2805	.3635	.450	.542
	$(D'/a^2)^{\frac{1}{2}}$	.02633	.02562	.02708	.02904	.03130
7	$(D't/a^2)^{\frac{1}{2}}$	.250	.343	.441	.541	.645
	$(D'/a^2)^{\frac{1}{2}}$	.03228	.03113	.03283	.03493	.03724
10	$(D't/a^2)^{\frac{1}{2}}$	.220	.304	.394	.483	.576
	$(D'/a^2)^{\frac{1}{2}}$	.02840	.02777	.02936	.03117	.03323

Lack of any constancy among the values of $(D'/a^2)^{\frac{1}{2}}$ indicates that the postulated diffusion model does not fit these data.

TABLE 31

CALCULATED VALUES OF VARIABLES FROM THE GENERALIZED CORRELATIONS FOR PEI-ECH RESIN

T (°K)	P_{CO_2} (atm)	K	M_∞ (meq/g)	βR (min^{-1})	$\frac{D_2}{a^2} \times 10^4$ (min^{-1})	R	$\beta \times 10^2$ (min^{-1})	$\beta a^2/D$
273	.01	108.3	4.64	44.2	1.133	3978	1.112	98.1
273	.003	108.3	2.04	44.2	1.133	5815	0.760	67.0
293	.01	68.9	2.95	93.9	2.960	4450	2.110	71.3
293	.0065	68.9	2.17	93.9	2.960	5090	1.845	62.4
293	.003	68.9	1.30	93.9	2.960	6510	1.444	48.8
313	.01	46.4	1.99	183	6.980	4918	3.717	53.3
313	.003	46.4	.873	183	6.980	7200	2.542	36.5
343	.01	27.9	1.19	426	20.40	5590	7.613	37.3
343	.003	27.9	.524	426	20.40	8185	5.210	25.5

PERCENTAGE DIFFERENCES BETWEEN CALCULATED AND EXPERIMENTAL VALUES

T	P_{CO_2}	K	M_∞	βR	D'/a^2	R	β	$\beta a^2/D'$
273	.01	+10.4	+14.3	+58.9	-33.9	+21.2	+31.4	-1.90
273	.003		+14.6	-40.3	-8.42	+21.4	-28.1	-46.4
293	.01		+1.72	+27.4	-13.4	+0.41	+27.1	+36.2
293	.0065	-0.58	-1.36	-29.5	+26.5	+1.74	-28.3	-43.2
293	.003		+2.36	-12.6	-10.6	+0.39	-12.9	-2.40
313	.01	-15.8	-3.24	-11.2	-12.9	-2.61	-8.97	+4.51
313	.003		-27.8	-17.3	+6.40	-18.1	+1.07	+6.85
343	.01		+12.6	-1.20	-0.30	+27.5	-22.6	+28.6
343	.003	+9.41	+16.4	-15.8	+12.3	+29.2	-10.3	+25.5

TABLE 32

FRACTIONAL MASS UPTAKE DATA (DERIVED FROM THE GENERAL CORRELATIONS) FOR DESIGN CONDITIONS OF 20°C, 0.65% CO_2, AND 100% RH IN A FRESH, WATER-SATURATED PACKED BED OF PEI - ECH RESIN (GRAPHICAL REPRESENTATION IS GIVEN IN FIGURE 35, IN CONJUNCTION WITH CORRESPONDING EXPERIMENTAL DATA)

TIME t(min)	$(D't/a^2)^{\frac{1}{2}}$	M_t/M_∞	M_t (gms/dry gm)
20	.0769	.054	.00516
40	.1088	.128	.01223
60	.1332	.203	.01940
80	.1539	.274	.02618
100	.1720	.334	.03193
120	.1885	.391	.03757
140	.2036	.440	.04205
160	.2176	.484	.04205
180	.2306	.522	.04632
200	.2434	.556	.04990
220	.2550	.587	.05311
240	.2664	.616	.05613
260	.2775	.641	.05885
280	.2878	.665	.06125
300	.2979	.684	.06305
320	.3078	.705	.06735
340	.3171	.724	.06918
360	.3263	.742	.07090
380	.3353	.758	.07240
400	.3440	.772	.07382

NOTES

From Figure 14, $D'/a^2 = 2.96 \times 10^{-4}$ (minutes)$^{-1}$

From Figure 16, $\beta R = 93.9$ (minutes)$^{-1}$

From Figure 3, $M_\infty = 2.17$ (meq/dry gram)

From Equation 24, $R = 4947\ (.0065)^{-.316} \exp(-910/(1.987 \times 293)) = 5090$

$\therefore\ \beta = (\beta R)/R = 93.9/5090 = 1.845 \times 10^{-2}$ (minutes)$^{-1}$

$\therefore\ \beta a^2/D' = 1.845 \times 10^{-2}/2.96 \times 10^{-4} = 62.35$

Values of M_t/M_∞ are gotten by linear interpolation between the M_t/M_∞ curves for $\beta a^2/D' = 60$ (Figure 75) and $\beta a^2/D' = 65$ (Figure 77).

M_t (gms/dry gram) = $(M_t/M_\infty)(M_\infty)$ (44/1000)

TABLE 33

TRIAL AND ERROR CALCULATION FOR BEST VALUES OF

(D'/a^2) AND $\beta a^2/D'$

FOR AMBERLITE IRA-93 RESIN

CONDITIONS: 20°C, 1.00% CO_2, 100% RH

t (min)	$t^{\frac{1}{2}}$	M_t/M_∞	$(D'/a^2)^{\frac{1}{2}}$	$(D't/a^2)^{\frac{1}{2}}$	$(D't/a^2)^{\frac{1}{2}}$	$(D'/a^2)^{\frac{1}{2}}$	$(D't/a^2)^{\frac{1}{2}}$	$(D'/a^2)^{\frac{1}{2}}$
5	2.237	.313	.102	.0456	.264	.1181	.192	.0858
10	3.161	.537	.191	.0601	.348	.1102	.264	.0834
15	3.873	.687	.264	.0682	.414	.1069	.324	.0836
20	4.470	.782	.324	.0724	.464	.1039	.372	.0832
25	5.000	.844	.373	.0746	.503	.1007	.413	.0826
30	5.475	.884	.409	.0747	.539	.0984	.447	.0817
35	5.915	.912	.440	.0774	.567	.0958	.476	.0804
40	6.325	.934	.472	.0746	.594	.0939	.515	.0814
45	6.710	.954	.509	.0758	.624	.0931	.548	.0816
50	7.070	.970	.553	.0782	.654	.0925	.580	.0820
55	7.415	.983	.600	.0809	.700	.0944	.628	.0846
60	7.750	.992	.665	.0858			.667	.0861
71		1.000						

$$D'/a^2 = 6.89 \times 10^{-3} \text{ min}^{-1}$$

$\beta = 36 \times 6.89 \times 10^{-3} = .248 \text{ min}^{-1}$

The manufacturer states that the particles have a diameter range of .40 to .50 mm, so that a is approximately $\frac{1}{2}(.40 + .50)$ mm $= 2.25 \times 10^{-2}$ cm.

$$R = \frac{11.97/78}{(1.173)(3.93 \times 10^{-2})(10^{-2})} - 1 = 331$$

$D = (D'/a^2)(R+1)(a^2) = (6.89\times10^{-3})(332)(5.07\times10^{-4})/60 = 1.93\times10^{-5}$ cm^2/sec

$60/\beta R = 60/(.248 \times 331) = .731 = (a^2/3)(\delta/a)/D_L$, and $D_L = 1.77\times10^{-5}$ cm^2/sec

$\therefore \delta/a = 0.077$

TABLE 34

TRIAL AND ERROR CALCULATIONS FOR BEST VALUES OF

(D'/a^2) AND $(\beta a^2/D')$

FOR DOWEX WGR RESIN

CONDITIONS: 0°C, 1.00% CO_2, 100% RH

	t(min)	80	160	240	320	400	480	560
	$t^{\frac{1}{2}}$	8.94	12.65	15.49	17.89	20.00	21.92	23.66
$\frac{\beta a^2}{D'}$	M_t/M_∞	.212	.325	.437	.549	.661	.774	.875
95	$(D'/a^2)^{\frac{1}{2}}$	.123	.151	.185	.225	.273	.335	.417
	$(D'/a^2)^{\frac{1}{2}}$	.01377	.01193	.01195	.01258	.01365	.01528	.01762
38	$(D't/a^2)^{\frac{1}{2}}$	.1567	.193	.226	.264	.308	.358	.438
	$(D'/a^2)^{\frac{1}{2}}$	.01751	.01526	.01459	.01476	.01540	.01634	.01849
26	$(D't/a^2)^{\frac{1}{2}}$	.176	.219	.257	.293	.335	.388	.455
	$(D'/a^2)^{\frac{1}{2}}$	.01968	.01733	.01659	.01638	.01675	.01770	.01923
29	$(D't/a^2)^{\frac{1}{2}}$	.170	.210	.249	.287	.329	.382	.450
	$(D'/a^2)^{\frac{1}{2}}$	.01901	.01661	.01608	.01604	.01645	.01742	.01902

$(D'/a^2)_{avg} = 2.97 \times 10^{-4}$ (minutes)$^{-1}$; $\beta = 29 \times 2.97 \times 10^{-4} = .861 \times 10^{-2}$

TABLE 35

TRIAL AND ERROR CALCULATIONS FOR BEST VALUES OF (D'/a^2) AND $(\beta a^2/D)$ FOR DOWEX WGR RESIN

CONDITIONS: 0°C, 0.30% CO_2, 100% RH

	t(min)	80	160	240	320	400	480
	$t^{1/2}$	8.94	12.65	15.49	17.89	20.00	21.92
$\frac{\beta a^2}{D}$	M_t/M_∞	.351	.558	.679	.775	.853	.917
48	$(D't/a^2)^{\frac{1}{2}}$	.190	.255	.306	.356	.408	.472
	$(D'/a^2)^{\frac{1}{2}}$	.02125	.02015	.01975	.01989	.02040	.02155
40	$(D't/a^2)^{\frac{1}{2}}$	.198	.264	.313	.361	.416	.481
	$(D'/a^2)^{\frac{1}{2}}$	.02213	.02086	.02023	.02020	.02080	.02194

By Interpolation: $\frac{\beta a^2}{D} = 43$; $(D'/a^2)_{avg} = 4.37 \times 10^{-4}$ (minutes)$^{-4}$

$\beta = 43 \times 4.37 \times 10^{-4} = 1.882 \times 10^{-2}$ (minutes)$^{-1}$.

TABLE 36

TRIAL AND ERROR CALCULATIONS FOR BEST VALUES OF (D'/a^2) AND $(\beta a^2/D')$ FOR DOWEX W G R RESIN

CONDITIONS: [FIRST] 20°C, 1.00% CO_2, 100% RH

	t(min)	60	120	180	240	300	360
	$t^{1/2}$	7.75	10.96	13.42	15.49	17.32	18.98
$\frac{\beta a^2}{D'}$	M_t/M_∞	.279	.440	.571	.689	.795	.882
80	$(D't/a^2)^{\frac{1}{2}}$	.1475	.194	.239	.292	.355	.425
	$(D'/a^2)^{\frac{1}{2}}$	.01902	.01772	.01780	.01885	.02051	.02239
51	$(D't/a^2)^{\frac{1}{2}}$	.166	.216	.261	.3085	.365	.435
	$(D'/a^2)^{\frac{1}{2}}$	.02141	.01971	.01945	.01992	.02107	.02293
38	$(D't/a^2)^{\frac{1}{2}}$	.179	.2265	.272	.320	.3765	.444
	$(D'/a^2)^{\frac{1}{2}}$	.02308	.02069	.02027	.02065	.02175	.02340
33	$(D't/a^2)^{\frac{1}{2}}$	.1865	.2365	.2825	.3315	.385	.452
	$(D'/a^2)^{\frac{1}{2}}$	.02405	.02160	.02104	.02141	.02222	.02382
36	$(D't/a^2)^{\frac{1}{2}}$	.181	.2315	.2775	.325	.380	.445
	$(D'/a^2)^{\frac{1}{2}}$	.02336	.02114	.02067	.02098	.02194	.02345

$\frac{\beta a^2}{D'} = 35$; $(D'/a^2)_{avg} = 4.90 \times 10^{-4}$ (minutes)$^{-1}$; $\beta = 35 \times 4.90 \times 10^{-4}$

$= 1.717 \times 10^{-2}$ (minutes)$^{-1}$.

TABLE 37

TRIAL AND ERROR CALCULATIONS FOR BEST VALUES OF (D'/a^2) AND $(\beta a^2/D')$ FOR DOWEX WGR RESIN

CONDITIONS: (SECOND) 20°C, 1.00% CO_2, 100% RH

$\frac{\beta a^2}{D'}$	t(min)	60	120	180	240	300	360
	$t^{1/2}$	7.75	10.96	13.42	15.49	17.32	18.98
	M_t/M_∞	.259	.431	.581	.707	.810	.892
23	$(D' t/a^2)^{\frac{1}{2}}$	.201	.262	.313	.365	.421	.482
	$(D'/a^2)^{\frac{1}{2}}$	.02594	.02392	.02331	.02358	.02430	.02542
25	$(D' t/a^2)^{\frac{1}{2}}$	.195	.255	.306	.358	.414	.477
	$(D'/a^2)^{\frac{1}{2}}$	.02517	.02345	.02281	.02312	.02390	.02515

$(D'/a^2)_{avg} = 5.73 \times 10^{-4}$ (minutes)$^{-1}$; $\beta = 25 \times 5.73 \times 10^{-4} = 1.433 \times 10^{-2}$ (minutes)$^{-1}$.

TABLE 38

TRIAL AND ERROR CALCULATIONS FOR BEST VALUES OF (D'/a^2) AND $(\beta a^2/D')$ FOR DOWEX WGR RESIN

CONDITIONS: 20°C, 0.65% CO_2, 100% RH

	t(min)	60	120	180	240	300	360
	$t^{1/2}$	7.75	10.96	13.42	15.49	17.32	18.98
$\frac{\beta a^2}{D'}$	M_t/M_∞	.231	.412	.567	.700	.808	.891
23	$(D't/a^2)^{\frac{1}{2}}$	.188	.256	.307	.3615	.420	.481
	$(D'/a^2)^{\frac{1}{2}}$	.02427	.02336	.02287	.02333	.02424	.02532
19	$(D't/a^2)^{\frac{1}{2}}$	.203	.270	.3235	.378	.433	.4935
	$(D'/a^2)^{\frac{1}{2}}$	.02621	.02464	.02412	.02439	.02498	.02599
20	$(D't/a^2)^{\frac{1}{2}}$	.2005	.268	.3195	.375	.428	.492
	$(D'/a^2)^{\frac{1}{2}}$	.02589	.02447	.02383	.02422	.02468	.02593

$(D'/a^2)_{avg} = 6.18 \times 10^{-4}$ (minutes)$^{-1}$; $\beta = 20 \times 6.18 \times 10^{-4}$

$\beta = 1.236 \times 10^{-2}$ (minutes)$^{-1}$.

TABLE 39

TRIAL AND ERROR CALCULATIONS FOR BEST VALUES OF (D'/a^2) AND $(\beta a^2/D')$ FOR DOWEX WGR RESIN

CONDITIONS: 20°C, 0.30% CO_2, 100% RH

	t(min)	60	120	180	240	300	360
	$t^{1/2}$	7.75	10.96	13.42	15.49	17.32	18.98
$\frac{\beta a^2}{D'}$	M_t/M_∞	.229	.330	.531	.671	.794	.875
21	$(D't/a^2)^{\frac{1}{2}}$	.194	.2525	.3033	.357	.418	.474
	$(D'/a^2)^{\frac{1}{2}}$	.02509	.02306	.02259	.02303	.02414	.02499
22	$(D't/a^2)^{\frac{1}{2}}$	.193	.249	.299	.354	.417	.473
	$(D'/a^2)^{\frac{1}{2}}$	.02490	.02272	.02228	.02284	.02408	.02492

$(D'/a^2)_{avg} = 5.58 \times 10^{-4}$ (minutes)$^{-1}$; $\beta = 22 \times 5.58 \times 10^{-4}$

$\beta = 1.228 \times 10^{-2}$ (minutes)$^{-1}$.

TABLE 40

TRIAL AND ERROR CALCULATIONS FOR BEST VALUES OF (D'/a^2) AND $(\beta a^2/D')$ FOR DOWEX WGR RESIN

CONDITIONS: 20°C, 0.30% CO_2, 100% RH (GAS) [WITHOUT RE-WETTING SURFACE]

	t(min)	20	60	100	140	180	220
	$t^{1/2}$	4.47	7.75	10.00	11.82	13.42	14.83
$\frac{\beta a^2}{D'}$	M_t/M_∞	.221	.409	.566	.699	.808	.891
55	$(D't/a^2)^{\frac{1}{2}}$	.144	.200	.253	.310	.372	.440
	$(D'/a^2)^{\frac{1}{2}}$	.03218	.02581	.02530	.02623	.02773	.02967
75	$(D't/a^2)^{\frac{1}{2}}$	.132	.188	.240	.299	.363	.437
	$(D'/a^2)^{\frac{1}{2}}$	.02950	.02426	.02400	.02528	.02703	.02948

$D'/a^2 = 7.07 \times 10^{-4}$ (minutes)$^{-1}$; $\beta = 75 \times 7.07 \times 10^{-4}$

$= 5.31 \times 10^{-2}$ (minutes)$^{-1}$.

TABLE 41

TRIAL AND ERROR CALCULATIONS FOR BEST VALUES OF (D'/a^2) AND $(\beta a^2/D')$ FOR DOWEX WGR RESIN

CONDITIONS: 40°C, 1.00% CO_2, 100% RH

	t(min)	20	50	80	110	140	170	200
	$t^{1/2}$	4.47	7.07	8.94	10.49	11.82	13.03	14.14
	$\frac{\beta a^2}{D'} M_t M_\infty$	.1587	.343	.482	.612	.727	.819	.894
28	$(D't/a^2)^{\frac{1}{2}}$	.150	.218	.266	.310	.358	.409	.472
	$((D'/a^2)^{\frac{1}{2}}$	.03352	.03082	.02975	.02955	.03030	.03141	.03339
29	$(D't/a^2)^{\frac{1}{2}}$	.147	.2165	.264	.3085	.3575	.408	.469
	$(D'/a^2)^{\frac{1}{2}}$	.03287	.03063	.02953	.02941	.03020	.03125	.03314

By interpolation: $\frac{\beta a^2}{D'} = 28.4$; $(D'/a^2)_{avg} = 9.71 \times 10^{-4}$ (minutes)$^{-1}$;

$\beta = 28.4 \times 9.71 \times 10^{-4} = 2.757 \times 10^{-2}$ (minutes)$^{-1}$.

TABLE 42

TRIAL AND ERROR CALCULATIONS FOR BEST VALUES OF (D'/a^2) AND $(\beta a^2/D')$ FOR DOWEX WGR RESIN

CONDITIONS. 40°C. 0.30% CO_2, 100%RH

	t(min)	20	50	80	110	140	170	200
	$t^{\frac{1}{2}}$	4.47	7.07	8.94	10.49	11.82	13.03	14.14
$\frac{\beta a^2}{D'}$	M_t/M_∞	.1664	.347	.497	.628	.739	.834	.903
26	$(D't/a^2)^{\frac{1}{2}}$	.156	.227	.277	.321	.371	.424	.483
	$(D'/a^2)^{\frac{1}{2}}$	.03488	.03210	.03099	.03060	.03137	.03254	.03414
31	$(D't/a^2)^{\frac{1}{2}}$	.147	.213	.264	.308	.359	.414	.4735
	$(D'/a^2)^{\frac{1}{2}}$	.03287	.03011	.02954	.02937	.03039	.03178	.03347
28	$(D't/a^2)^{\frac{1}{2}}$	.1515	.221	.271	.315	.365	.419	.480
	$(D'/a^2)^{\frac{1}{2}}$	.03388	.03123	.03033	.03003	.03089	.03217	.03394

$(D'/a^2)_{avg} = 10.12 \times 10^{-4}(\text{minutes})^{-1}$;

$\beta = 28 \times 10.12 \times 10^{-4} = 2.837 \times 10^{-2}(\text{minutes})^{-1}$

TABLE 43

TRAIL AND ERROR CALCULATIONS FOR BEST VALUES OF (D'/a^2) AND $(\beta a^2/D')$ FOR DOWEX WGR RESIN

CONDITIONS: 70°C, 1.00% CO_2, 100%RH

	t(min)	5	10	15	20	25	30	35	40	45
	$t^{\frac{1}{2}}$	2.237	2.162	3.872	4.470	5.000	5.480	5.915	6.324	6.710
$\frac{\beta a^2}{D'}$	M_t/M_∞	.2773	.4325	.5534	.6290	.7045	.770	.826	.873	.911
29	$(D't/a^2)^{\frac{1}{2}}$	.193	.2475	.288	.316	.348	.380	.4115	.448	.486
	$(D'/a^2)^{\frac{1}{2}}$	.082	.0782	.0744	.0707	.0696	.0693	.0696	.0707	.0724
36	$(D't/a^2)^{\frac{1}{2}}$	.180	.229	.271	.300	.332	.3645	.401	.436	.475
	$(D't/a^2)^{\frac{1}{2}}$	.0805	.0724	.0699	.0671	.0664	.0666	.0679	.0689	.0708
51	$(D't/a^2)^{\frac{1}{2}}$	.1653	.2133	.2545	.2835	.3165	.350	.387	.4265	.466
	$(D'/a^2)^{\frac{1}{2}}$	.0739	.0674	.0657	.0634	.0633	.0639	.0654	.0675	.0694
65	$(D't/a^2)^{\frac{1}{2}}$	.1535	.199	.239	.271	.306	.341	.380	.418	.461
	$(D'/a^2)^{\frac{1}{2}}$	.0686	.0629	.0617	.0606	.0612	.0622	.0641	.0660	.0687

$$(D'/a^2)_{avg} = 40.96 \times 10^{-4} (\text{minutes})^{-1};$$

$$\beta = 65 \times 40.96 \times 10^{-4} = 26.63 \times 10^{-2} \ (\text{minutes})^{-1}$$

TABLE 44

TRIAL AND ERROR CALCULATIONS FOR BEST VALUES OF (D'/a^2) AND $(\beta a^2/D')$ FOR DOWEX WGR RESIN

CONDITIONS: 70°C, 0.30% CO_2, 100% RH

	t(min)	5	10	15	20	25	30	35	40
	$t^{\frac{1}{2}}$	2.237	2.162	3.872	4.470	5.000	5.480	5.915	6.325
$\frac{\beta a^2}{D'}$	M_t/M_∞	.2538	.408	.5364	.646	.739	.8135	.8735	.919
51	$(D't/a^2)^{\frac{1}{2}}$	.158	.206	.249	.291	.333	.378	.427	.475
	$(D'/a^2)^{\frac{1}{2}}$	.0623	.0651	.0643	.0651	.0666	.0690	.0722	.0751
36	$(D't/a^2)^{\frac{1}{2}}$	.1717	.2215	.264	.306	.3485	.3905	.4375	.487
	$(D'/a^2)^{\frac{1}{2}}$	.0765	.0699	.0682	.0684	.0697	.0713	.0739	.0770
33	$(D't/a^2)^{\frac{1}{2}}$	.1785	.2265	.269	.312	.356	.396	.446	.493
	$(D'/a^2)^{\frac{1}{2}}$	.0798	.0717	.0694	.0697	.0712	.0723	.0753	.0779

$\frac{\beta a^2}{D} \approx 35$; $(D'/a^2)_{avg} = 52.87 \times 10^{-4}$ (minutes)$^{-1}$

$\beta = 35 \times 52.87 \times 10^{-4} = 18.52 \times 10^{-2}$ (minutes)$^{-1}$

TABLE 45

DETERMINATION OF WATER CAPACITY OF RESINS

SAMPLE	WEIGHTS	DOWEX WGR	PEI-ECH
A	Tare	1.3461 gms	1.3337 gms
	Wet+Tare	3.6300 gms	4.1376 gms
	Dry+Tare	2.3587 gms	2.2840 gms
	Water	1.2713 gms	1.8536 gms
	Resin	1.0126 gms	0.9503 gms
	Ratio	1.255 gms/gm	1.952 gms/gm
B	Tare	1.3353 gms	1.3432 gms
	Wet+Tare	3.7670 gms	4.4135 gms
	Dry+Tare	2.4193 gms	2.3958 gms
	Water	1.3477 gms	2.0177 gms
	Resin	1.0840 gms	1.0526 gms
	Ratio	1.242 gms/gm	1.915 gms/gm
C	Tare	1.3350 gms	1.3399 gms
	Wet+Tare	3.6798 gms	4.5396 gms
	Dry+Tare	2.3800 gms	2.4795 gms
	Water	1.2998 gms	2.0601 gms
	Resin	1.0450 gms	1.1396 gms
	Ratio	1.243 gms/gm	1.807 gms/gm
D	Tare	1.3399 gms	1.3351 gms
	Wet+Tare	3.5500 gms	7.9086 gms
	Dry+Tare	2.3255 gms	3.6938 gms
	Water	1.2245 gms	4.2148 gms
	Resin	0.9856 gms	2.3587 gms
	Ratio	1.242 gms/gm	1.788 gms/gm

For Dowex WGR, the average value of the ratio of water to dry resin is 1.245 grams per gram. For PEI-ECH, it was assumed that, since weight loss to the atmosphere must have been rapid right from the instant that filtration ceased, the true value of the water capacity should be slightly greater than that exhibited by the first sample. Therefore, the capacity was assumed to be 2.00 grams of water per gram of dry resin.

APPENDIX C: GRAPHS OF EXPERIMENTAL RESULTS

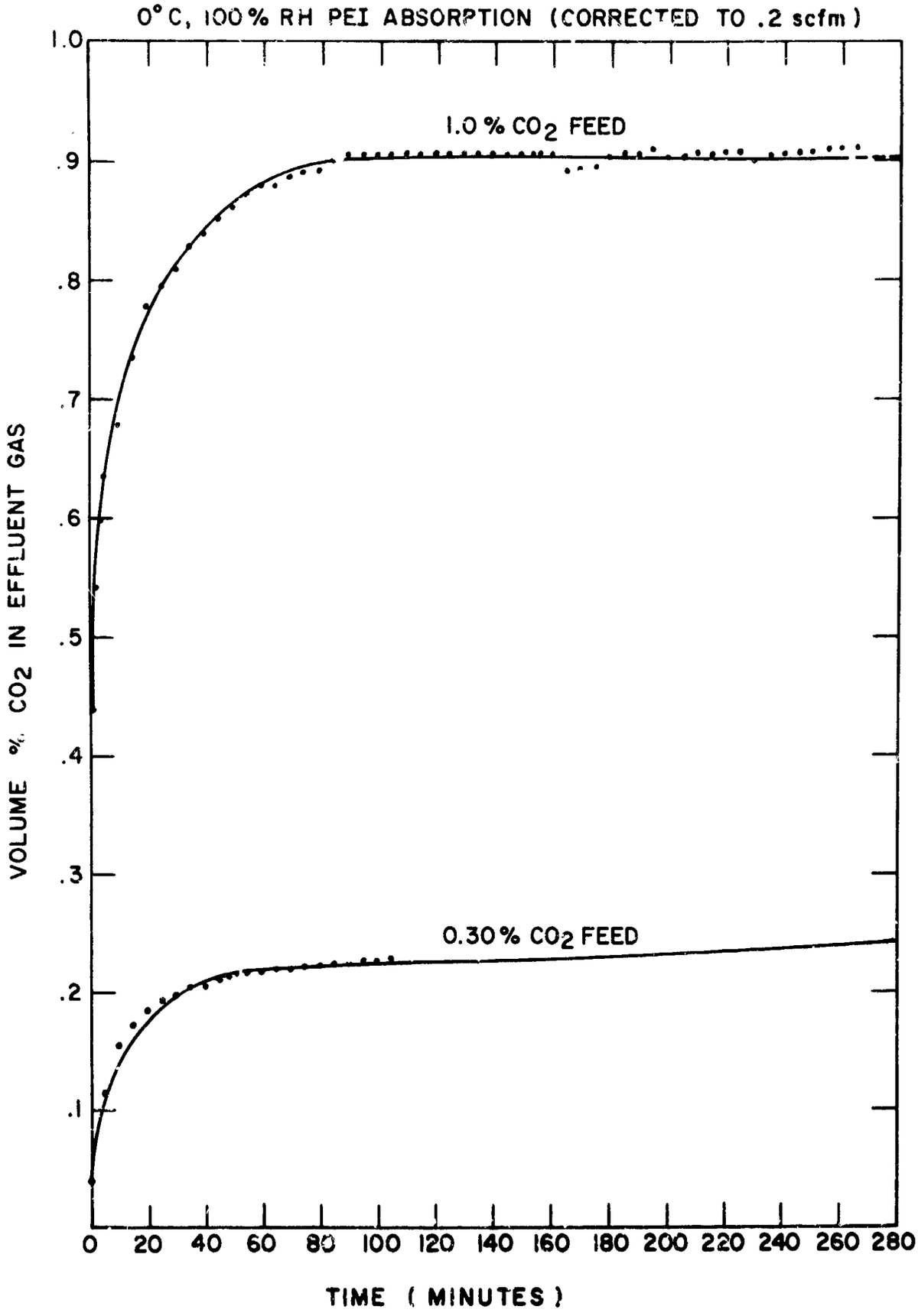
0° C, 100% RH PEI ABSORPTION (CORRECTED TO .2 scfm)
1.0 % CO2 FEED
0.30 % CO2 FEED
VOLUME % CO2 IN EFFLUENT GAS
1.0
.9
.8
.7
.6
.5
.4
.3
.2
.1
0
20
40
60
80
100
120
140
160
180
200
220
240
260
280
TIME (MINUTES)

FIGURE 24

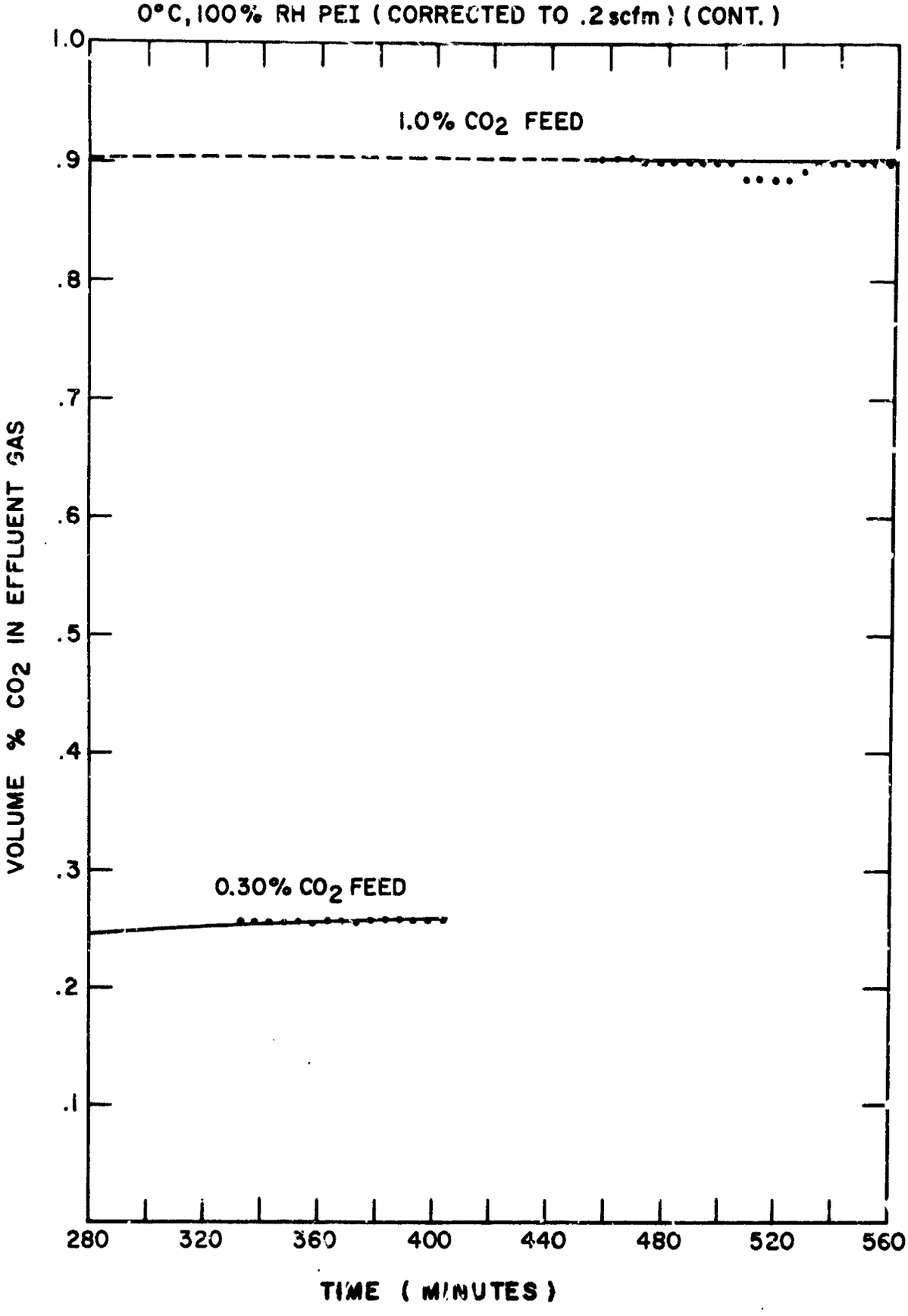

FIGURE 24 (CONTINUED)

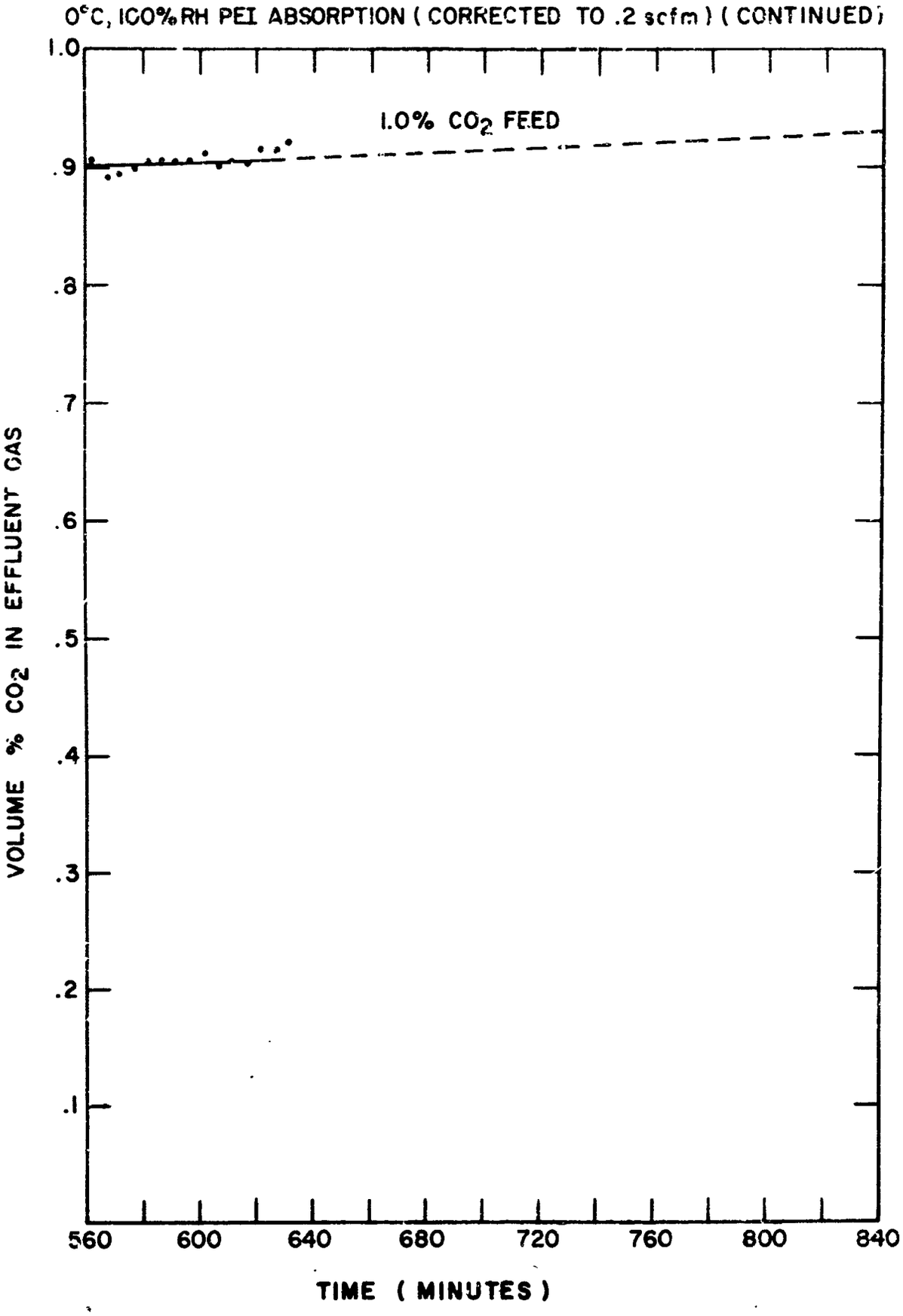

FIGURE 24 (CONTINUED)

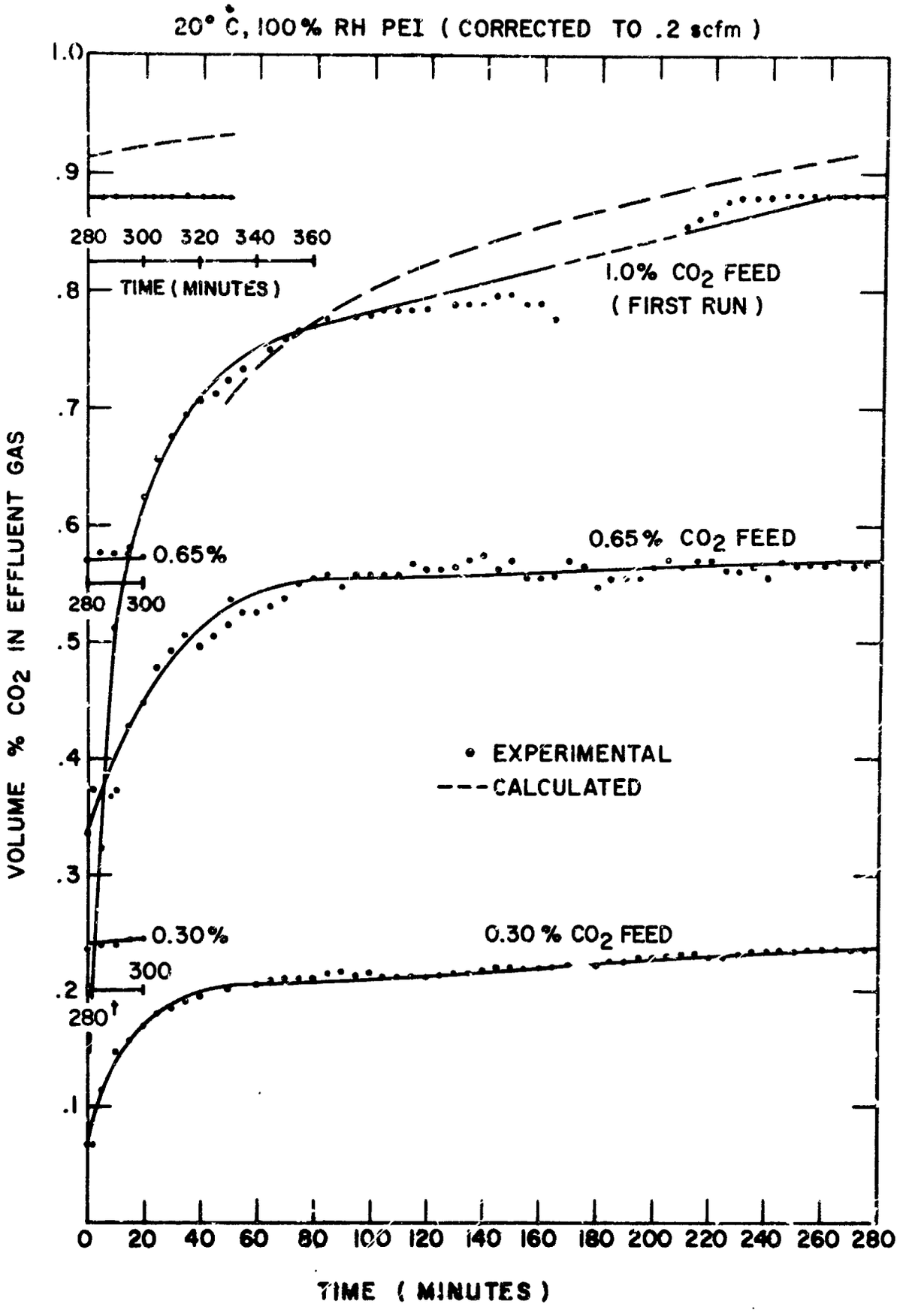

FIGURE 25
PAGE 148

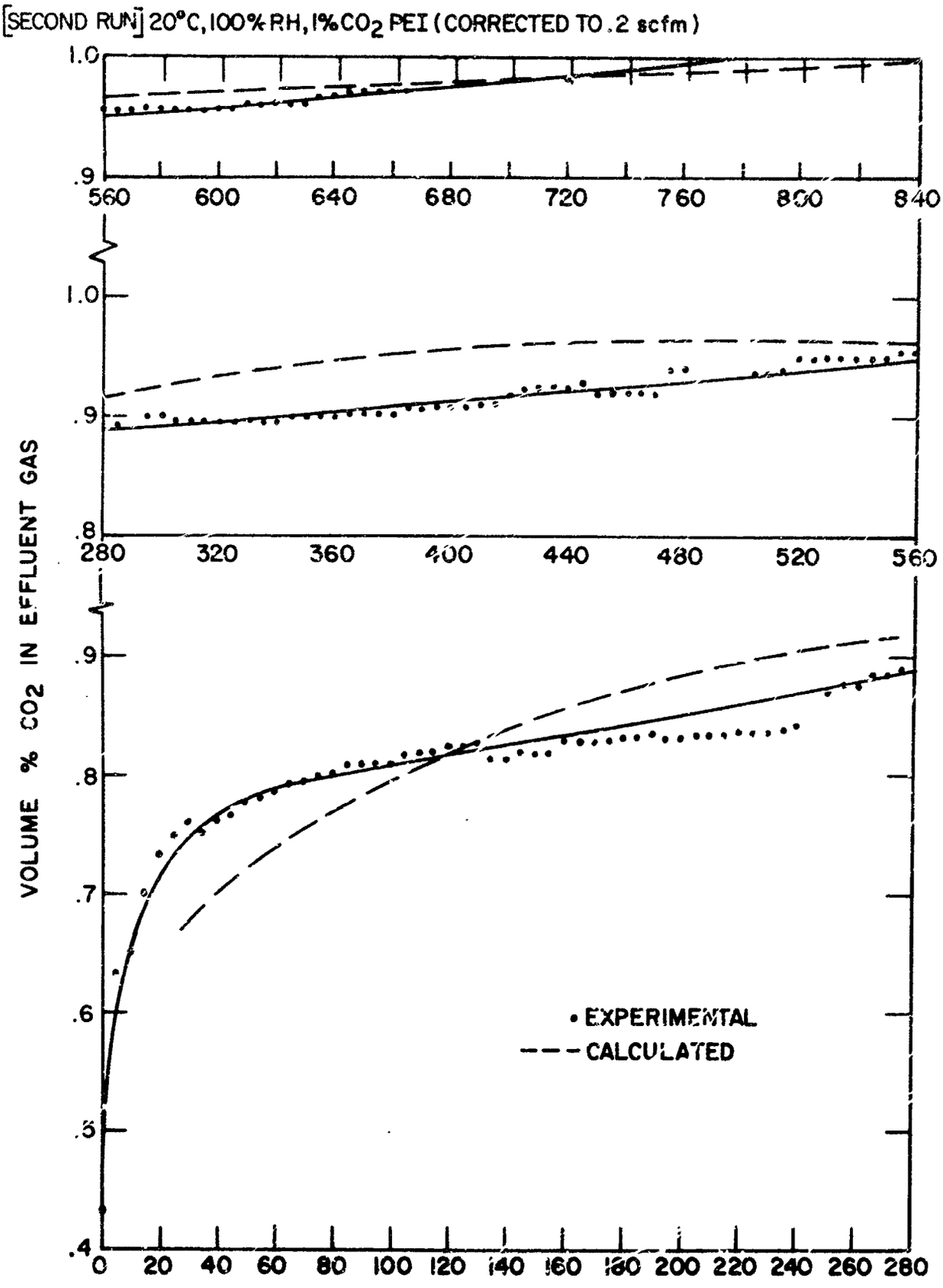
[SECOND RUN] 20°C, 100% RH, 1% CO_2 PEI (CORRECTED TO .2 scfm)
VOLUME % CO_2 IN EFFLUENT GAS
TIME (MINUTES)
• EXPERIMENTAL
– – – CALCULATED

FIGURE 26

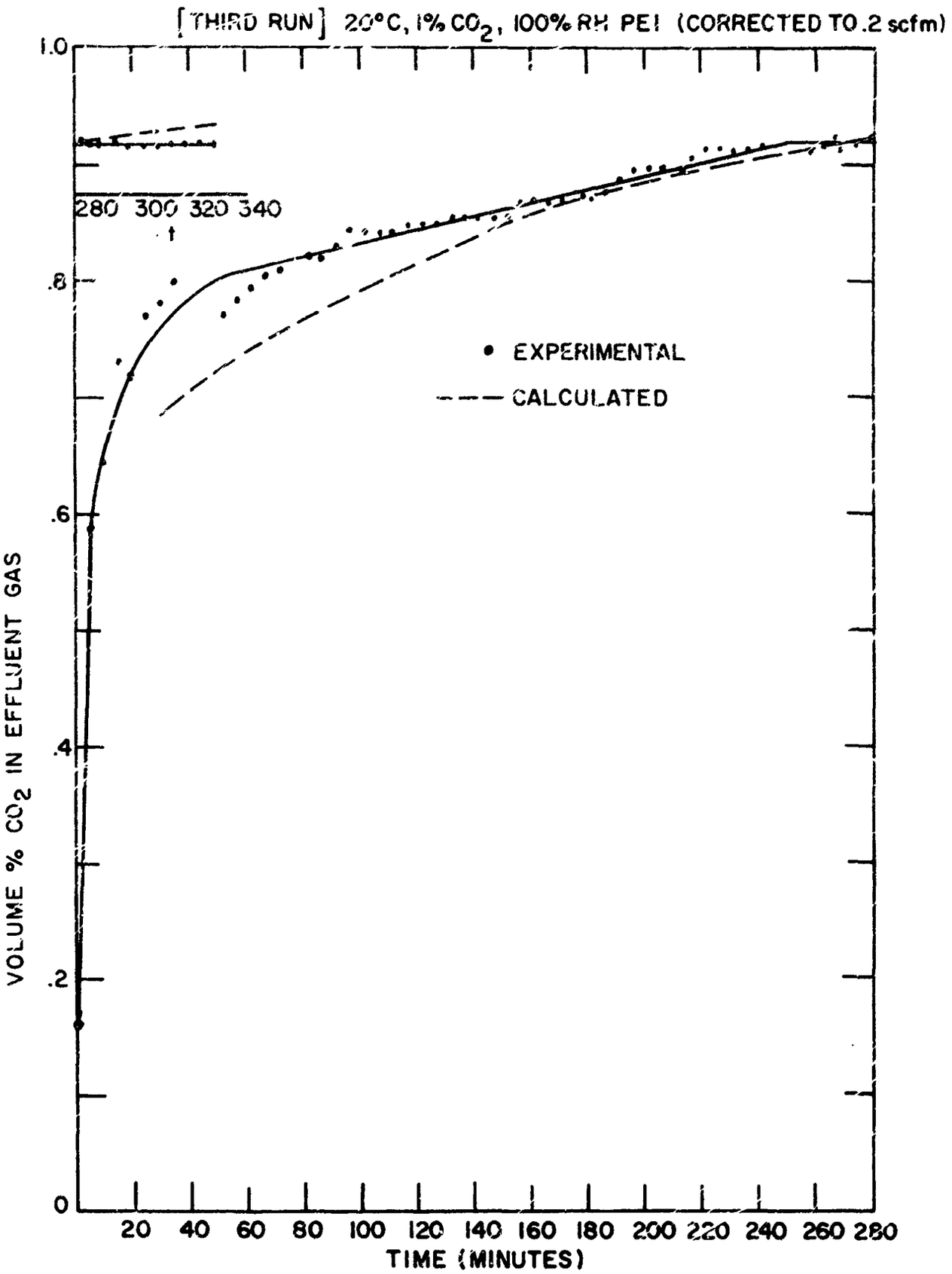
[THIRD RUN] 20°C, 1% CO_2, 100% RH PEI (CORRECTED TO .2 scfm)
1.0
.8
.6
.4
.2
0
280 300 320 340
t
• EXPERIMENTAL
CALCULATED
VOLUME % CO_2 IN EFFLUENT GAS
20 40 60 80 100 120 140 160 180 200 220 240 260 280
TIME (MINUTES)

FIGURE 27

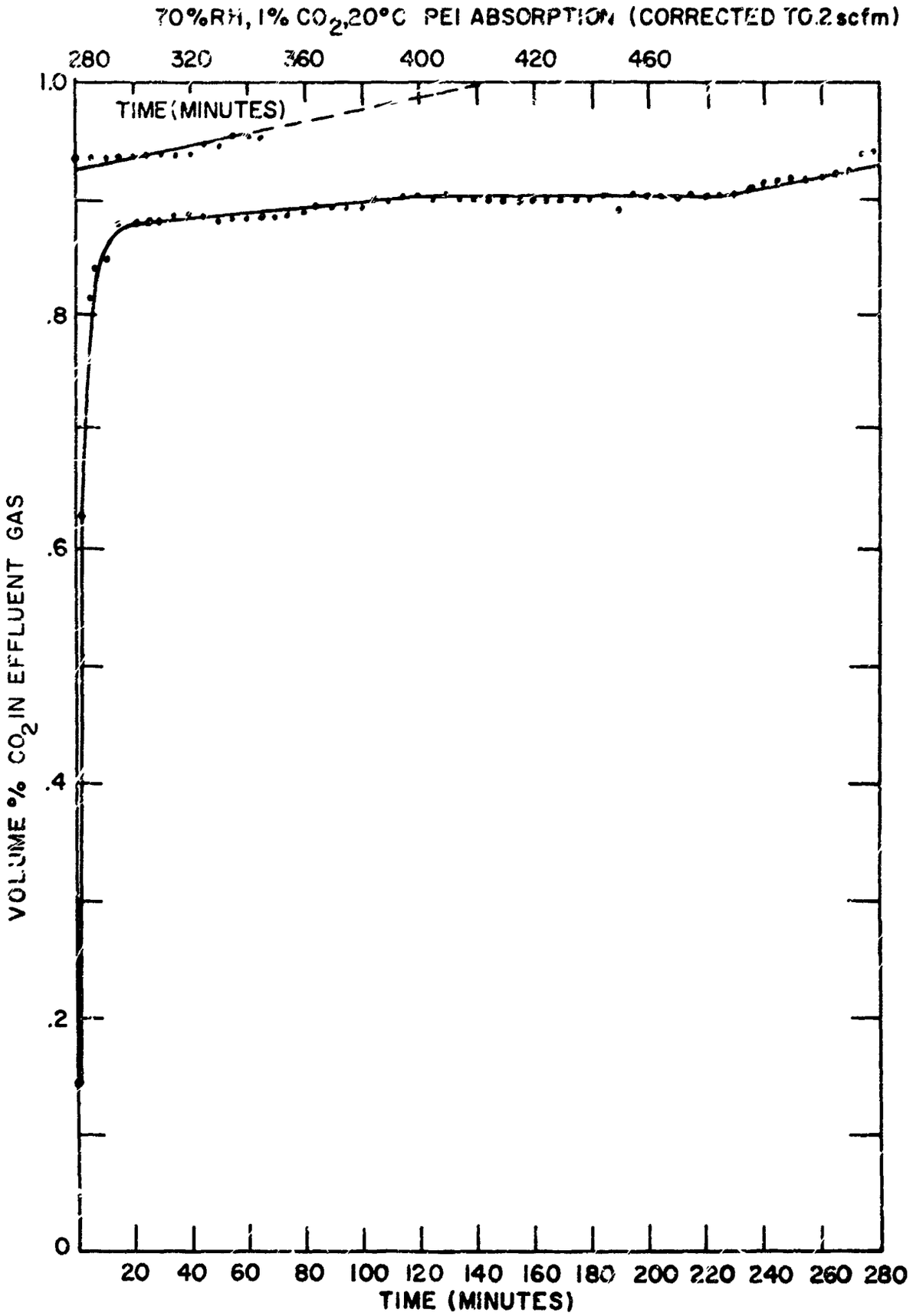
70%RH, 1% CO_2, 20°C PEI ABSORPTION (CORRECTED TO 2 scfm)
280
320
360
400
420
460
TIME (MINUTES)
1.0
.8
.6
.4
.2
0
VOLUME % CO_2 IN EFFLUENT GAS
20
40
60
80
100
120
140
160
180
200
220
240
260
280
TIME (MINUTES)

FIGURE 28

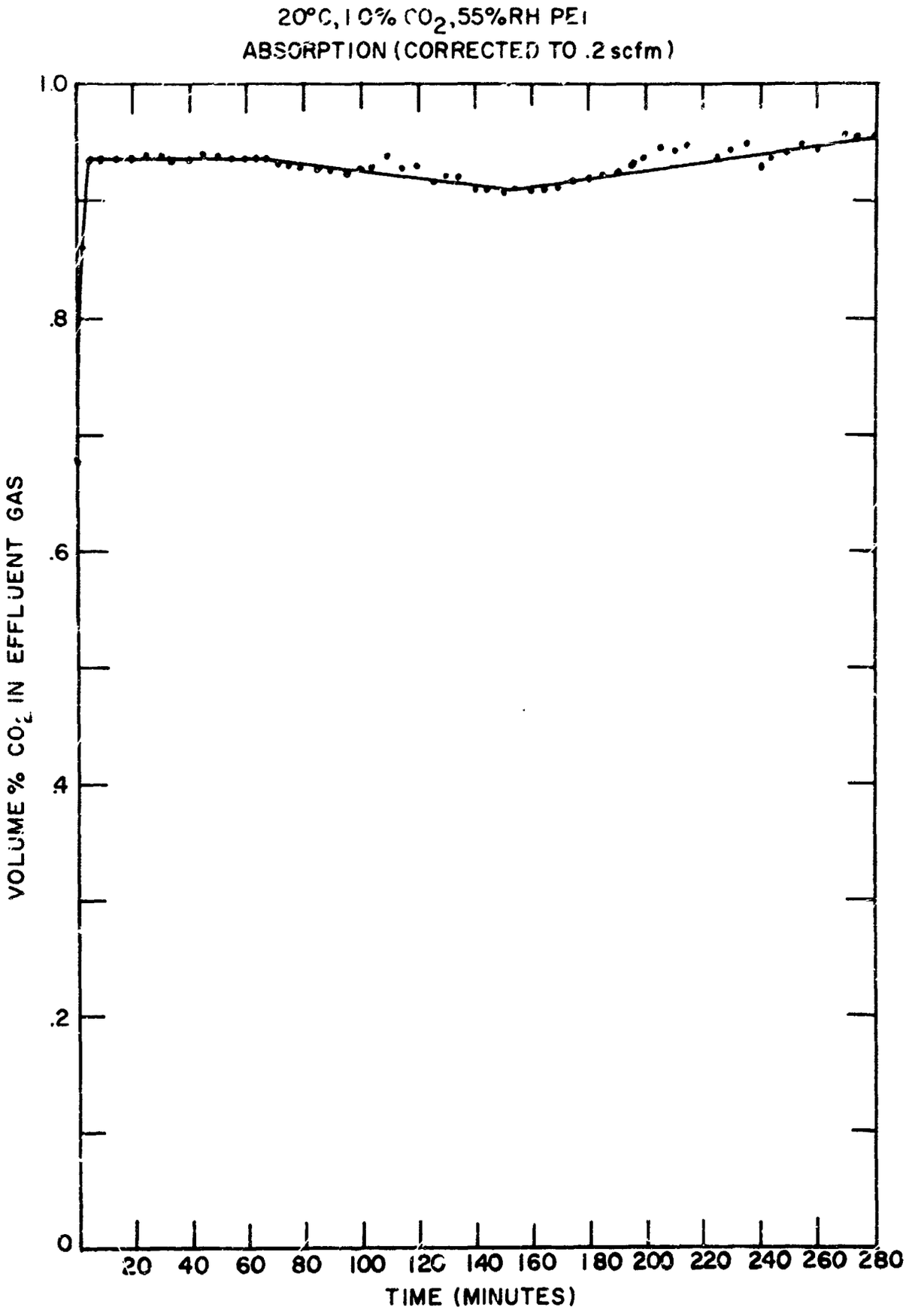
20°C, 10% CO_2, 55%RH PEI
ABSORPTION (CORRECTED TO .2 scfm)
VOLUME % CO_2 IN EFFLUENT GAS
1.0
.8
.6
.4
.2
0
20 40 60 80 100 120 140 160 180 200 220 240 260 280
TIME (MINUTES)

FIGURE 29

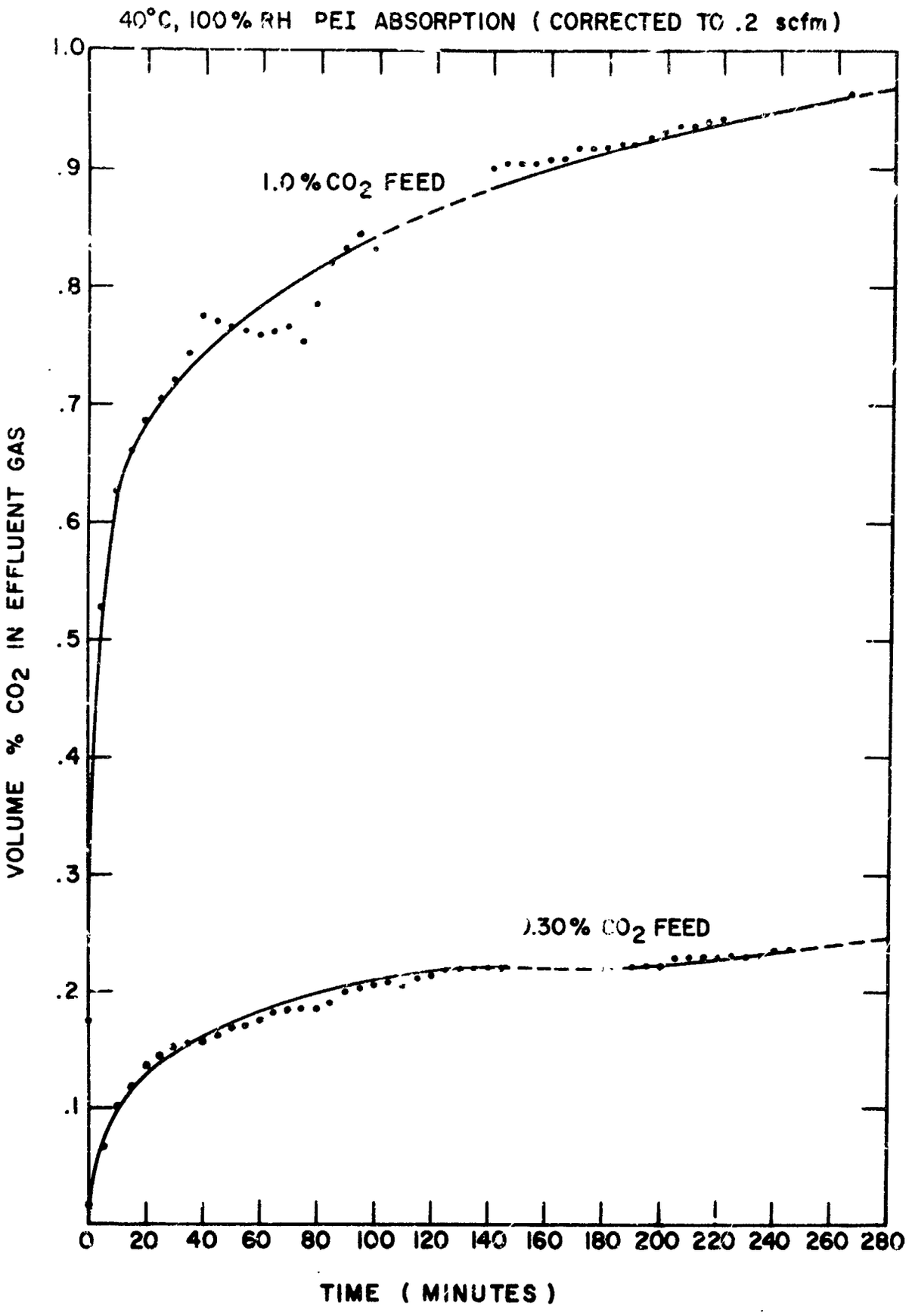

FIGURE 30

PAGE 153

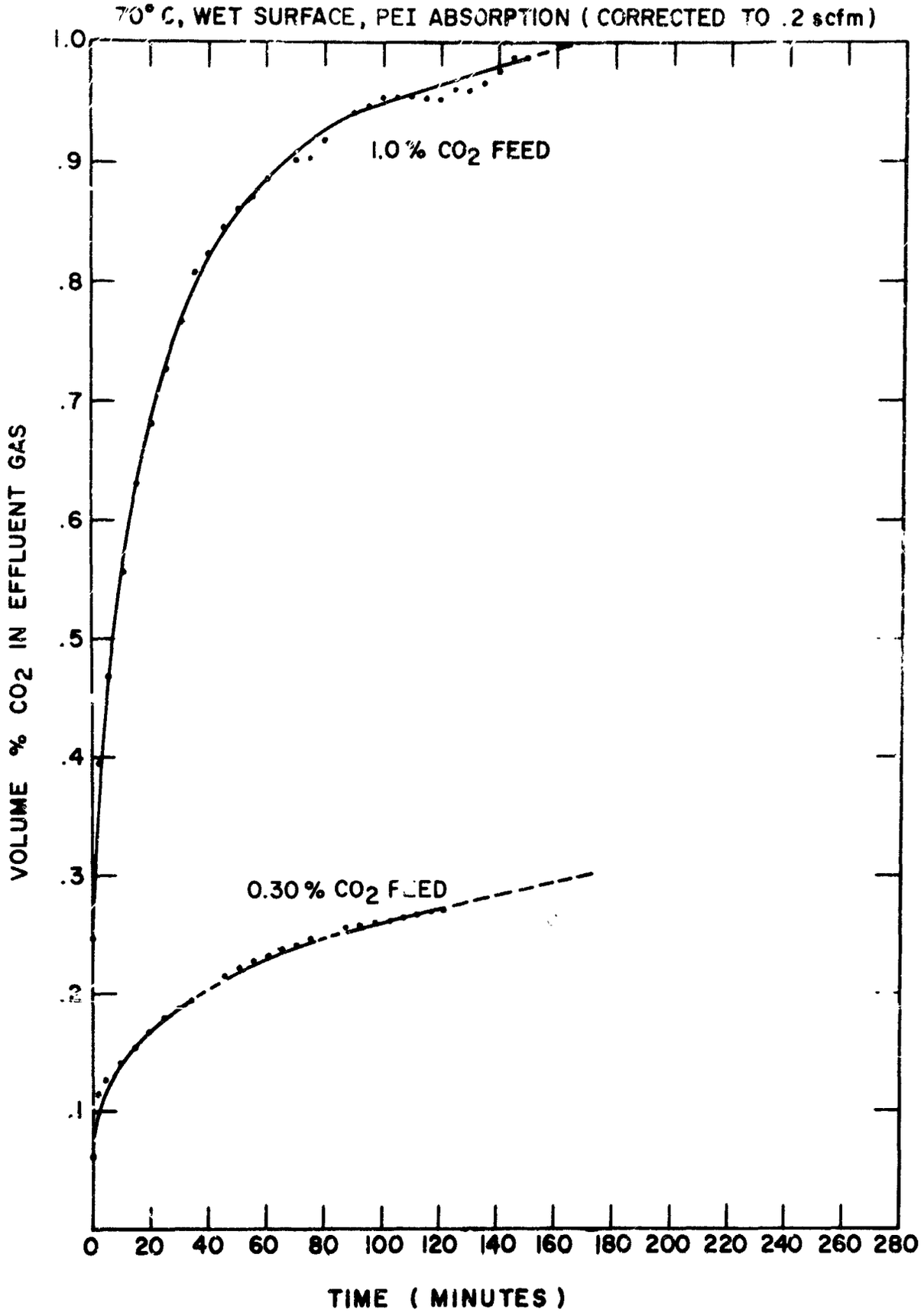

FIGURE 31

PAGE 154

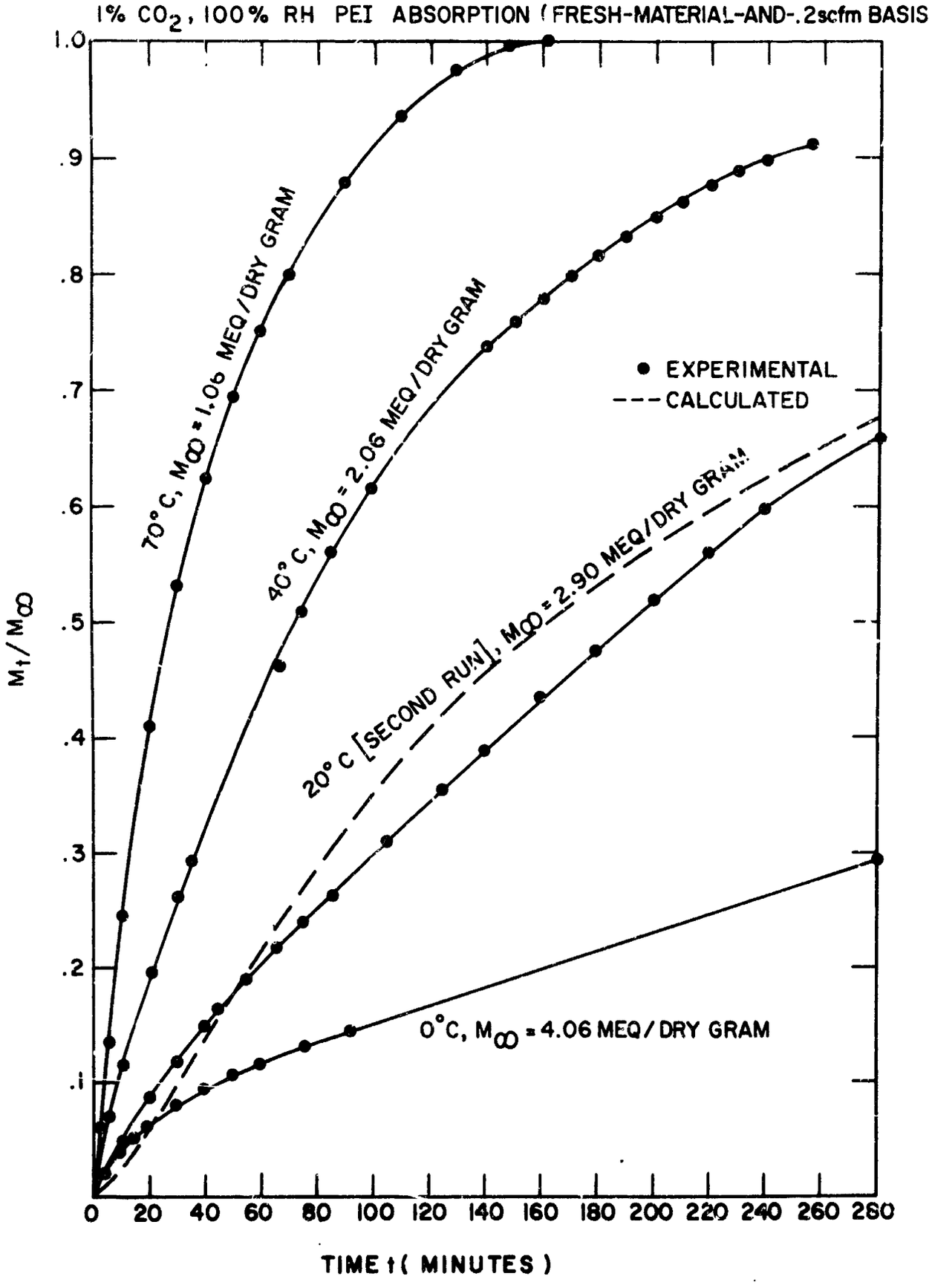

FIGURE 32

PAGE 155

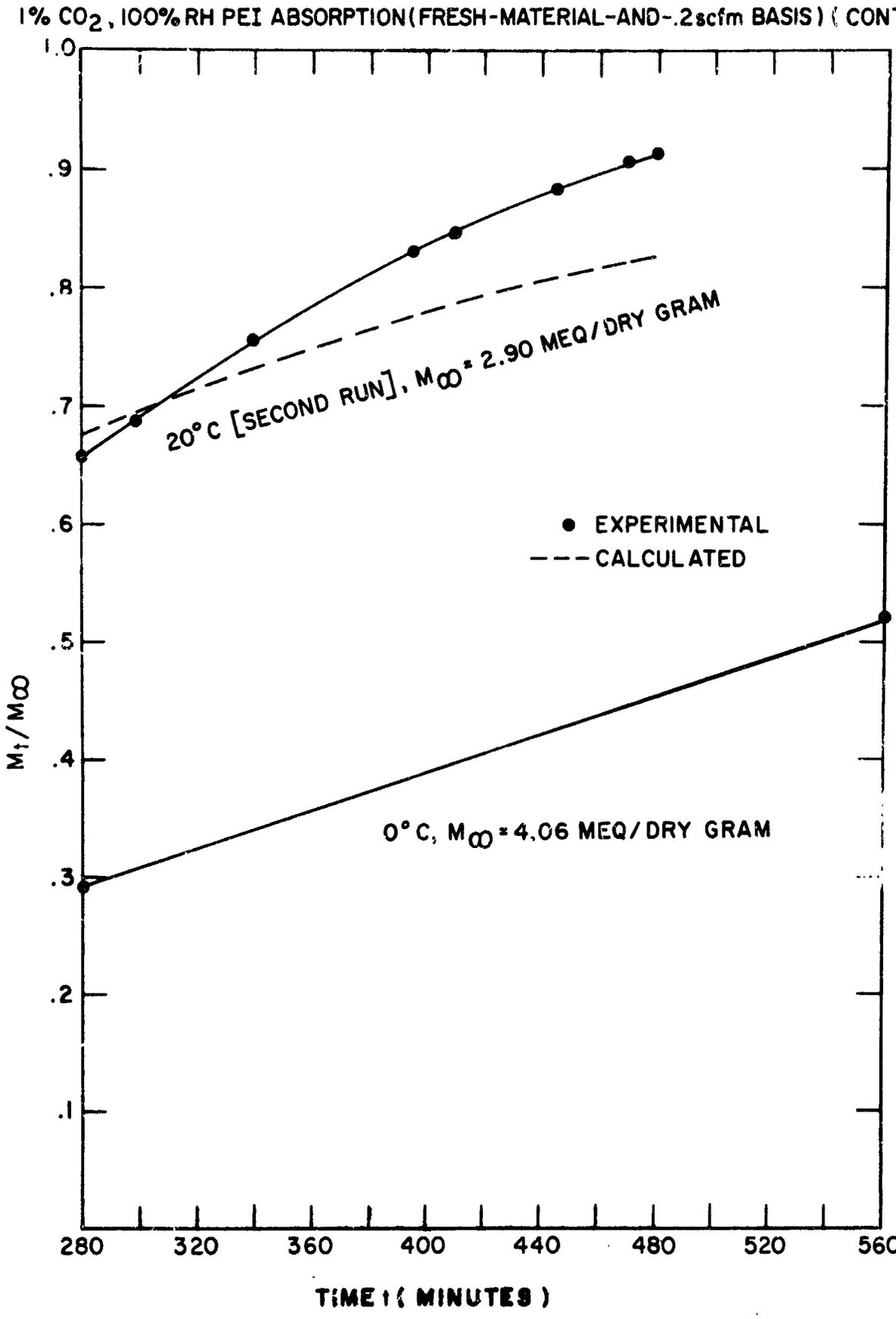

FIGURE 32 (CONTINUED)

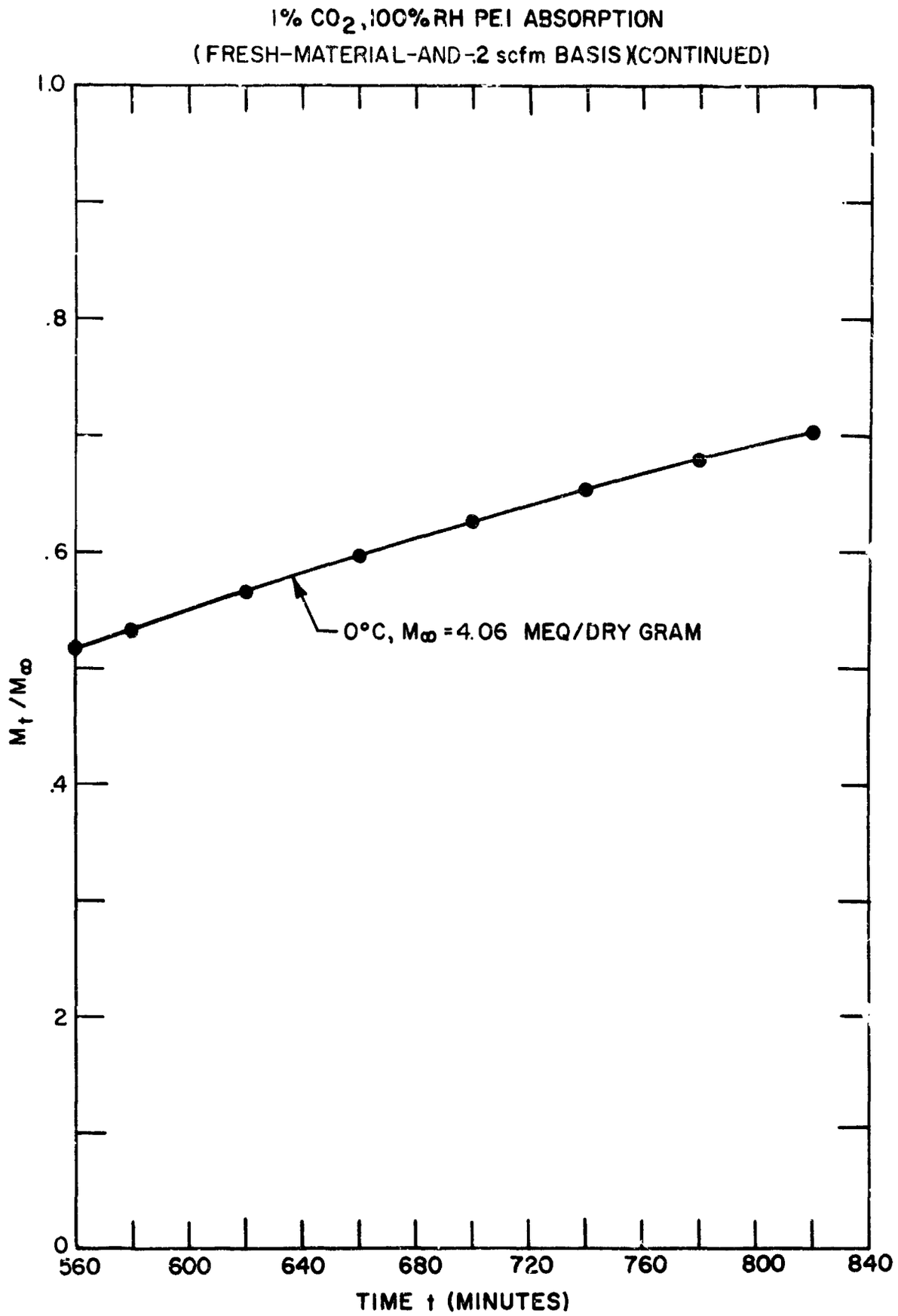

FIGURE 32 (CONTINUED)

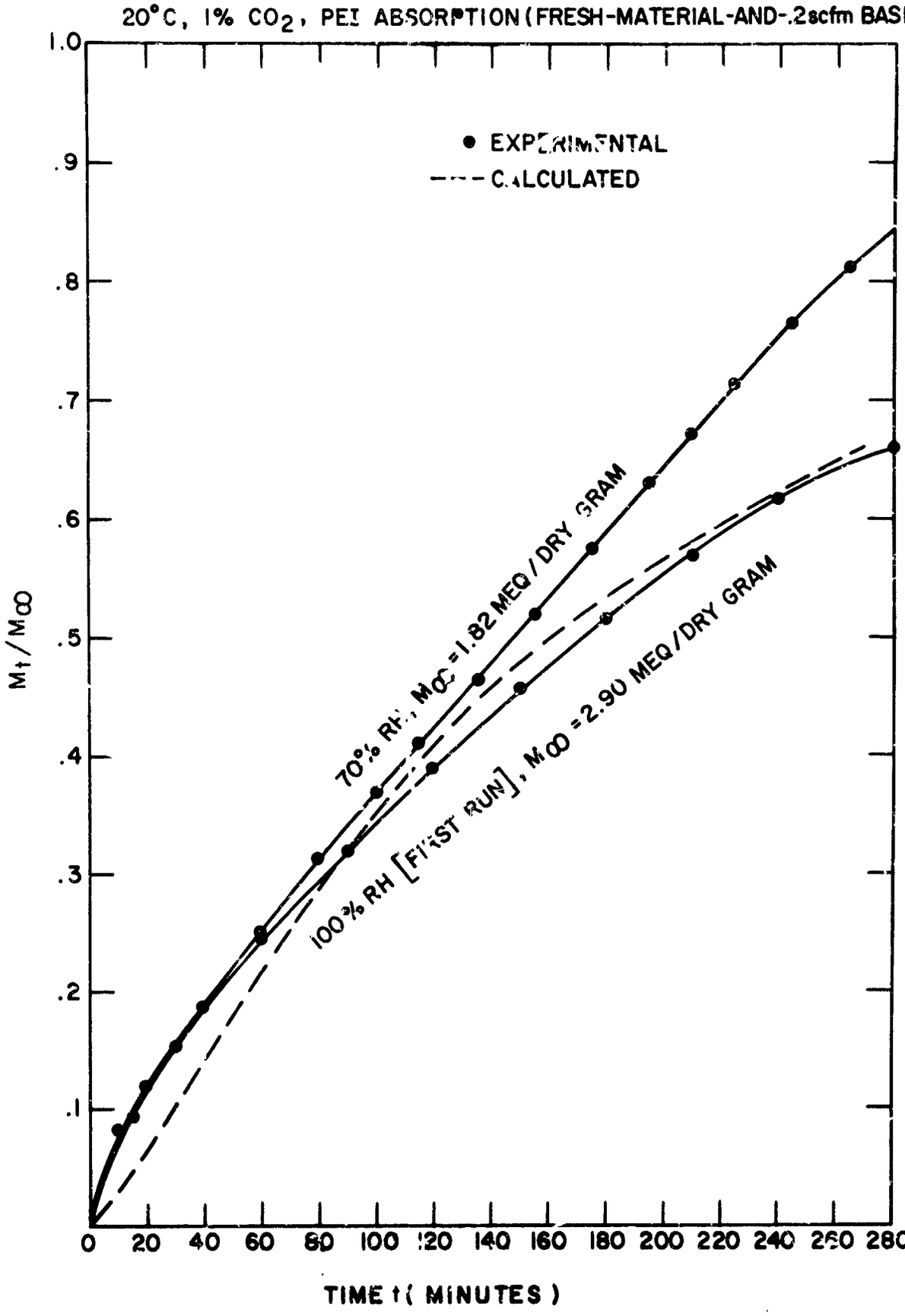
20°C, 1% CO_2, PEI ABSORPTION (FRESH-MATERIAL-AND-.2scfm BASIS)
● EXPERIMENTAL
---- CALCULATED
70% RH, M_∞ = 1.82 MEQ/DRY GRAM
100% RH [FIRST RUN], M_∞ = 2.90 MEQ/DRY GRAM
M_t/M_∞
TIME t (MINUTES)
1.0
.9
.8
.7
.6
.5
.4
.3
.2
.1
0 20 40 60 80 100 120 140 160 180 200 220 240 260 280

FIGURE 33

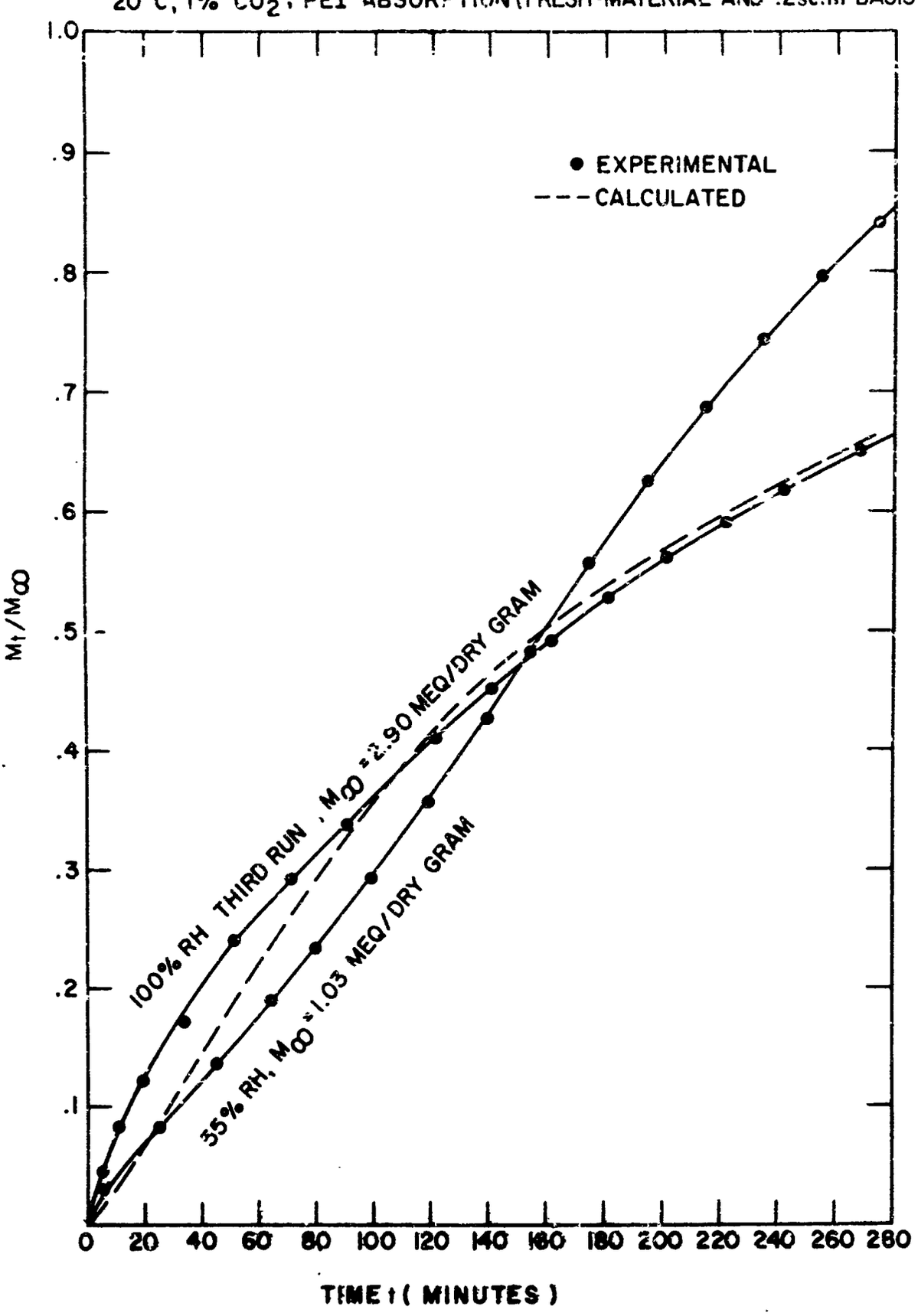

FIGURE 34

PAGE 159

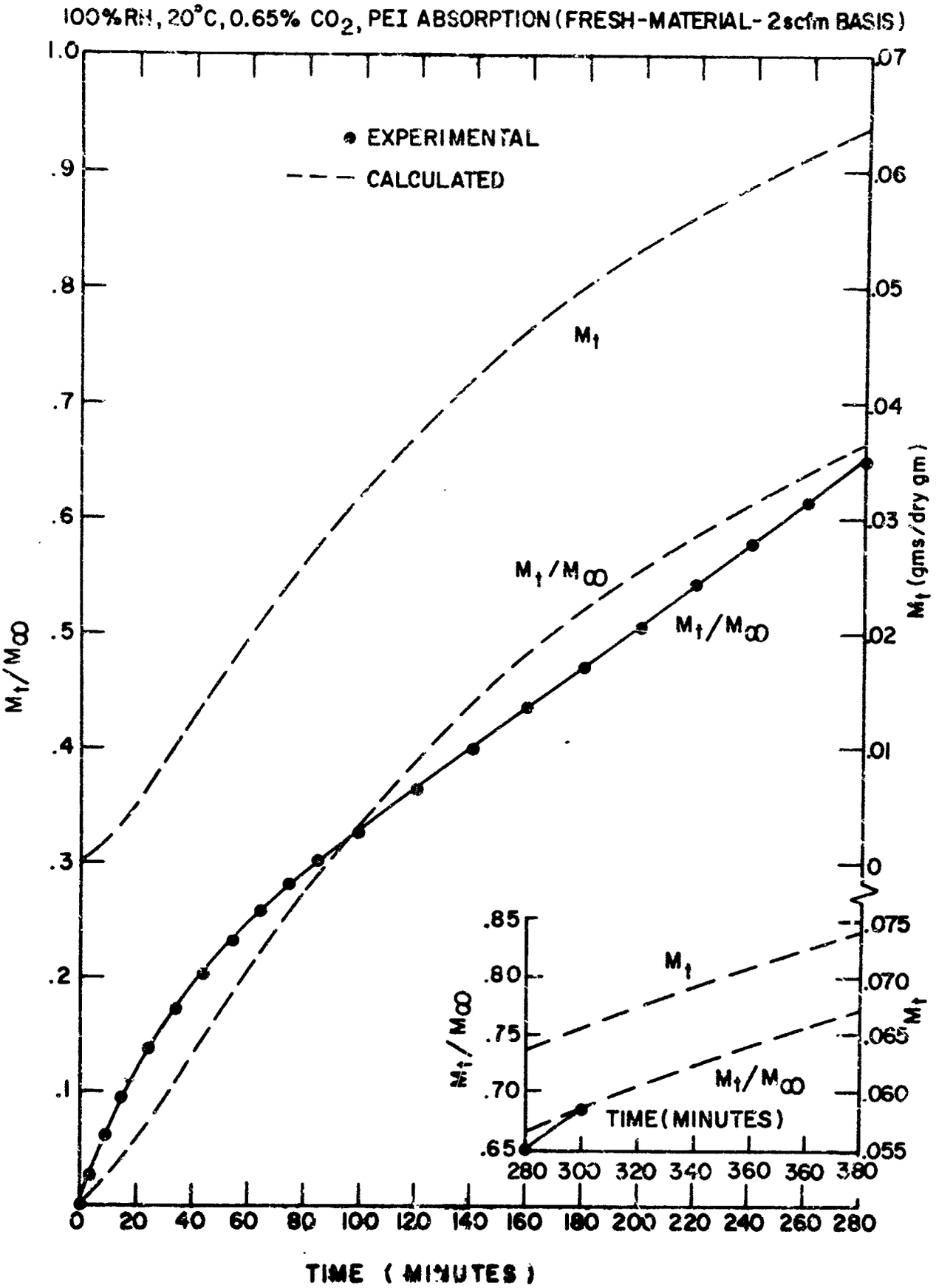

FIGURE 35

PAGE 160

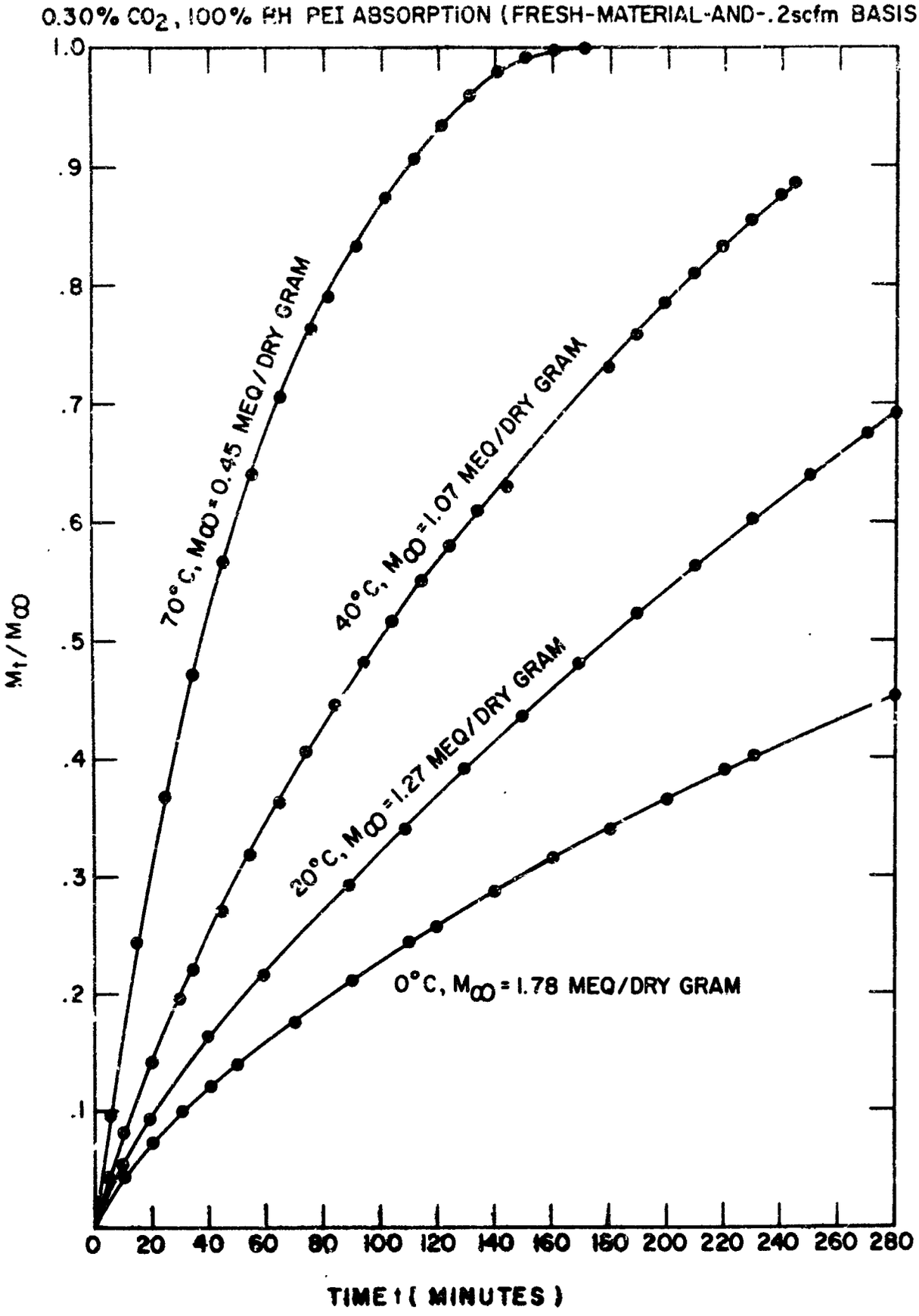
0.30% CO_2, 100% RH PEI ABSORPTION (FRESH-MATERIAL-AND-.2scfm BASIS)
M_t/M_∞
1.0
.9
.8
.7
.6
.5
.4
.3
.2
.1
70°C, M_∞ = 0.45 MEQ/DRY GRAM
40°C, M_∞ = 1.07 MEQ/DRY GRAM
20°C, M_∞ = 1.27 MEQ/DRY GRAM
0°C, M_∞ = 1.78 MEQ/DRY GRAM
0 20 40 60 80 100 120 140 160 180 200 220 240 260 280
TIME t (MINUTES)

FIGURE 36

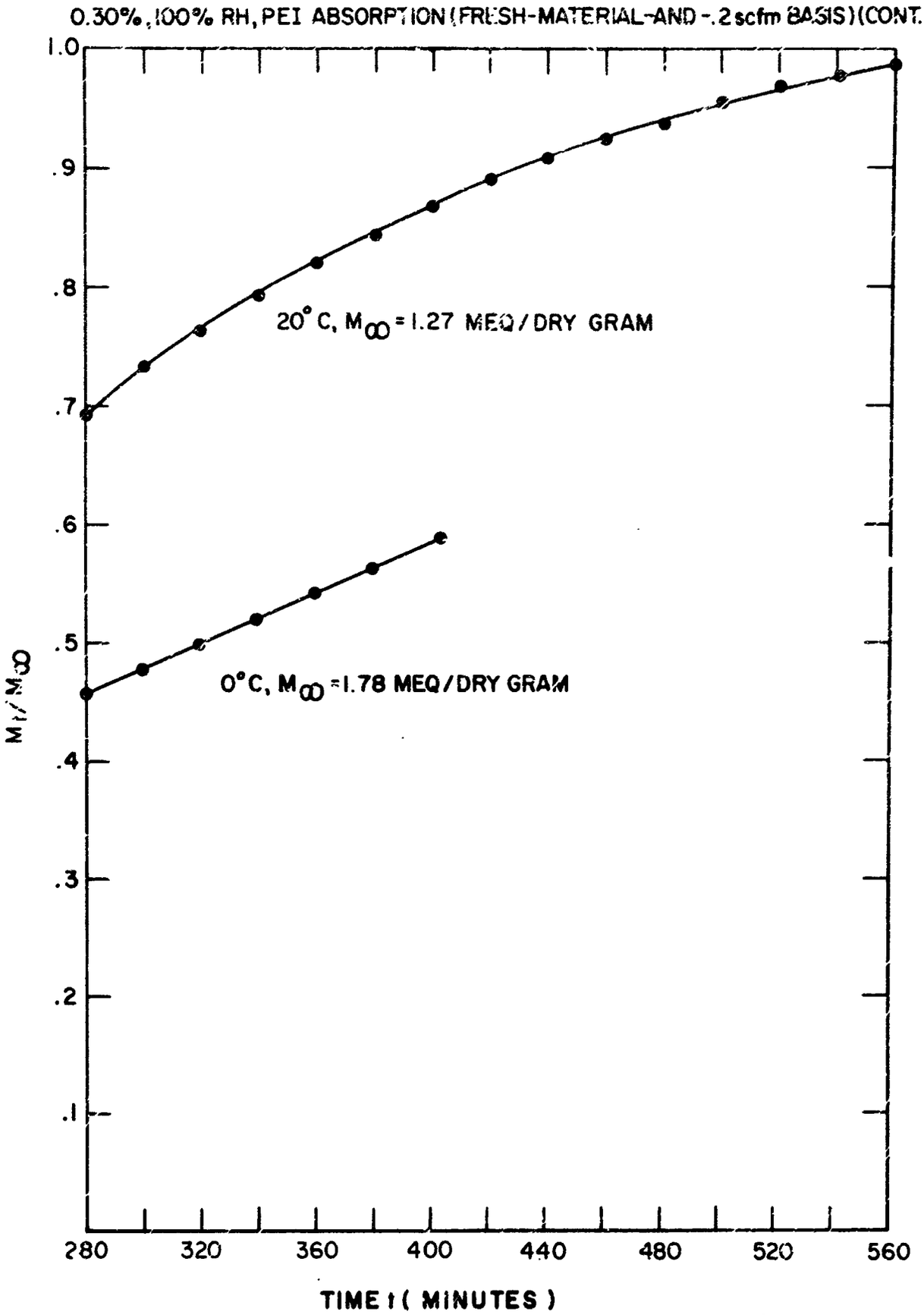

FIGURE 36 (CONTINUED)

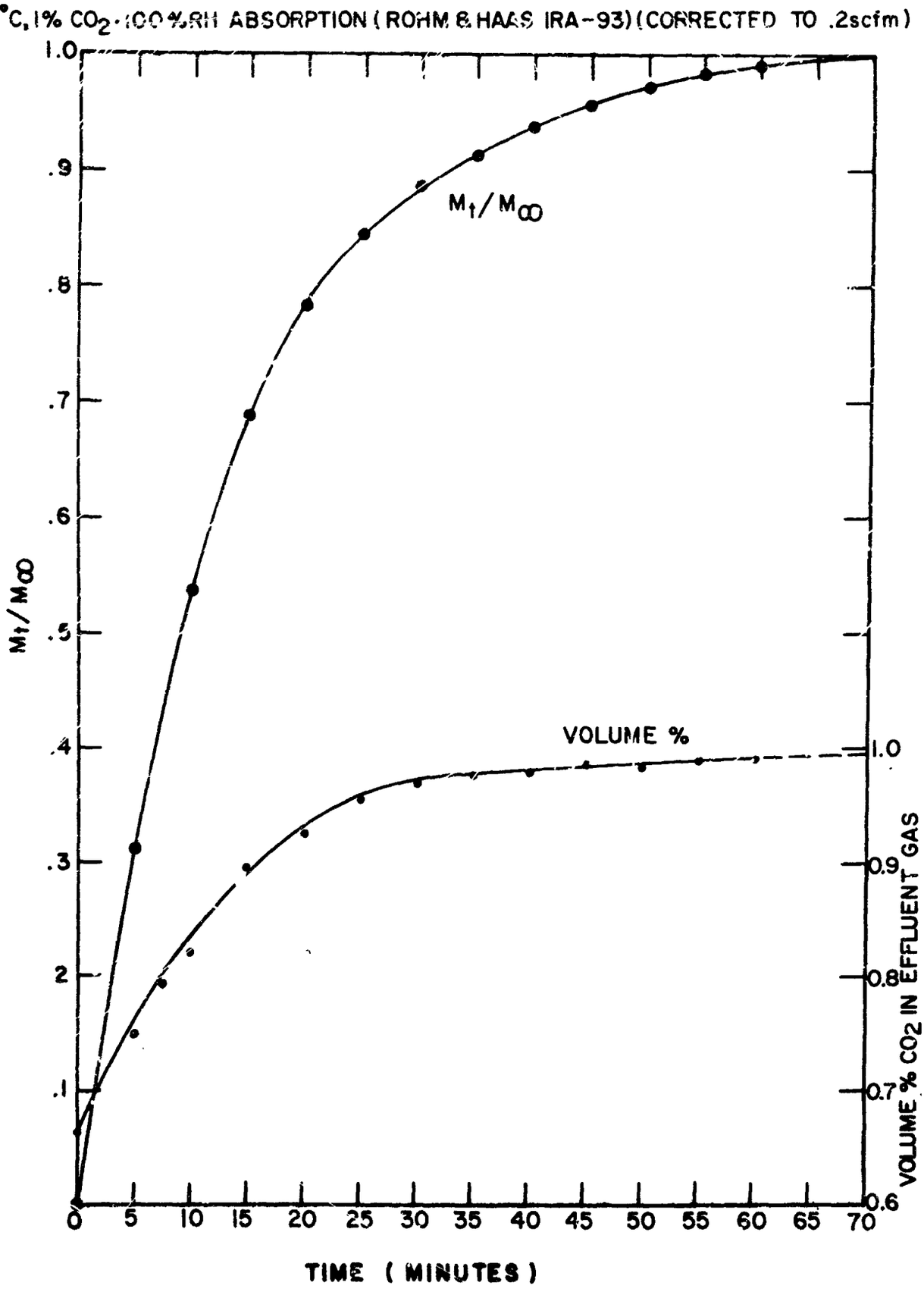

FIGURE 37

PAGE 163

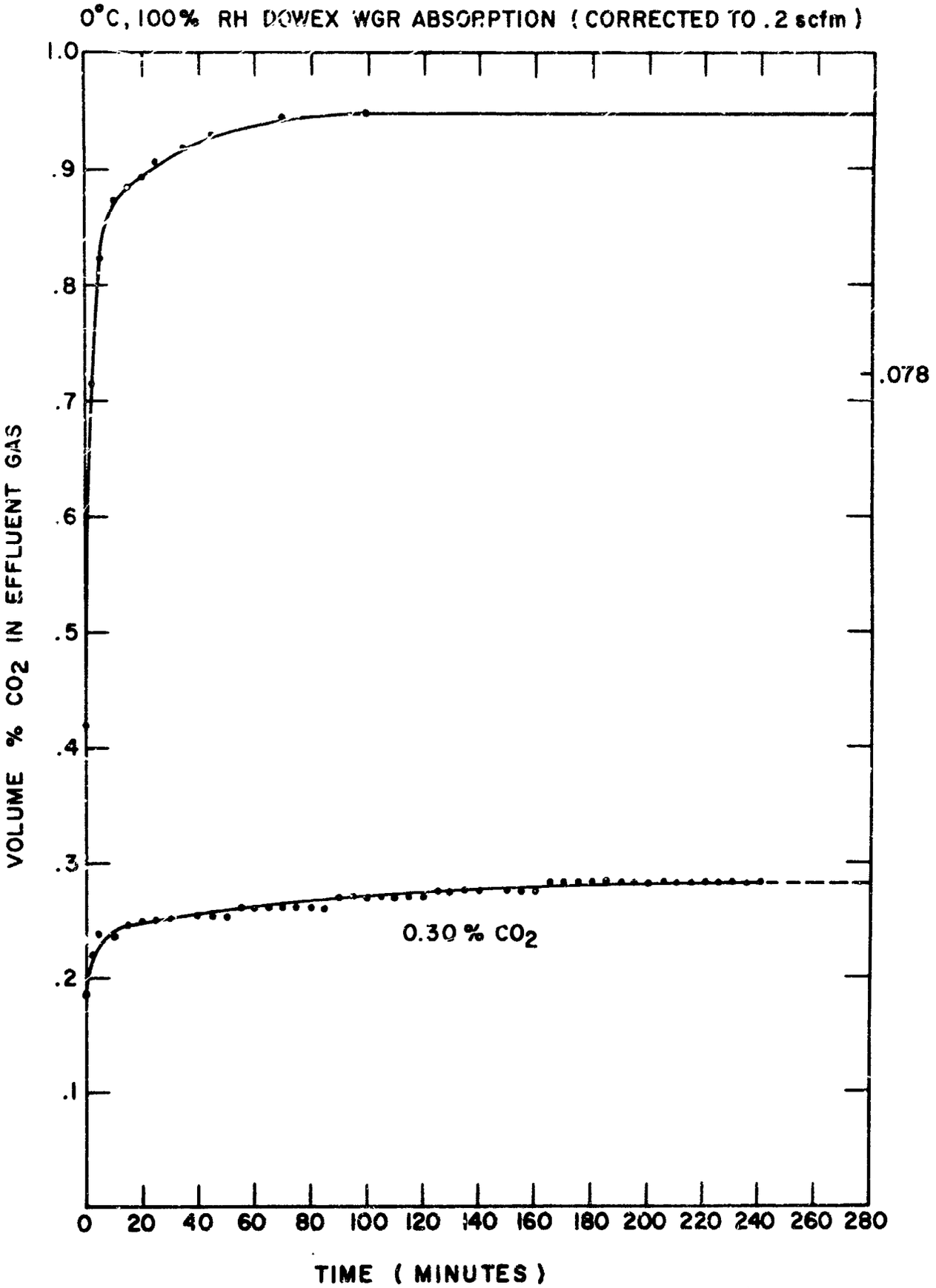
0°C, 100% RH DOWEX WGR ABSORPTION (CORRECTED TO .2 scfm)
VOLUME % CO_2 IN EFFLUENT GAS
1.0
.9
.8
.7
.6
.5
.4
.3
.2
.1
.078
0.30 % CO_2
0
20
40
60
80
100
120
140
160
180
200
220
240
260
280
TIME (MINUTES)

FIGURE 38

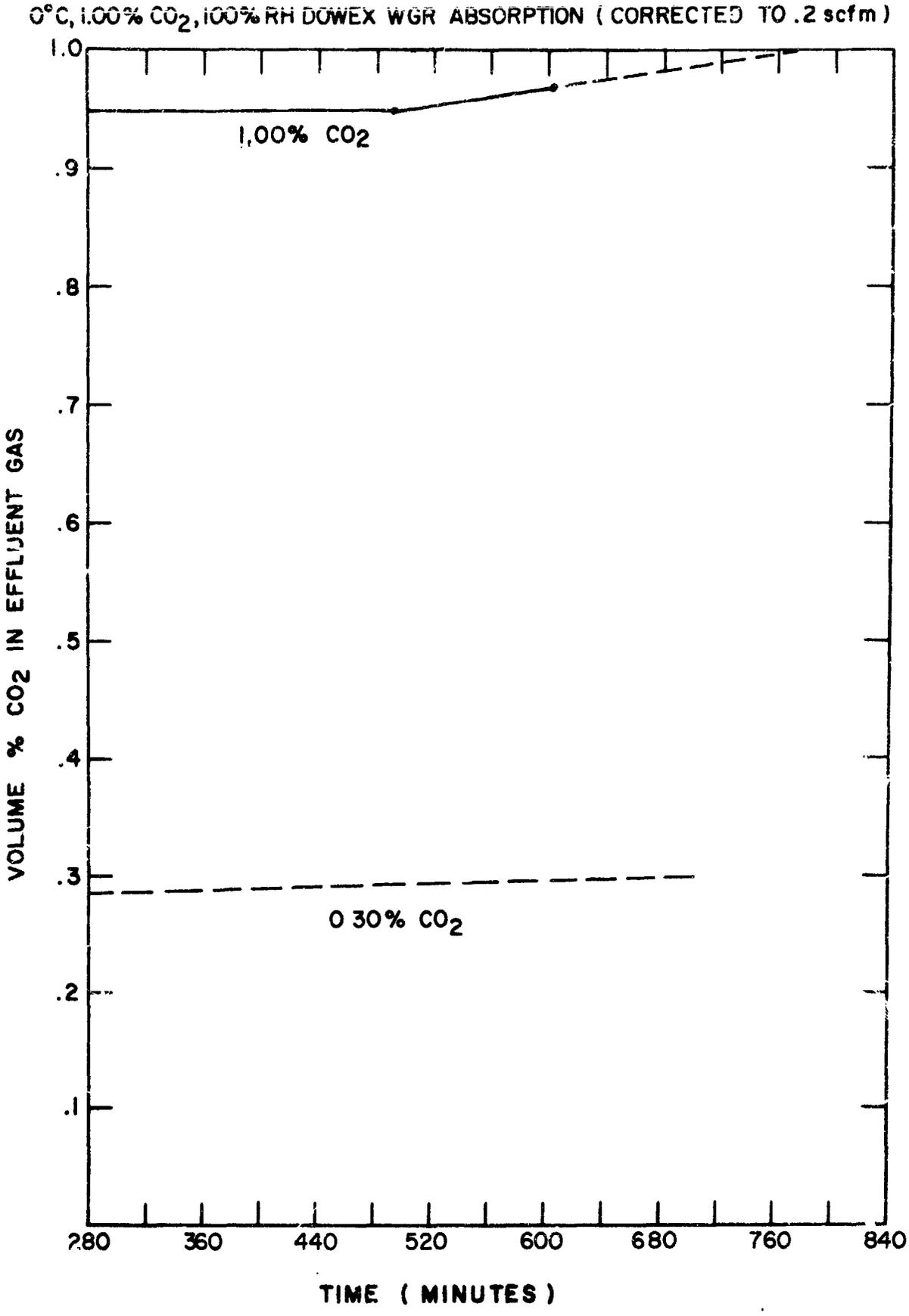

FIGURE 38 (CONTINUED)

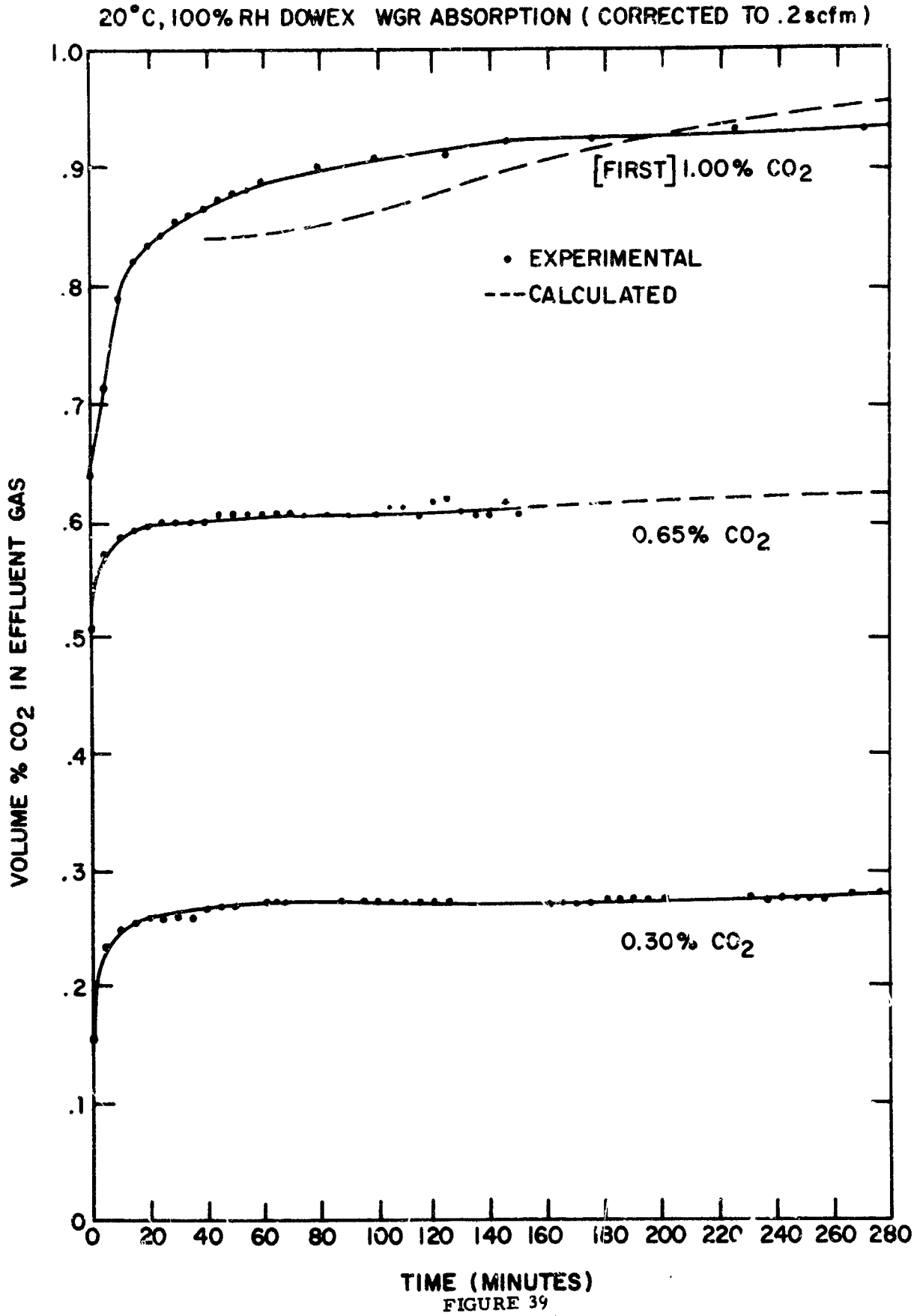
20°C, 100% RH DOWEX WGR ABSORPTION (CORRECTED TO .2 scfm)
VOLUME % CO_2 IN EFFLUENT GAS
1.0
.9
.8
.7
.6
.5
.4
.3
.2
.1
0
[FIRST] 1.00% CO_2
• EXPERIMENTAL
---CALCULATED
0.65% CO_2
0.30% CO_2
0 20 40 60 80 100 120 140 160 180 200 220 240 260 280
TIME (MINUTES)

FIGURE 39

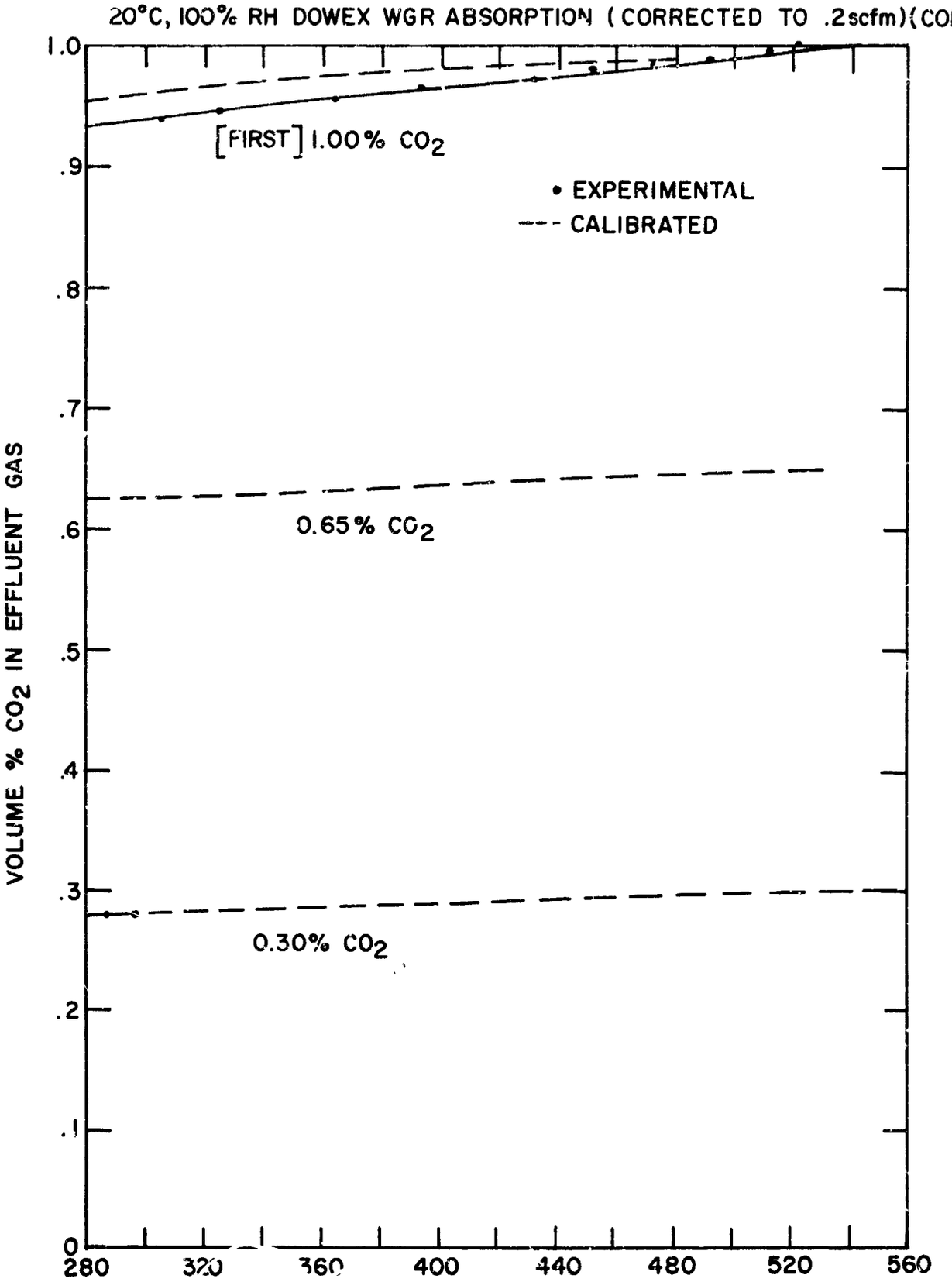

FIGURE 39 (CONTINUED)

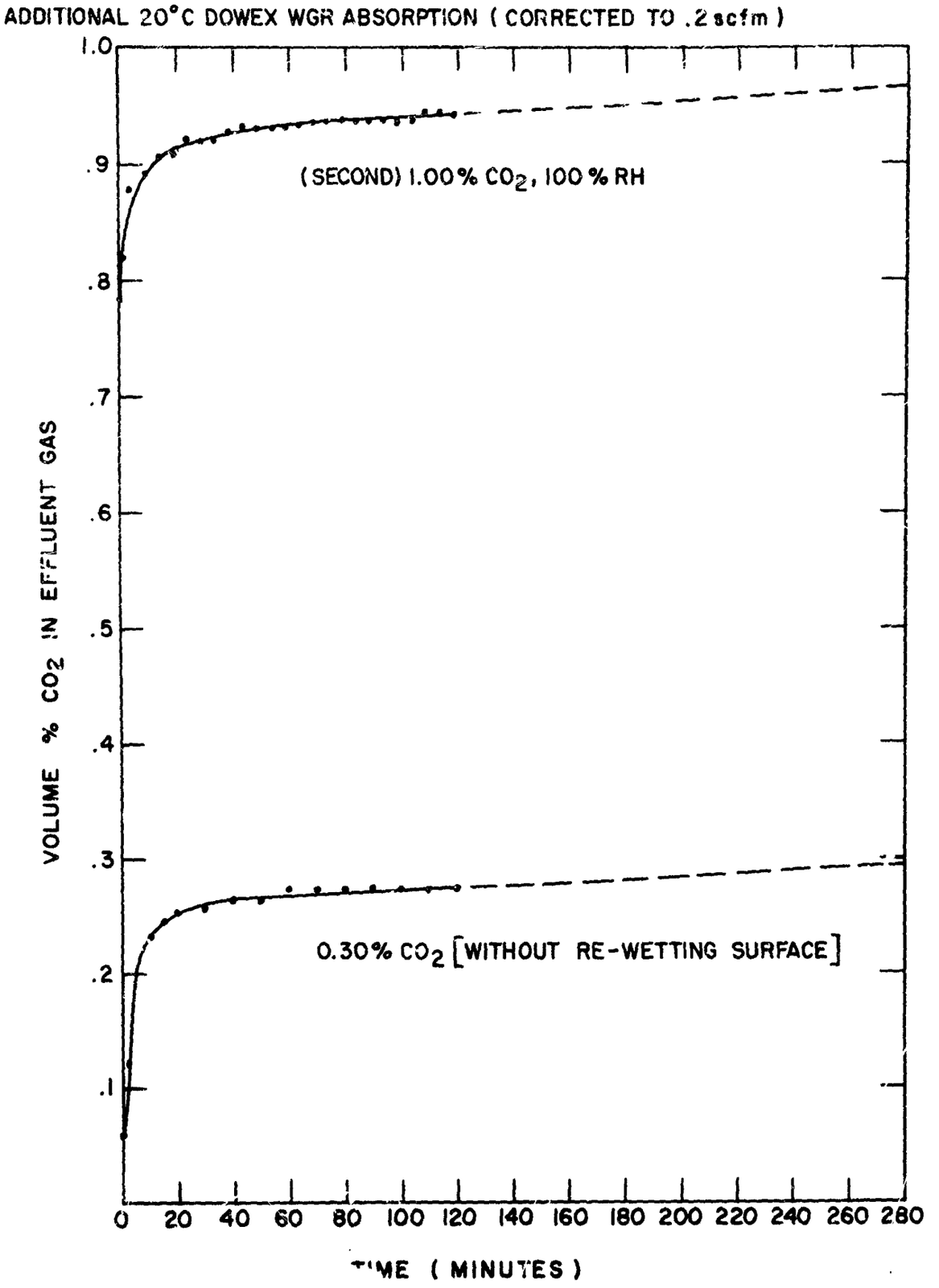

FIGURE 40
PAGE 168

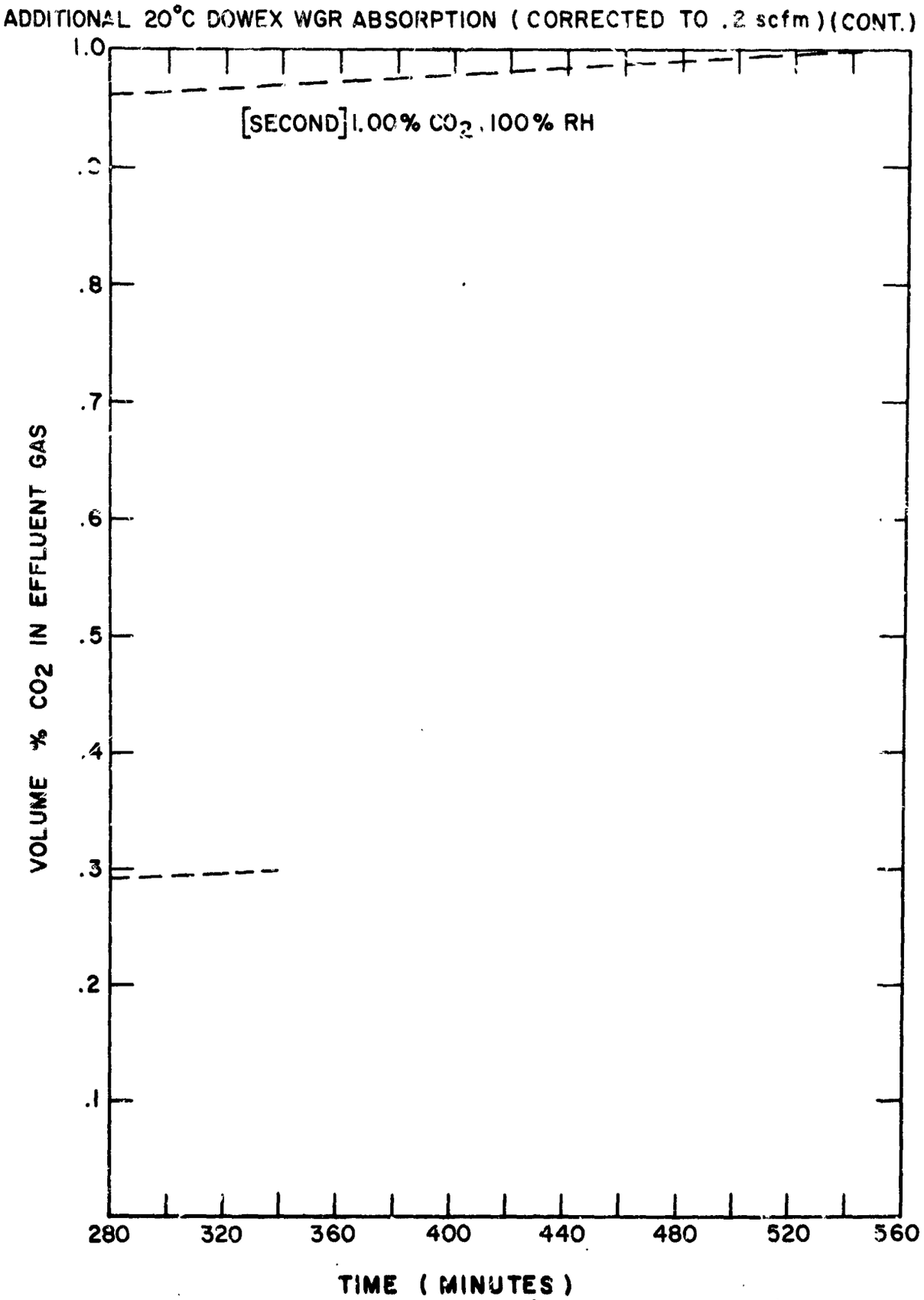

FIGURE 40 (CONTINUED)

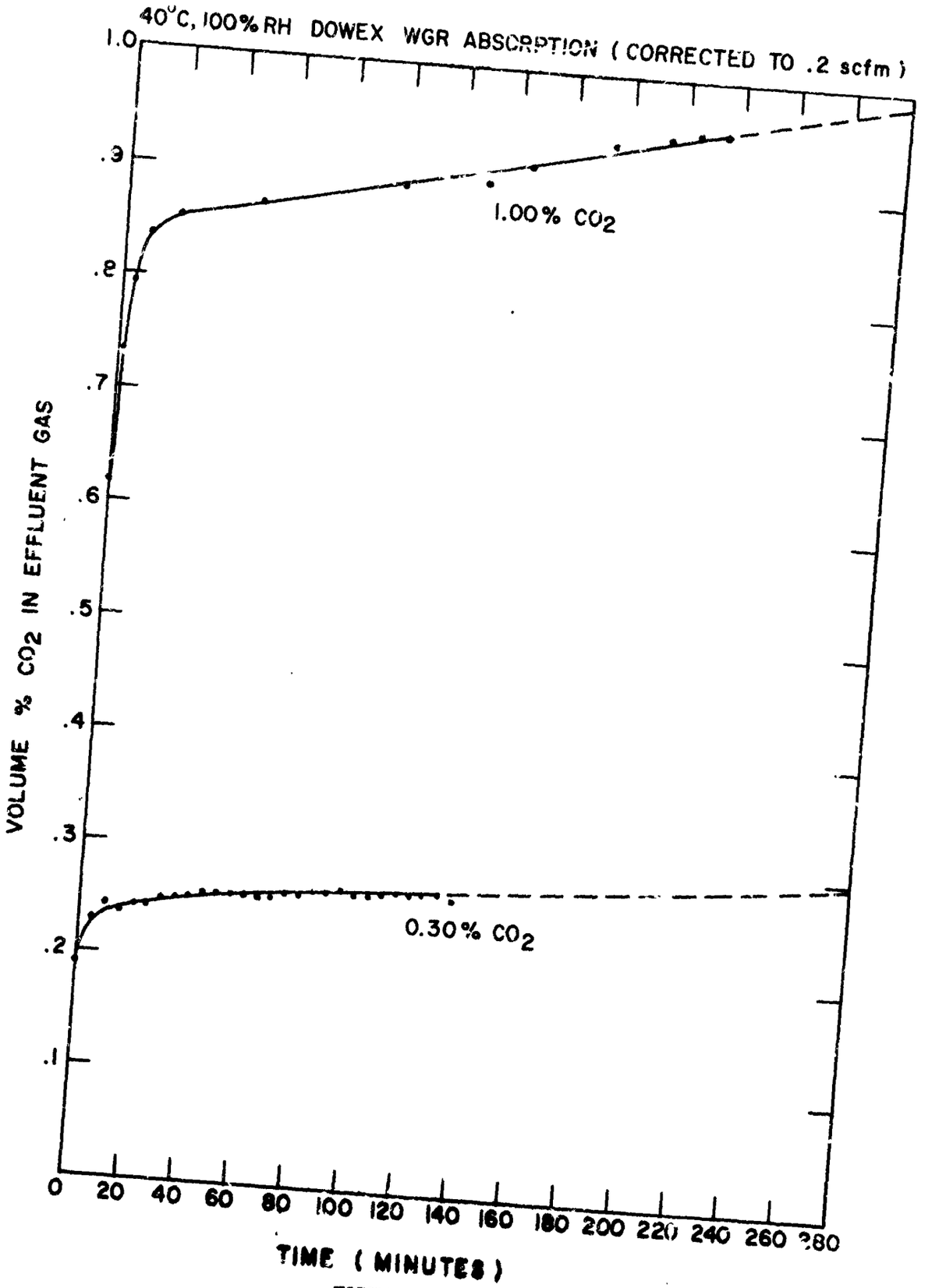

FIGURE 41

PAGE 170

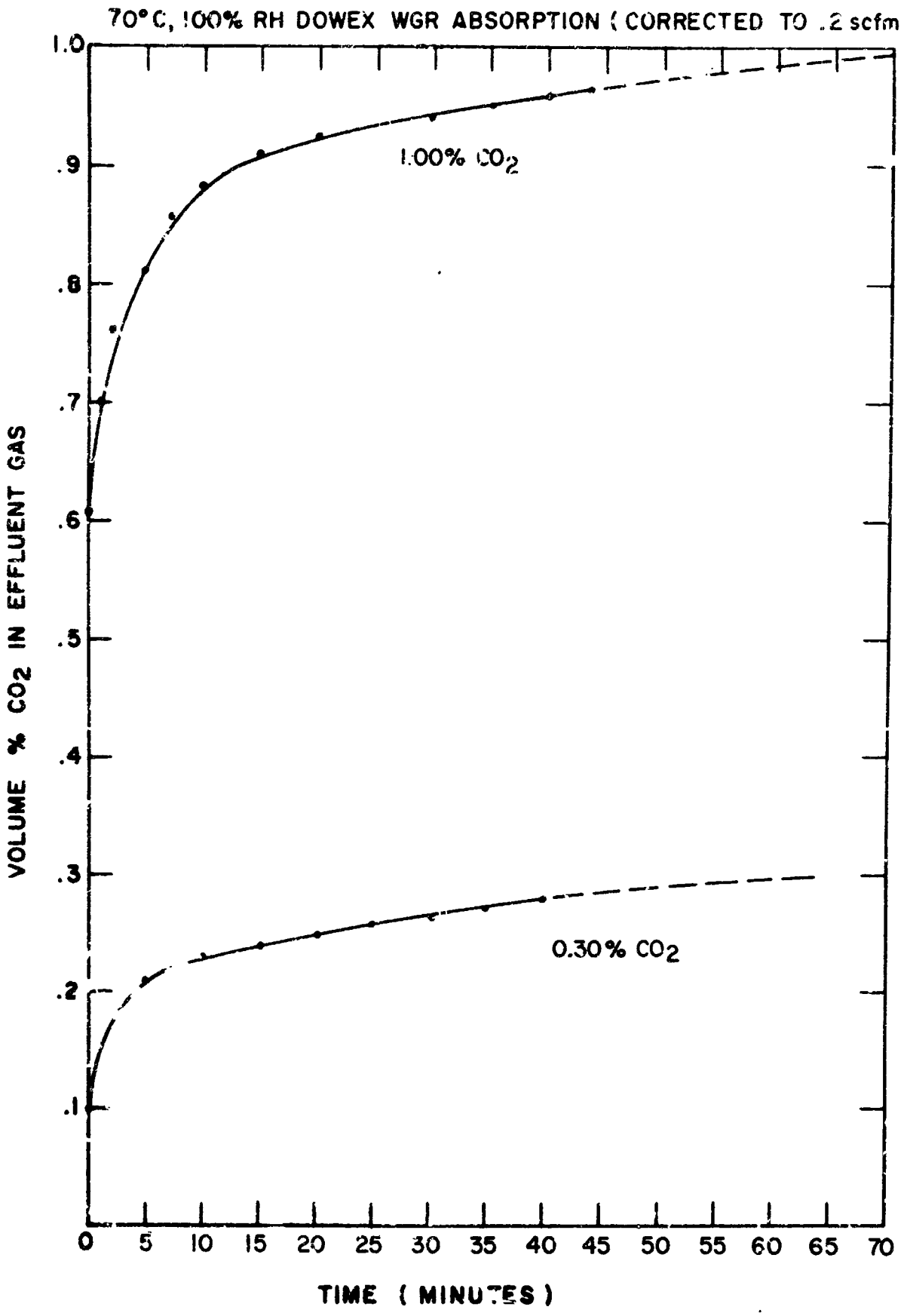
70°C, 100% RH DOWEX WGR ABSORPTION (CORRECTED TO .2 scfm)
1.00% CO_2
0.30% CO_2
VOLUME % CO_2 IN EFFLUENT GAS
1.0
.9
.8
.7
.6
.5
.4
.3
.2
.1
0
5
10
15
20
25
30
35
40
45
50
55
60
65
70
TIME (MINUTES)

FIGURE 42

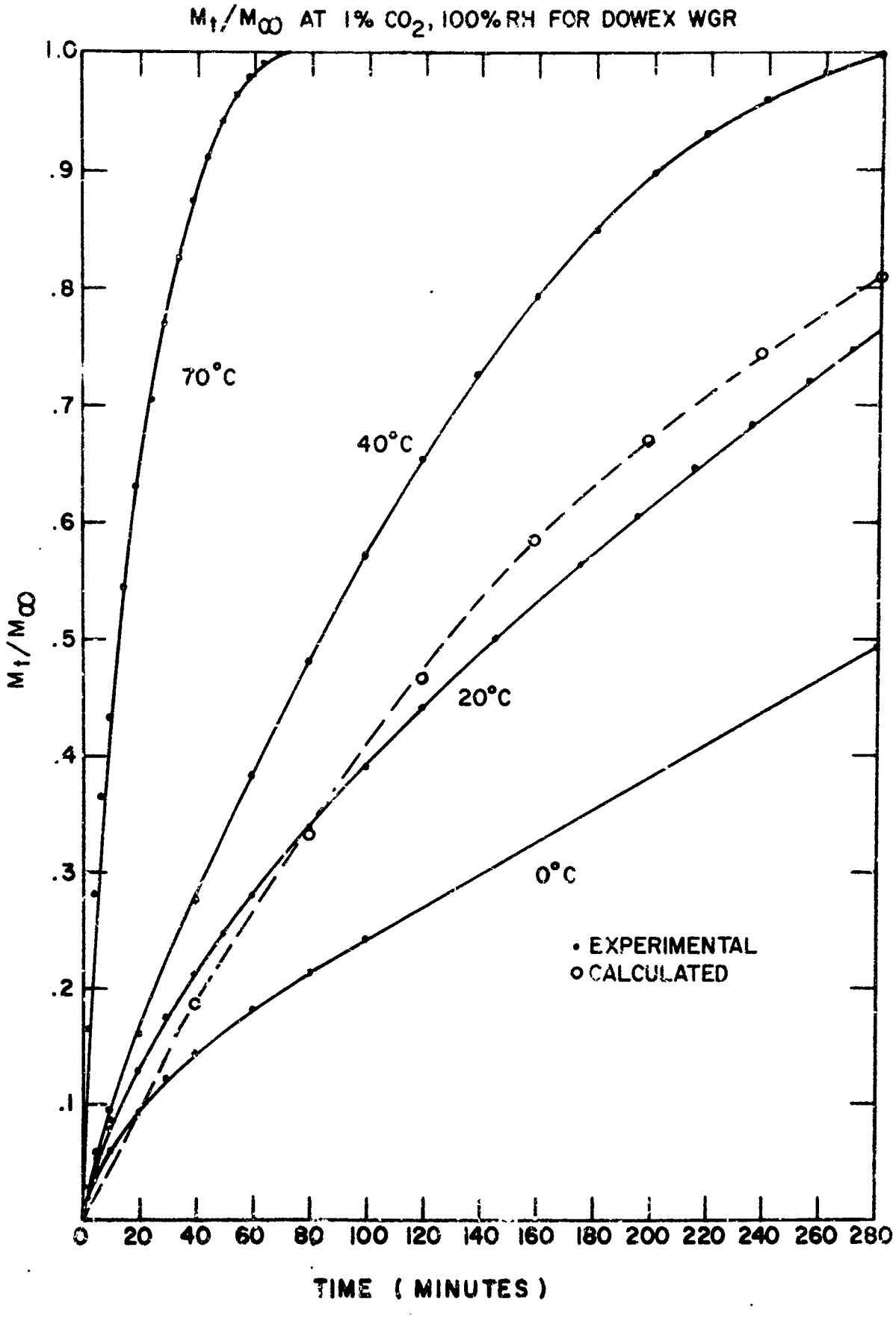

FIGURE 43

PAGE 17

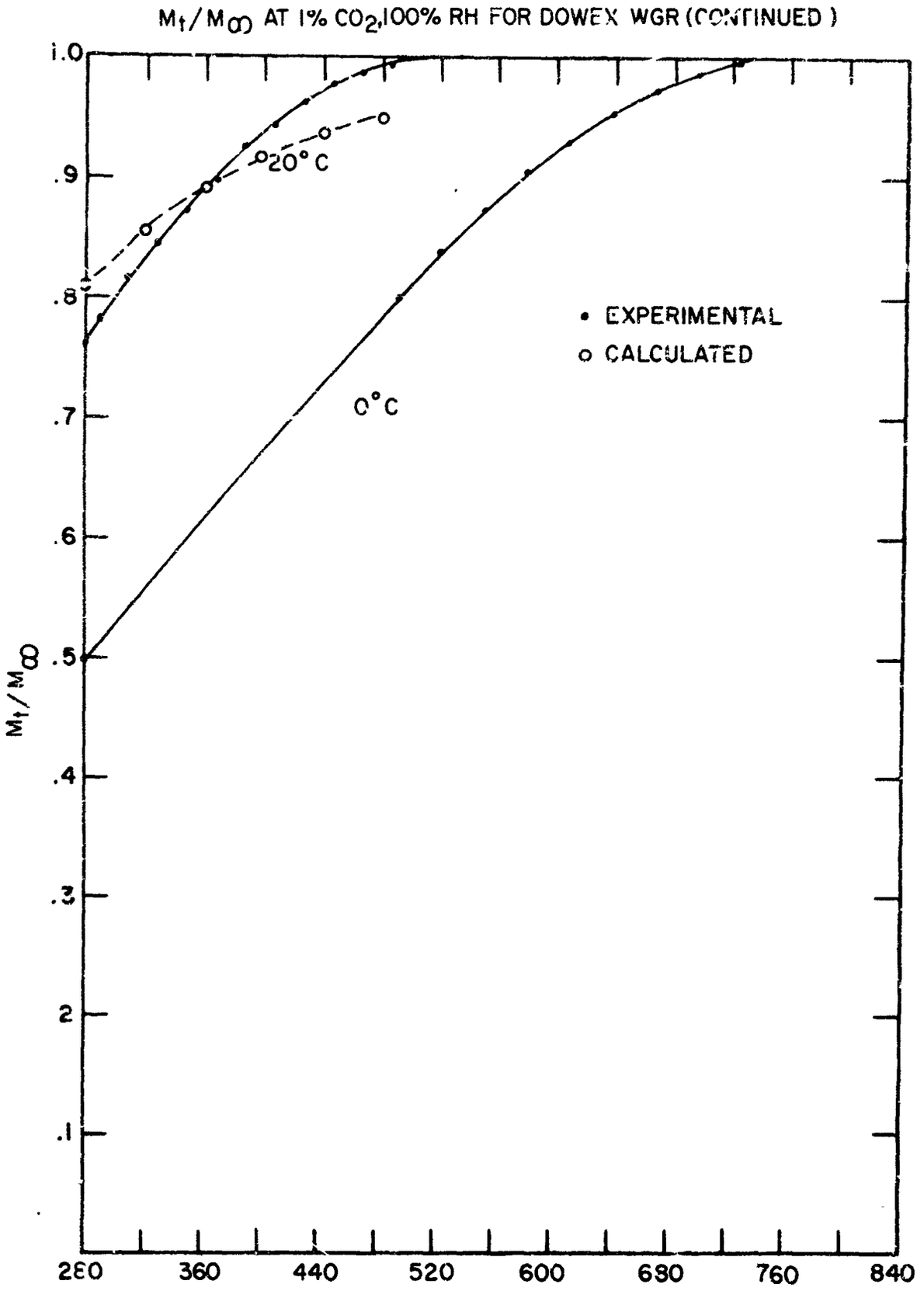

FIGURE 43 (CONTINUED)

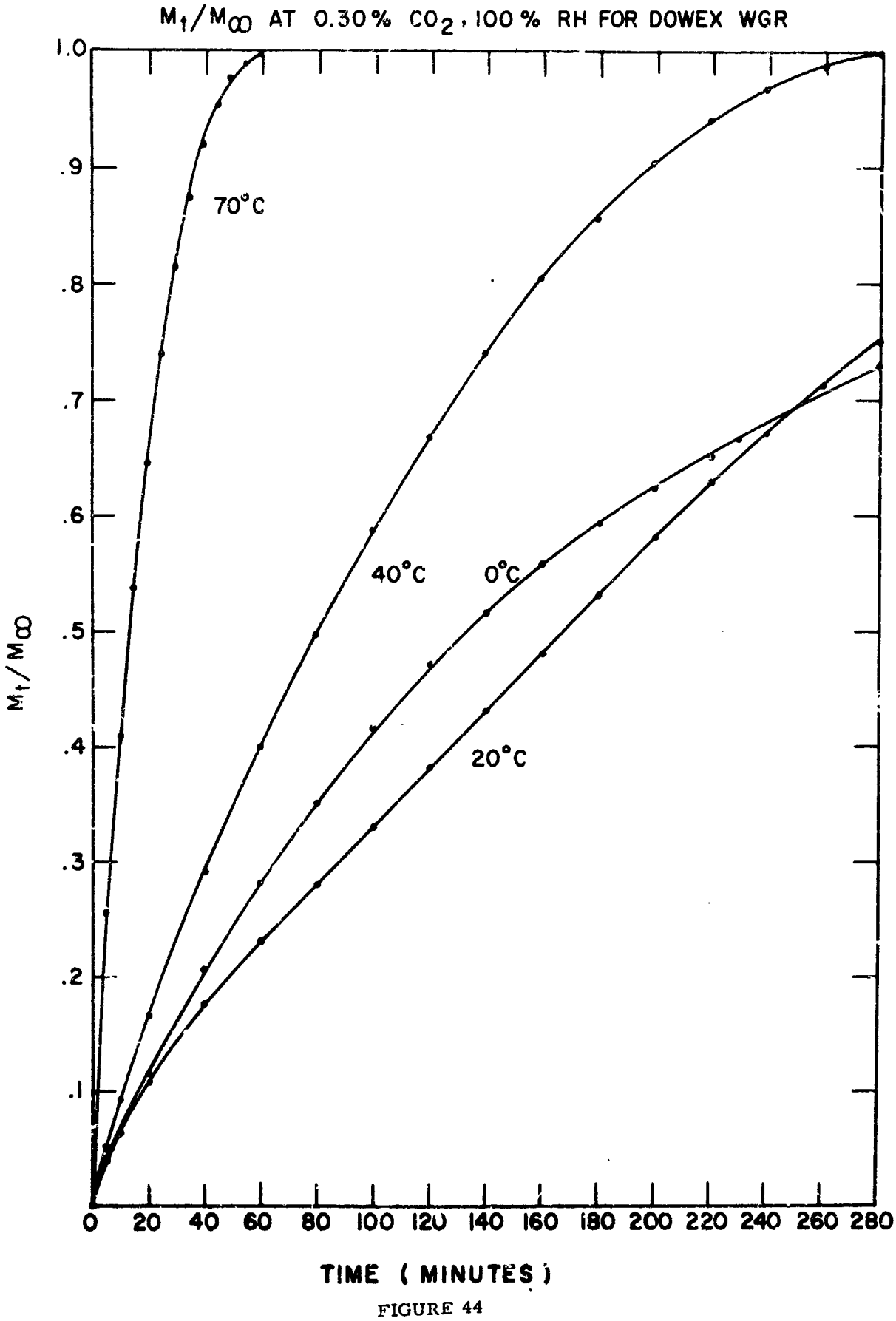
M_t/M_∞ AT 0.30% CO_2, 100% RH FOR DOWEX WGR
1.0
.9
.8
.7
.6
.5
.4
.3
.2
.1
M_t/M_∞
70°C
40°C
0°C
20°C
0
20
40
60
80
100
120
140
160
180
200
220
240
260
280
TIME (MINUTES)

FIGURE 44

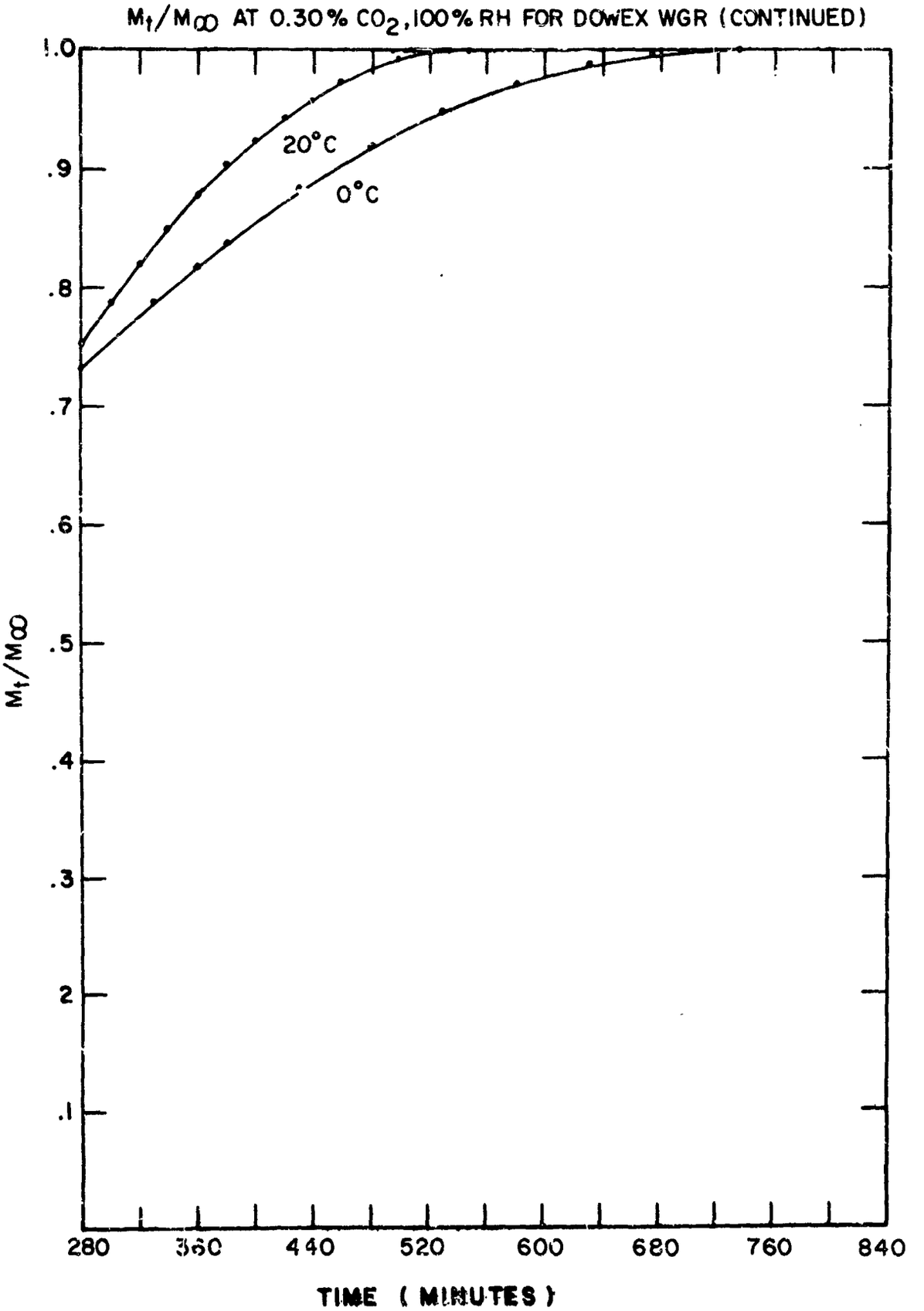

FIGURE 44 (CONTINUED)

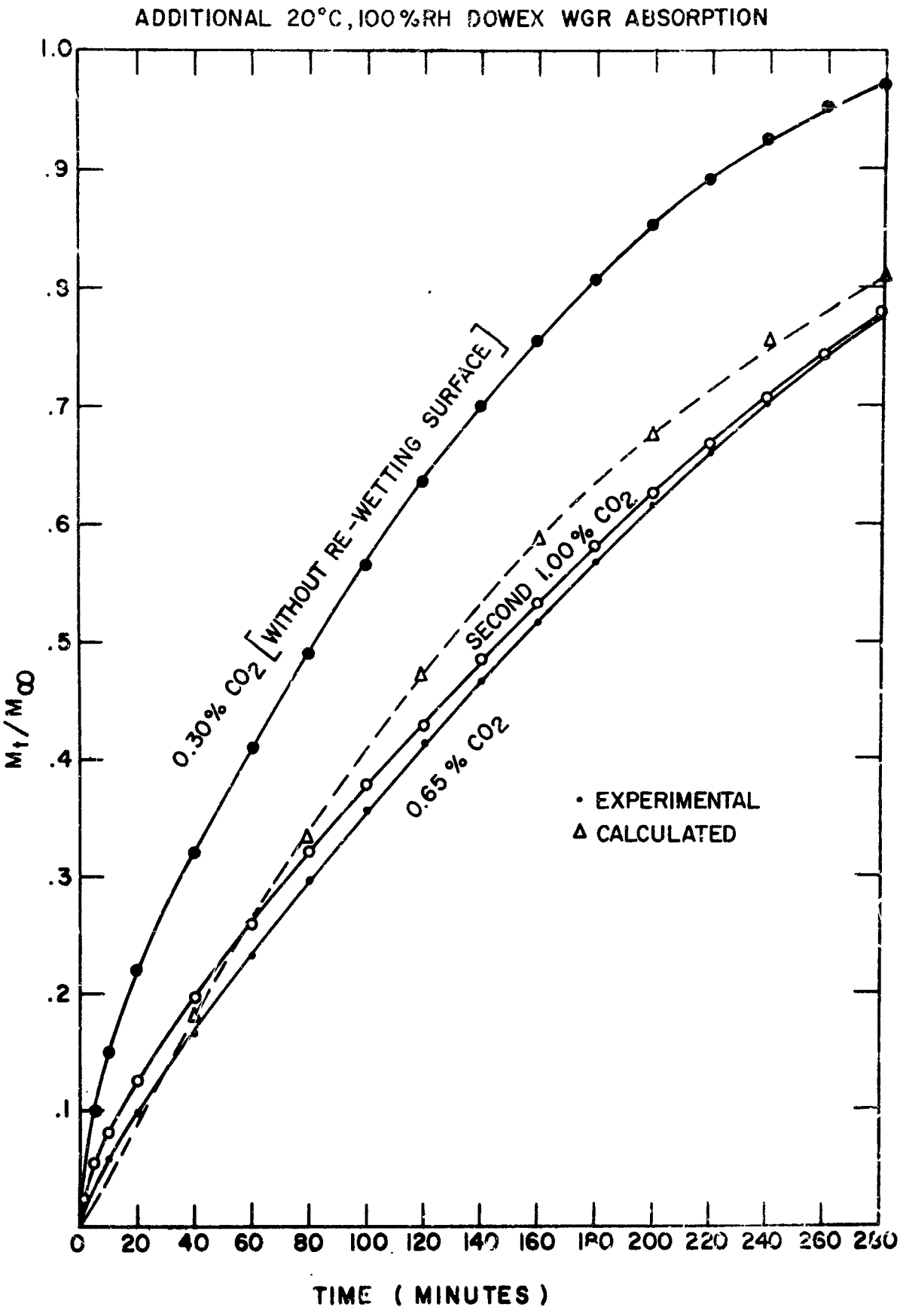

FIGURE 45

PAGE 176

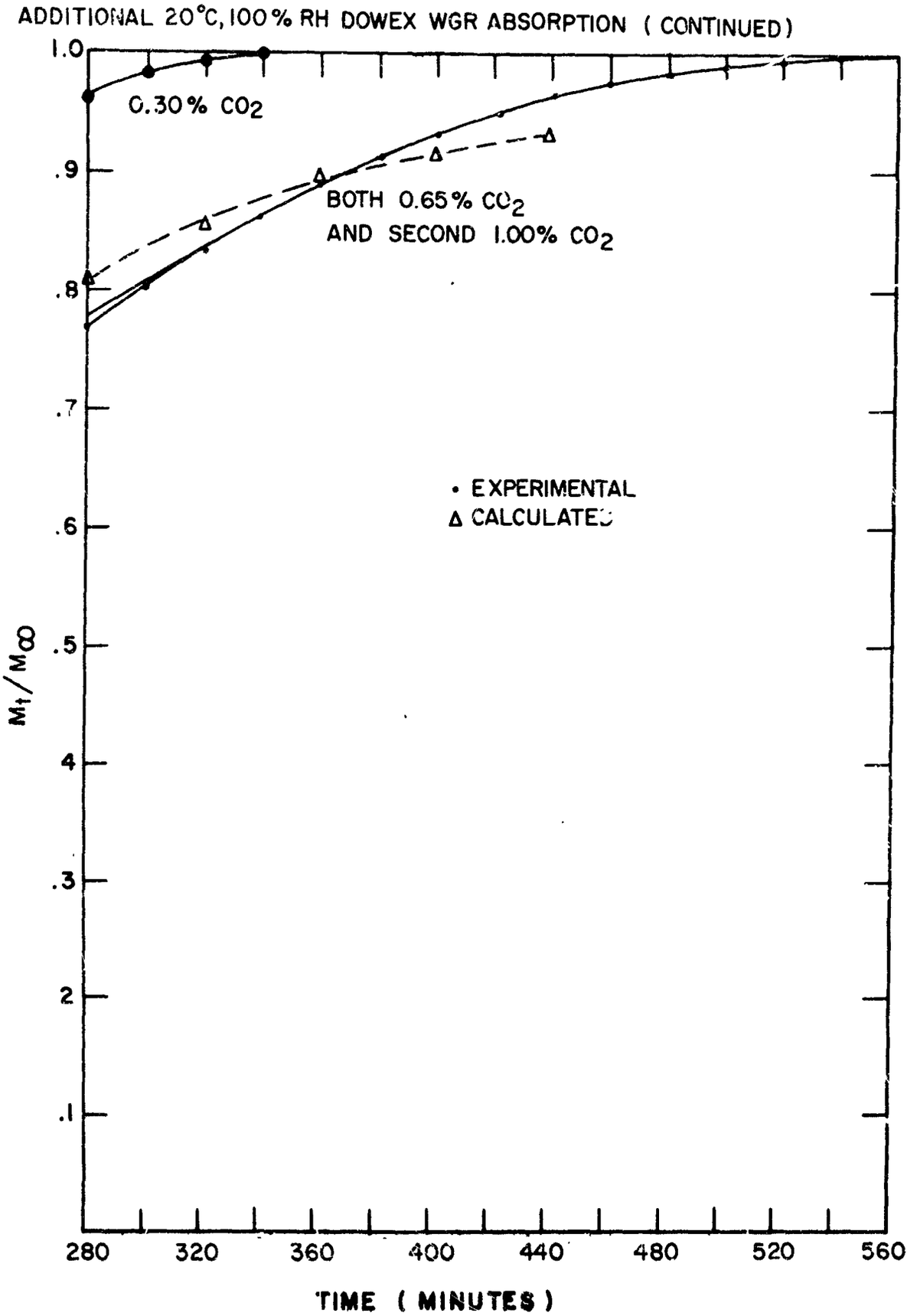

FIGURE 45 (CONTINUED)

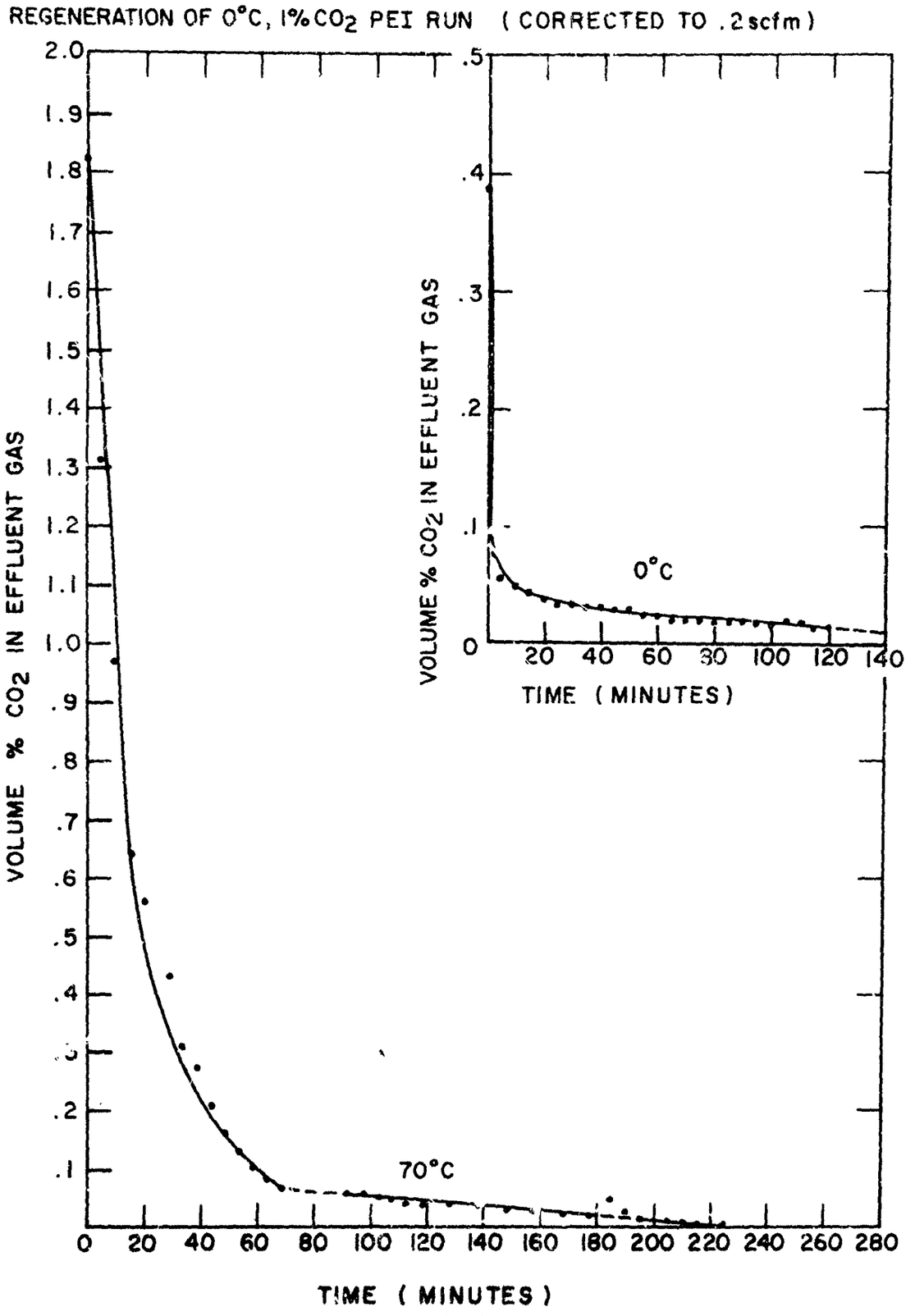
REGENERATION OF 0°C, 1% CO_2 PEI RUN (CORRECTED TO .2 scfm)
VOLUME % CO_2 IN EFFLUENT GAS
TIME (MINUTES)
70°C
0°C
0 20 40 60 80 100 120 140 160 180 200 220 240 260 280
0 20 40 60 80 100 120 140
.1 .2 .3 .4 .5 .6 .7 .8 .9 1.0 1.1 1.2 1.3 1.4 1.5 1.6 1.7 1.8 1.9 2.0
0 .1 .2 .3 .4 .5

FIGURE 46

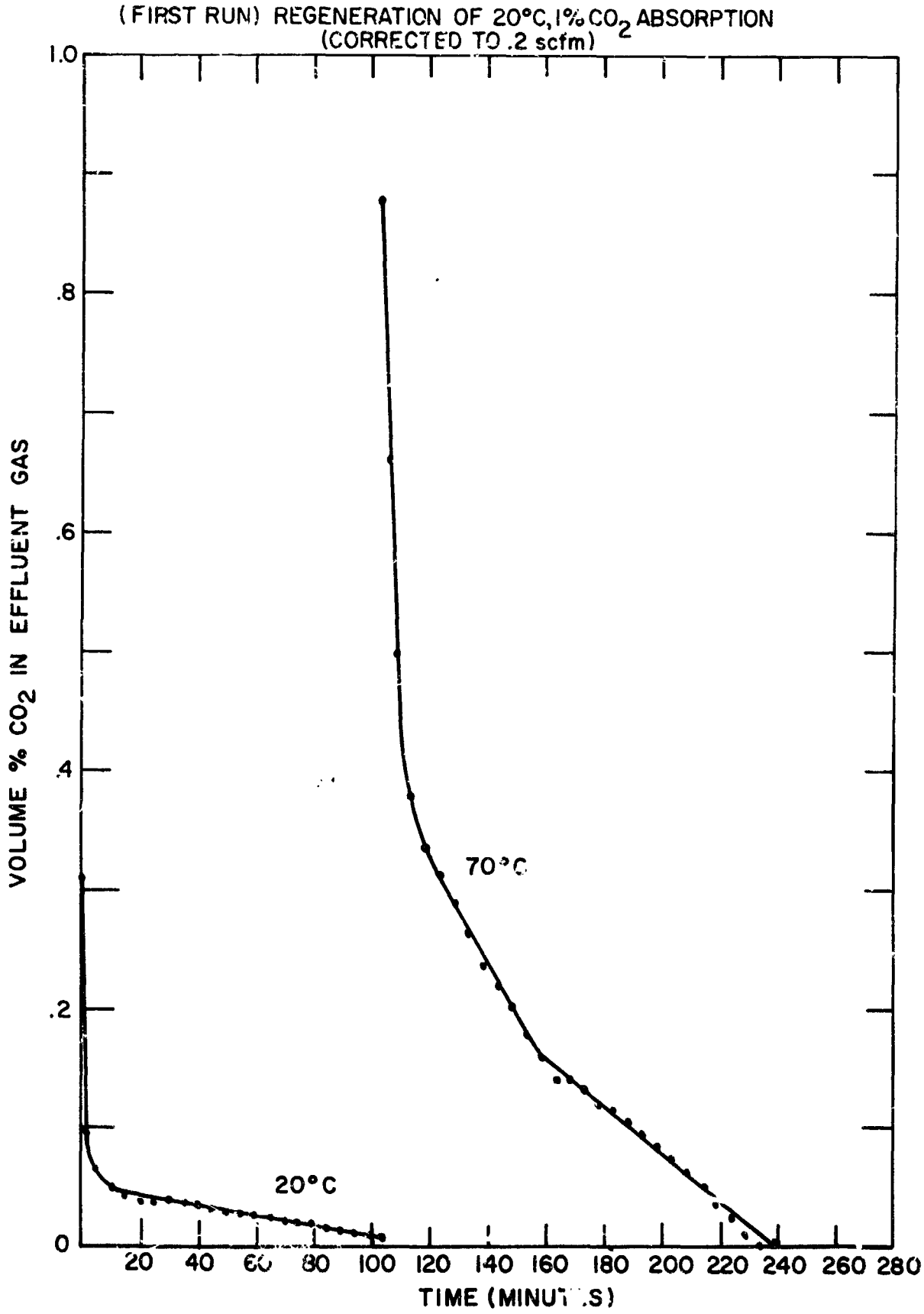
(FIRST RUN) REGENERATION OF 20°C, 1% CO_2 ABSORPTION
(CORRECTED TO .2 scfm)
VOLUME % CO_2 IN EFFLUENT GAS
1.0
.8
.6
.4
.2
0
20°C
70°C
20 40 60 80 100 120 140 160 180 200 220 240 260 280
TIME (MINUTES)

FIGURE 47

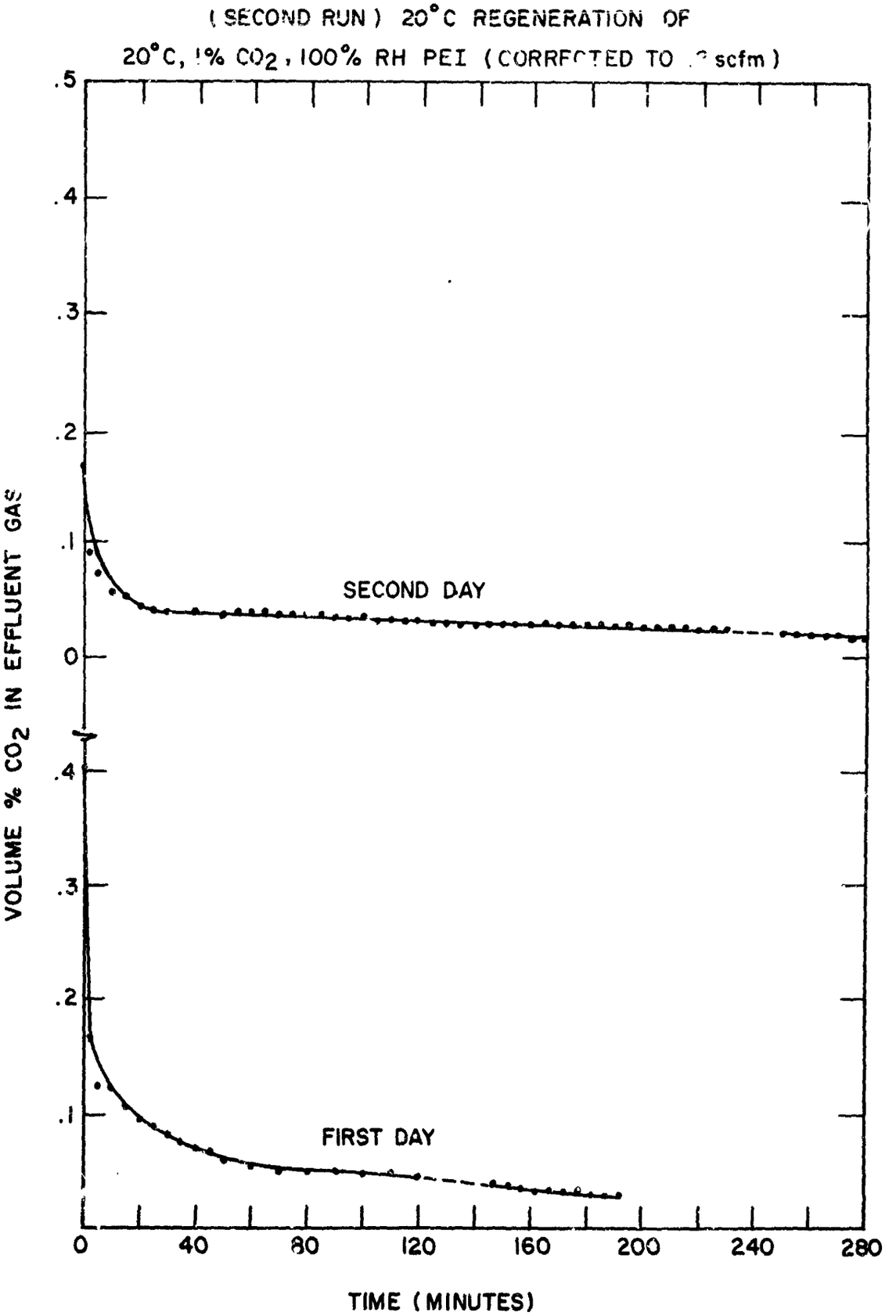

FIGURE 48

PAGE 180

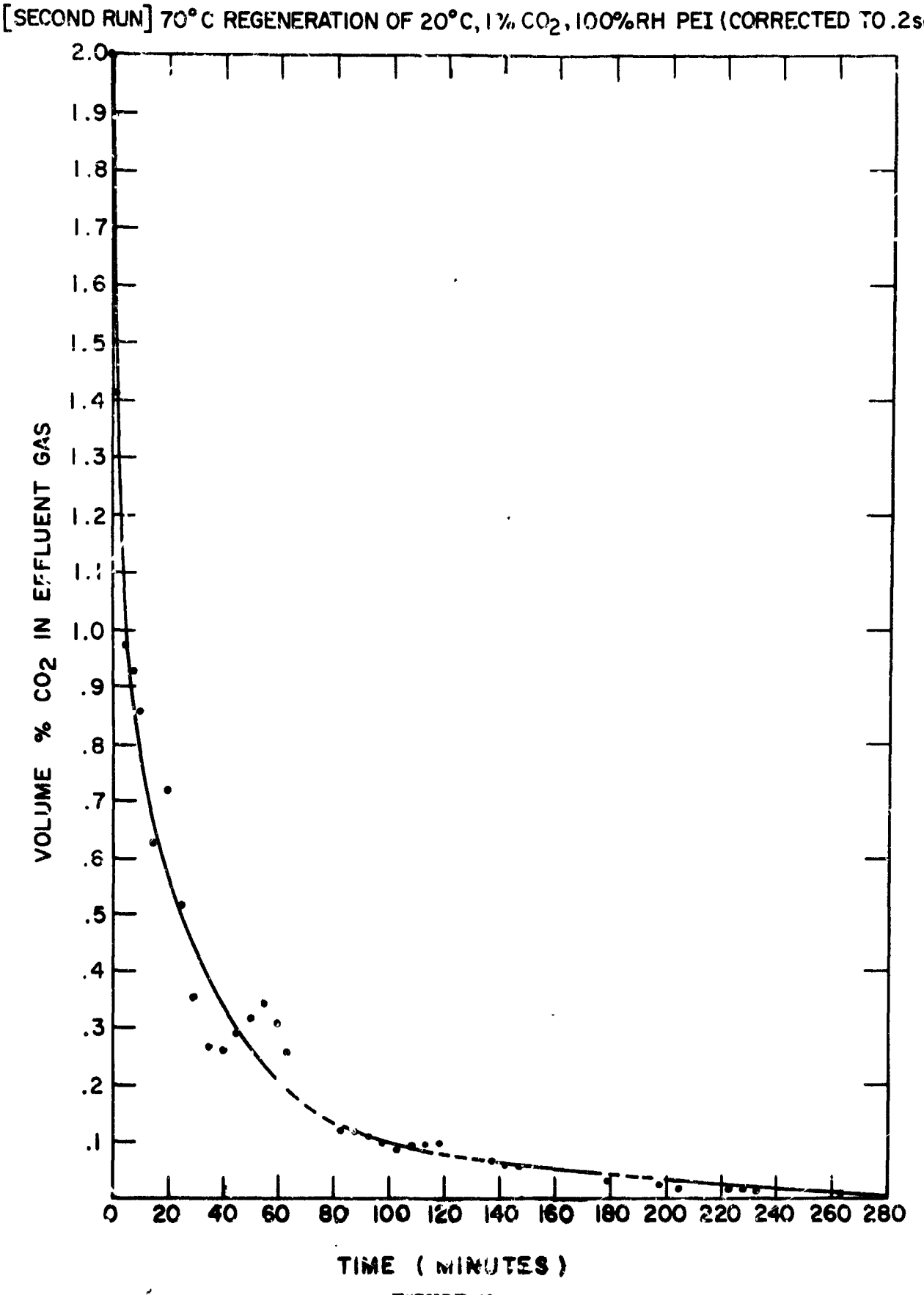
[SECOND RUN] 70°C REGENERATION OF 20°C, 1% CO_2, 100%RH PEI (CORRECTED TO .2scfm)
VOLUME % CO_2 IN EFFLUENT GAS
2.0
1.9
1.8
1.7
1.6
1.5
1.4
1.3
1.2
1.1
1.0
.9
.8
.7
.6
.5
.4
.3
.2
.1
0 20 40 60 80 100 120 140 160 180 200 220 240 260 280
TIME (MINUTES)

FIGURE 49

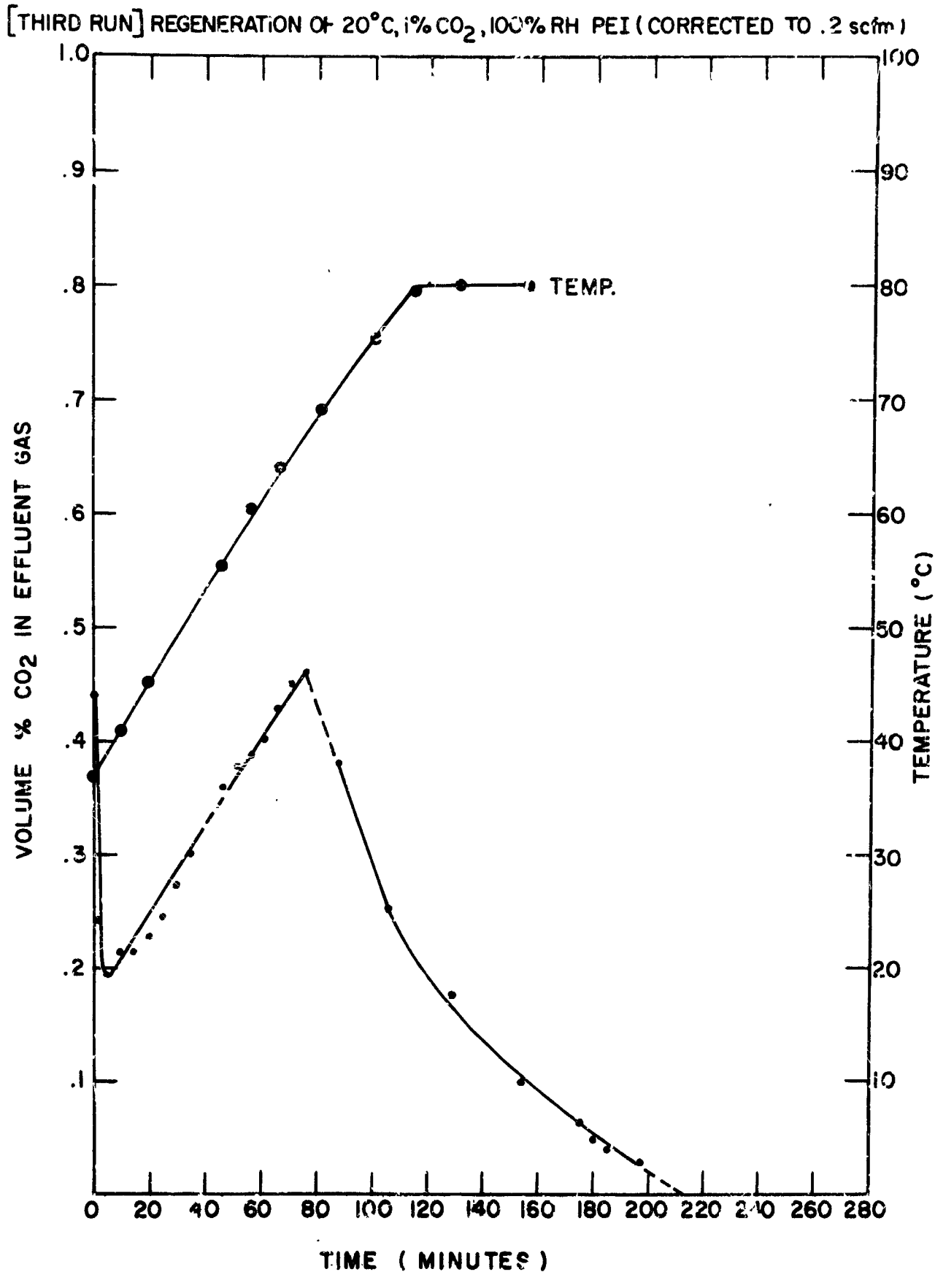

FIGURE 50

PAGE 182

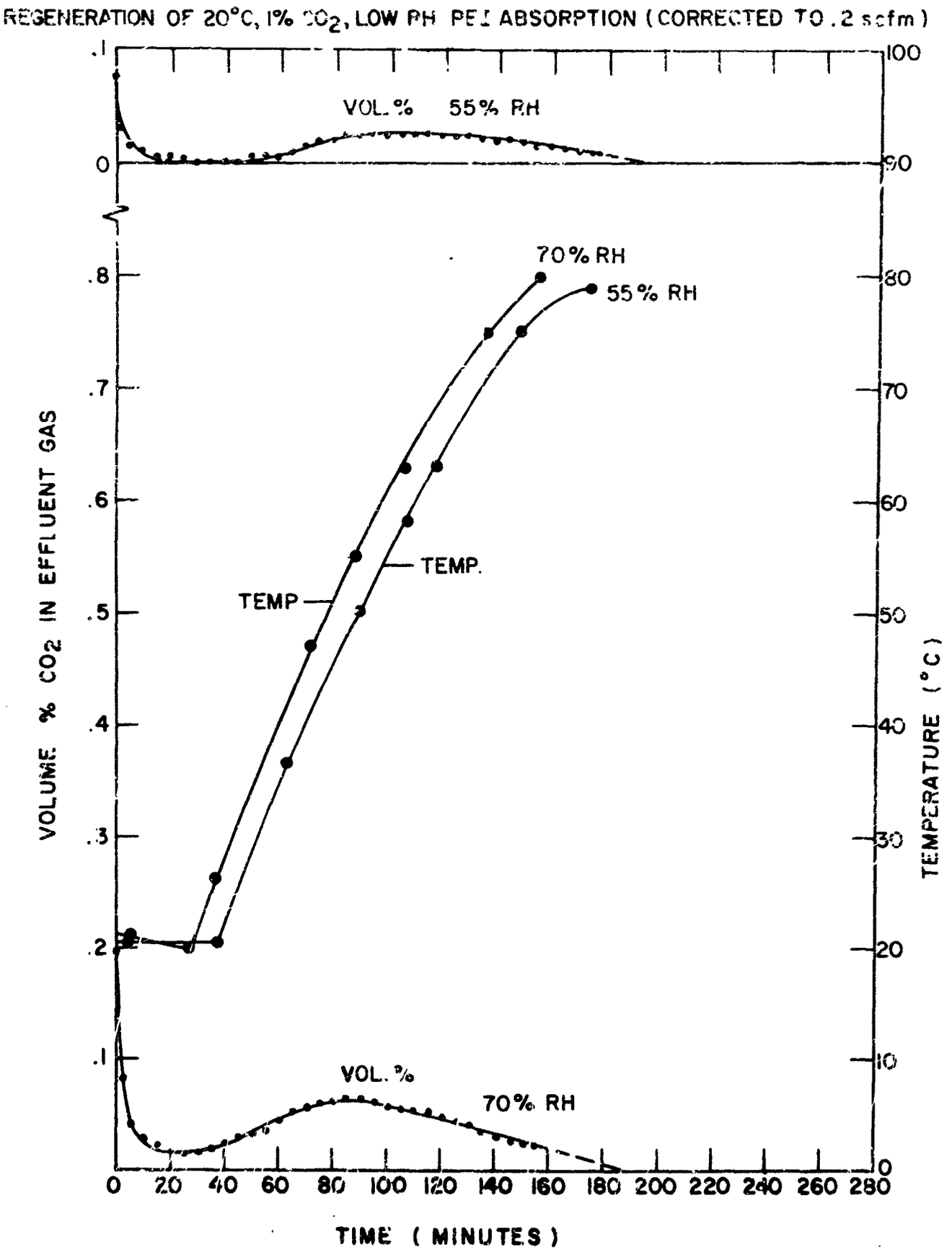
REGENERATION OF 20°C, 1% CO_2, LOW RH PEI ABSORPTION (CORRECTED TO .2 scfm)
VOL.% 55% RH
70% RH
55% RH
TEMP.
TEMP
VOL.%
70% RH
VOLUME % CO_2 IN EFFLUENT GAS
TEMPERATURE (°C)
TIME (MINUTES)
0
.1
.2
.3
.4
.5
.6
.7
.8
10
20
30
40
50
60
70
80
90
100
0 20 40 60 80 100 120 140 160 180 200 220 240 260 280

FIGURE 51

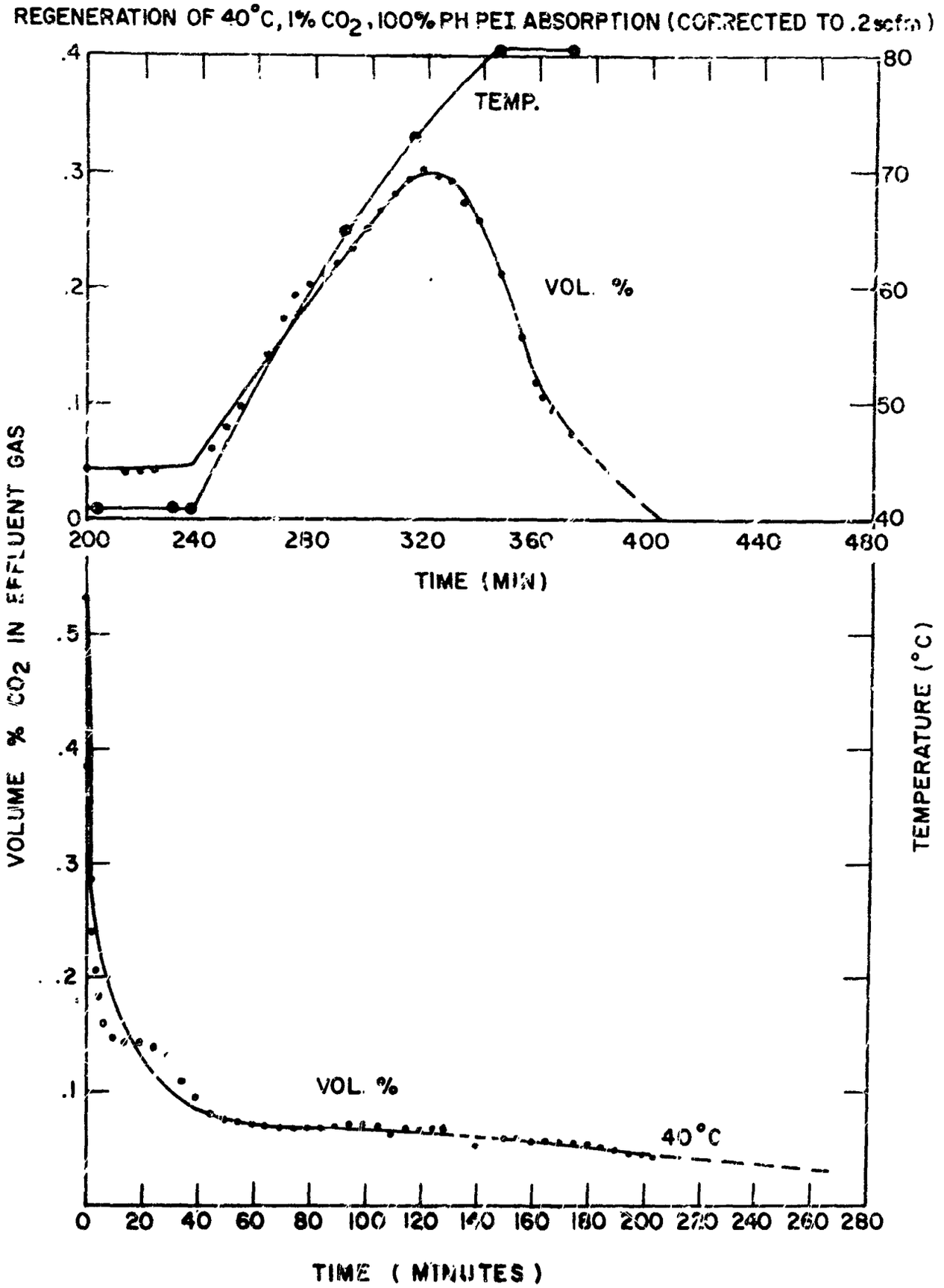

FIGURE 52

PAGE 184

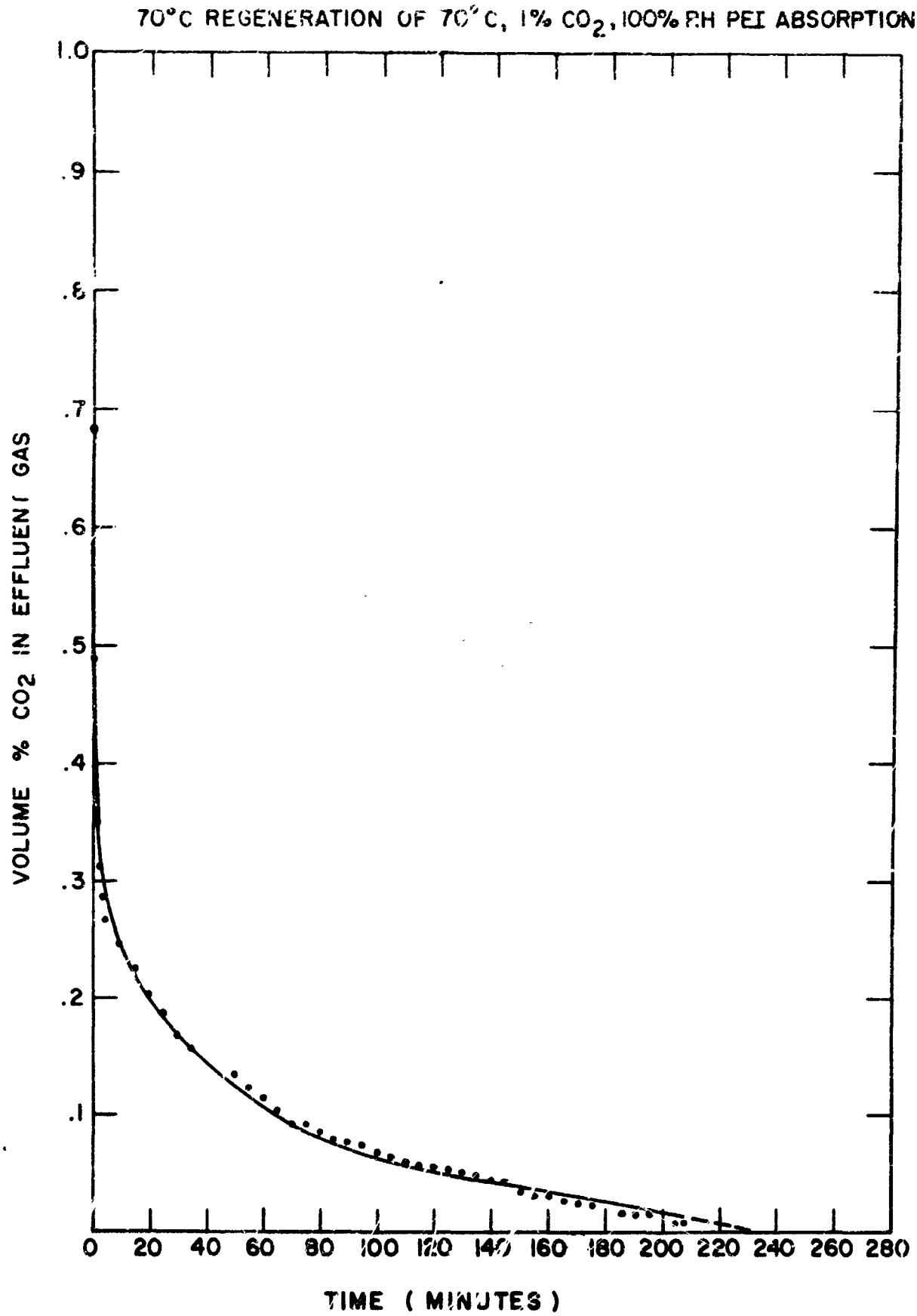

FIGURE 53

PAGE 185

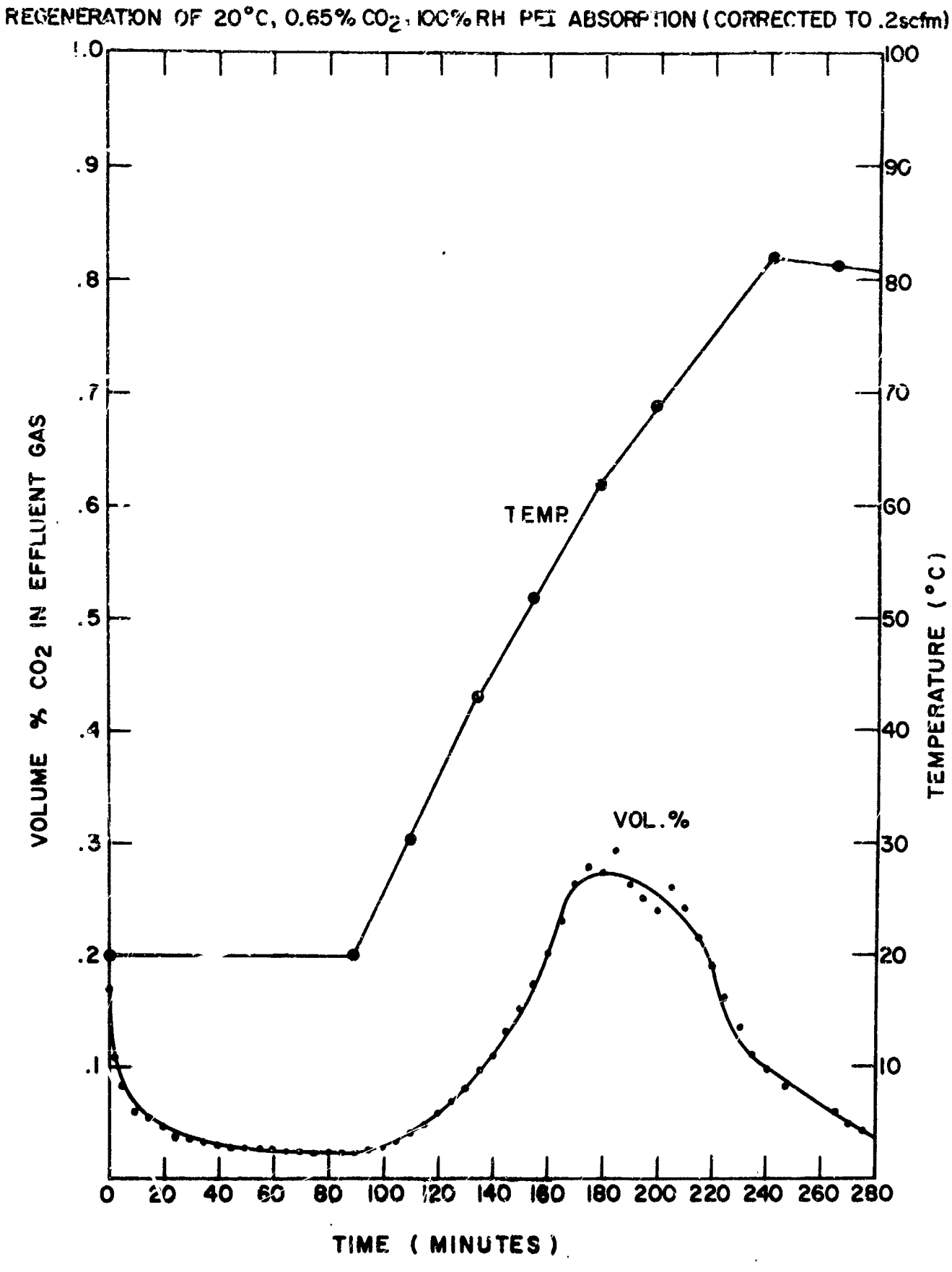

FIGURE 54

PAGE 186

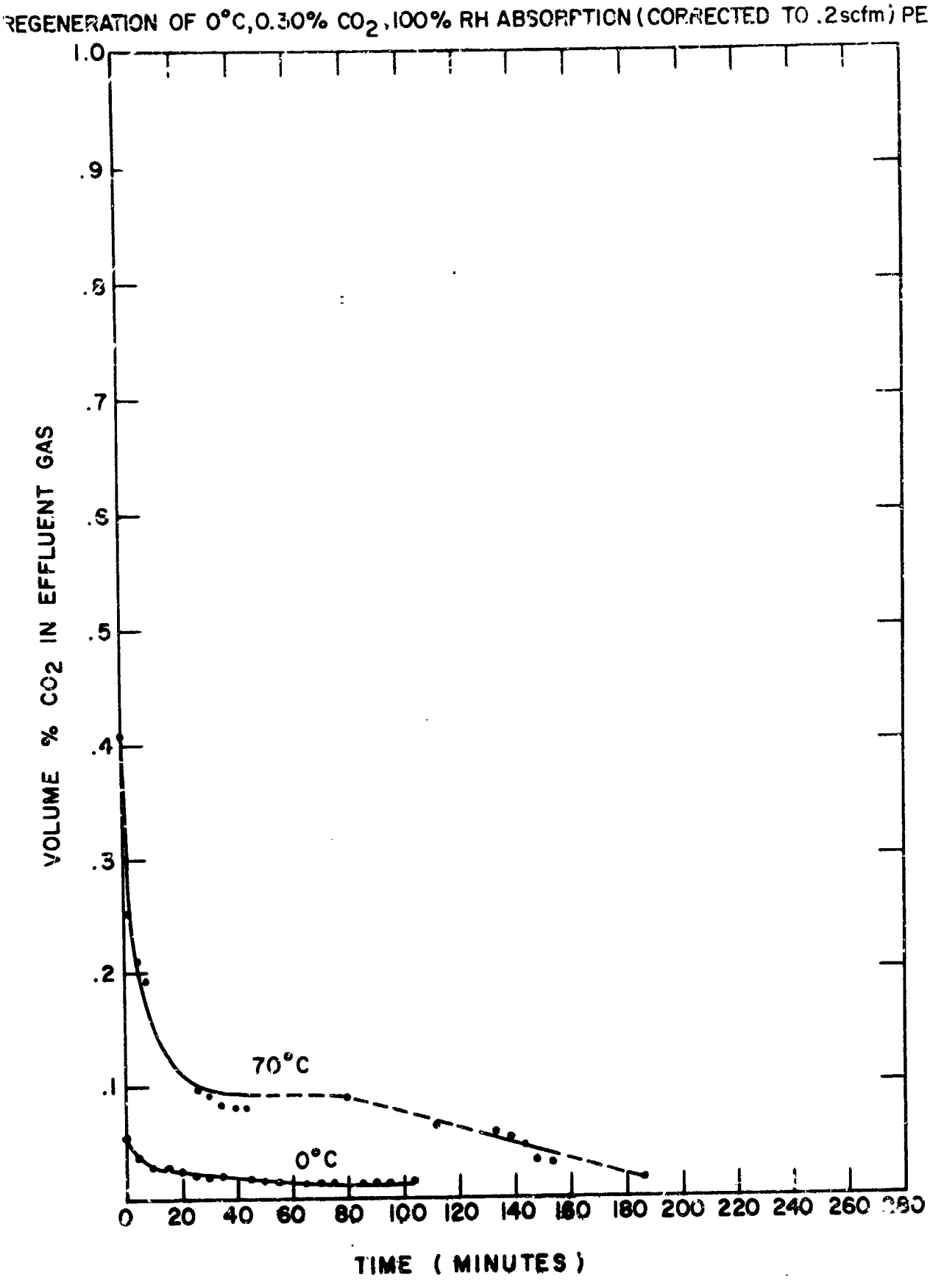
REGENERATION OF 0°C, 0.30% CO_2, 100% RH ABSORPTION (CORRECTED TO .2scfm) PEI
VOLUME % CO_2 IN EFFLUENT GAS
1.0
.9
.8
.7
.6
.5
.4
.3
.2
.1
70°C
0°C
0 20 40 60 80 100 120 140 160 180 200 220 240 260 280
TIME (MINUTES)

FIGURE 55

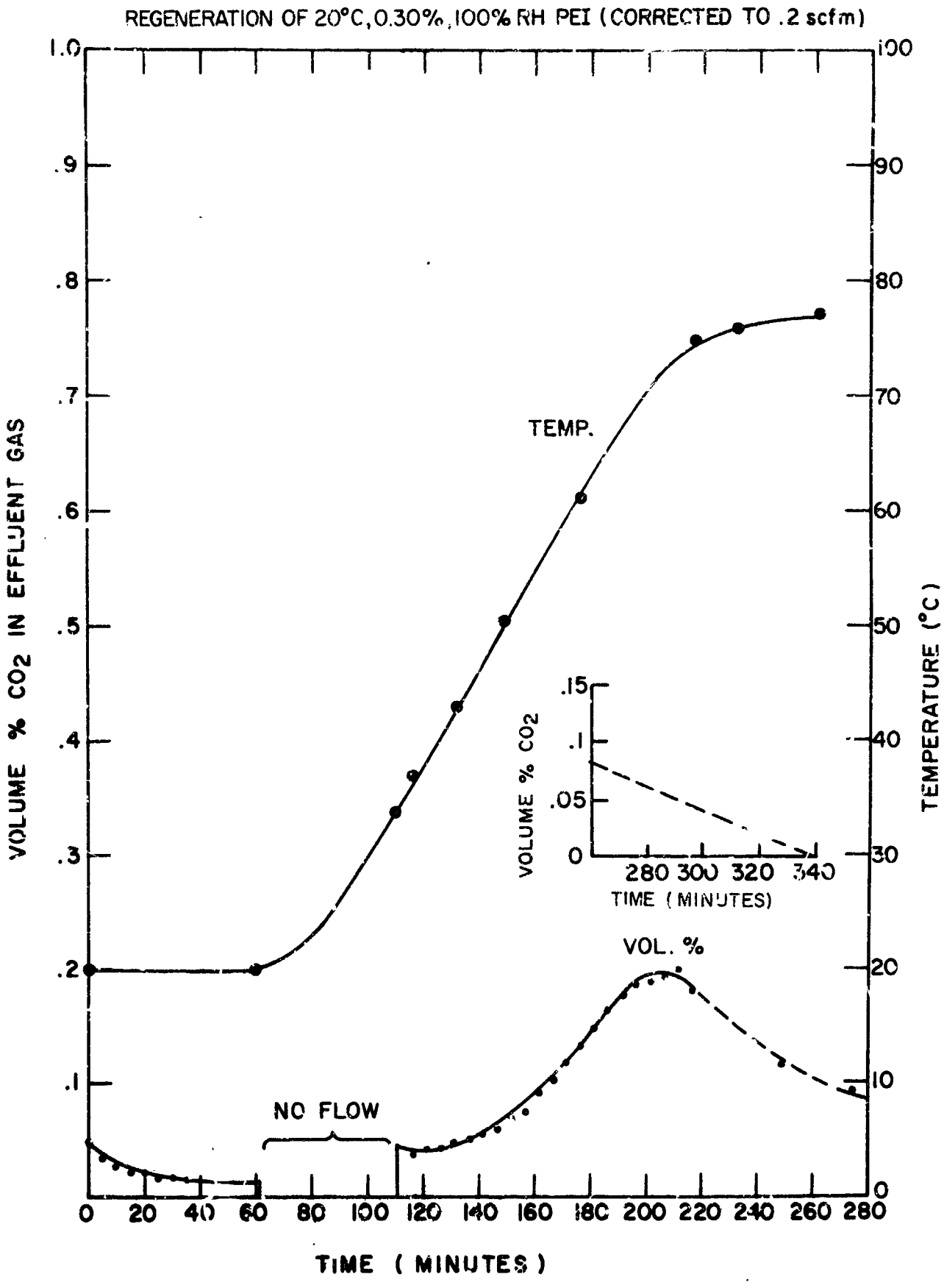

FIGURE 56

PAGE 188

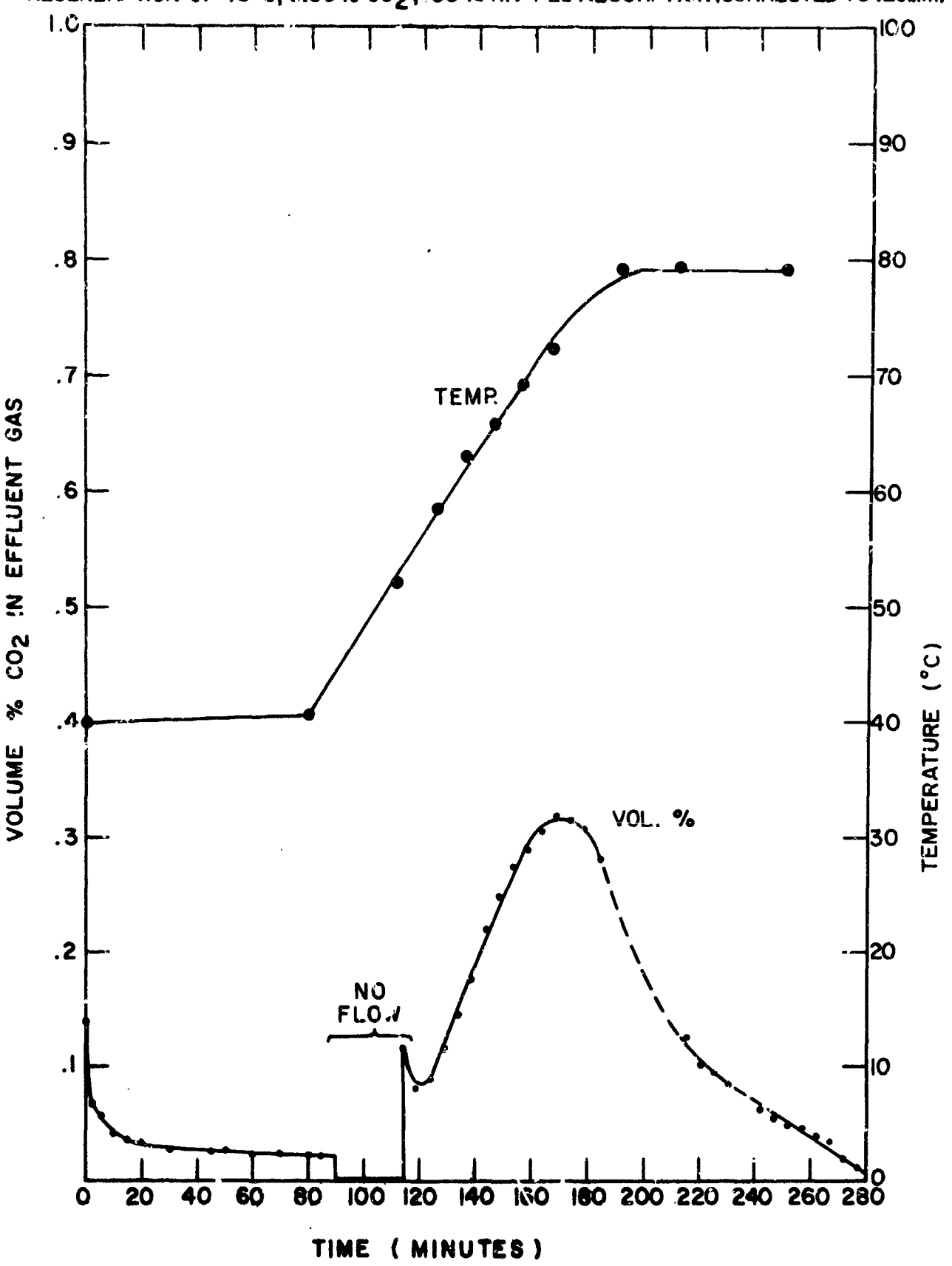

FIGURE 57

PAGE 189

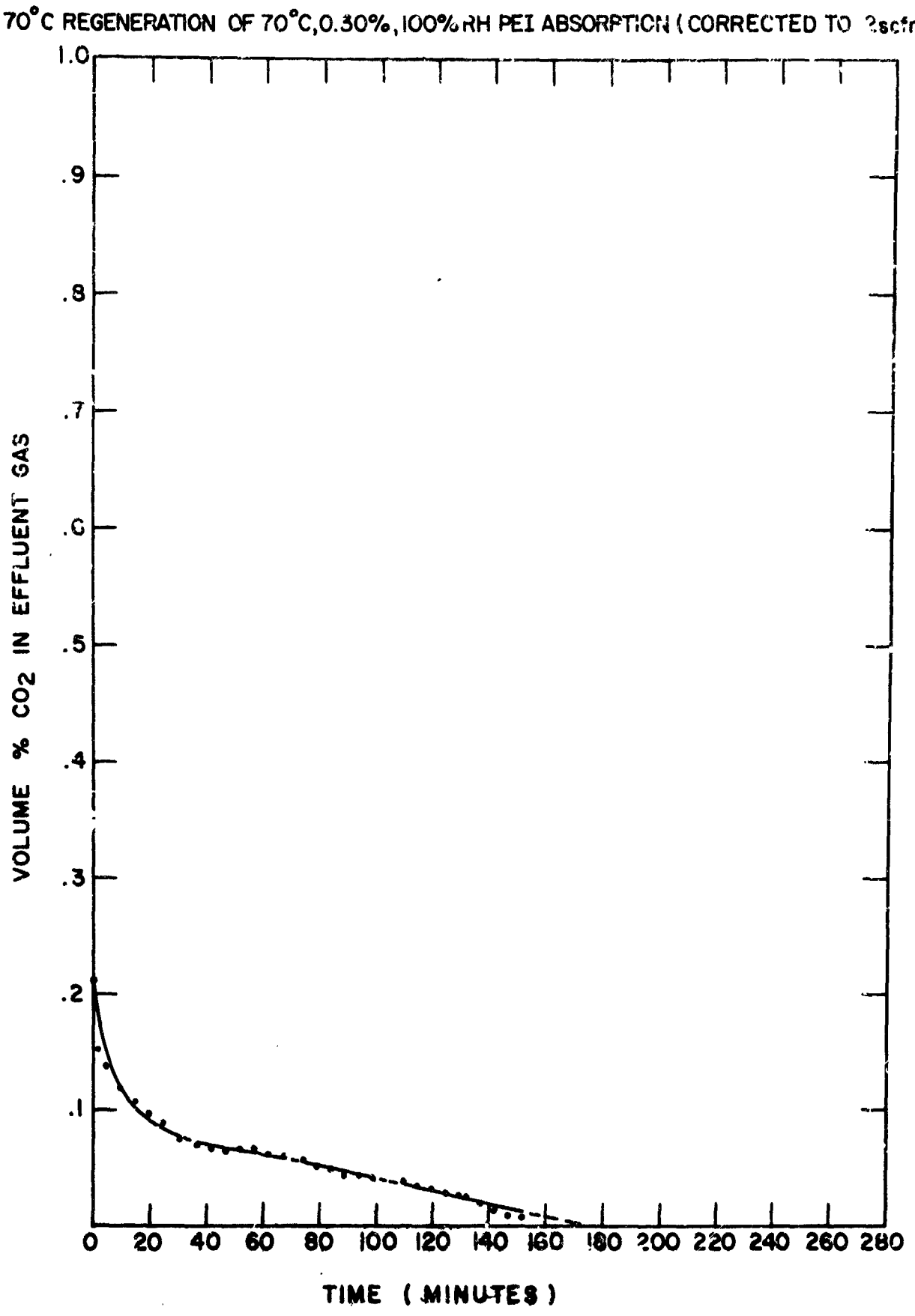

FIGURE 58

PAGE 190

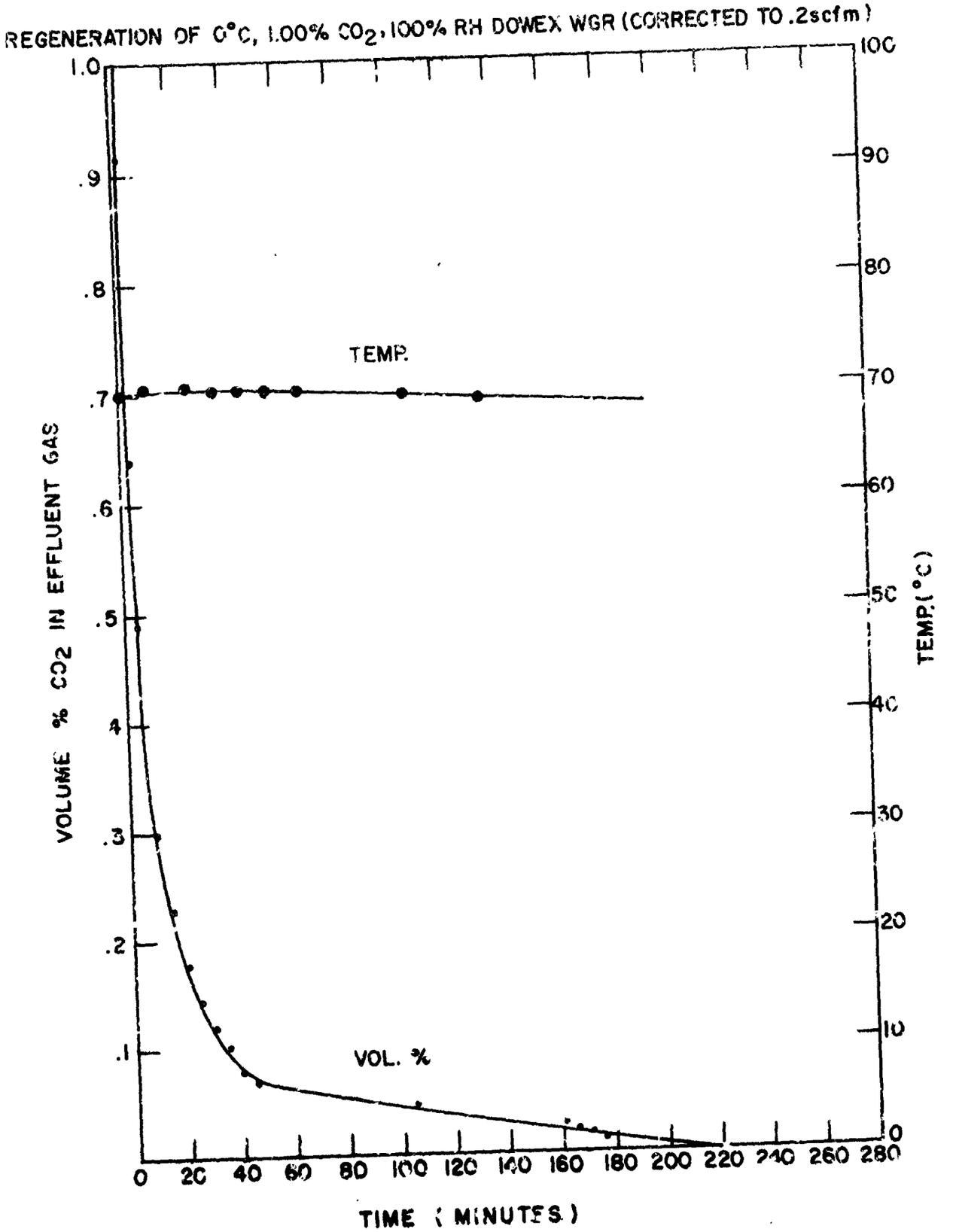

FIGURE 59
PAGE 191

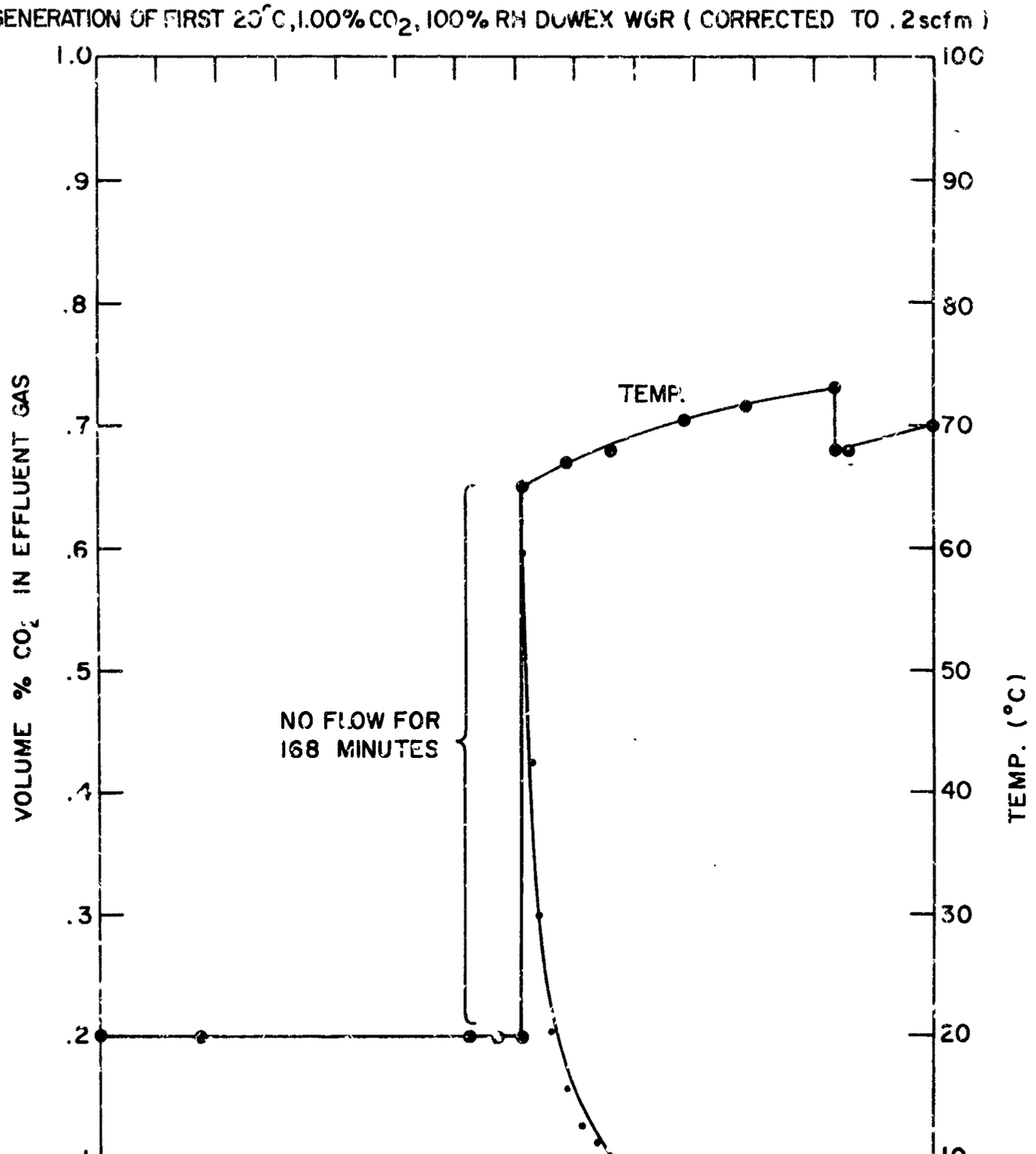
REGENERATION OF FIRST 25°C, 1.00% CO_2, 100% RH DOWEX WGR (CORRECTED TO .2 scfm)
VOLUME % CO_2 IN EFFLUENT GAS
TEMP. (°C)
TEMP.
NO FLOW FOR
168 MINUTES
VOL. %
TIME (MINUTES)
1.0
.9
.8
.7
.6
.5
.4
.3
.2
.1
0
100
90
80
70
60
50
40
30
20
10
0
0 20 40 60 80 100 120 140 160 180 200 220 240 260 280

FIGURE 60

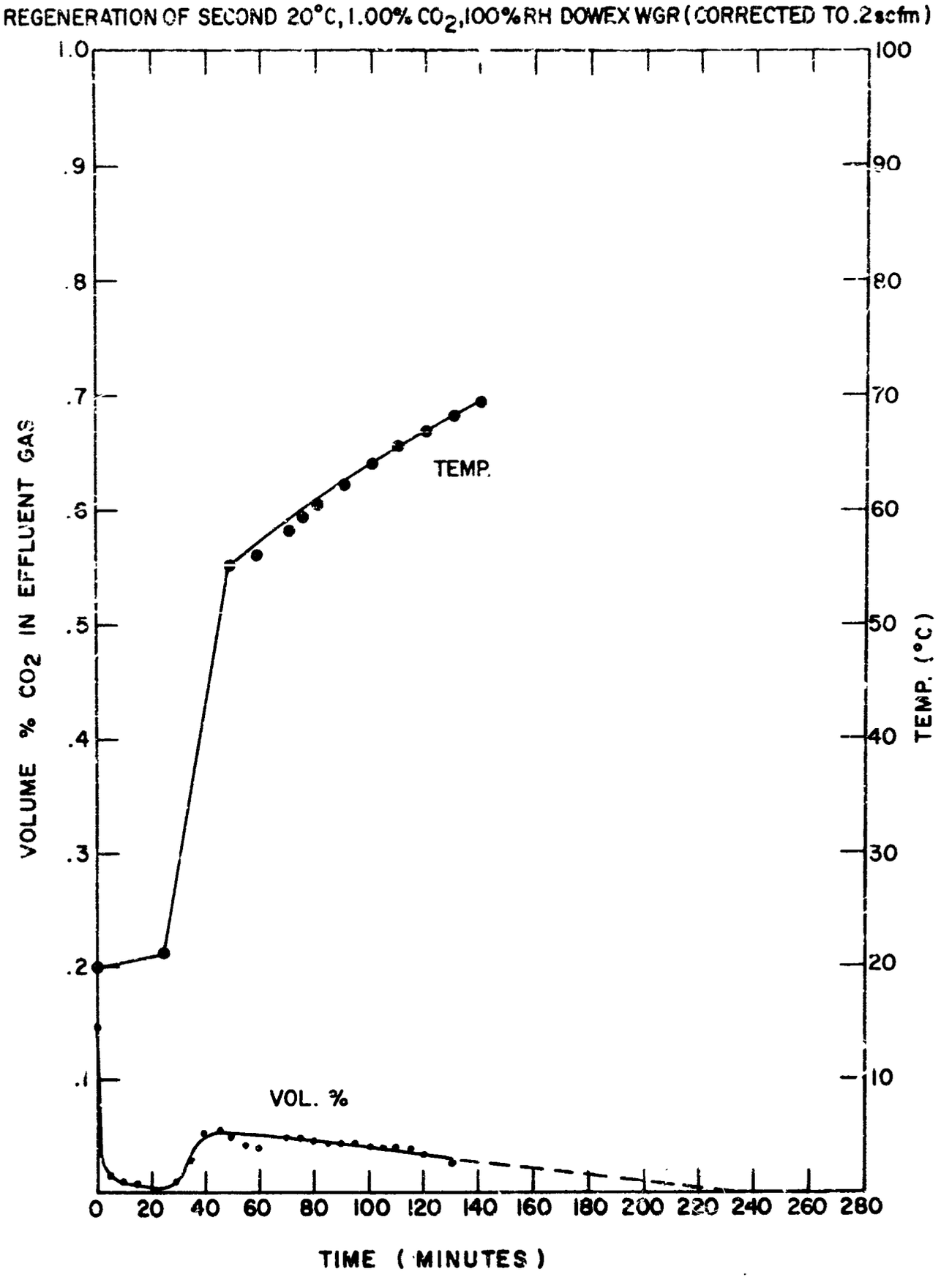

FIGURE 61

PAGE 193

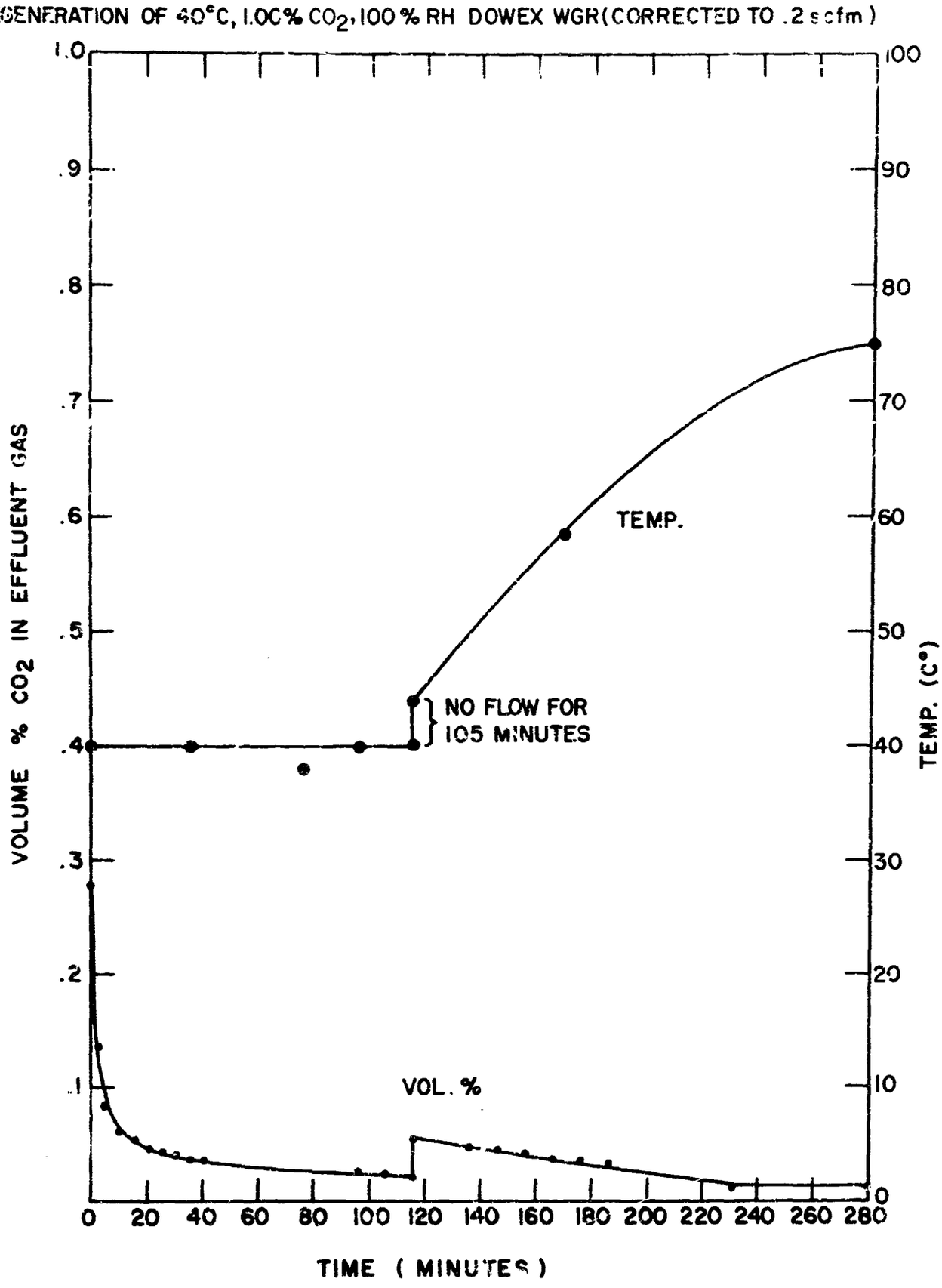

FIGURE 62

PAGE 194

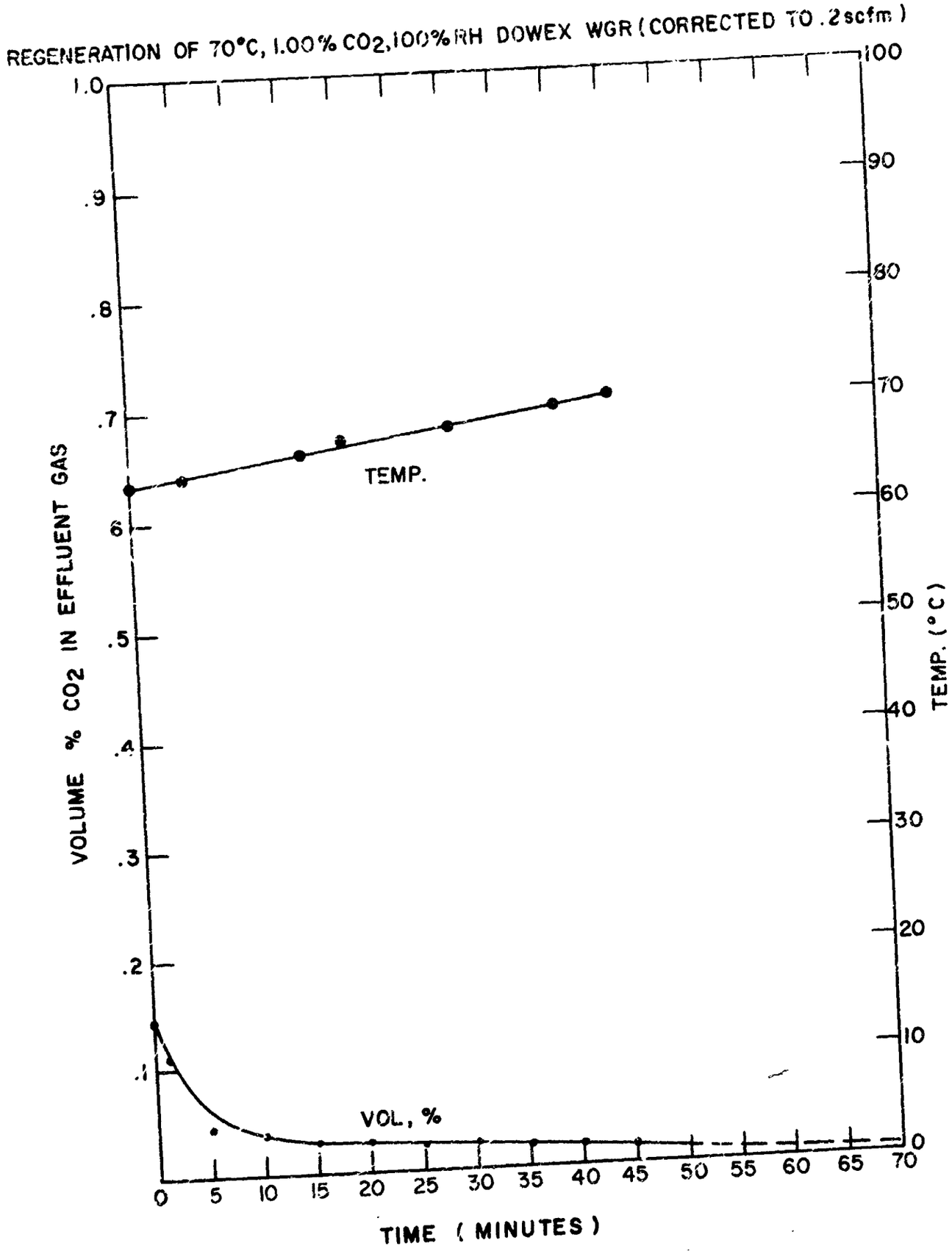

FIGURE 63

PAGE 195

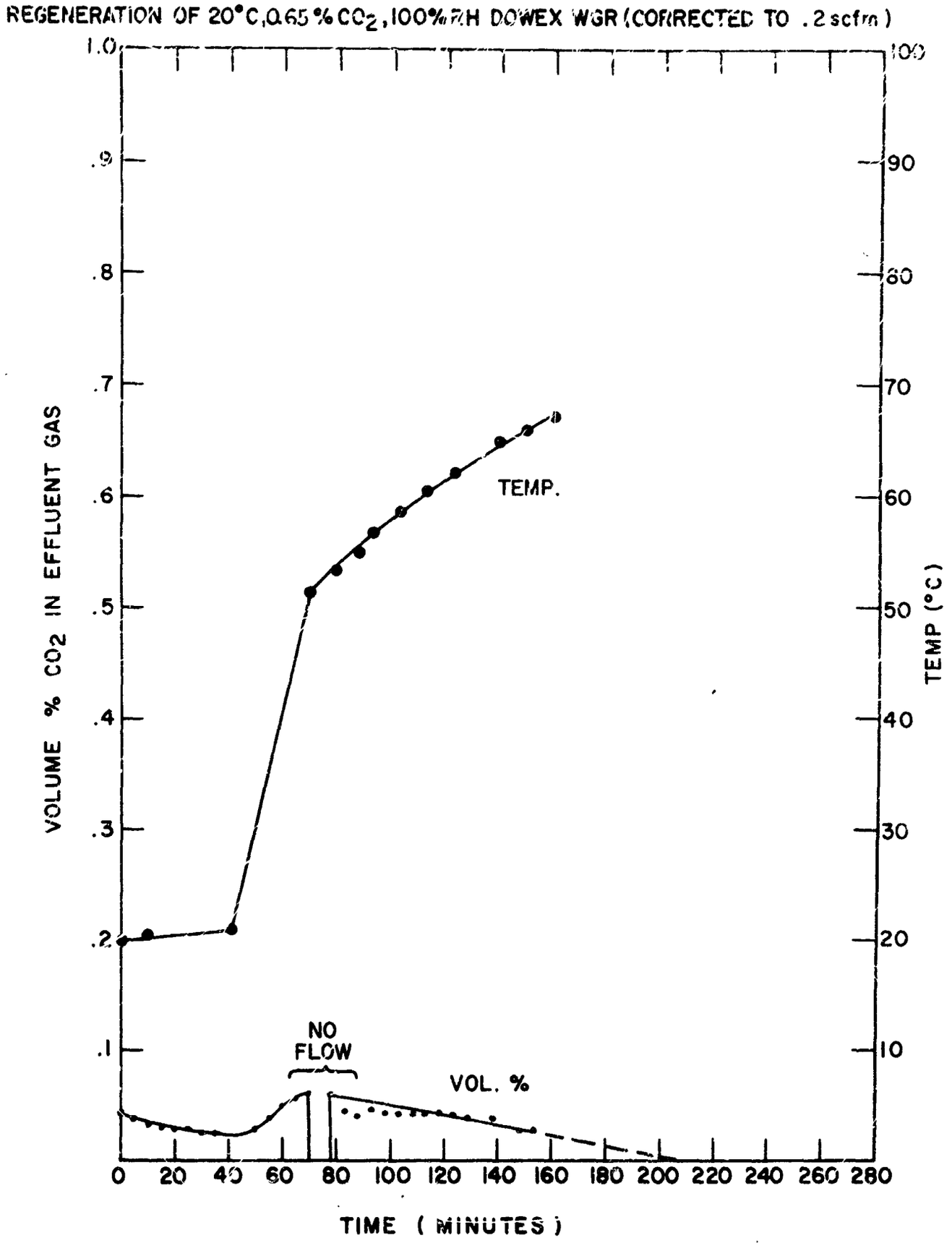

FIGURE 64

PAGE 196

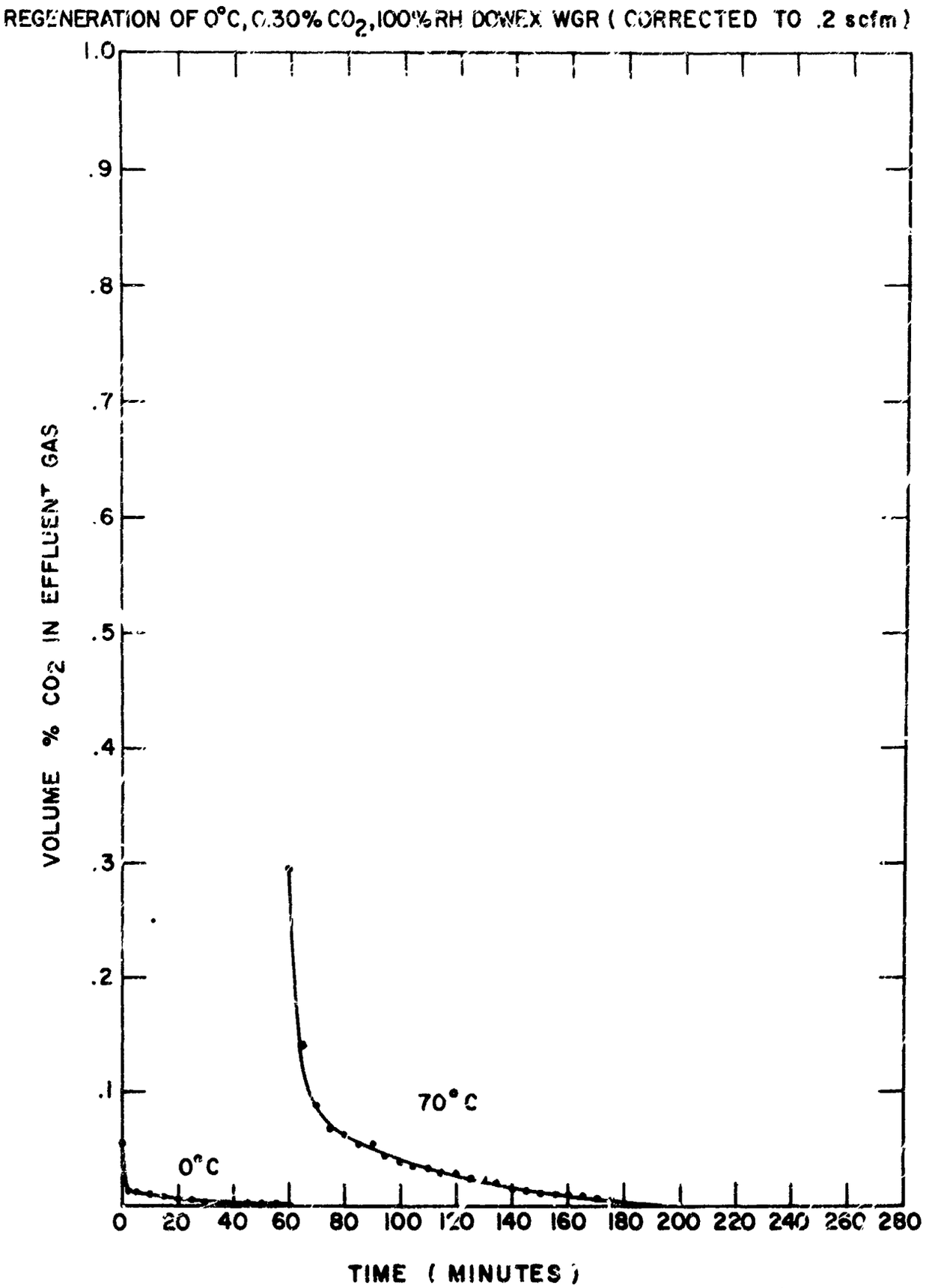

FIGURE 65

PAGE 197

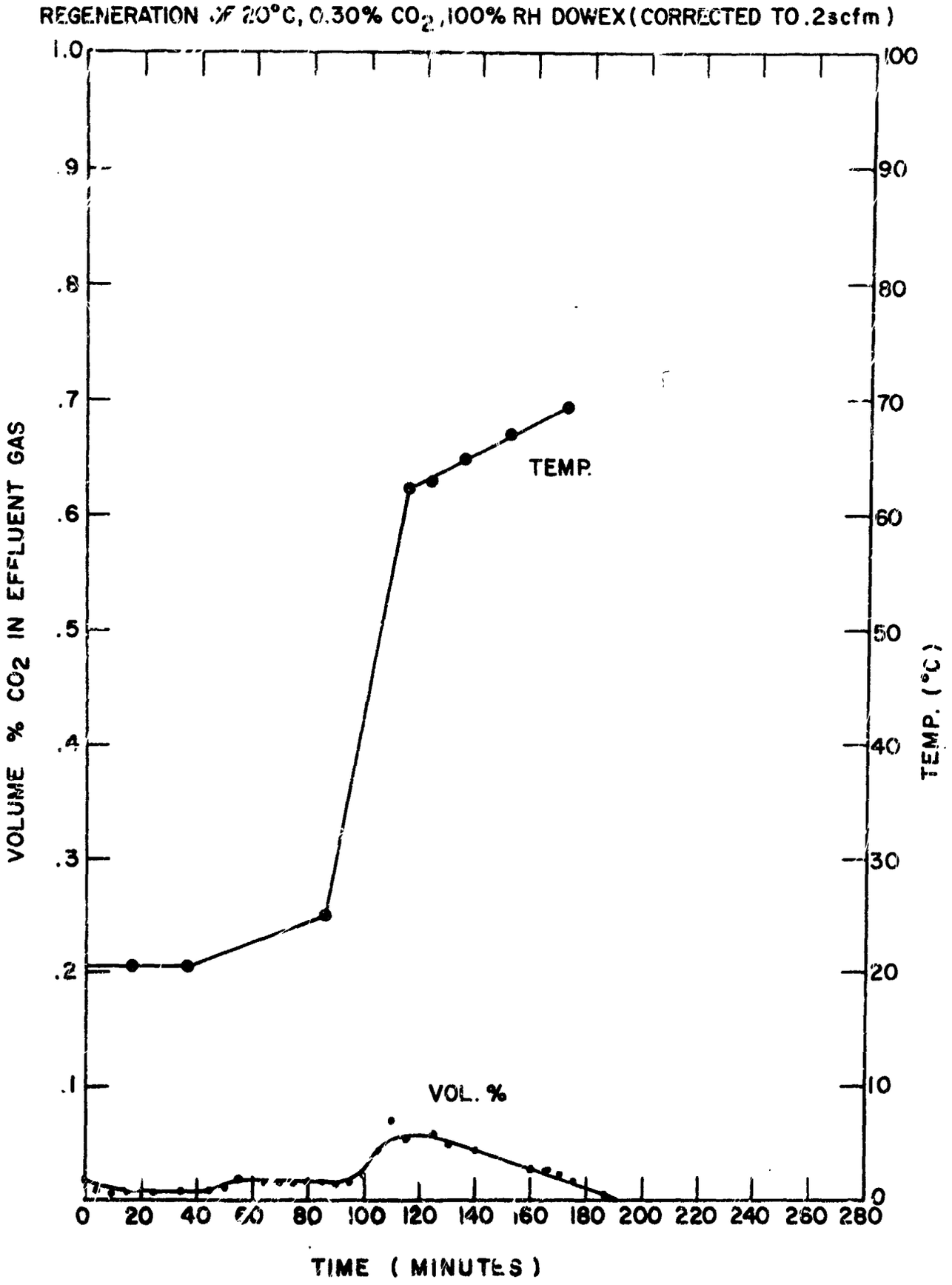

FIGURE 66

PAGE 198

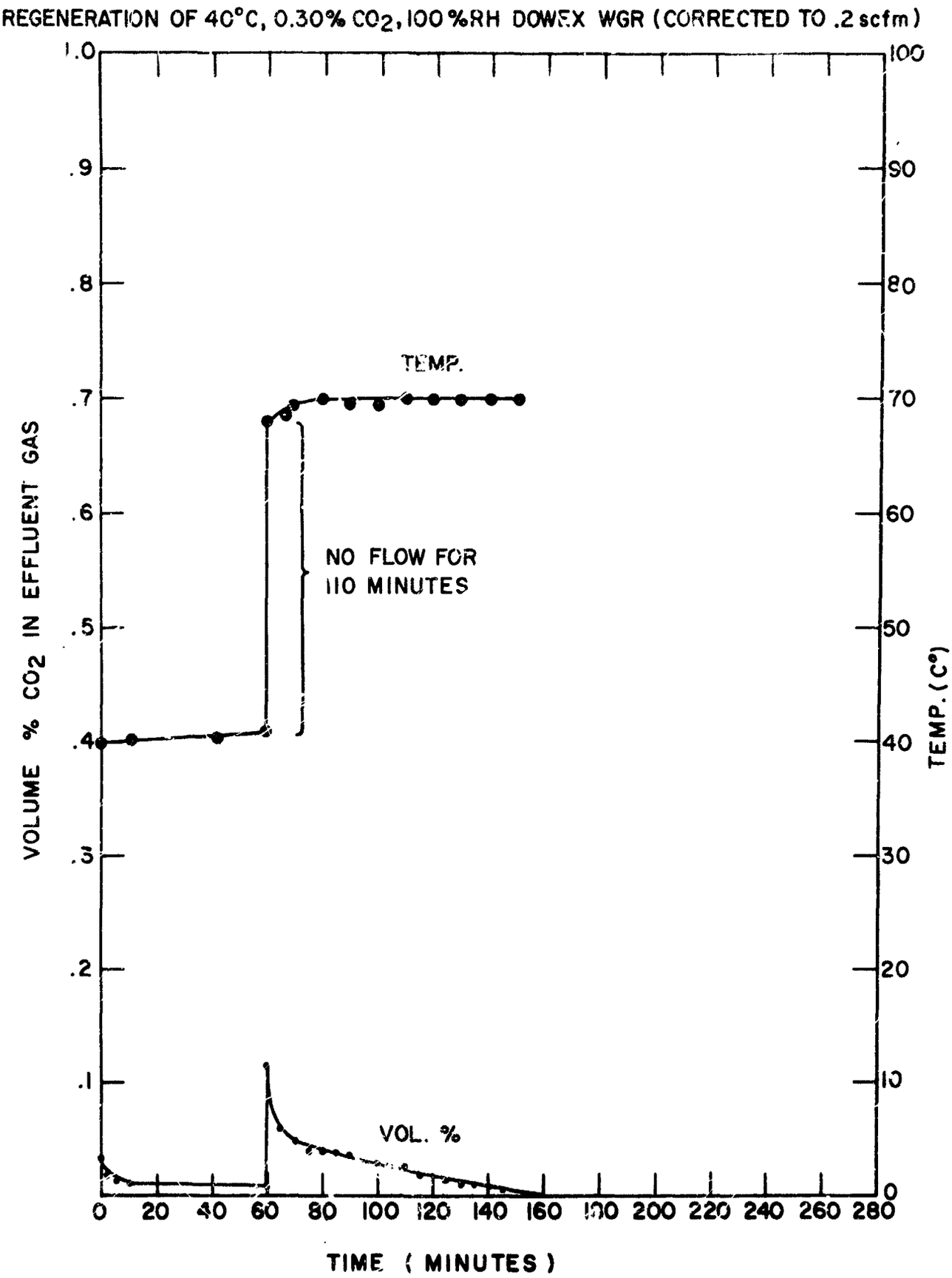
REGENERATION OF 40°C, 0.30% CO_2, 100 %RH DOWEX WGR (CORRECTED TO .2 scfm)
VOLUME % CO_2 IN EFFLUENT GAS
TEMP. (C°)
TEMP.
NO FLOW FOR
110 MINUTES
VOL. %
TIME (MINUTES)
1.0
.9
.8
.7
.6
.5
.4
.3
.2
.1
100
90
80
70
60
50
40
30
20
10
0
0 20 40 60 80 100 120 140 160 180 200 220 240 260 280

FIGURE 67

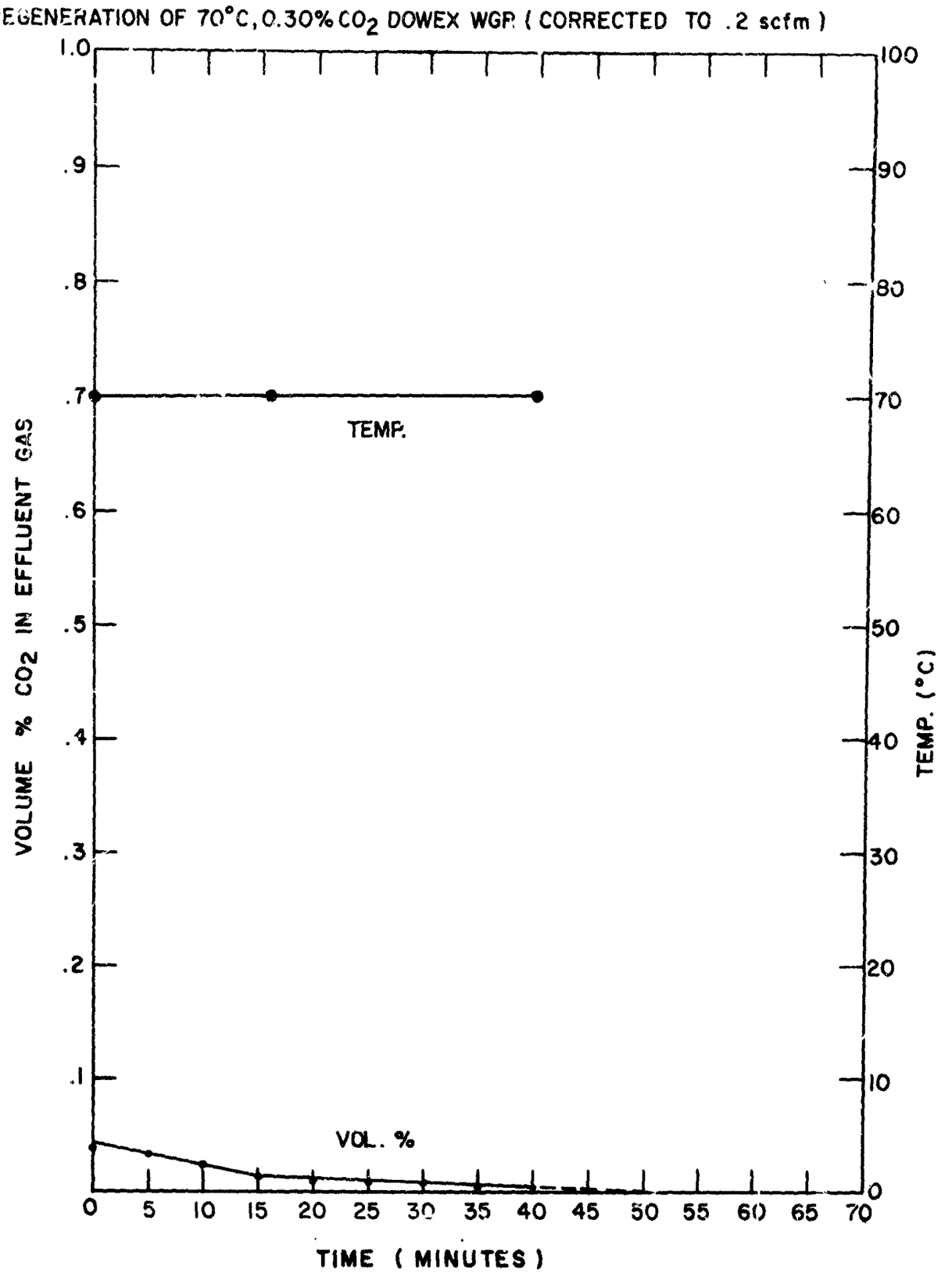

FIGURE 68
PAGE 200

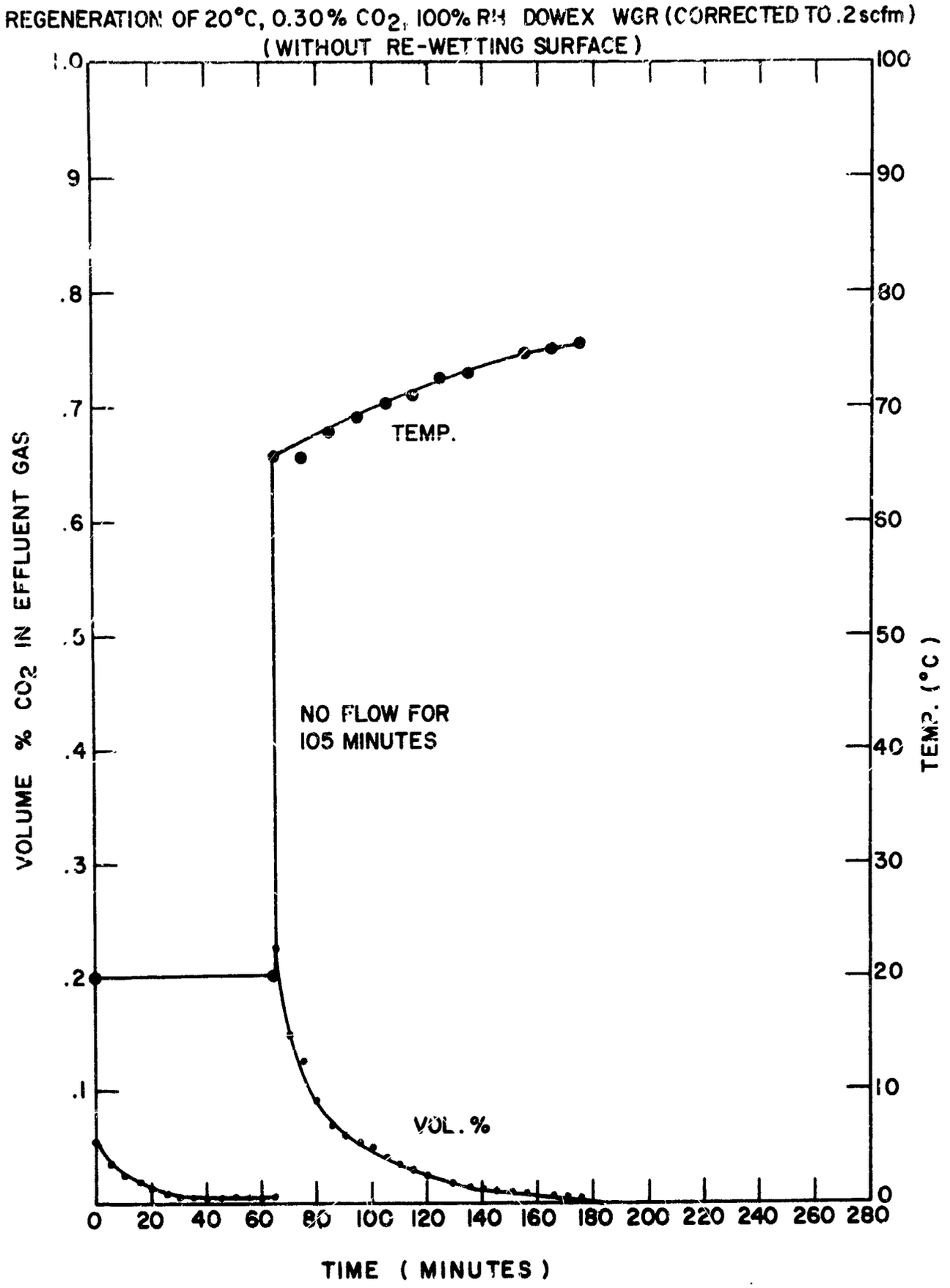

FIGURE 69

PAGE 201

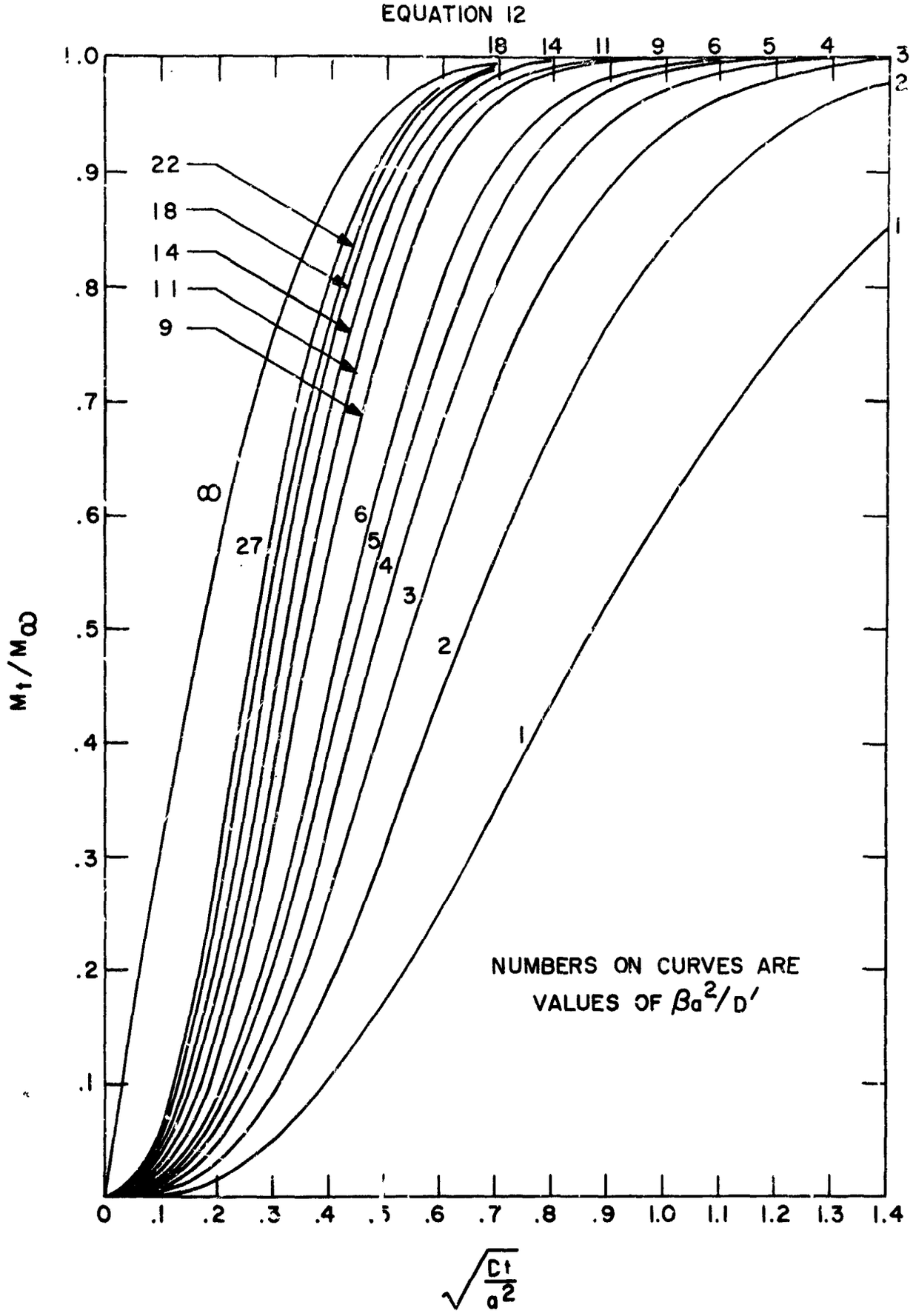
EQUATION 12
18
14
11
9
6
5
4
3
2
1
22
18
14
11
9
8
27
6
5
4
3
2
1
1.0
.9
.8
.7
.6
.5
.4
.3
.2
.1
M_t/M_∞
NUMBERS ON CURVES ARE
VALUES OF $\beta a^2/D'$
0
.1
.2
.3
.4
.5
.6
.7
.8
.9
1.0
1.1
1.2
1.3
1.4
$\sqrt{\frac{Dt}{a^2}}$

FIGURE 70

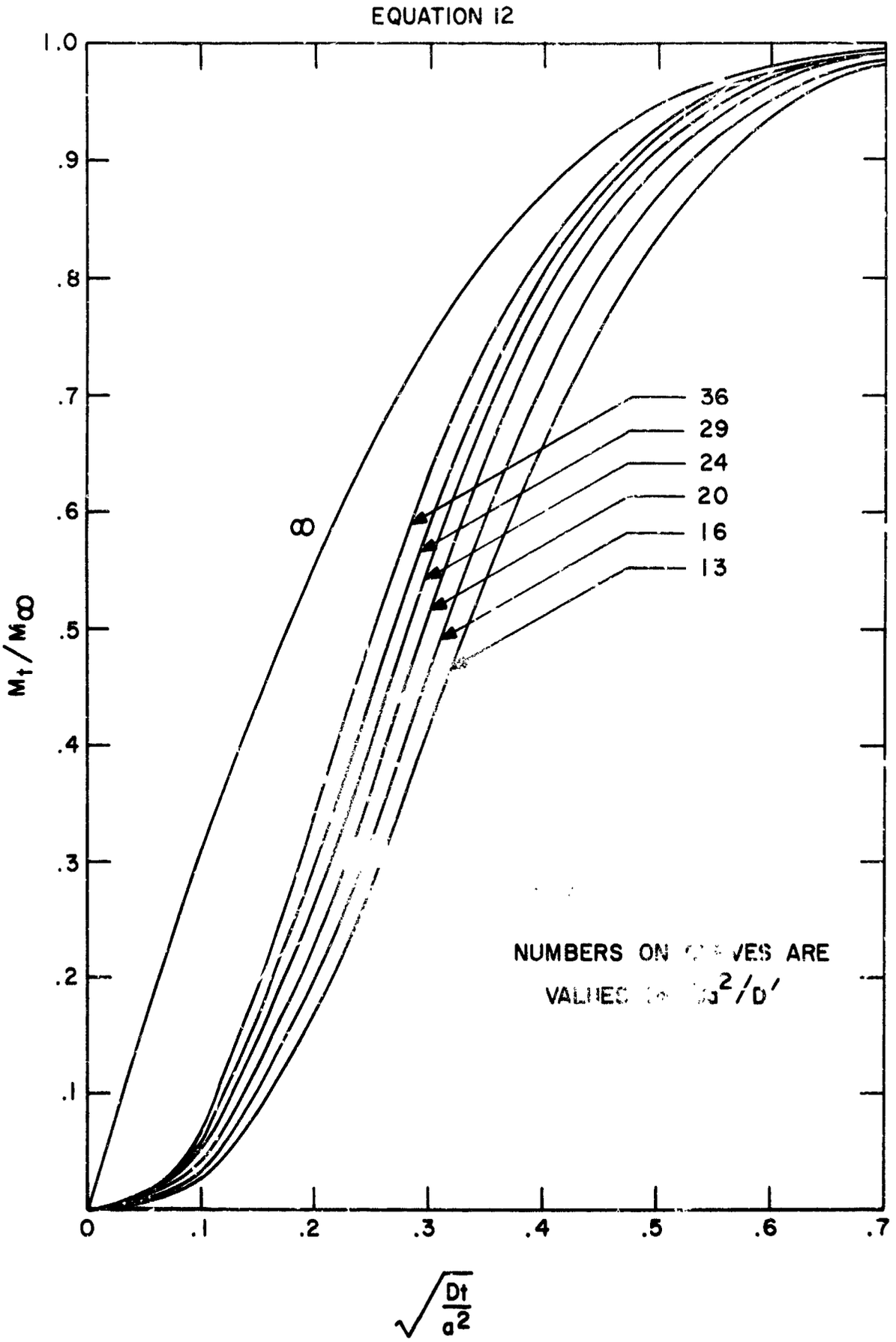
EQUATION 12
1.0
.9
.8
.7
.6
.5
.4
.3
.2
.1
0
.1
.2
.3
.4
.5
.6
.7
M_t/M_∞
$\sqrt{\frac{Dt}{a^2}}$
∞
36
29
24
20
16
13
NUMBERS ON CURVES ARE
VALUES OF a^2/D'

FIGURE 71

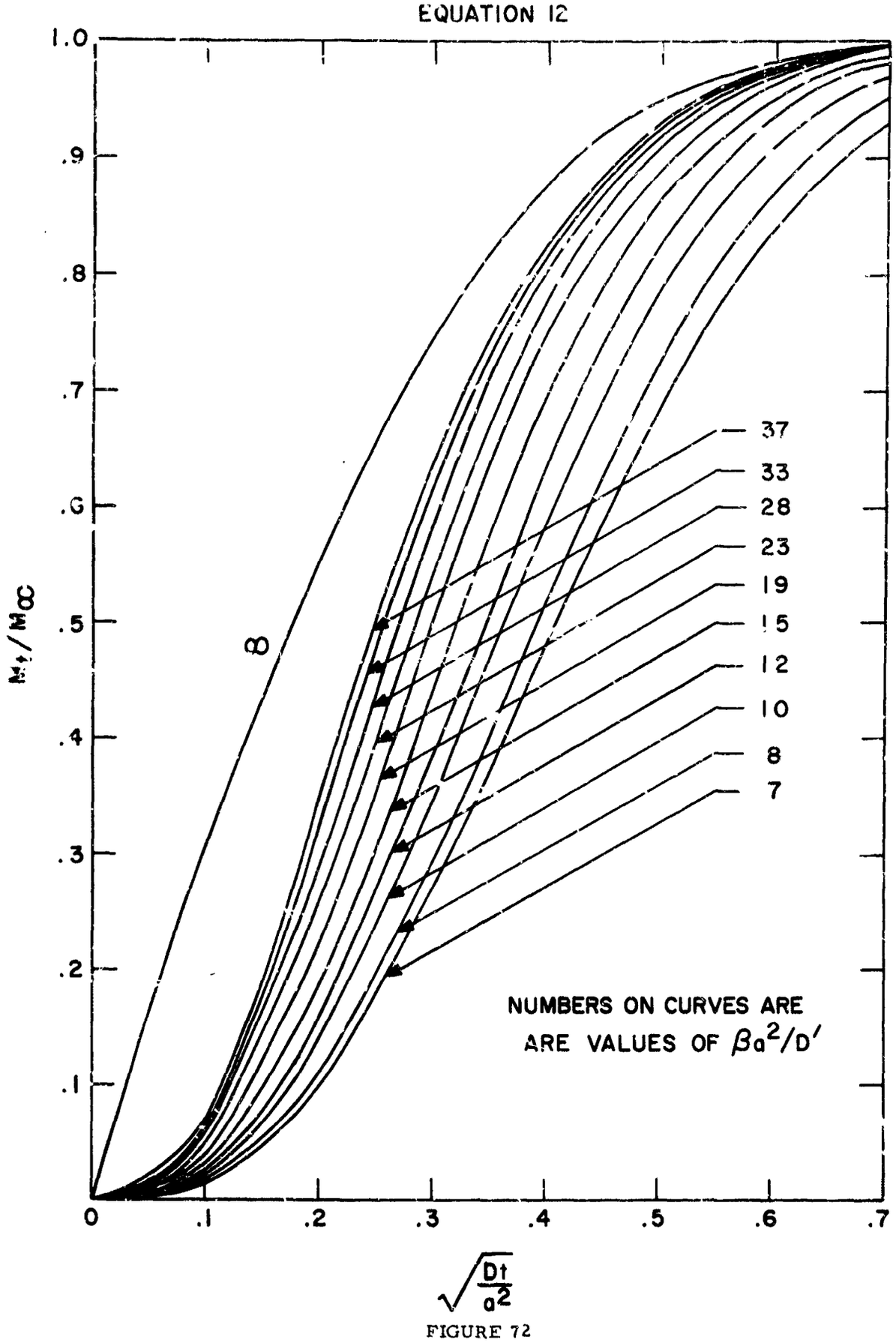
EQUATION 12
1.0
.9
.8
.7
.6
.5
.4
.3
.2
.1
0
.1
.2
.3
.4
.5
.6
.7
M_t/M_∞
$\sqrt{\frac{Dt}{a^2}}$
∞
37
33
28
23
19
15
12
10
8
7
NUMBERS ON CURVES ARE
ARE VALUES OF $\beta a^2/D'$

FIGURE 72

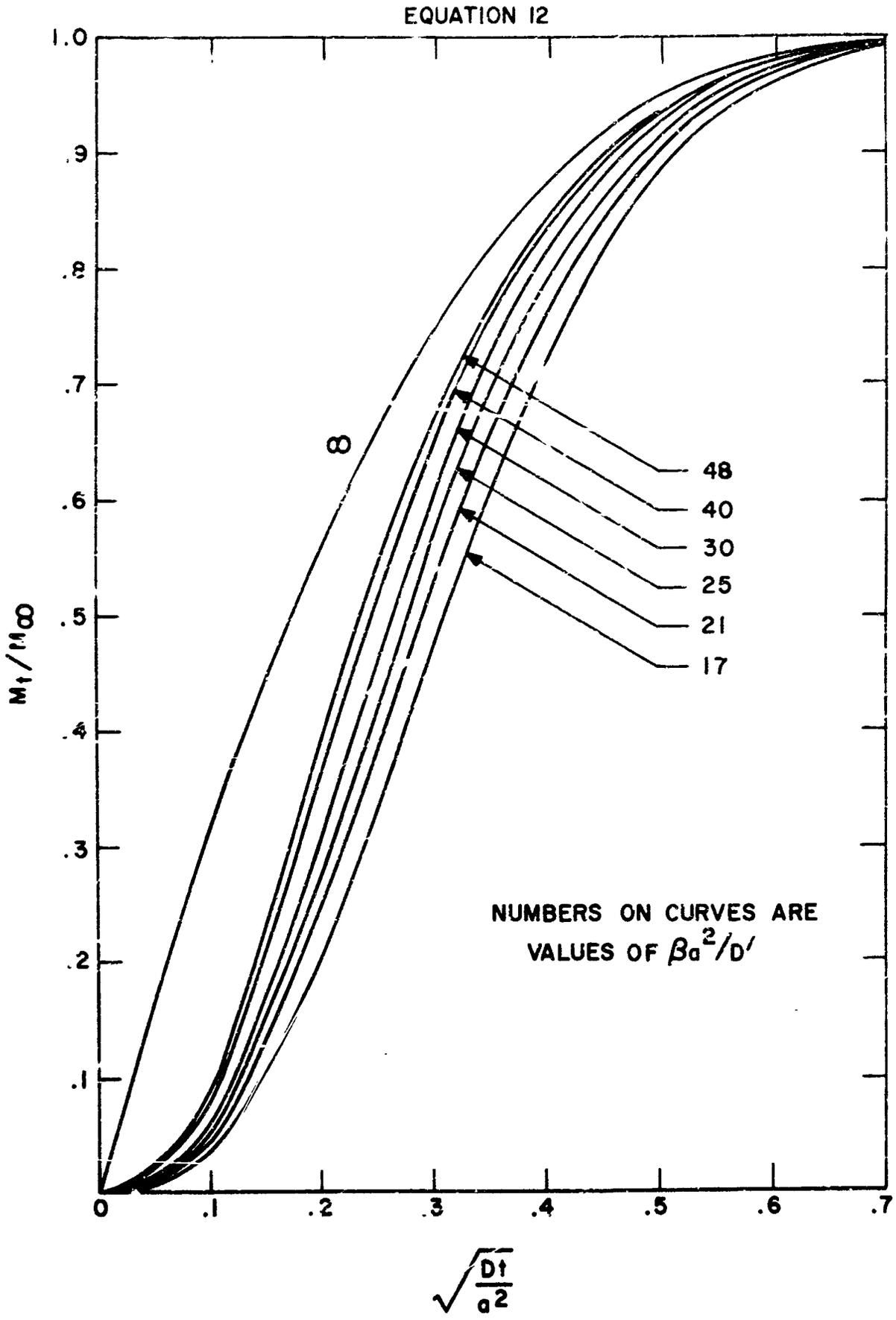
EQUATION 12
1.0
.9
.8
.7
.6
.5
.4
.3
.2
.1
0
.1
.2
.3
.4
.5
.6
.7
M_t/M_∞
$\sqrt{\frac{Dt}{a^2}}$
∞
48
40
30
25
21
17
NUMBERS ON CURVES ARE
VALUES OF $\beta a^2/D'$

FIGURE 73.

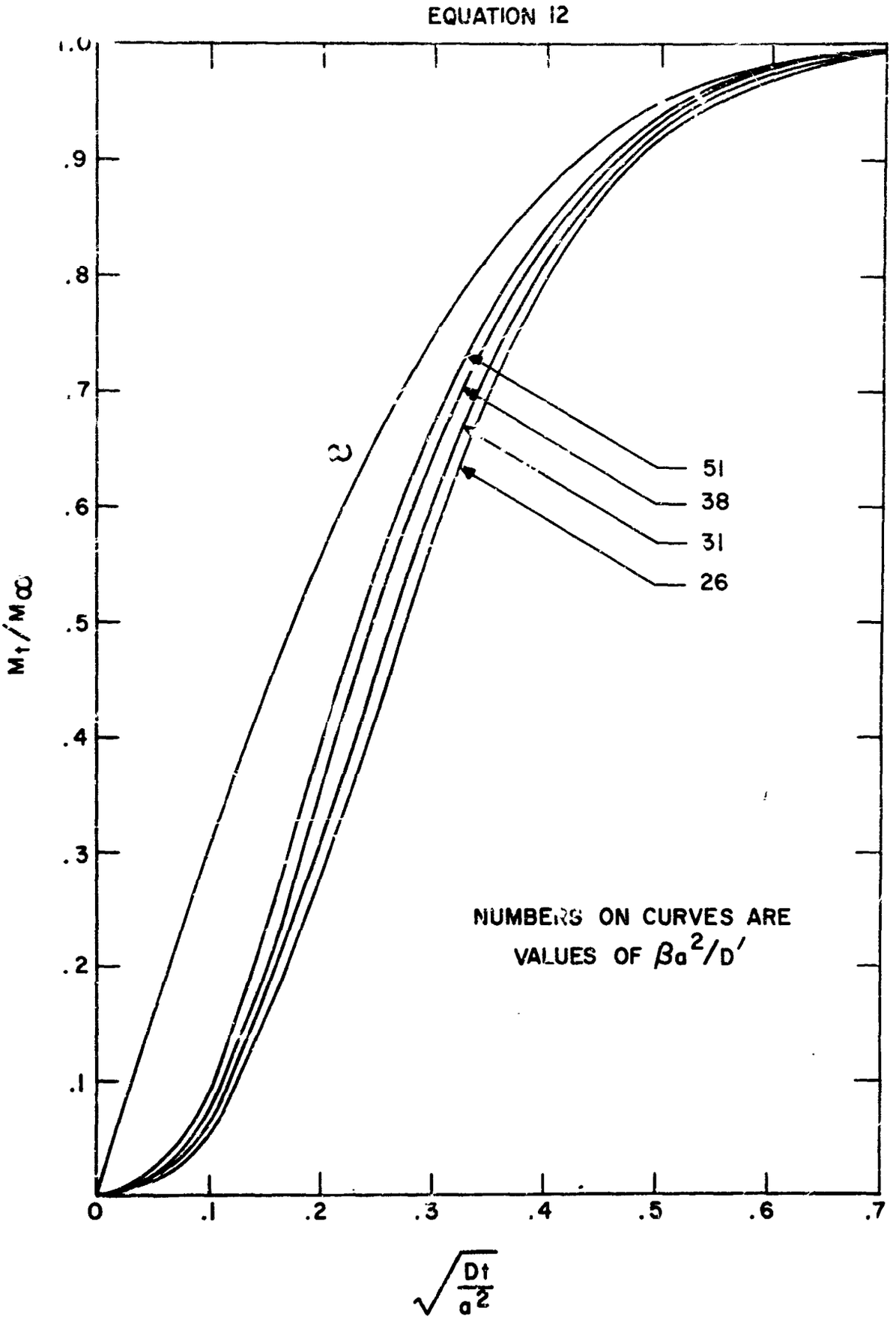

FIGURE 74
PAGE 206

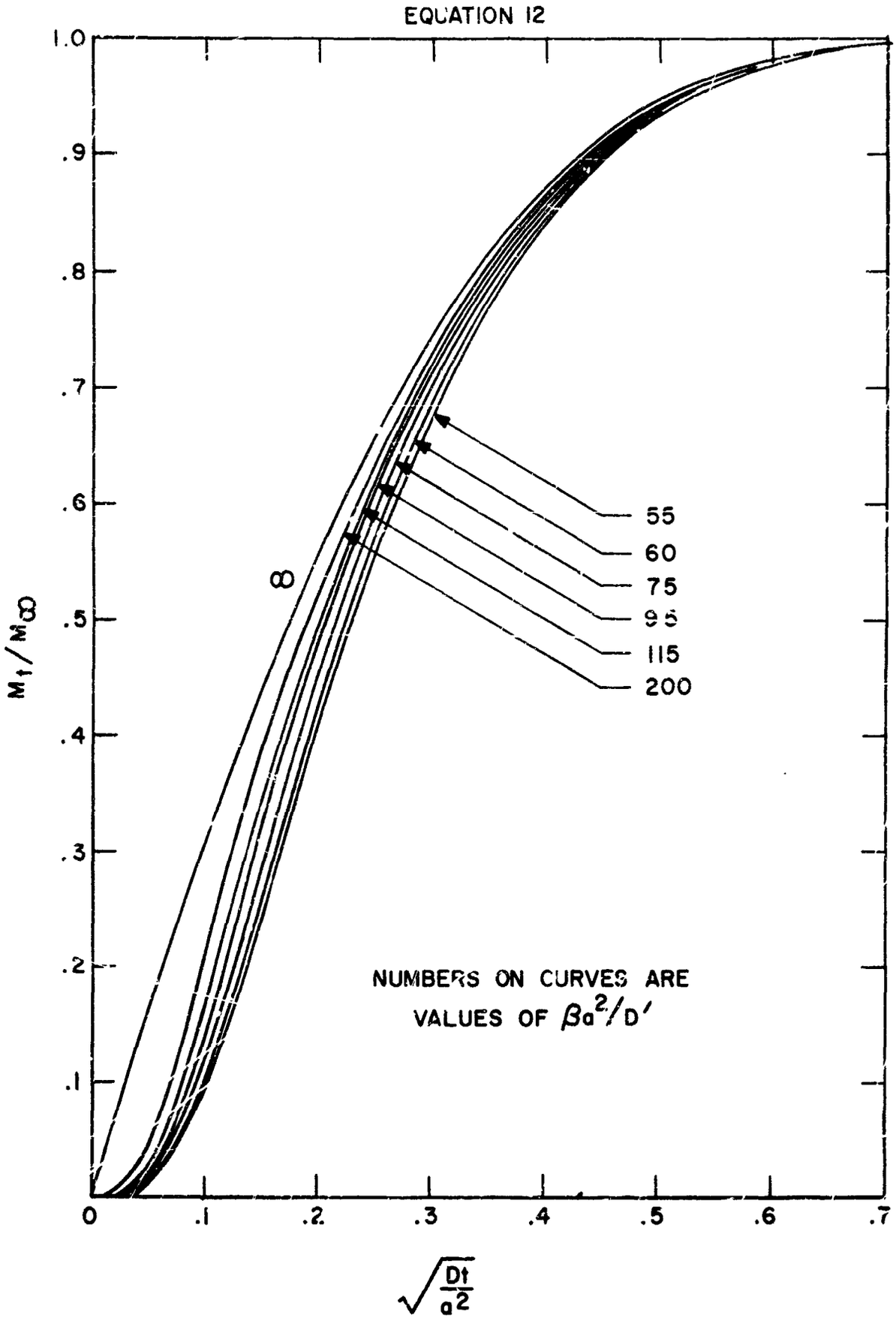
EQUATION 12
1.0
.9
.8
.7
.6
.5
.4
.3
.2
.1
0
.1
.2
.3
.4
.5
.6
.7
M_t/M_∞
$\sqrt{\frac{Dt}{a^2}}$
∞
55
60
75
95
115
200
NUMBERS ON CURVES ARE
VALUES OF $\beta a^2/D'$

FIGURE 75

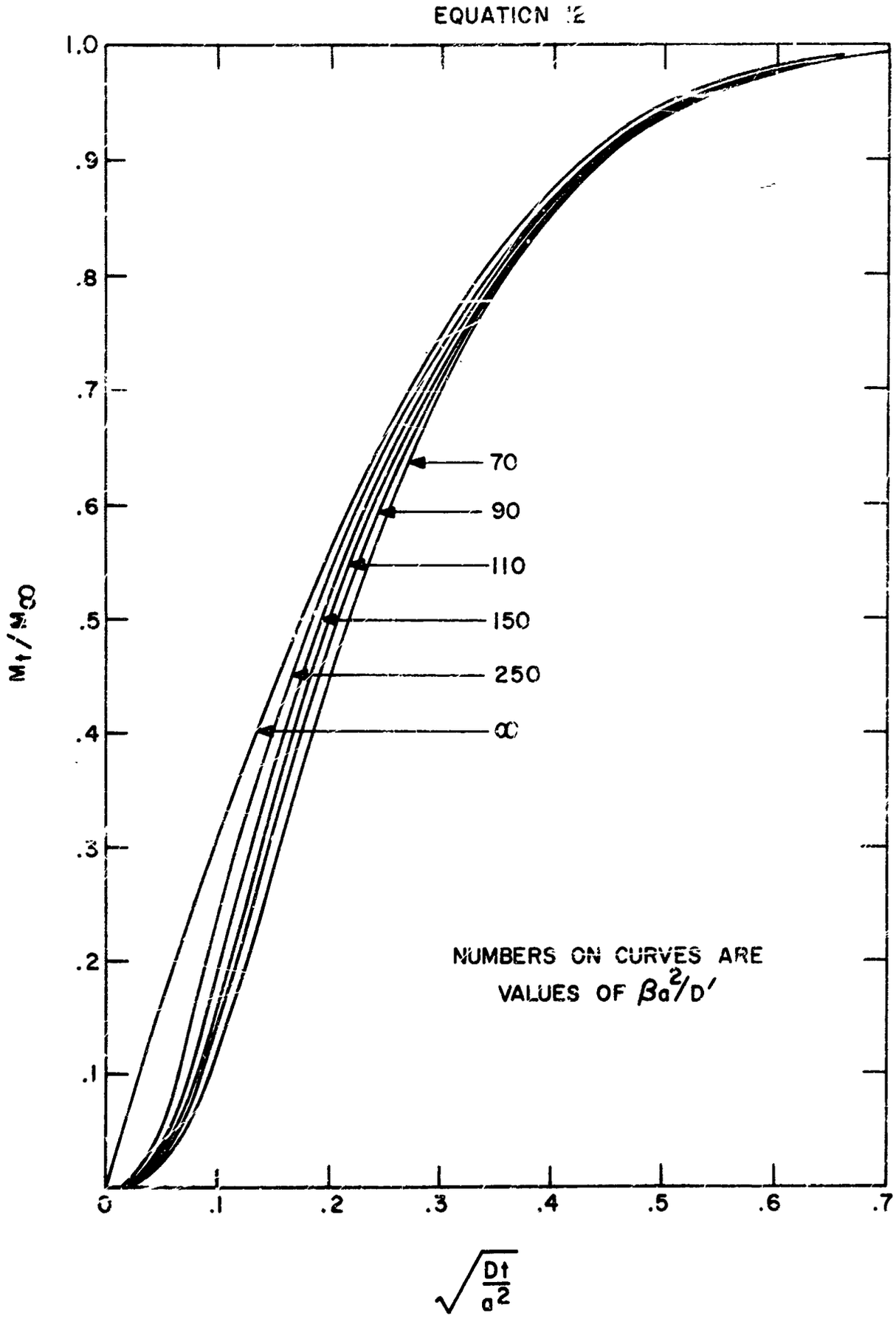
EQUATION 12
1.0
.9
.8
.7
.6
.5
.4
.3
.2
.1
0
.1
.2
.3
.4
.5
.6
.7
M_t/M_∞
70
90
110
150
250
∞
NUMBERS ON CURVES ARE
VALUES OF $\beta a^2/D'$
$\sqrt{\frac{Dt}{a^2}}$

FIGURE 76

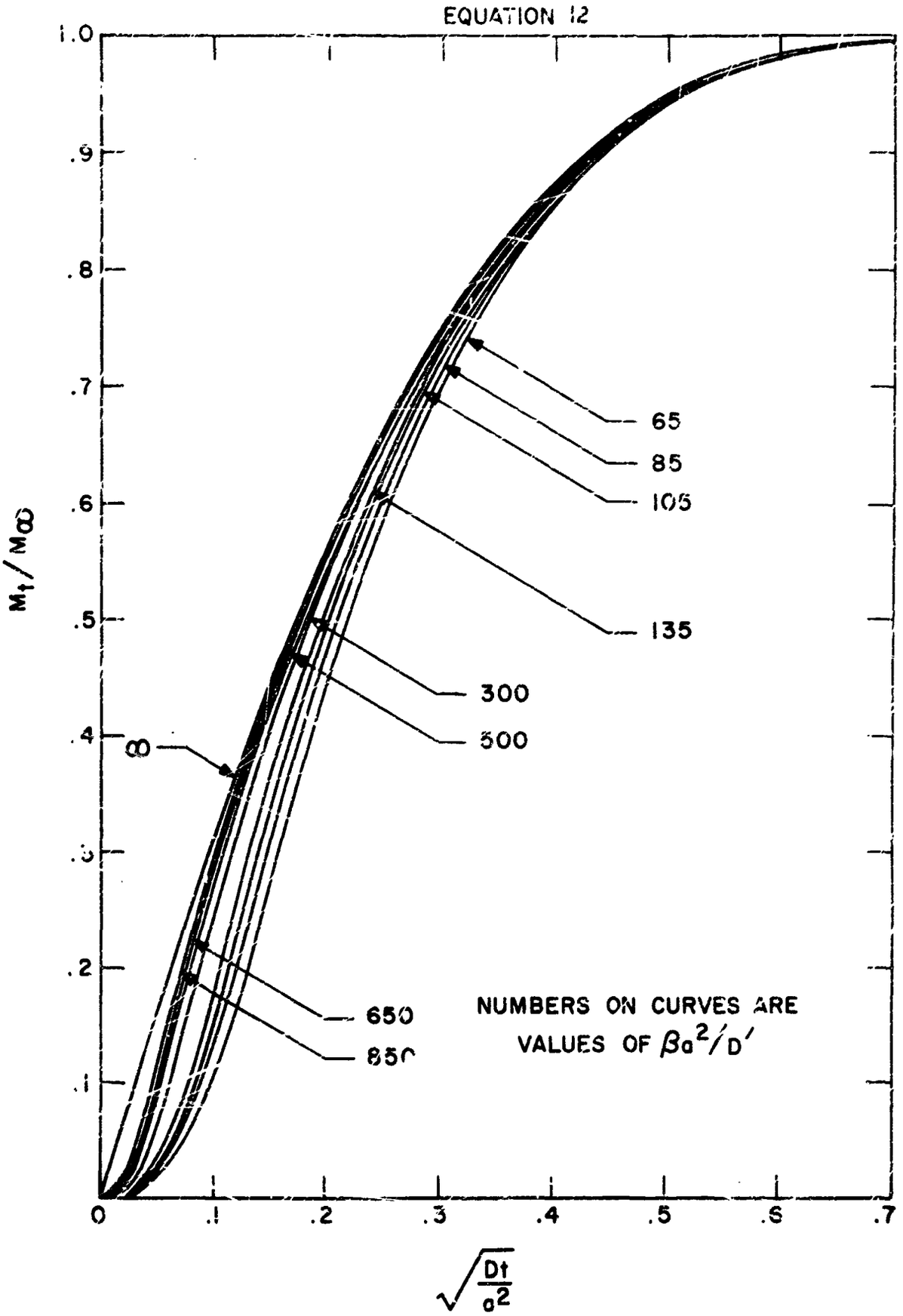
EQUATION 12
1.0
.9
.8
.7
.6
.5
.4
.3
.2
.1
0
.1
.2
.3
.4
.5
.6
.7
M_t / M_∞
$\sqrt{\frac{Dt}{a^2}}$
65
85
105
135
300
500
650
850
∞
NUMBERS ON CURVES ARE
VALUES OF $\beta a^2/D'$

FIGURE 77

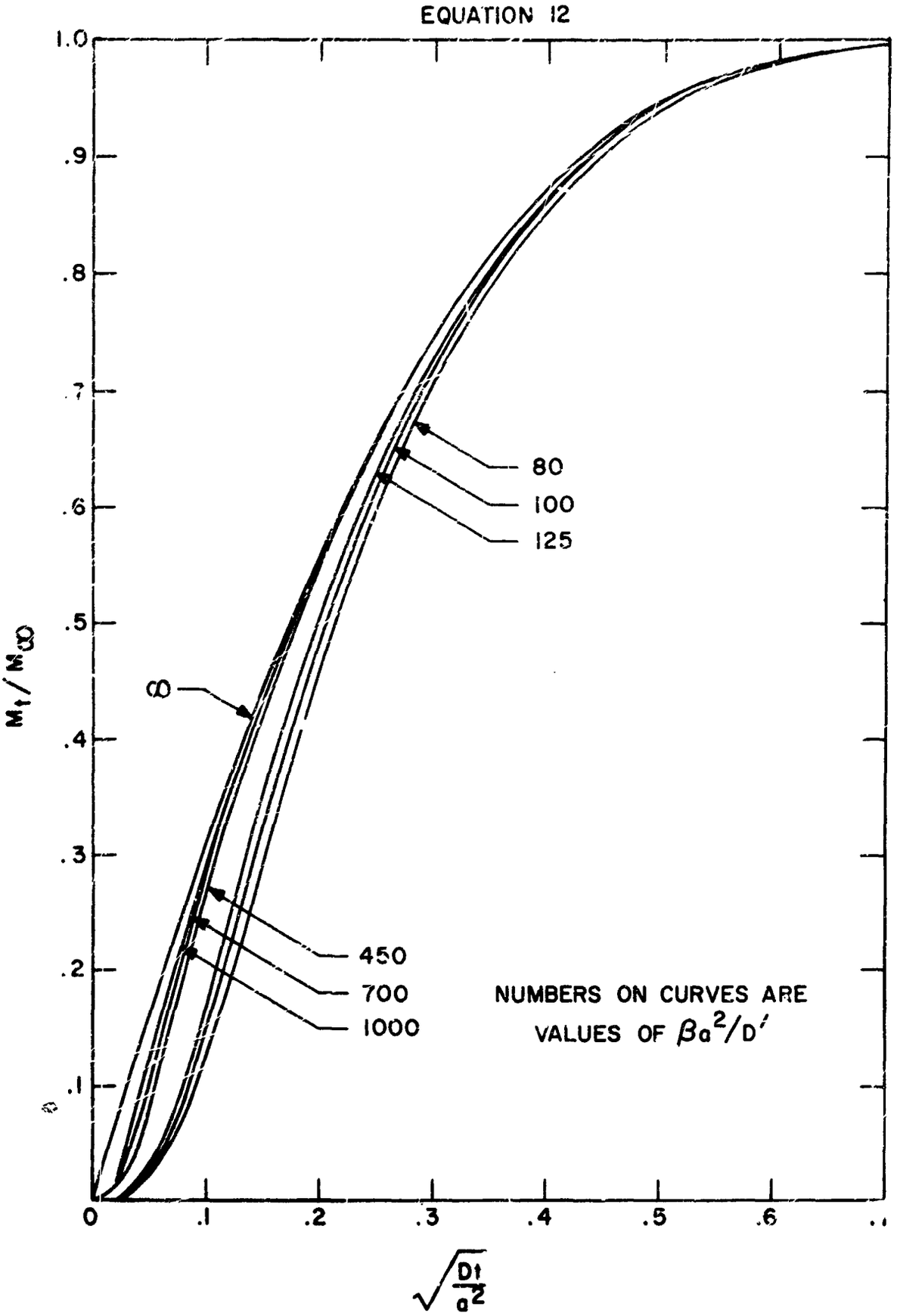

FIGURE 78

PAGE 210

APPENDIX D: DESIGN CALCULATIONS

CALCULATIONS FOR DESIGN OF OPERATIONAL AIR PURIFICATION SYSTEM

1.) From reference 2, CO_2 production by exhalation is .56 $ft^3/hr \cdot man$ at 760 mm and 0^oC and from reference 29, H_2O production by exhalation is 1.72 moles of H_2O per mole of CO_2 or .704 grams of H_2O per gram of CO_2. The CO_2 estimate seems low, and perspiration as a source of gaseous water is not taken into account.

2.) More reasonable estimates are available in reference 30, which is a comprehensive review. This gives .106 pounds CO_2/hr per man by exhalation and .090 pounds H_2O/hr-man by both exhalation and perspiration.

3.) From step 2, two men will produce (2)(.106)(453.6)=96.2 grams CO_2/hr and (2)(.09)(453.6)=81.7 grams H_2O/hr.

4.) To provide a resin reserve to compensate for incomplete regeneration assume that each absorption cycle runs until 70% of total absorption is reached, i.e $M_t/M_\infty = .7$.

5.) From Figure 35, $M_t/M_\infty = .7$ is reached at 20^oC with 0.65% CO_2 in the gas phase and 100% RH after 314 minutes.

6.) From Figure 7, $M_{co} = 2.17$ meg per gram of resin, or (2.17)(44/1000)=.0955 grams of CO_2 per gram of resin.

7.) From steps 4 and 6 then, (.7)(.0955)=.06685 grams of CO_2 are actually absorbed per gram of resin.

8.) From steps 3 and 5, $(96.2 \frac{\text{grams } CO_2}{\text{hr.}})(\frac{314 \text{ min}}{60 \text{ min hr.}})$=503.7 grams of CO_2 must be absorbed during each 314 minute cycle.

9.) From steps 7 and 8, $(503.7 \text{ grams } CO_2)(\frac{1 \text{ gram resin}}{.06685 \text{ grams } CO_2})$ = 7538 grams of resin are required per CO_2 absorber bed.

10.) Since the water capacity of this resin is 2 grams of water per gram of resin, each CO_2 bed will contain 2x7538 or 15076 grams of water.

11.) From steps 2 and 5, the total amount of water vapor added to the air during one cycle is 428 grams.

12.) Since the rate of CO_2 absorption is independent of the gas flow rate, the minimum gas flow is the one which passes 503.7 grams of CO_2 into the column in 314 minutes at P_{CO_2} = .0065 atm.:

$$(\frac{503.7 \text{ grams } CO_2}{314 \text{ minutes}})(\frac{1 \text{ gram mole } CO_2}{44 \text{ grams } CO_2})(\frac{1 \text{ gram mole gas}}{.0065 \text{ gram mole } CO_2})$$

$$(\frac{1 \text{ pound mole}}{453.6 \text{ gram moles}}) \times (\frac{359 \text{ scf}}{1 \text{ pound mole}}) = 4.432 \text{ scfm.}$$

13.) The minimum gas flow for water absorption of 50% RH is to be maintained is: $(\frac{428 \text{ grams } H_2O}{314 \text{ minutes}})(\frac{1 \text{ gram dry air}}{.00732 \text{ grams } H_2O})$

$$(\frac{1.0073 \text{ grams wet air}}{1 \text{ gram dry air}})(\frac{1 \text{ gram mole air}}{29 \text{ grams air}}) \times (\frac{1 \text{ pound mole}}{453.6 \text{ gram moles}}) \times$$

$(\frac{359 \text{ scf}}{1 \text{ pound mole}})$ = 5. 114 scfm.

14.) From 12 and 13, the minimum gas flow rate is 5.114 scfm.

15.) The water which must be added to the air in the air humidifier column to provide 100% RH air to the CO_2 absorber column is:

$(.00732 \frac{\text{grams } H_2O}{\text{gram dry air}})(\frac{528^\circ R}{492^\circ R})(\frac{29 \text{ pounds}}{359 \text{ scf}})$ (5. 114 scfm) $(453.6 \frac{\text{grams}}{\text{pound}})$ (314 min) = 471. 3 grams.

16.) Total water removal in the water absorber beds must then be 428 + 471. 3 = 899. 3 grams.

17.) The theoretical resin requirement is then (899. 3 grams H_2O) $(\frac{1 \text{ gram resin}}{2 \text{ grams } H_2O})$ = 449. 7 grams. However, since 50%RH air is to be produced, and not 100% RH air as would be the case if complete water saturation of the particles were attained, $(\frac{100}{50})$ (449. 7) = 899. 3 grams of resin per water absorber bed is required.

18.) Since two beds of each type are needed for continuous operation, the total resin on hand must be 2(7538+899. 3) = 16875 grams or 37. 2 pounds.

19.) The total water is 2 [2(7538) + 899. 3] = 2(15975. 3) = 31951 grams = 70.4 pounds.

20.) The total volume occupied is approximately 1.5 ft^3 for the four beds.

21.) The water storage container should be able to hold all the condensed water from one regeneration, a maximum of 12.1 pounds. Its volume should then be: $\frac{12.1}{62.4} = .194\ ft^3$.

REGENERATION

The PEI-ECH resin bed has been saturated to 70% of its equilibrium capacity in contact with 0.65% CO_2 in air at 20°C and 100% RH. The amount of CO_2 present on the resin is (.70) (2.17 meq/g) = 1.519 meq/g. It is desired to find the equilibrium composition of the gas above this bed if the temperature is raised to 30, 40, 50, 60, 70, and 80°C. CAPACITY = $K P_{CO_2}^{.684}$ and $K = .1397 \times e^{\frac{+3616}{R_o T}} = .1397 \times 10^{789/T}$ Vapor pressures of water are from reference 31.

T(°C)	T(°K)	789/T	K	$P^o_{H_2O}$(mm)	$(\frac{141.7}{K})$	P_{CO_2}(mm)
30	303	2.604	56.1	31.8	2.526	3.88
40	313	2.522	46.4	55.8	3.050	5.11
50	323	2.444	38.8	92.9	3.649	6.64
60	333	2.370	32.7	149.1	4.332	8.52
70	343	2.301	27.9	234.4	5.075	10.76
80	353	2.237	24.1	355.0	5.880	13.32
20	293	2.693	68.9	17.6	2.054	2.87

Resin is saturated at 0.65% (if 0.65% gas is left above it) when $K = 1.519/(.0065)^{.684} = 47.6$, i.e. $T \approx 39°C$. At 20°C, this gas has 100% RH, but, if heated to 80°C its RH is only 5%. This means that this gas will not inhibit water vaporization to any great extent, but it will certainly inhibit CO_2 removal. Hence this gas must be purged first.

Now we will determine P_{CO_2} above the bed if there is initially no CO_2 above it at all. $P_{CO_2} = (CAPACITY/K)^{1.462} (760) = (1.519/K)(932)^{1.462}$ mm $P_{CO_2} = (141.7/K)^{1.462}$.

The ratio of water to CO_2 in the bed is:

$\frac{2/18 \text{ mole } H_2O/\text{gram resin}}{1.519\times10^{-3} \text{ moles } CO_2/\text{gram resin}}$ = 111/1.519 = 73.1. This ratio, at 80°C, in the gas phase, must be 355/13.32 = 26.65. This means that CO_2 will come off the resin 73.1/26.65 = 2.74 times as fast as H_2O initially.

Assuming that the ratio of H_2O to CO_2 is a constant, then the ratio of partial pressures will always be $\frac{P_{H_2O}}{P_{CO_2}} = \frac{P^c_{H_2O}}{P_{CO_2}}$ which we have seen to be $\frac{355}{13.32}$ = 26.65. With CO_2 coming off the resin 2.74 times as fast as water, all the CO_2 should have been removed when only $\frac{100}{2.74}$ = 36.5% of the water has vaporized.

It must be argued that this gaseous pressure ratio cannot be expected to remain constant because the supply of CO_2 (on the resin) is being depleted so much faster than the supply of water. There are two compensating points however. First, the depletion means that the H_2O/CO_2 ratio in the solid phase is also increasing (although not as rapidly). The relative value of $(H_2O/CO_2)_{RESIN}/(H_2O/CO_2)_{GAS}$ will not increase as rapidly as either of the individual ratios. Second, the vapor pressure of water above the resin is substantially less than that above pure water (i.e. 355 mm). (For an ideal solution, which this assuredly is not, $P^o_{H_2O}$ would be 303 mm, based on two grams of water per gram of resin.) The ratio in the denominator of the above expression is thereby decreased. Thus, it is felt that the method employed gives a reasonable estimate of the water vaporized.

HEAT LOAD

HEAT OF REACTION: $(1x10^4 \frac{cal}{mole})(\frac{503.7}{44} \text{ moles})(x \frac{1 \text{ Btu}}{252 \text{ cal}}) = 454 \text{ Btu}$

SENSIBLE HEAT:

CO_2 ABSORBER: $(60C^o)(1 \frac{cal}{gram \cdot C^o})(\frac{1 \text{ Btu}}{252 \text{ cal}})(7538x3 \text{ grams})$

$= 5385$ Btu

H_2O ABSORBER: $(60C^o)(1 \frac{cal}{gram \cdot C^o})(\frac{1 \text{ Btu}}{252 \text{ cal}})(899.3x2 \text{ grams})$

$= 429$ Btu

LATENT HEAT:

CO_2 ABSORBER: $(.365)(\frac{15076}{453.6} \text{ pounds})(992.6 \frac{\text{Btu}}{\text{pound}}) = 12040$ Btu

H_2O ABSORBER: $(\frac{899.3}{453.6} \text{ pounds})(992.6 \frac{\text{Btu}}{\text{pound}}) = 1970$ Btu

TOTAL HEAT REQUIREMENT = 20278 Btu per cycle

POWER = $(\frac{20278 \text{ Btu}}{314 \text{ min}})(\frac{60 \text{ minutes}}{\text{hr}})(\frac{1000 \text{ watt. hr}}{3413 \text{ Btu}}) = 1134$ watts

MAXIMUM CONDENSER COOLING REQUIREMENT (provided all the water vaporized is recondensed):

LATENT HEAT + WATER SENSIBLE HEAT + CO_2 SENSIBLE HEAT = $(12040+1970)+ (.365)(\frac{2}{3})(7385)+\frac{1}{2}(429)$ $+(503.7 \text{ grams})(.22\frac{cal}{gram \cdot C^o})(60C^o)(\frac{1 \text{ Btu}}{252 \text{ cal}}) = 14010 + 1525 + 26 = 15561$ Btu in 314 min, or an average of 2970 Btu/hr

HEAT REMOVED FROM BEDS (to return them to 20^oC) = 20278-15561 = 4717 Btu

Introduction of a membrane which separates CO_2 and water vapor (32) does not yield any decrease in cooling requirements. Even though the ratio of water to CO_2 permeability is low enough (3200/280 = 11.43 for silicone rubber), so that some separation could take place before condensation, the water retained would still be in the vapor phase. Separation after condensation is unnecessary, since it it hoped that only a small amount of water will be lost. If the loss is substantial, however, such a membrane, placed after the condenser where the water to CO_2 ratio should be quite a bit less than 11.43, could recycle some water vapor back to the condenser.

HUMIDIFIER DESIGN

This device will be built along the lines of a conventional shell and tube heat exchanger. The "tubes" will consist of cylinders of thin, stiff wire mesh lined with a porous felt-like material. Liquid water from the shell side diffuses through the felt and evaporates into the tube-side air stream from the inside surface. As is shown in the following set of calculations, a square shell 25 inches on a side and one foot long which contains 86 one-foot long, $1\frac{1}{4}$" outside diameter tubes of mesh, each lined with $\frac{1}{8}$" thick wicking material, should be adequate to process 5.114 scfm of 50% RH 20°C air to a humidity in excess of 90% RH at 20°C. This device occupies 2.2 cubic feet and contains 106 pounds of liquid water at 20°C (see step 12 of the calculations).

CALCULATIONS:

1.) The molar rate of water transfer N_A is to be:

(5.114 scfm)(29 lbs. air/359 scf)(60 min/hr)(.00732 lbs water/lb. air) x (1 lb.-mole water/18 lbs.) = 1.01×10^{-2} lb.-moles/hr

2.) The inlet water mole fraction in the air $y_{in} = \frac{H_{in}/18}{1/29 + H_{in}/18} = 1.167 \times 10^{-2}$

3.) For 90% RH exit conditions, $y_{out} = 2.077 \times 10^{-2}$

4.) The interfacial water mole fraction for a completely wet surface is calculated from the saturation humidity at the water temperature, $y_i = \frac{.01464}{18/29 + .01464} = 2.300 \times 10^{-2}$

5.) Assuming that the usual logarithmic mean driving force prevails, then $\Delta y = \frac{y_{out} - y_{in}}{\ln\left(\frac{y_i - y_{in}}{y_i - y_{out}}\right)} = 5.60 \times 10^{-3}$

6.) The interfacial area for a bundle of n tubes of diameter D_T and length L is $\pi n D_T L$

7.) The mass transfer coefficient k_y is related to the gaseous heat transfer coefficient h_y by $\frac{h_y}{29\, k_y} = 0.26$

8.) For heat transfer to a fluid in laminar flow the equation (31) for h_y is $h_y = 2 \frac{k_{TH}}{D_T} \left(\frac{W C_P}{k_{TH} L}\right)^{\frac{1}{3}}$, where k_{TH} is the thermal conductivity, C_P the heat capacity at constant pressure, and $\underline{W}$ the mass flow rate.

9.) For air inside a tube bundle flowing at 5.114 scfm at 20°C, $h_y = \frac{2.67}{D_T (nL)^{1/3}}$ where D_T is in inches and $\underline{L}$ is in feet

10.) Applying the mass transfer equation (31):

$N_A = k_y (\Delta y) A$ yields: $nL = 85.6$, so that 86 one-foot long tubes should suffice.

11.) Taking a 1" inside diameter, $\frac{1}{8}$" thickness wicking, triangular pitch stacking and $2\frac{1}{2}$" center-to-center distance in a square shell, 2.18 ft^3 are taken up.

12.) If no problem of dry spots on the wicking material exist, the center-to-center distance can be reduced, so that the total volume and the amount of stored water can be substantially decreased. (see Table 17).

ESTIMATE OF HEAT EXCHANGER-CONDENSER SIZE

1.) From the section on heat loads, the average cooling requirement of the condenser is 2970 Btu/hr.

2.) If the inlet gas is at 80°C (176°F) and the exit gas is at 20°C (68°F) and the coolant at t_c (°F) the logarithmic means temperature gradient is:

$\Delta t = \frac{176 - 68}{\ln \frac{176 - tc}{68 - tc}}$. This assumes that the liquid droplets of condensate are carried along with the gas because of the zero gravity environment. The gas centrifuge separates them just prior to venting.

3.) The area for heat transfer in a tube bundle of $\underline{n}$ tubes of inside diameter D_T and length $\underline{L}$ is: $\pi\ n\ D_T\ L$.

4.) Assuming a heat transfer coefficient of 2 Btu/hr·ft^2·°F and employing the usual heat transfer equation (31):

$q = n\ A\ \Delta t$ yields: $52.6\ (\ln \frac{176 - t_c}{68 - t_c}) = n\ D_T\ L$ where D_T is in inches and $\underline{L}$ is in feet.

5.) For 1" ID tubes used with 32°F coolant:

$n\ L = 72.9.$

6.) If 73 1" ID, one-foot long tubes are packed on triangular pitch, with $2\frac{1}{2}$ inch center-to-center distance in a cylindrical shell, less than 2 ft^3 of space is required.